PRECLINICAL STUDY FOR THE TREATMENT OF MITOCHONDRIAL ENCEPHALOPATHY ASSOCIATED WITH COENZYME Q DEFICIENCY

RESEARCH GROUP CTS-101

CENTRO DE INVESTIGACIÓN BIOMÉDICA (CIBM)

DEPARTMENT OF PHYSIOLOGY. FACULTY OF MEDICINE

PTS-GRANADA

UNIVERSIDAD DE GRANADA

AGUSTÍN HIDALGO GUTIÉRREZ

BIOMEDICINE DOCTORAL PROGRAMME

Granada, 2020

Editor: Universidad de Granada. Tesis Doctorales
Autor: Agustín Hidalgo Gutiérrez
ISBN: 978-84-1306-718-6
URI: http://hdl.handle.net/10481/653668

PREDOCTORAL CONTRACTS:

1. **Type:** Predoctoral contract associated to grant SAF2013-47761R (MCINN, Spain). Full time 01/02/2015-01/08/2016.

   Organism: Universidad de Granada.

   Center: Centro de Investigación Biomédica y Facultad de Medicina.

   Departament: Physiology.

2. **Type:** FPU Contract, Ministry of Science and Innovation, Spain. Position 17/1000. (FPU15/01448). Full time 15/09/2016-21/12/2020.

   Organism: Universidad de Granada.

   Center: Centro de Investigación Biomédica y Facultad de Medicina.

   Departament: Physiology.

PARTICIPATION IN RESEARCH PROJECTS:

1. **Title:** Looking for the connection between clock genes and mitochondrial impairment in aging and age-related loss of muscule fibers.
   Reference: CB/10/00238.
   Principal Investigator: Dario Acuña Castroviejo.
   Agency: INSTITUTO DE SALUD CARLOS III.
   Date: 29/11/2013-29/12/2016.

2. **Title:** Estudio preclínico para el tratamiento de la encefalopatía mitocondrial asociada a la deficiencia en Coenzima Q.
   Reference: SAF2013-47761-R.
   Principal Investigator: Luis Carlos López García.
   Agency: MINECO.

Date: 01/01/2014-31/12/2015.

Funds: 102,850.00 €

3. **Title:** Patogénesis y Tratamiento de la Deficiencia en Coenzima Q.
   Reference: SAF2015-65786-R.
   Principal Investigator: Luis Carlos López.
   Agency: Ministerio de Economía y Competitividad, Gobierno de España (MINECO).
   Date: 01/2015-12/2018.
   Funds: 181,500.00 €

4. **Title:** New therapeutic molecules for the treatment of mitochondrial diseases.
   Reference: MDA-602322.
   Principal Investigator: Luis Carlos López.
   Agency: Muscular Dystrophy Association (MDA, USA)
   Date: 01/2/2019-31/01/2022.
   Funds: 289,865.00 $

FUNDING AND AWARDS:

1. **Initation fellowship**, Universidad de Granada. 1,800 € 01/04/2015-31/03/2016.

2. **Europe COST ACTION (CA)**, MITOEAGLE Action, Ref . COST-STSM-CA15203-37564. 2,500 €. 19/06/2017-02/08/2017.

3. **FPU short-term stay**, EST17/00858, Ministry of Science and Innovation, Spain. Position 1/120. 5,200 €. 29/04/2018-26/07/2018.

4. **Best paper published in February** 2019 for ‘’β-RA reduces DMQ/CoQ ratio and rescues the encephalopathic phenotype in *Coq9*^{R239X} mice’’ paper. Biochemical and Biomolecular Spanish Society (SEBMM). 2/2019

5. **European Consortium**, EPIC-XS. 1,494 €. 13/10/2019-27/10/2019.

PUBLICATIONS:

Main publications supporting this doctoral thesis:

1. **Hidalgo-Gutiérrez A**, et al. (2019). β-RA reduces DMQ/CoQ ratio and rescues the encephalopathic phenotype in Coq9R239X mice. EMBO molecular medicine. DOI: 10.15252/emmm.201809466 (**First Author**). IF: 8,821; D1, 9/138, Medicine, Research & Experimental. Article awarded with best paper of the month (February) by the Biochemistry and Molecular Biology Spanish Society (SEBBM).

2. Gonzalez-García P, **Hidalgo-Gutiérrez A**, et al. (2020). Coenzyme Q10 modulates sulfide metabolism and links the mitochondrial respiratory chain to pathways associated to one carbon metabolism. Human Molecular Genetics. DOI: 10.1093/hmg/ddaa214. (**Co-First Author**). IF: 5.1; Q1, 27/177 , Genetics and Heredity.

3. **Hidalgo-Gutiérrez A**, et al. (2020). Toxic vs Therapeutic: The Dose-Dependent Effects of β-Resorcylic Acid Depend on Mitochondrial Metabolism. Authorea Repository. DOI: 10.22541/au.158938611.16011582. (**First Author**). Pending of submission.

Doctoral thesis related publications:

4. Barriocanal-Casado E, Cueto-Urena C, Benabdellah K, Gutierrez-Guerrero A, Cobo M, **Hidalgo- Gutierrez A**, et al (2016). Gene Therapy Corrects Mitochondrial Dysfunction in Hematopoietic Progenitor Cells and Fibroblasts from *Coq9*^{R239X} Mice. PLoS One. 2016;11(6):e0158344. IF: 3.057; Q1, 11/63 Multidisciplinary science.

5. Luna-Sánchez M, **Hidalgo-Gutiérrez A**, Hildebrandt TM, Chaves-Serrano J, Barriocanal-Casado E, Santos-Fandila A, Romero M, Sayed RKA, Duarte J, Prokisch H, Schuelke M, Escames G, Acuña- Castroviejo D, Lopez LC (2017). CoQ Deficiency Causes Disruption of Mitochondrial Sulfide Oxidation, a new Pathomechanism Associated to this Syndrome. *EMBO molecular medicine* 9(1):78-95. (**Co-Fist Author**). IF: 10.293; 7/133 (D1), Medicine, Research & Experimental.

6. Quinzii CM, Luna-Sanchez M, Ziosi M, **Hidalgo-Gutierrez A**, et al (2017). The Role of Sulfide Oxidation Impairment in the Pathogenesis of Primary CoQ Deficiency. Frontiers in physiology 2017;8: 525

10.3389/fphys.2017.00525. Review. IF: 3.394; Q1, 20/83, Physiology. **International collaboration**.

7. Rodríguez-Hidalgo M, Luna-Sánchez M, **Hidalgo-Gutiérrez** A, et al (2018). Reduction in the levels of CoQ biosynthetic proteins is related to an increase in lifespan without evidence of hepatic mitohormesis. Sci Rep. 8(1):14013. (**Third Author**) IF: 4.011; Q1, 15/69, Multidisciplinary Sciences.

8. Kleiner G, Barca E, Ziosi M, Emmanuele V, Xu Y, **Hidalgo-Gutierrez A**, et al (2018). CoQ_{10} supplementation rescues nephrotic syndrome through normalization of H2S oxidation pathway. Biochim Biophys Acta Mol Basis Dis. 2018 Nov; 1864(11):3708-3722. doi: 10.1016/j.bbadis.2018.09.002. IF 4.328; Q1, 74/298 Biochemistry and molecular biology. **International collaboration**.

9. Barriocanal-Casado E, **Hidalgo-Gutiérrez A**, et al. (2019). Rapamycin administration is not a valid therapeutic strategy for every case of mitochondrial disease. eBioMedicine. DOI: 10.1016/j.ebiom.2019.03.025. (**Second Author**). IF: 5.736; Q1, 18/138, Medicine, Research & Experimental.

Doctoral thesis not related publications:

10. Rahim I, Djerdjouri B, Sayed RK, Fernandez-Ortiz M, Fernandez-Gil B, **Hidalgo-Gutierrez A**, et al (2017). Melatonin administration to wild-type mice and non-treated NLRP3 mutant mice share similar inhibition of the inflammatory response during sepsis. J Pineal Res. 10.1111/jpi.12410. IF: 11.613; D1 6/142, Endocrinology & Metabolism. 3/83, Physiology. **Local collaboration**.

11. Huertas JR, Al-Fazazi S, **Hidalgo-Gutierrez A** et al (2017). Antioxidant effect of exercise: Exploring the role of the mitochondrial complex I superassembly. Redox biology 2017;13: 477-481 10.1016/j.redox.2017.07.009. (**Third Author**) IF: 7.126; Q1, 31/293, Biochemistry and molecular biology. **National collaboration**.

12. Díaz-Casado María E, Rusanova I, Aranda P, Fernández-Ortiz M, Sayed RK, Fernández-Gil B, **Hidalgo-Gutiérrez A**, et al (2018). In Vivo Determination of Mitochondrial Respiration in 1-Methyl-4-Phenyl-1,2,3,6-Tetrahydropyridine-Treated. Zebrafish Reveals the Efficacy of Melatonin in Restoring Mitochondrial Normalcy. Zebrafish 2017; 10.1089/zeb.2017.1479. IF: 1.742; Q1, 41/170, Zoology. **Local collaboration**.

13. Casuso RA, Al-Fazazi S, **Hidalgo-Gutiérrez A**, et al. (2019). Hydroxytyrosol influences exercise-induced mitochondrial respiratory complex assembly into supercomplexes in rats. Free Radical Biology and Medicine. DOI: 10.1016/j.freeradbiomed.2019.01.027 (**Co-First Author**). IF: 6.17; Q1, 16/143, Endocrinology & Metabolism. **National collaboration**.

CONFERANCE ATTENDANCE:

1. 11th MiP conference on Mitochondrial Physiology. International Conference. Organized by the Mitochondrial Physiology Society. Lucni Bouda, Pec pod Snezkou, Czech Republic. Contribution: First Author, **Oral communication by competitive process.** 07-11/09/2015.

2. III Scientific journeys of Genyo. National Conference. Organized by Pfizer Genyo center. Universidad de Granada, Granada. Contribution: First Author, **Oral communication by competitive process.** 14-15/12/2015.

3. IV Scientific journeys of Genyo. National Conference. Organized by Pfizer Genyo center. Universidad de Granada, Granada. Contribution: First Author, **Poster** 14-15/12/2016.

4. Euromit Cologne 2017. International Conference. Euromit. University of Cologne, Cologne, Germany. Contribution: First Author, **Poster** 11-15/06/2017.

5. The 9th Conference of the International Coenzyme Q10 Association. International Conference. International Coenzyme Q10 Association. Columbia University, New York, USA. Contribution: First Author, **Poster** 21-24/06/2018.

6. I Congreso Nacional de Investigadores del PTS. National Conference. UGR, Granada, Spain. Contribution: First Author, **Oral communication** by competitive process. 13-15/02/2019.

To my family

AGRADECIMIENTOS

A mi familia.

A mi gente. A estas alturas no es necesario pararse a nombrarlos, ya que, son los que son y deben darse por aludidos.

A mis mentores y compañer@s que, con horas de interminable trabajo, me han ayudado a conseguir mis objetivos durante esta etapa.

A todos los colaboradores nacionales e internacionales con los que he tenido el placer de trabajar, los cuales también han sido indispensables para mi desarrollo laboral.

Los que me conocen saben que no soy dado al pensamiento o escritura emotiva o lacrimógena, así que voy a dedicaros unas citas que me parecen interesantes.

> "Cada cual forja su fortuna con su comportamiento" (Frase griega antigua extraída de los ensayos de Montaigne).
>
> "Yo soy yo y mi circunstancia, y si no la salvo a ella no me salvo yo", (José Ortega y Gasset).

Y por supuesto, un poco de humor de la mano de Groucho Marx:

> "Si eres capaz de hablar sin parar, al final te saldrá algo gracioso, brillante e inteligente"
>
> "Todo el mundo debe creer en algo, yo creo que voy a seguir bebiendo, discúlpenme"
>
> "Estuve tan ocupado escribiendo la crítica que nunca pude sentarme a leer el libro"

¡Always look on the bright side of life! (Monty Python)

ACKNOWLEDGEMENT

To my family

To my people. It is not necessary to stop and name them, because they must be taken for granted.

To my mentors and colleagues who, with hours of endless work, have helped me to achieve my goals during this stage.

To all the national and international collaborators with whom I have had the pleasure of working with. They have also been indispensable for my carreer development.

Those who know me know that I am not given to emotional or tearful thinking or writing. So I will dedicate some quotes that I find interesting.

> "Everyone makes their fortune with their behavior" (Ancient Greek phrase extracted from Montaigne's essays).
>
> "I am I and my circumstance; and, if I do not save it, I do not save myself" (José Ortega y Gasset).

And of course, a little humor by Groucho Marx (literally traduced from Spanish version):

> 'If you're able to talk nonstop, eventually you'll come up with something funny, bright and smart".
>
> "Everyone must believe in something, I think I'll keep drinking, excuse me"
>
> "I was so busy writing the review that I could never sit down and read the book"

¡Always look on the bright side of life! (Monty Python)

ABBREVIATIONS

ABBREVIATIONS

4-HB: 4-Hydroxybenzoate

ATP: Adenosine triphosphate

ADP: Adenosine diphosphate

BBB: Blood brain barrier

BNGE: Blue native gel electrophoresis

CBS: cystathionine β-synthase

CoQ: Coenzyme Q

CSE: cystathionine γ-lyase

DMQ: Demetoxyubiquinone

DNA: Deoxyribonucleic acid

FAD: Flavin adenine dinucleotide

H_2S: Hydrogen sulfide

HPLC: High-resolution liquid chromatography

IMM: Inner mitochondrial membrane

LC-HRMS: Liquid chromatography coupled to high-resolution mass spectrometry

LOHN: Hereditary Leber optic neuropathy

MD: Mitochondrial diseases

MEFs: Mouse embryonal fibroblasts

MELAS: Mitochondrial encephalopathylactic acidosis and stroke

MLD: Metachromatic leukodystrophy

MNGIE: mitochondrial neurogastrointestinal encephalopathy

mPTP: mitochondrial permeability transition pore

mRNA: messenger RNA

mtDNA: mitochondrial DNA

mtETC: Mitochondrial electron transfer chain

mtUPR: Mitochondrial unfolded protein response

NAD: Nicotinamide adenine dinucleotide

NMD: Non-sense mediated mRNA decay.

OXPHOS: Oxidative phosphorylation system.

RNA: ribonucleic acid

ROS: reactive oxygen species

SAAR: Sulfur amino acids restriction

SC: Supercomplexes

SQOR: Sulfide:quinone oxidoreductase

TIM: Translocase internal membrane

TOM: Translocase outer membrane translocase

TP: Thymidine phosphorylase

UCP: uncoupling protein

VDAC: Voltage-dependent anionic channel

INDEX

INDEX

Resumen **..1**

Summary **..9**

1. INTRODUCTION **..17**

1.1 THE MITOCHONDRION 17

1.1.1 GENERAL DESCRIPTION 17

1.1.2 ORIGINS 17

1.1.3 STRUCTURE 20

1.1.4 MITOCHONDRIAL GENOME 22

1.1.5 FUNCTION 23

1.1.5.1 The OXPHOS system 25

1.1.5.2 Supercomplexes 27

1.1.5.3 Coenzyme Q 30

1.1.5.3.1 History 30

1.1.5.3.2 Structural, physical and chemical proprieties of Coenzyme Q 32

1.1.5.3.3 Biosynthesis and distribution of CoQ.. 33

1.1.5.3.3.1 Complex Q 36

1.1.5.3.3.2 CoQ localization.. 40

1.1.5.3.4 CoQ functions: 42

1.1.5.3.4.1 The role of CoQ in the mitochondrial respiratory chain. 42

1.1.5.3.4.2 CoQ and uncoupled proteins (UCP). 43

1.1.5.3.4.3 CoQ and the mitochondrial permeability transition pore (mPTP). 44

1.1.5.3.4.4 CoQ as antioxidant. 44

1.1.5.3.4.5 Other functions 46

1.1.5.3.4.6 Sulfide metabolism 47

1.2 RARE DISEASES 49

1.2.1 MITOCHONDRIAL DISEASES 50

1.2.1.1 CoQ deficiency 53

1.2.1.1.1 Pathological mechanisms associated to CoQ deficiency: experimental studies 58

1.2.1.1.2 Experimental treatments for CoQ deficiency. 64

1.2.1.1.3 Treatment of patients with CoQ deficiency. 66

1.2.1.1.4 Alternative treatments for CoQ deficiency using analogs of 4HB 68

2. HYPOTHESIS & OBJECTIVES 73

3. MATERIALS & MÉTHODS 79

3.1 EXPERIMENTAL DESIGN 79

3.2 HEMOGRAM, PLASMA AND URINE ANALYSIS 81

3.3 HISTOLOGY AND IMMUNOHISTOCHEMISTRY 82

3.4 IN VIVO MRI AND PROTON MRS 83

3.5 TRANSCRIPTOME ANALYSIS BY RNA-seq 84

3.6 MITOCHONDRIAL PROTEOMICS ANALYSIS 86

3.7 MITOCHONDRIAL RESPIRATION 89

3.8 CoQ-DEPENDENT RESPIRATORY CHAIN ACTIVITIES 91

3.9 EVALUATION OF SUPERCOMPLEXES FORMATION BY BNGE....................... 92

3.10 SAMPLE PREPARATION AND WESTERN BLOT ANALYSIS IN TISSUES......... 93

3.11 QUANTIFICATION OF CoQ$_9$ AND CoQ$_{10}$ LEVELS IN MICE TISSUES 94

3.12 QUANTIFICATION OF β-RA AND 4-HB LEVELS IN MICE TISSUES................ 95

3.13 QUANTIFICATION OF PRO-INFLAMMATORY MEDIATORS IN MURINE RAW 264.7 MACROPHAGES AND BRAINSTEM EXTRACTS.................................. 96

3.14 STATISTICAL ANALYSIS 96

3.15 DATA AVAILABILITY.. 97

4. RESULTS 103

4.1 CoQ DEFICIENCY ALTERNATIVE THERAPY: 4-HB ANALOGUE. β-RESORCYLIC ACID 103

4.1.1 THE TREATMENT WITH β-RA RESCUES THE PHENOTYPE OF *Coq9*^{R239X} MICE 103

4.1.2 THE TREATMENT WITH B-RA INDUCES A REDUCTION IN THE HISTOPATHOLOGICAL SIGNS OF THE ENCEPHALOPATHY 107

4.1.3 TRANSCRIPTOMICS PROFILE REVEALS A REDUCTION IN THE NEUROINFLAMMATORY GENES 111

4.1.4 β-RA DOES NOT DIRECTLY ACT AS ANTI-INFLAMMATORY AGENT 114

4.1.5 β-RA IMPROVES MITOCHONDRIAL BIOENERGETICS IN PERIPHERAL TISSUES OF *Coq9*^{R239X} MICE 115

4.1.6 β-RA REDUCES DMQ$_9$ IN PERIPHERAL TISSUES OF *Coq9*^{R239X} MICE.................... 120

4.1.7 THE EFFECT OF β-RA OVER COQ BIOSYNTHETIC PATHWAY IS PARTIALLY MEDIATED BY A STABILIZATION OF THE COMPLEX Q 128

4.1.8 THE LEVELS OF DMQ_9 CONTRIBUTE TO THE DISEASE PHENOTYPE. 132

4.1.9 STEROIDS HORMONES OR FGF21 DO NOT MEDIATE THE TISSUES COMMUNICATION UNDER COQ DEFICIENCY. 135

4.2 TOXIC OR THERAPEUTIC? - THE DOSE-DEPENDENT EFFECTS OF β-RESORCYLIC ACID DEPEND ON MITOCHONDRIAL METABOLISM..............138

4.2.1 THE HIGH DOSE OF β-RA INDUCES DETRIMENTAL EFFECTS IN THE PHENOTYPE OF WILD-TYPE ANIMALS, WITH SEVERE MORPHOLOGICAL AND FUNCTIONAL ALTERATIONS IN THE LIVER, KIDNEYS AND BRAIN. 138

4.2.2 THE HIGH DOSE OF β-RA AFFECTS THE HOMEOSTASIS OF THE MITOCHONDRIAL PROTEOME AND COQ METABOLISM IN WILD-TYPE ANIMALS.......................... 150

4.2.3 A LOWER DOSE OF β-RA AVOIDS ITS TOXIC EFFECTS IN WILD-TYPE ANIMALS, MAINTAINING ITS POTENTIAL TO REDUCE THE PHENOTYPIC AND HISTOPATHOLOGICAL SIGNS IN *Coq9*^{R239X} MICE. 160

4.2.4 THE THERAPEUTIC EFFECT OF THE LOW DOSE OF β-RA IS DUE TO THE REDUCTION OF THE DMQ/COQ RATIO IN PERIPHERAL TISSUES OF *Coq9*^{R239X} MICE, LEADING TO A BIOENERGETICS IMPROVEMENT. 164

4.2.5 CO-ADMINISTRATION OF 4-HB MODIFIES THE EFFECTS OF β-RA.................... 170

4.3 SULFIDE METABOLISM AND CoQ DEFICIENCY...174

4.3.1 MODULATION OF SULFIDE METABOLISM PATHWAY TO PREVENT THE PATHOLOGY... 174

5. DISCUSSION 181

5.1 β-RA SUPLEMENTATION AS ALTERNATIVE THERAPY FOR PRIMARY COQ DEFICIENCY. 181

5.2 DUAL EFFECTS OF β–RA: THE INFLUENCE OF COQ METABOLISM. 190

5.3 MODULATION OF SULFIDE METABOLISM AS THERAPEUTIC APPROACH FOR PRIMARY COQ DEFICIENCY. 196

6. CONCLUSIONS 201

7. BIBLIOGRAPHY 205

RESUMEN

Resumen

La mitocondria es uno de los orgánulos celulares más fascinantes. Está formada por una bicapa lipídica y hay de entre cientos a miles de copias por célula. La mitocondria actúa como la central energética de la célula, por lo que es necesaria para la generación de energía que la célula necesita para llevar a cabo una correcta actividad. Además, es un orgánulo indispensable para muchos procesos metabólicos. Debido a esto, un defecto en la mitocondria, producido principalmente por mutaciones en genes que codifican proteínas mitocondriales, podría desencadenar en alguna de las llamadas enfermedades mitocondriales (MD).

Las enfermedades mitocondriales son un grupo raro de enfermedades neurometabólicas que son extremadamente complejas y encuadran un grupo heterogéneo de desórdenes genéticos que resultan en una fosforilación oxidativa alterada, incluyendo la cadena de transporte de electrones mitocondrial (mtETC), produciendo defectos en la producción de energía celular que se da en forma de adenosina trifosfato (ATP). Las enfermedades mitocondriales afectan a 12,5 de cada 100.000 (1 de cada 8.000) personas. El tratamiento de estos pacientes es difícil ya que, en la mayoría de los casos, no hay intervenciones posibles que proporcionen una perspectiva real de cura, y la mayoría de las opciones terapéuticas se limitan a cuidados paliativos.

Agustín Hidalgo Gutiérrez

Una afección considerada como MD es la deficiencia primaria de Coenzima Q (CoQ), que puede estar asociada a diferentes presentaciones clínicas. En muchos casos, incluso los tratamientos con los mejores resultados fallan en la mejora de la bioenergética mitocondrial y/ o características fenotípicas en los modelos de ratón, como el aumento de peso o fuerza, y, en consecuencia, no hay mejoría en la calidad de vida o supervivencia. Por lo tanto, es de vital importancia encontrar opciones terapéuticas con mayor efectividad.

El tratamiento convencional se basa en la administración exógena de altas dosis de CoQ_{10}. Este tratamiento, sin embargo, tiene efectos limitados en un alto porcentaje de pacientes debido a diferentes factores: 1) la baja absorción y biodisponibilidad de la CoQ_{10} exógena, junto con su baja capacidad para cruzar la barrera hematoencefálica (BBB); 2) la falta de efecto sobre la acumulación de metabolitos intermedios en la síntesis de CoQ (es importante destacar que algunos de estos metabolitos, p. ej., la demetoxiubiquinona, pueden contribuir al fenotipo de enfermedad al inhibir la transferencia de electrones en la mtETC); y 3) la falta de efecto sobre el Complejo Q y la biosíntesis endógena de CoQ. Debido a esto, la terapia utilizando CoQ_{10} exógena no induce ningún cambio en los niveles de CoQ_9.

En el modelo de ratón *Coq9*^{R239X}, el cual desarrolla una encefalopatía mitocondrial fatal debido a la deficiencia en CoQ, hemos probado el potencial terapéutico del ácido β-resorcílico (β RA), un análogo estructural del ácido 4-

hidroxibenzoico (4-HB), precursor de CoQ y del ácido salicílico, usado como antiinflamatorio. El β-RA mejoró notablemente los caracteres fenotípicos, morfológicos e histopatológicos de la encefalopatía, consiguiendo un aumento significativo en la supervivencia. Estos efectos se debieron a la disminución de los niveles de DMQ_9 y a una mejoría de la bioenergética mitocondrial en los tejidos periféricos. Sin embargo, ni la biosíntesis de la CoQ, ni la función mitocondrial, cambiaron en el cerebro después de la terapia, lo que sugiere que algunas interacciones endocrinas entre los tejidos periféricos y el cerebro pueden estar induciendo la reducción de la astrogliosis y la espongiosis, así como una regulación secundaria *downstream* de los genes promotores de la inflamación relacionados con astrocitos. Debido a que los resultados terapéuticos del tratamiento con β-RA fueron superiores a los de la suplementación con CoQ_{10}, su uso en la clínica debería considerarse en las deficiencias de CoQ. Igualmente, antes de aplicar el tratamiento de β-RA en la clínica, deben desarrollarse estudios de seguridad y dosis-respuesta incluidos en un ensayo clínico.

En este sentido, el β-RA, como otros derivados de los ácidos hidroxibenzoicos, son compuestos fenólicos naturales que se utilizan con fines médicos. Algunos de estos compuestos (p. ej., ácido salicílico), sin embargo, han reportado toxicidad en condiciones particulares, pero los mecanismos de esta toxicidad siguen siendo desconocidos. En la segunda parte de este estudio, se llevó a cabo una evaluación del efecto de una dosis alta de β-RA, aproximadamente 1 g/kg de peso corporal/día en ratones, la misma dosis utilizada previamente para el tratamiento preclínico de la deficiencia de CoQ, en animales *wild-type*. Además, se probó el potencial terapéutico de una dosis más baja de β-RA, tres veces menor que la dosis alta, tanto en animales *wild-type,* como en nuestro modelo de ratón *Coq9*$^{\mathrm{R239X}}$ de encefalopatía mitocondrial causada por deficiencia de CoQ. Los resultados demuestran que, la dosis alta de β-RA, previamente utilizada para el tratamiento preclínico de la deficiencia de CoQ, induce toxicidad hepática, renal y cerebral en animales *wild-type* con una alteración en los perfiles transcriptómicos y proteómicos mitocondriales. Esos efectos tóxicos dependen del uso del β-RA en la vía biosintética de la CoQ. En el caso de la dosis baja de β-RA, se disminuye drásticamente la toxicidad en animales *wild-type*, preservando la capacidad terapéutica en los ratones *Coq9*$^{\mathrm{R239X}}$. En conjunto, nuestros resultados muestran nuevos efectos tóxicos producidos por los HBA, además de proporcionar una perspectiva traslacional segura para el uso del β-RA en el tratamiento de las deficiencias de CoQ.

Por ultimo, la CoQ está involucrada en muchos otros procesos metabólicos, recibiendo electrones de otras enzimas de vías metabólicas diferentes. Así, actúa como cofactor de la dihidroorotato deshidrogenasa (DHOH), que está implicada en la síntesis *de novo* de pirimidinas; en la transferencia de electrones mediada por flavoproteína (ETF), que recibe electrones de la β-oxidación de ácidos grasos; en la glicerol 3-fosfato deshidrogenasa mitocondrial (G3PDH), que conecta la glucólisis, la OXPHOS y el metabolismo de los ácidos grasos; en la colina deshidrogenasa (CHDH), que participa en el metabolismo de la glicina; en la prolina deshidrogenasa (PDH), que está relacionada con el metabolismo de la prolina y la arginina; y en la sulfuro:quinona oxidoreductasa (SQOR), enzima catalítica de la vía metabólica de oxidación del sulfuro de hidrógeno (H_2S). Sobre esta última enzima, nuestro grupo, junto con el grupo de la Dra. Catarina Quinzii en Nueva York, han publicado recientemente dos estudios independientes que muestran que la deficiencia en CoQ disminuye severamente los niveles de SQOR. Esta disminución de SQOR conduce a un defecto en la oxidación del H_2S, lo que conduce a la acumulación de este y un agotamiento del sistema de glutation. Así, una modulación de la disponibilidad de aminoácidos sulfurados en la dieta, como fuente de H_2S podría proporcionar beneficios terapéuticos. Para probar esto, tratamos los ratones *Coq9*^{R239X} con N-acetilcisteina (NAC), un aminoácido sulfurado que además puede estimular la biosíntesis de glutatión, o con una dieta con restricción de aminoácidos sulfurados (SAAR). Sin embargo, tras los tratamientos, no encontramos ningún cambio en el sistema de glutation ni en las enzimas del metabolismo del sulfuro de hidrógeno. En consecuencia, la supervivencia o el fenotipo de nuestros ratones mutantes no mejoraron. En general, estos datos prueban la ineficacia de la modulación de la disponibilidad de aminoácidos sulfurados en el rescate de la patología en los ratones *Coq9*$^{\mathrm{R239X}}$, y confirman que el metabolismo del sulfuro influye en los niveles de glutatión, pero de forma independiente a la disponibilidad de aminoácidos sulfurados.

SUMMARY

Summary

Mitochondrion is one of the most fascinating organelles of the cell. It is formed by a lipid bilayer and it is present in hundreds to thousands of copies per cell. It acts as the powerplant of the cell and, therefore, it is necessary for the generation of the energy needed for the activity of the cell. Furthermore, it is a critical organelle for many metabolic processes. Because of it, a defect in mitochondria, mainly produced by mutations of genes encoding mitochondrial proteins, could triggers some of the so-called mitochondrial diseases (MD).

MD are a group of rare neurometabolic disorders that are extremely complex and refer to a heterogeneous group of genetic disorders resulting from abnormal oxidative phosphorylation, including the mitochondrial electron transfer chain (mtETC) and leading to defective cellular energy production in the form of adenosine triphosphate (ATP). MD affect 12.5 per 100,000 (1/8,000) persons, and the management of these patients remains difficult since, in most cases, there are no interventions that provide a realistic prospect of cure, and the therapeutic options for these disorders are mostly limited to palliative care and remain woefully inadequate. The treatment of MD is, in most cases, still limited to a palliative care.

An affection considered as MD is primary CoQ deficiency, which can be associated to different clinical presentations. In many cases, even the

treatments with the best results still fail in improving the mitochondrial bioenergetics and/or phenotypic features on mouse models, as weight or strength gaining, and consequently, the quality of life or survival are not improved. So, it is of vital importance to find therapeutic options that approach to a real cure for these patients.

The conventional treatment is based in the exogenous administration of high doses of CoQ_{10}. This treatment, however, has limited effects in a high percentage of patients due to different factors: 1) the low absorption and bioavailability of the exogenous CoQ_{10}, together with its low capacity to cross the Blood Brain Barrier (BBB); 2) the lack of effect over the accumulation of intermediate metabolites in the synthesis of CoQ (importantly, some of these metabolites, e.g. Demethoxyubiquinone, may contribute to the disease phenotype by inhibiting the transfer of electrons in the mtETC); and 3) the lack of effect over the Complex Q and the endogenous biosynthesis of CoQ. For that reason, CoQ_{10} therapy does not induce any change in the levels of CoQ_9.

In the *Coq9*^{R239X} mouse model with fatal mitochondrial encephalopathy due to CoQ deficiency, we have tested the therapeutic potential of β-resorcylic acid (β-RA), a structural analog of the CoQ precursor 4-hydroxybenzoic acid (4-HB) and the anti-inflammatory salicylic acid. β-RA noticeably rescued the phenotypic, morphological, and histopathological signs of the encephalopathy, leading to a significant increase in the survival. Those effects were due to the decrease of the levels of DMQ_9 and the increase of mitochondrial bioenergetics in peripheral tissues. However, neither CoQ biosynthesis nor mitochondrial function changed in the brain after the therapy, suggesting that some endocrine interactions may induce the reduction of the astrogliosis, spongiosis, and the secondary down-regulation of astrocytes-related neuroinflammatory genes. Because the therapeutic outcomes of β-RA administration were superior to those after CoQ_{10} supplementation, its use in the clinic should be considered in CoQ deficiencies. Somehow, to apply the β-RA treatment into the clinic, the safety and dose–response studies included in a clinical trial should be first developed.

β-RA, as other hydroxybenzoic acids derivatives, are natural phenolic compounds that are being used for medical purposes. Some of these compounds (e.g. salicylic acid), however, have reported toxicity in particular conditions but the mechanisms of this effect remain obscure. In this study, we used biased and unbiased approaches to evaluate the effect of a high dose of β-RA, approximately 1g/kg body weight/day in mice, previously used for the preclinical treatment of CoQ deficiency, in wild-type animals, and to test the therapeutic potential of a lower dose of β-RA, three time less than the high dose, in both wild-type and our mouse model *Coq9*^{R239X} of mitochondrial encephalopathy caused by CoQ deficiency. We show that the high dose of β-RA, previously used for the preclinical treatment of CoQ deficiency, induces hepatic, renal and cerebral toxicity in wild-type animals, with a disruption in transcriptomic profiles and mitochondrial proteomes. Those toxic effects are dependent of the metabolic use of β-RA in the CoQ biosynthetic pathway. Thus, the low dose of β-RA, dramatically decreases the toxicity in wild-type animals, preserving the therapeutic capability in *Coq9*$^{\mathrm{R239X}}$ mice by modulating CoQ metabolism. Collectively, our results highlight novel toxic mechanisms of HBAs and provide a safe translational perspective for the use the β-RA in the treatment of CoQ deficiencies.

Besides, CoQ is involved in many other metabolic processes, receiving electrons from enzymes of other metabolic pathways. CoQ is cofactor of the dihydroorotate dehydrogenase (DHOH), which is involved in the synthesis de novo of pyrimidines; the electron transfer flavoprotein (ETF), which receives electrons from the fatty acids β-oxidation; the mitochondrial glycerol 3-phosphate dehydrogenase (G3PDH), which connects glycolysis, OXPHOS and fatty acids metabolism; the choline dehydrogenase (CHDH), which is involved in the glycine metabolism; the proline dehydrogenase (PDH), which is related with proline and arginine metabolism; and the sulfide:quinone oxidoreductase (SQOR), catalytic enzyme of the sulfide oxidation metabolic pathway. So, it is possible that a defect in CoQ could affect any of these pathways and influence in the pathology. In fact, our group, together with the group of Dr. Catarina Quinzii in New York, have recently published two independent studies that show that CoQ deficiency severely decreases the levels of SQOR. Thus, the decrease in SQOR leads to an impairment of H_2S oxidation, leading to accumulation of H_2S and depletion on the glutathione system. Consequently, the modulation of sulfur amino acids availability in the diet, as sources of H_2S could provide therapeutic benefits. Thus, we treated *Coq9*^{R239X} mice with N-acetylcysteine (NAC), which is a sulfur amino acid and it can stimulate glutathione biosynthesis, or a diet with sulfur amino acids restriction (SAAR). However, we did not find any changes in the glutathione system or sulfide metabolism enzymes after the treatments. Consequently, the survival or phenotype of the mutant mice were not improved. Globally, these data probe the inefficiency of the modulation of sulfur amino acids availability in rescuing the pathology in *Coq9*^{R239X} mice and confirm that sulfide metabolism influences the levels of glutathione, independently of the sulfur amino acids availability.

INTRODUCTION

1. INTRODUCTION

1.1 THE MITOCHONDRION

1.1.1 GENERAL DESCRIPTION

Mitochondrion is one of the most fascinating organelles of the cell. It is formed by a lipid bilayer and it is present in hundreds to thousands of copies per cell. It acts as the powerplant of the cell and, therefore, it is essential for the generation of the energy needed for the activity of the cell. Furthermore, it is a critical organelle for many metabolic processes (Gorman *et al*, 2016; Nunnari & Suomalainen, 2012; Spinelli & Haigis, 2018).

1.1.2 ORIGINS

Mitochondria have existed for more than a billion years, but it was not until the middle of the nineteenth century that they were officially recognized in cells, at first, as a grainy appearance in the cell cytoplasm when observed by light microscopy. The anatomist Kölliker (1856) observed mitochondria in muscle cells in the 1850s, while Altman (1890) suggested that his “bioblasts” (granules microscopically observable throughout the cell) were symbionts, a fact that Schimper (1883) had suggested for chloroplasts 7 years earlier. This idea was taken further and developed by Mereschkowsky (1905). The name mitochondrion was first coined by Benda (1898), and it comes from two Greek words, mitos (thread) and chondros (granule), which describes the appearance of mitochondria during spermatogenesis. In the following years, many people speculated on the role of mitochondria in the cell, with Warburg, (1913) recognizing the particulate nature of cell respiration, and Keilin, (1925) associating the cytochrome system with cellular structures. The first direct evidence for this functional association depended on the isolation of the mitochondria from the rest of the cell, which became possible in the 1930s. The first isolations of mitochondria by cell fractionation were made by Bensley and Hoerr (1934), and, following this breakthrough, the path opened for studies of the biochemical reactions occurring in mitochondria (Martin, 2007).

Even, the evolutionary origin of mitochondria is interesting and still nowadays remains unconcluded. From the classical point of view, two possible models have been described. First, the autogenous model, which hold that the nucleus and cytoplasm formed through evolutionary changes in a single prokaryotic lineage and a latter event originated mitochondria by splitting off a portion of DNA from this nucleus and evolved by membranes vesicles from cytoplasm (Baum, 2015; Martin, 2007). With the arrival of modern biochemical technics, the analysis of mitochondrial DNA and structures, and its similarities with bacteria, the second model was proposed as the endosymbiosis theory of Lynn Margulis. According to this theory, a bacterial specie merged with another host microbe, presumably an archaeon, by phagocytosis and stablished a symbiosis relationship between and giving rise to eukaryotes (Margulis, 1970). Anyway, nowadays it remains unclear the organisms involved or the direction of the relationship of this protoorganism, parasitism, commensalism, mutualism, symbiosis but there is a general agreement that the mitochondria have descend from a free-living bacterium (Martin, 2007; Zachar & Boza, 2020) (Introduction figure 1).

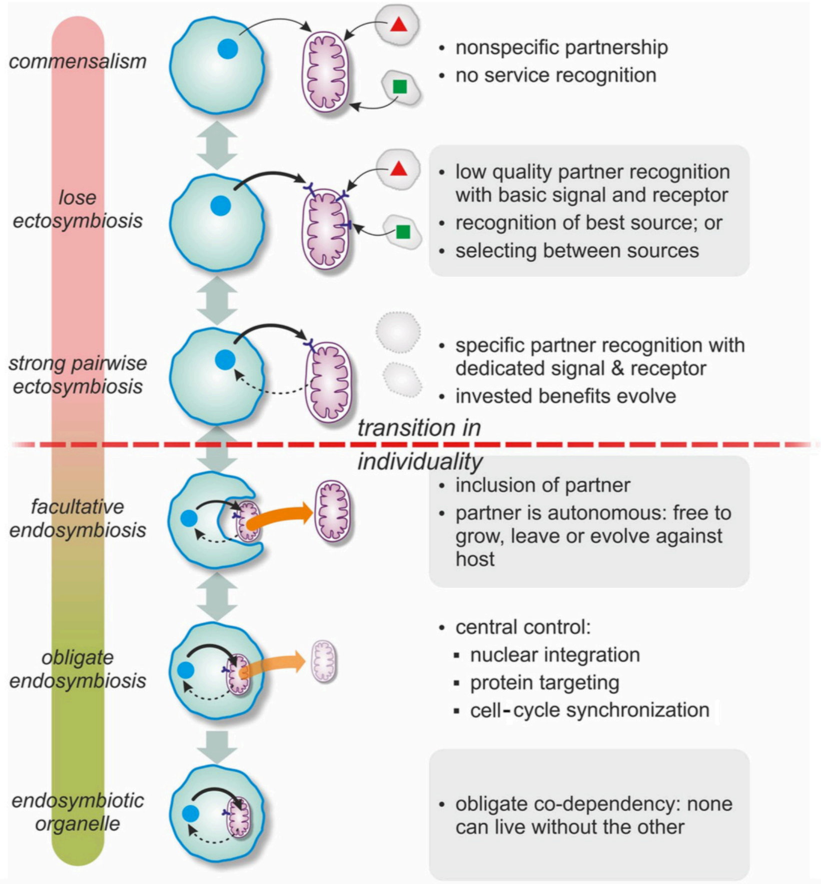
commensalism
nonspecific partnership
no service recognition
lose ectosymbiosis
low quality partner recognition with basic signal and receptor
recognition of best source; or
selecting between sources
strong pairwise ectosymbiosis
specific partner recognition with dedicated signal & receptor
invested benefits evolve
transition in individuality
facultative endosymbiosis
inclusion of partner
partner is autonomous: free to grow, leave or evolve against host
obligate endosymbiosis
central control:
nuclear integration
protein targeting
cell-cycle synchronization
endosymbiotic organelle
obligate co-dependency: none can live without the other

Introduction Figure 1. **Basic steps of endosymbiosis and organellogenesis.** (Zachar & Boza, 2020)

1.1.3 STRUCTURE

Mitochondrion has been described as a membranous organelle that contains about 1,500 proteins in vertebrates. It is organized in four main compartments: the outer membrane, the intermembranes space, the inner membrane and the matrix (Zhao *et al*, 2013).

The outer membrane is similar to the eukaryotic bilayer membrane, with a composition of 50/50 protein/phospholipids. The outer membrane features make it a semi-permeable barrier to the cytosol (<5000-10000 MW) (Cogliati *et al*, 2016). This outer membrane contains different kind of channels that allow the interchange of molecules between the cytosol and the mitochondrion, as voltage dependent channels (VDACs) and porins, to control the movement of small molecules. For bigger molecules, e.g. proteins, the mitochondria precursors use the translocation outer membrane (TOM) complex (Brown *et al*, 2020). The outer membrane can stablish connection with other cell parts, as other mitochondria, the endoplasmic reticulum, the nucleus or ribosomes (Zhao *et al.*, 2013) (Introduction figure 2).

The intermembranes space is a compartment with low amount of proteins. The proteins of intermembranes space are involved in different kind of processes as apoptosis, inner membrane remodeling (e.g. OPA1) or protein importation (Zhao *et al.*, 2013) (Introduction figure 2).

Contrary to the outer membrane, the inner membrane is less permeable to ions and molecules, letting pass just a few of molecules, as the oxygen. The remaining molecules can only pass through the membrane with the help of specific membrane transporters, each of which is specific to a particular ion or molecule. This allows mitochondria to maintain an electrochemical membrane potential through the inner mitochondrial membrane (IMM) (van der Laan *et al*, 2016). The IMM has a higher protein content 80/20 protein/phospholipids (similar to the bacterial membranes) compared to the outer membrane, within its you can find oxidative phosphorylation system (OXPHOS), uncoupling proteins, translocase of the inner membrane system (TIM) proteins, etc. This membrane separates the intermembranes space and the mitochondrial matrix; and form invaginations around the matrix, the so called mitochondria cristae, where the oxidative phosphorylation occurs (Kuhlbrandt, 2015) (Introduction figure 2).

The last compartment, the mitochondrial matrix, represent almost the 70% in protein amount of the organelle. The matrix contains proteins involved in different enzymatic reactions pathways as krebs cycle, fatty acid oxidation and heme synthesis proteins (Kuznetsov & Margreiter, 2009). Also located in the matrix are the mitochondrial DNA (mtDNA) and the ribosomal machinery for the transduction of mitochondrial genes (Introduction figure 2).

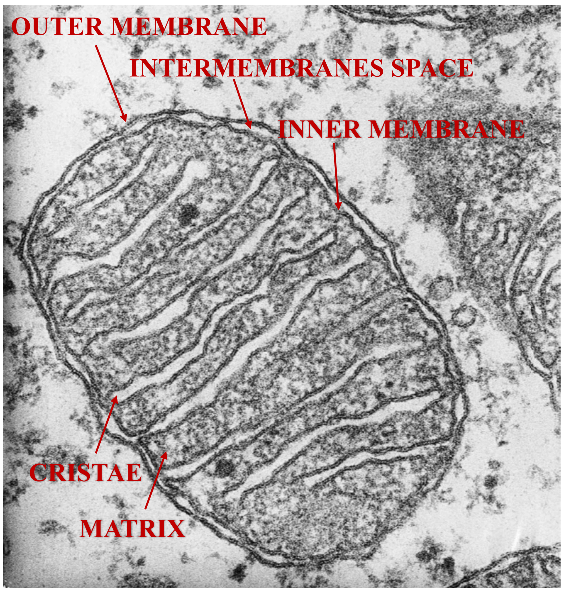

Introduction Figure 2. **Compartment of the mitochondrion.** Image modified from (Scheffler, 2007).

1.1.4 MITOCHONDRIAL GENOME

mtDNA is a small, double stranded, circular, bacterial like, DNA that, in mammals, ranges from 16-18 kbs (16.5 in human) and consists of a guanine rich strand (heavy strand) and a cytosine rich strand (light strand). The amount of mtDNA varies from 2 to 15 copies in each cell, resulting in thousands of copies per cell (Satoh & Kuroiwa, 1991). mtDNA encodes 2 ribosomal RNA and 22 transference RNA, needed for the own transcription of this mtDNA; and 13 subunits of OXPHOS complexes, 7 for complex I, 1 for complex III, 3 for complex IV and 2 for complex V. Complex II subunits are entirely encoded by nucleus DNA (Wallace, 2016) (Introduction figure 3).

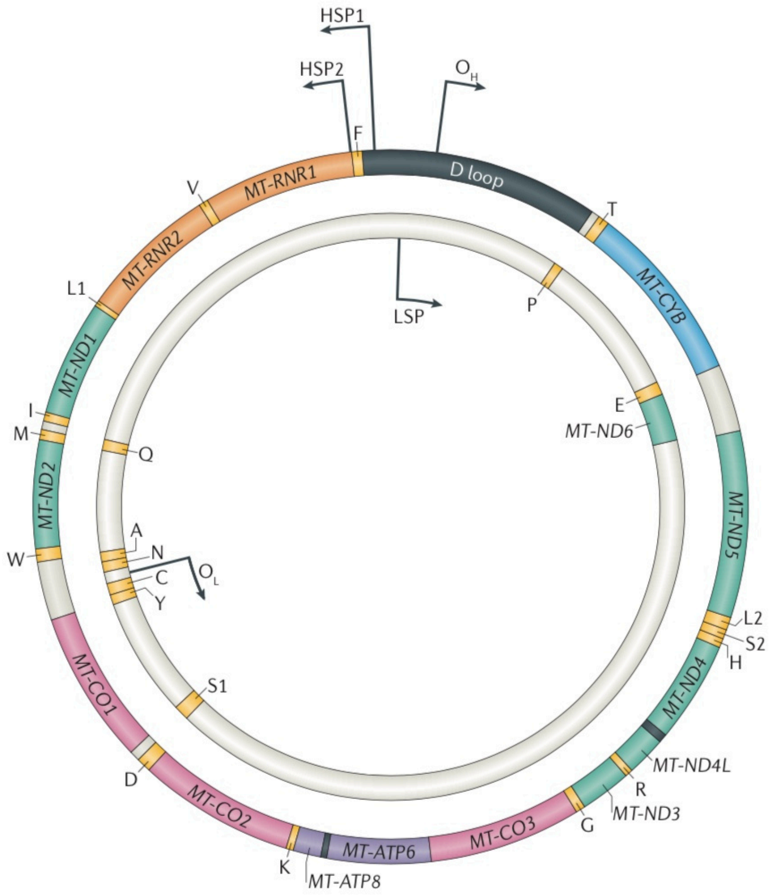
HSP1
HSP2
O_H
F
D loop
T
MT-RNR1
V
MT-RNR2
L1
MT-ND1
I
M
MT-ND2
W
LSP
P
E
MT-ND6
Q
A
N
C
Y
O_L
S1
MT-CYB
MT-ND5
L2
S2
H
MT-ND4
MT-ND4L
R
MT-ND3
G
MT-CO3
MT-ATP6
MT-ATP8
K
MT-CO2
D
MT-CO1

Introduction Figure 3. **Human mitochondrial genome** (Gorman *et al.*, 2016).

1.1.5 FUNCTION

As mentioned before, the main function of the mitochondria is to provide the cell with the necessary energy for its activity, in form of ATP. Besides the ATP synthesis, mitochondria are essential organelles for the metabolism and cell biology since they are involved in diverse process as Krebs cycle, amino acids metabolism, lipid metabolism, sulfide metabolism, urea cycle, gluconeogenesis, and ketogenesis; in addition, they are needed for other cellular processes as thermogenesis, homeostasis, cell cycle progression, redox status, immune response or apoptosis (Gorman *et al.*, 2016; Nunnari & Suomalainen, 2012; Spinelli & Haigis, 2018). Nevertheless, many processes that occur in mitochondria are not totally understood, and further research is required to understand the complexity and importance of this organelle.

In fact, mitochondria are considered the main metabolic center of the cell thanks to the control over multiple cellular processes. They are dynamic organelles that changes depending on the stress, the ambient and even according to the tissue type. Depending on the tissue, the mitochondrion can use different types of substrates or synthesize a variety of compounds. For example, mitochondria are involved in the urea cycle, and sulfide cycle in the liver, gluconeogenesis in the liver and kidney, beta-oxidation of lipids in skeletal muscle or ketone bodies in the brain (Liesa & Shirihai, 2013) (Introduction figure 4).

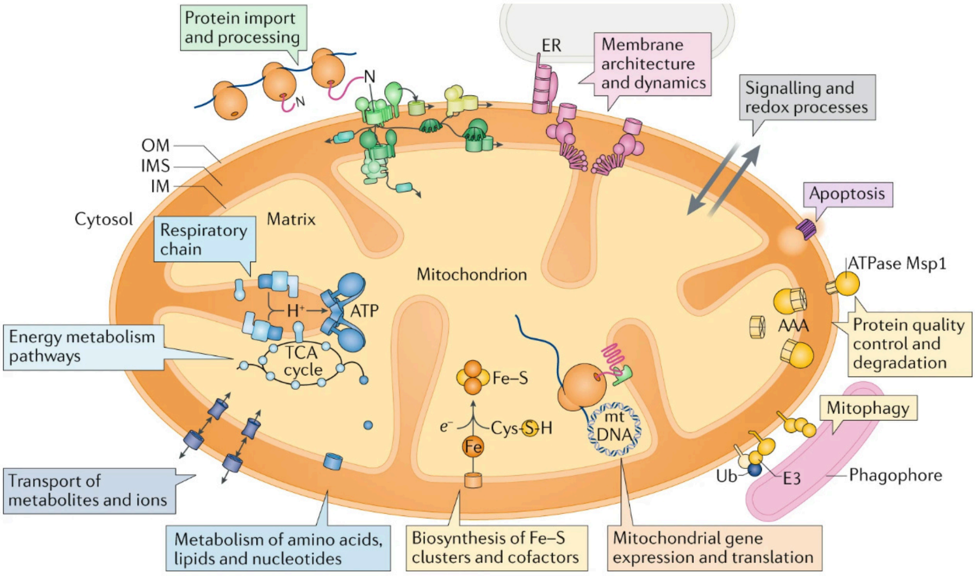
Protein import and processing
N
N
ER
Membrane architecture and dynamics
Signalling and redox processes
OM
IMS
IM
Cytosol
Matrix
Respiratory chain
Apoptosis
Mitochondrion
ATPase Msp1
H⁺
ATP
Energy metabolism pathways
TCA cycle
AAA
Protein quality control and degradation
Fe–S
e⁻
Cys-S-H
Fe
mt DNA
Mitophagy
Ub
E3
Phagophore
Transport of metabolites and ions
Metabolism of amino acids, lipids and nucleotides
Biosynthesis of Fe–S clusters and cofactors
Mitochondrial gene expression and translation

Introduction Figure 4. **Mitochondrial Function** (Pfanner *et al*, 2019).

1.1.5.1 The OXPHOS system

The OXPHOS system is a group of proteins and molecules that are located in the IMM. Their main final function is to create the necessary energy for the correct operation of the cell. Each main functional protein is formed by different subunits, so they are called complexes. Additionally, there are two electron mobile carriers, Coenzyme Q (CoQ) and cytochrome c. The five protein complexes with their particular functions are:

- Complex I or NADH ubiquinone oxidoreductase, which transfers electrons from NADH to CoQ (or Ubiquinone), pumping also protons (H^+) to the inner membrane space.

- Complex II or Succinate dehydrogenase, which transfers electrons from Succinate (via flavin adenine dinucleotide (FAD)) to CoQ.
- Complex III or $CoQH_2$-cytochrome c reductase, which obtains the electrons from the CoQ and transfer them to cytochrome c, pumping also H^+ to the inner membrane space.
- Complex IV or cytochrome c oxidase, which takes the electrons from cytochrome c and transfer them to oxygen, producing 2 molecules of water, pumping also H^+ to the inner membrane space.
- Complex V or ATP synthase complex, which uses the H^+ gradient generated in the inner membrane to generate ATP from ADP, introducing the H^+ into the mitochondrial matrix again.

Basically, the oxidative phosphorylation is an indispensable cellular process divided in three processes. First, it transfers electron from reducing equivalent (as NADH or $FADH_2$, obtained from diverse metabolic processes as Glycolysis, Citric acid cycle or b-oxidation of fatty acid…) to oxygen; second, coupled to the electron transfer, CI, CIII and CIV pump protons to the inner membrane space, causing a proton motive force across the IMM; and third, this proton motive force produced is used to convert ADP to ATP using the ATP synthase (Enriquez, 2016) (Introduction figure 5).

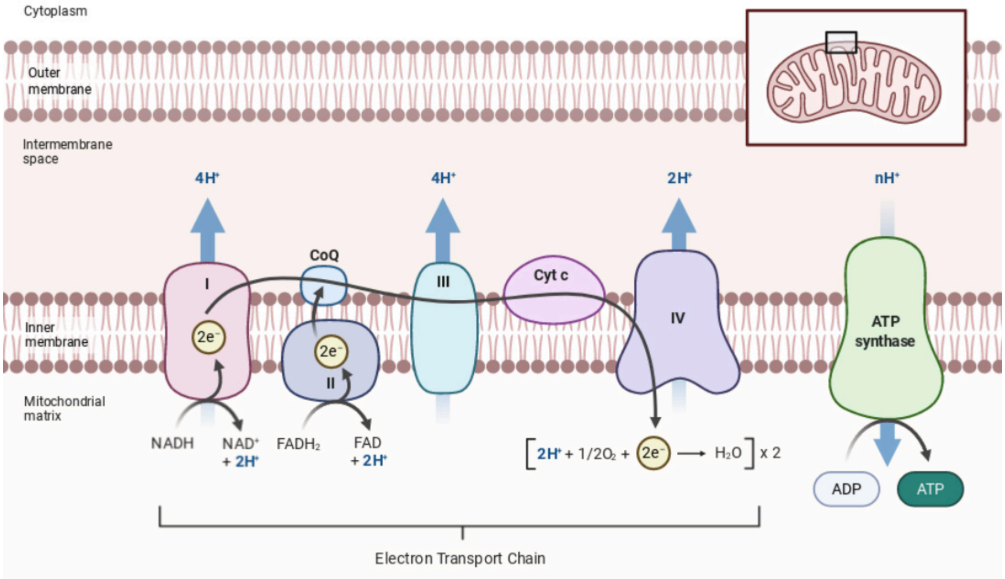
Cytoplasm
Outer membrane
Intermembrane space
4H⁺
4H⁺
2H⁺
nH⁺
CoQ
I
III
Cyt c
IV
ATP synthase
Inner membrane
2e⁻
2e⁻
II
Mitochondrial matrix
NADH
NAD⁺ + 2H⁺
FADH₂
FAD + 2H⁺
[2H⁺ + 1/2O₂ + 2e⁻ → H₂O] x 2
ADP
ATP
Electron Transport Chain

Introduction Figure 5. **OXPHOS system.** Image extracted from Biorender.

1.1.5.2 Supercomplexes

The physical and functional organization of the OXPHOS system has long been discussed during years. Three main models have been proposed:

The solid model: This model proposes that the mitochondrial respiratory chain components were tied forming a rigid supramolecular structure that allowed the transference of the electrons from one component to other giving a maximum efficiency to this structure. In 1963 this model won wide acceptance since Chance and collaborators proposed the concept of Oxysome: ‘’a functional unit for electron transfer and oxidative phosphorylation” (Chance *et al*, 1963; Keilin & Hartree, 1947) (Introduction figure 6).

The fluid model: The first non-official fluid model was proposed by Green and Tzagoloff in 1966. It postulates that in the mitochondrial respiratory chain there are rigids components as the complexes and mobile components as the CoQ or cytochrome c that were in charge of the electron transfer from the rigid components. Later, Hackenbrock presented a number of experiments that showed a high degree of molecules motive freedom of the IMM and proposed the first official fluid model also called ‘’random collision model’’, where he said: ‘’The IMM is a fluid-state rather than a solid-state membrane and... all membrane proteins and redox components which catalyze electron transport and ATP synthesis are in constant and independent diffusional motion...’’(Green & Tzagoloff, 1966; Hackenbrock *et al*, 1986) (Introduction figure 6).

The plasticity model: The pioneers of this model were Schägger and Pfeiffer who published in 2000 the first analysis of yeast and bovine mitochondrial preparations by blue native gel electrophoresis (BNGE), describing the formation of supercomplexes, a supramolecular organization that joined the mitochondrial individual complexes in one single structure (Introduction figure 6). The plasticity model postulates that the individual complexes can be found individually or in association in different combinations depending on the energetics needs of the cell (Schagger & Pfeiffer, 2000). The grade of association between individual or tied complexes varies according to the cell type or the metabolic status. Since individual complexes and supercomplexes have been demonstrated to be functional (Enriquez, 2016), it has been proposed different advantages for the supercomplexes, i.e.: better stability; lower ROS production, since the supercomplexes can enclose reactive intermediaries inside them; or a better mobilization of the electron transfer from the transporters, CoQ or cytochrome c, to their targets (Acin-Perez *et al*, 2008).

In addition, it has been demonstrated that the formation of supercomplexes is a dynamic mechanism that allow the cells to adapt to different source of carbon or different physiological or environmental conditions, e.g. hypoxia or thermogenesis. For example, in a starving situation, with more active β-oxidation of fatty acids, the formation of SCs involving CI is reduced, letting the CIII free and accessible for the incoming electrons from the $FADH_2$ (transferred by the CII) (Lapuente-Brun *et al*, 2013).

The fail in this system can cause a pathological situation that can derivate in a mitochondrial disease. Besides, it has been probed that there is a tight connection between the different components of the mitochondrial respiratory chain, so, a defect in one component could affect other component, destabilizing all the system (Enriquez, 2016). Anyway, much effort in research is still needed to achieve a better understanding of this complex system and the relation between its components.

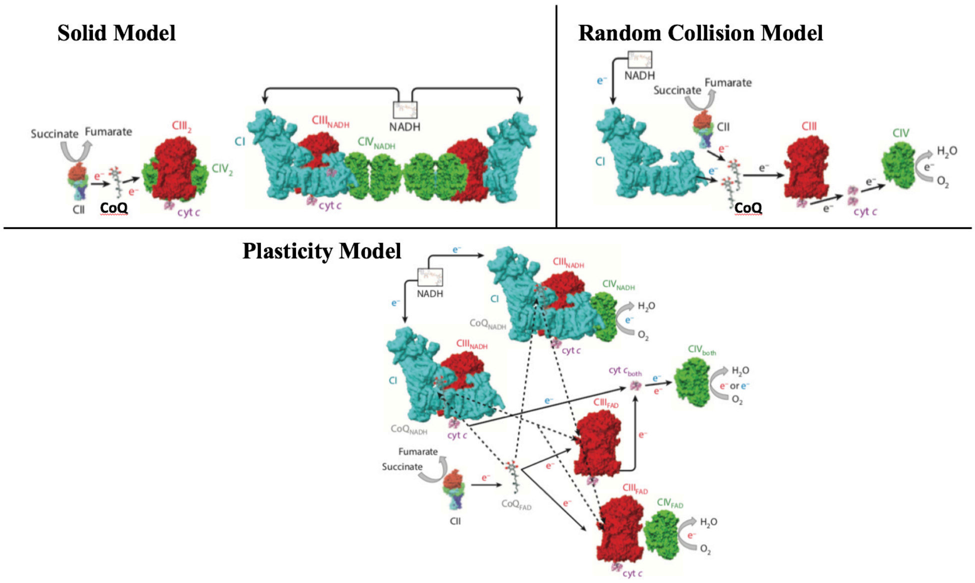
Solid Model
Random Collision Model
Plasticity Model
Succinate
Fumarate
CII
CoQ
CIII$_2$
CIV$_2$
cyt c
CI
CIII$_{NADH}$
NADH
CIV$_{NADH}$
CIII
CIV
H$_2$O
O$_2$
e$^-$
CoQ$_{NADH}$
cyt c$_{both}$
CIV$_{both}$
e$^-$ or e$^-$
CIII$_{FAD}$
CIV$_{FAD}$
CoQ$_{FAD}$

Introduction Figure 6. **Supercomplexes Models.** Image modified from (Enriquez, 2016).

1.1.5.3 Coenzyme Q

CoQ forms the "Q-junction", which has a central role in the OXPHOS system and other metabolic pathways. It receives electrons from different components, including complex I and II; and it donates electrons to complex III.

1.1.5.3.1 History

CoQ was first isolated in 1955 from an unsaponifiable fraction of horse and pig's gut (Festenstein *et al*, 1955). Two years later, Crane was able to isolate mitochondria from beef heart, describing the presence and function of CoQ in the respiratory chain (Crane *et al*, 1957). In 1958, Wolf determined its structure, as an unusual lipid formed by a benzoquinone ring joint to an isoprenoid chain to be inserted into biological membranes (Turunen *et al*, 2004; Wolf *et al*, 1958). In 1961, Mitchell included the CoQ in his chemiosmotic theory for its role in cellular respiration and received the chemistry Nobel prize in 1978 thanks to its theory.

In 1969, the importance of this lipid was corroborated with the studies of Ernster and collaborators in submitochondrial particles. They observed the deactivation and reactivation of NADH and succinate dehydrogenase activity when quinones were depleted and reincorporated into submitochondrial particles (Ernster *et al*, 1969).

The synthesis and distribution of CoQ were initially attributed to the IMM, where it could act in the transport of electrons from complex I and II to III (Lenaz *et al*, 2007).

Later studies described other functions associated with its redox capabilities in extramitochondrial membranes (Santos-Ocana *et al*, 1998). Nowadays, the role and applications of CoQ has been studied in different fields of research, including aging, sport physiology, immune system, cardiovascular diseases, metabolic syndrome and MD, among others (Alcazar-

Fabra *et al*, 2018; Diaz-Casado *et al*, 2019; Hernandez-Camacho *et al*, 2018; Martinez-Rodriguez *et al*, 2020).

1.1.5.3.2 Structural, physical and chemical proprieties of Coenzyme Q

CoQ, chemically 2,3-dimethoxy-5-methyl-6-(polyprenyl)-1,4-benzoquinone, is a lipophilic molecule formed by a benzoquinone ring hydroxylated in 1,4 position, which provides its redox caracteristics; and attached to a lateral isoprenoid chain that confers hydrophobicity and the solubility in polar solvents. It is more soluble as less isoprene units form the isoprenoid chain (Crane & Dilley, 1963) (Introduction figure 7).

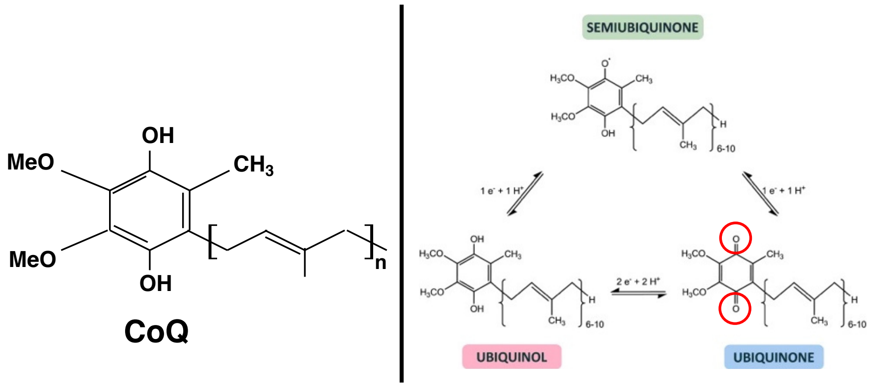

Introduction Figure 7. **CoQ structure and redox status.** Figure modified from (Alcazar-Fabra *et al*, 2016).

In nature exists different types of CoQ according to:

- Number of isoprenes of lateral chain: The length can vary between species. The reason of this variability is still unknow but we can find 6 units of isoprene (CoQ_6) in the yeast *Sacharomyces cerevisae*, 8 units (CoQ_8) in the bacillus *Escherichia coli*, 9 units (CoQ_9) in C*aenoradbditis elegans* and 10 units (CoQ_{10}) in the yeast *Schizosaccharomyces pombe*. However, some species can possess different kinds of CoQ together as CoQ_9 and CoQ_{10} in mice, human or zebrafish; or CoQ_7, CoQ_8, CoQ_9 and CoQ_{10} in *Pneumocystis* (Kawamukai, 2009; Sul & Kaneshiro, 2001).

- The redox state: In the fully oxidized state is called ubiquinone (CoQ) which has two keto groups in position *para*. The addition of a proton and an electron originates the ubisemiquinone form ($CoQH^-$). The addition of the second proton and electron originates the totally reduced form, the ubiquinol ($CoQH_2$) which has two hydroxyl groups (Crane & Dilley, 1963). (Introduction figure 7).

1.1.5.3.3 Biosynthesis and distribution of CoQ

The biosynthetic pathway of CoQ has long been studied in eukaryotes and procaryotes (Abby *et al*, 2020; Kawamukai, 2016; Payet *et al*, 2016). It has been partially characterized by the identification of biosynthetic intermediates accumulated in strains of *Saccharomyces cerevisiae* mutants deficient in CoQ (Turunen *et al.*, 2004). At least 14 genes (*COQ1-COQ11, YAH1,ARH1* and *PTC7*) are currently known to encode proteins involved in CoQ biosynthesis in yeasts (Payet *et al.*, 2016; Stefely & Pagliarini, 2017; Tran & Clarke, 2007).

The function of many of these proteins in other eukaryotes cells is analogous to that of yeasts and is therefore known, while others, such as COQ4, COQ8, COQ9, COQ10 o COQ11 have to been deeper studied (Stefely & Pagliarini, 2017)

CoQ biosynthesis begins with the formation of hydroxybenzoic acid to which a polyisoprenoid lipophilic tail is attached. The aromatic precursor of the benzoquinone ring is 4-HB derived from tyrosine or phenylalanine (Kawamukai, 2016; Pierrel, 2017), and it is known to be synthesized in the cytosol, and, therefore, the ring must be imported into the matrix through an unidentified transporter (Stefely & Pagliarini, 2017). On the other hand, the polyisoprenoid chain is formed by the addition of isopentenyl diphosphate molecules from the mevalonate pathway to the farnesil or geranyl-geranyl diphosphate in multiple steps catalyzed by the polyprenyl diphosphate synthase or Coq1 (Grunler et al., 1994) (Figure 3). Once the polyisoprenoid chain is synthesized, it is condensed with 4-HB by a reaction catalyzed by PHB-polyprenyl transferase or Coq2p, causing an intermediate molecule called 3-hexaprenyl-4-hydroxybenzoic acid (in *S. Cerevisiae*). Nine other enzymes, COQ3-8A and B, COQ9 and COQ11, are found in human, in the IMM and modify the CoQ quinone ring through regulation or catalyzation of hydroxylation, methylation and decarboxylation reactions (Awad *et al*, 2018;

Diaz-Casado *et al.*, 2019; Luna-Sanchez *et al*, 2015; Tran & Clarke, 2007) (Introduction figure 8).

The order in which the following aromatic ring modification reactions occur is speculative. Thus, the proposed ring modifications currently begin with hydroxylation, followed by O-methylation and decarboxylation to form the 6-methoxy-2-polyprenile phenolic intermediate. Then two hydroxylation steps, a C-methylation and an O-methylation, are required to fully generate the CoQ (Tran & Clarke, 2007).

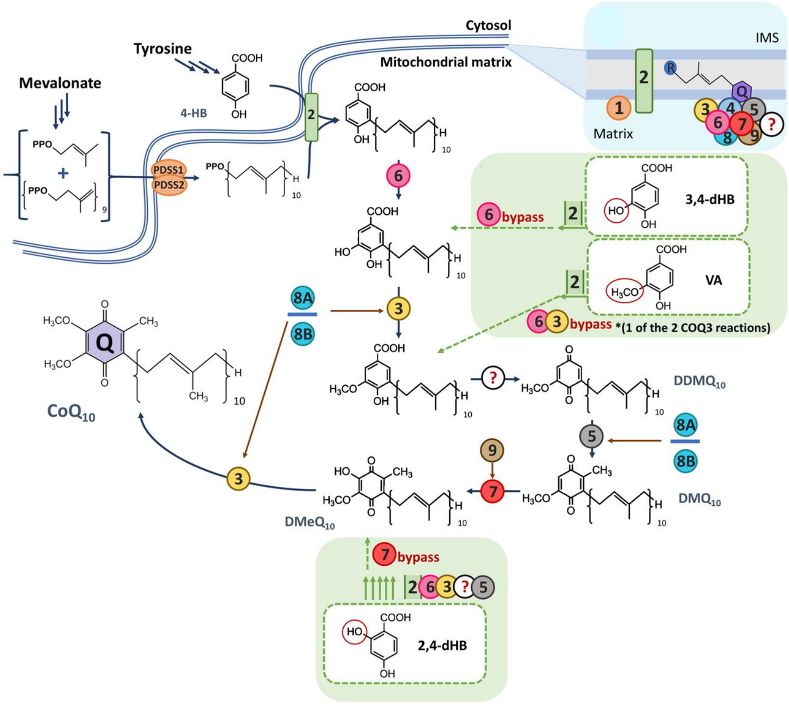
Cytosol
Mitochondrial matrix
IMS
Matrix
Tyrosine
Mevalonate
4-HB
COOH
OH
PPO
PDSS1
PDSS2
2
1
3
4
5
6
7
8
9
Q
R
?
3,4-dHB
VA
HO
H_3CO
6 bypass
6 3 bypass *(1 of the 2 COQ3 reactions)
8A
8B
DDMQ$_{10}$
DMQ$_{10}$
DMeQ$_{10}$
CoQ$_{10}$
CH_3
10
7 bypass
2,4-dHB

Introduction Figure 8. **Coenzyme Q byosinthetic proteins** (Alcazar-Fabra *et al.*, 2018).

1.1.5.3.3.1 Complex Q

The biosynthesis of CoQ commit:

1. The synthesis of benzoquinone ring.
2. The synthesis of the isoprenoid chain.
3. The condensation of both molecules.
4. The later modifications of the benzoquinone ring.

These processes mainly happen in the mitochondria and involves many proteins. Some of these proteins interact each to the other and form a protein complex denominated CoQ synthome or complex Q, which is essential for the CoQ biosynthesis, improving the catalysis or the scape of possible toxic intermediaries as DMQ (Yang *et al*, 2011). The proteins involved in the CoQ biosynthesis are (Introduction figure 9):

COQ1 or trans-polyprenile diphosphate synthase (PDSS1/2 in humans), which catalyzes the formation of the polyisoprenoid chain, being responsible for the specific length in different species (Okada *et al*, 1996). COQ1 is peripherally associated with the IMM on the matrix side (Barros *et al*, 2005).

COQ2 or 4-HB: polyprenyltransferase, which catalyzes the covalent bond between the 4-HB ring and the polyisoprenoid chain, generating the first membrane-binding intermediate, 4-hydroxy-3-polyprenylbenzoic acid (Tran

& Clarke, 2007). This protein behaves as an integral membrane protein, associated with the IMM on the matrix side.

COQ3, which catalyzes O-methylation steps in the biosynthetic pathway. It is a peripheral protein associated with the matrix on the side of the IMM (Poon *et al*, 1999).

COQ4, which is located in the matrix, attached to the IMM (Belogrudov *et al*, 2001), and is essential for the synthesis of CoQ. Although its exact function in the biosynthetic pathway is currently unknown, it has been hypothesized that acts as scaffold protein to attach proteins and lipids (Awad *et al.*, 2018; Stefely & Pagliarini, 2017).

COQ5 or 2-methoxy-6-polyprenyl-1,4-benzoquinone methyltransferase, catalyzes the single step of C-methylation, generating the intermediate 2-methoxy-5-methyl-6-polyprenyl-1,4-benzoquinone. It is located in the matrix, stuck to the IMM (Baba *et al*, 2004).

COQ6, which is exclusively involved in C5-hydroxylation of HHB or 3-hexaprenyl 4-aminobenzoate but not in C1 or C6. It is located peripheral to the IMM on the side of the matrix (Gin et al., 2003).

COQ7, which catalyzes the hydroxylation of DMQ to 5-hydroxyquinone. It has an interfacial location in the IMM (Berthold & Stenmark, 2003; Stenmark *et al*, 2001).

COQ8A or ADCK3 and COQ8B or ADCK4, which are atypical kinases that phosphorylates other biosynthetic proteins (as COQ3, COQ5 and COQ7), stabilizing the multiprotein complex and increasing CoQ synthesis. It has been hypothesized that they both have regulatory functions. Besides, it has been speculated an ATPase function. However, it has to be deeper studied to confirm these proprieties (Stefely & Pagliarini, 2017).

COQ9, which physically interacts with COQ7, since *Coq9* mutant mice have reduced levels of COQ7 and accumulation of DMQ, the substrate for COQ7. Thefore, COQ9 is essential for the stability and activity of COQ7 (Garcia-Corzo *et al*, 2013). Later, crystallography analysis confirmed that COQ9 is associated to COQ7 (Lohman *et al*, 2014). In addition, it is able to bind to lipids, so it is thought that it could provide the DMQ to the protein COQ7 (Garcia-Corzo *et al.*, 2013; Luna-Sanchez *et al.*, 2015). It is peripheral associated with the IMM on the matrix side (Hsieh *et al*, 2007).

COQ10 (COQ10A and COQ10B in humans) seems not to be part of the complex Q and is thought not to be directly involved in CoQ biosynthesis, as null coq10 mutants in yeasts have CoQ levels close to wild-type (Barros *et al.*, 2005). However, it seems to be important for the functionality of the CoQ. It contains a conserved lipid-binding domain, capable of binding CoQ. It has been hypothesized that COQ10 could act as a lipid chaperone involved in transferring CoQ from one side to the other within the mitochondrial membrane (Barros *et al.*, 2005; Kawamukai, 2009).

COQ11, which seems to be part of complex Q but it is not essential for the biosynthesis (Allan *et al*, 2015). It has been observed that COQ11 has homology with NDUFA9, an auxiliary subunit of Complex I in humans important for complex stability, but its relation or function is yet unknown (Awad *et al.*, 2018).

Yah1 and Arh, ferredoxin and ferredoxin oxidase, respectively, which may transfer electrons to COQ6. However, the functions of their mammalian analogues, FDX2 and FDXR, are still unknown (Awad *et al.*, 2018).

PTC7 is a phosphatase that regulates COQ7 (Acosta *et al*, 2016).

Therefore, the complex Q involves many protein and steps that must to be regulated in different ways: transcriptionally, by transcription factors; post-transcriptionally, by modulation of the transcripts of COQ; post-transductionally, by proteases or phospho-dephosphorylations; and by modulation of the own complex Q (Brea-Calvo *et al*, 2009; Hidalgo-Gutierrez *et al*, 2019; Lapointe *et al*, 2018; Martin-Montalvo *et al*, 2013).

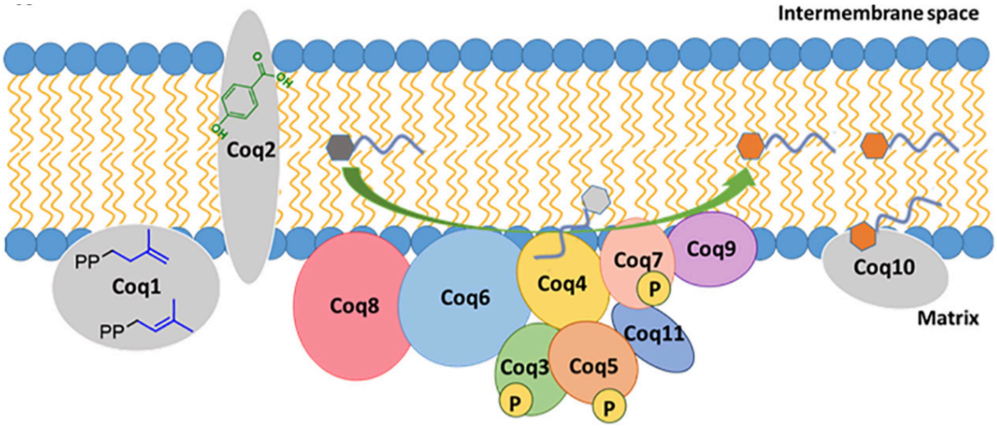

Introduction Figure 9. **Coenzyme Q byosinthetic proteins** (Awad *et al*, 2020).

1.1.5.3.3.2 CoQ localization

At membrane level: Once the lipids of the mevalonate pathway, including ubiquinone, have been synthesized, they will take different intramembranous positions that will be responsible for the membrane properties. The polyisoprenoid side chain of ubiquinone is located in the hydrophobic central region of the lipid bilayer. It is thought that this position destabilizes the membrane, promoting an increase in its fluidity and permeability. On the other hand, the benzoquinone ring is exposed on the inner or outer face of the membranes, depending on its functional requirement (Kawamukai, 2016; Stefely & Pagliarini, 2017).

At cellular level: Ubiquinone is mainly located in the IMM along with the other components of the electron transport chain, where it performs its electron transport function. In addition, it is present in all cell membranes, such as the plasma membrane and endomembranes (Kalen *et al*, 1987; Stefely & Pagliarini, 2017; Takahashi *et al*, 1993), indicating its involvement in multiple cellular functions.

The presence of CoQ in extramitochondrial membranes suggests the existence of membrane-linked mechanisms of synthesis and/or distribution. This fact is supported by the finding of enzymatic activity in endoplasmic reticulum, Golgi apparatus and peroxisomes (Kovacs *et al*, 2002; Tekle *et al*, 2002). However, the existence of mitochondrial recognition sequences in genes involved in biosynthesis and, its products located in mitochondria but not in other organelles, indicates that the biosynthesis of CoQ is completed in the mitochondria and is transported to other membranes (Baba *et al.*, 2004; Belogrudov *et al.*, 2001; Jiang *et al*, 2001).

A study in human cells (HL-60) corroborated this idea, in experiments using radiolabeled CoQ precursor to observe the intracellular distribution of the newly synthesized CoQ_{10} and CoQ_9. The study concluded that the first location of endogenous CoQ is the mitochondria. The study also suggested that a Brefeldin A-sensitive pathway is then used to distribute CoQ to other extramitochondrial membranes. On the other hand, the exogenous CoQ is incorporated into the endolysosomal fraction and is subsequently transported to the mitochondria following the route previously mentioned (Fernandez-Ayala *et al*, 2005).

1.1.5.3.4 CoQ functions:

As indicated, CoQ is a ubiquitous molecule that is present in every cell membrane, where it has different functions.

1.1.5.3.4.1 The role of CoQ in the mitochondrial respiratory chain.

CoQ is an essential component of the mitochondrial respiratory chain. It is located in the IMM where it acts as an electron carrier from complex I and complex II to complex III (Figure 5) (Alcazar-Fabra *et al.*, 2016) (Introduction figure 10).

This transfer of electrons is favored by the formation of the previously mentioned supercomplexes, in which CoQ is an essential component. Their participation allows a flow of electrons from NADH or succinate to molecular oxygen coupled to a flow of protons into the intermembrane space that generates an electrochemical gradient, which is used by ATP synthase for the synthesis of ATP (Acin-Perez *et al.*, 2008; Enriquez, 2016).

Besides of the classical electron flux direction from CI to CoQ and to CIII, it has been probed that in some particular physiological conditions, e.g. a shift from glucose to fatty acids that increases electron flux through FAD, the CoQ can be saturated and generate reactive oxygen species (ROS). To prevent this, CoQ serves as a sensor and the electron transport flux is inverted from CoQ to

CI. This mechanism produces a local increase of ROS that oxidizes CI subunits triggering its degradation and the subsequent degradation of CI to allow the transfer of FAD to CoQ. Therefore, CoQ acts as a metabolic sensor of the metabolism of complexes/supercomplexes (Guaras *et al*, 2016).

1.1.5.3.4.2 CoQ and uncoupling proteins (UCP).

There are some evidences that CoQ may have other functions that are not directly related to the electron transport chain. One of them is to function as a cofactor in the activity of UCP. These are proteins located in the IMM that translocate H^+ from the intermembrane space to the mitochondrial matrix. Therefore, and alluding to their name, they decouple the proton gradient (generated in the respiratory chain) from the oxidative phosphorylation, releasing the energy in the form of heat without production of ATP. This mechanism is used by mammals in brown fat to maintain body temperature in low temperature situations (Nedergaard *et al*, 2001).

Echtay and collaborators. showed that CoQ is a mandatory cofactor for UCPs overexpressing different types of UCPs in liposomes of *E. coli.* Liposomes were unable to transport H^+ in the absence of CoQ and transport was reactivated by adding CoQ to membranes in the presence of fatty acids. In addition, chain length and CoQ oxidation status are important for transport activation, with short-chain CoQs being less effective (Echtay *et al*, 2001;

Echtay *et al*, 2000). However, these initial studies of the role of CoQ in the function of the UCPs gave rise to a further later studies in cell cultures that questioned the physiological role of CoQ in the activity of the UCPs (Esteves *et al*, 2004; Jaburek & Garlid, 2003).

1.1.5.3.4.3 CoQ and the mitochondrial permeability transition pore (mPTP).

The electrochemical gradient, generated during electron transfer in the IMM, is maintained by the low permeability to ions and solutes of the membranes. The passage of molecules through the internal membrane appears to be regulated by a series of channels and ionic transporters that together are called mPTP, which is a voltage-dependent and Ca^{2+} sensitive channel that, among other thing, plays a key role in apoptosis (Green & Reed, 1998). Several studies have shown that the isoprenoid tail length of CoQ analogues modulates the permeability of mPTP (Fontaine *et al*, 1998). In this way, CoQ_{10}, with a long chain of isoprenes, prevents the opening of the channel, avoiding the depolarization of the membrane potential, ATP depletion, activation of caspase-9 with cytochrome c release and DNA fragmentation in keratinocytes under apoptotic stimuli (Bentinger *et al*, 2010; Papucci *et al*, 2003).

1.1.5.3.4.4 CoQ as antioxidant.

Most mitochondrial oxygen consumption is coupled to ATP synthesis, while a small percentage (about 1-2%) forms ROS by reacting with electrons scaping from the respiratory chain. These ROS can function as intracellular markers at physiological concentrations, but under pathophysiological conditions, where the production of ROS is highly elevated, these ROS react with different biomolecules such as DNA, proteins and lipids, oxidizing them and causing cell damage in a process known as oxidative stress (D'Autreaux & Toledano, 2007).

To counteract an increase in oxidative stress, a series of cellular antioxidant systems are activated to prevent or repair the damage caused. These antioxidants are classified into enzymes, such as, superoxide dismutase, glutathione peroxidase, catalase, thiredoxin reductase and peroxiredoxin (Holmgren & Bjornstedt, 1995); or non-enzymes, such as, vitamin C and E, carotenoids, glutation, α-lipoic acid, flavonoids, melatonin and $CoQH_2$(Chahbouni *et al*, 2010; Ibrahim *et al*, 1997).

CoQ is a powerful antioxidant that protects lipids against oxidative damage and maintains other antioxidants in their reduced forms (Alcazar-Fabra *et al.*, 2018). *In vitro* studies on submitochondrial particles have revealed that $CoQH_2$ is capable of inhibiting peroxidation (Bentinger *et al*, 2007; Takayanagi *et al*, 1980). Other studies also show how $CoQH_2$ can prevent oxidation to proteins

(Forsmark-Andree *et al*, 1995). As well as DNA, both in vitro and in vivo (Ernster & Dallner, 1995).

1.1.5.3.4.5 Other functions

CoQ can act as cofactor, receiving electrons from enzymes of other metabolic pathways. CoQ is cofactor of the dihydroorotate dehydrogenase (DHOH), which is involved in the synthesis *de novo* of pyrimidines; the electron transfer flavoprotein (ETF), which receives electrons from the fatty acids β-oxidation; the mitochondrial glycerol 3-phosphate dehydrogenase (G3PDH), which connects glycolysis, OXPHOS and fatty acids metabolism; the choline dehydrogenase (CHDH), which is involved in the glycine metabolism; the proline dehydrogenase (PDH), which is related with proline and arginine metabolism; and the SQOR, the main catalytic enzyme of the sulfide oxidation metabolic pathway (Alcazar-Fabra *et al.*, 2018; Enriquez, 2016; Enriquez & Lenaz, 2014) (Introduction figure 10).

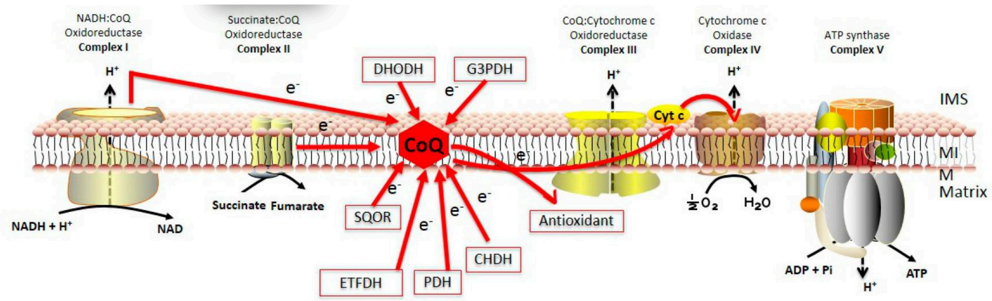
NADH:CoQ
Oxidoreductase
Complex I
Succinate:CoQ
Oxidoreductase
Complex II
CoQ:Cytochrome c
Oxidoreductase
Complex III
Cytochrome c
Oxidase
Complex IV
ATP synthase
Complex V
H+
e-
DHODH
G3PDH
CoQ
Cyt c
IMS
MI
M
Matrix
SQOR
ETFDH
PDH
CHDH
Antioxidant
NADH + H+
NAD
Succinate Fumarate
½O2
H2O
ADP + Pi
ATP

Introduction Figure 10. Integration of the Coenzyme Q in the electron transport chain (Diaz-Casado *et al.*, 2019).

1.1.5.3.4.6 Sulfide metabolism

Hydrogen sulfide (H_2S) is a molecule in gas state that is essential for cell metabolism since it can modulate many processes as cell proliferation, angiogenesis, neural development, redox status and apoptosis (Quinzii *et al*, 2017). In mammals, the H_2S equilibrium is maintained by 2 processes:

- The generation of H_2S (or transulfuration pathway), where H_2S is obtained by the desulfuration of cysteine or homocysteine produced by the cystathionine β-synthase (CBS) and cystathionine γ-lyase (CSE) in the cytosol. H_2S can also be produced by the mitochondrial or cytosolic enzyme 3-mercaptopyruvate sulfurtransferase (3-MST) in a reaction that uses 3-mercaptopyruvate as substrate (Kabil *et al*, 2014).
- The catabolism of H_2S (or oxidation pathway), which occurs entirely in the mitochondria, where H_2S is oxidized in three or four steps to thiosulfate or sulfite. The pathway is initiated by the SQOR, which catalyzes the formation of thiosulphate (SSO_3^{-2}) from hydrogen sulfide (H_2S) and sulfite (SO_3-^{2}), using CoQ as an electron acceptor (Figure 6). The thiosulphate (SSO_3^{-2}) formed reacts with glutathione (GS-) to form glutathione persulfide (GSS^-) in a reaction catalyzed by thiosulphate sulfotransferase (TST). Glutathione

persulfide (GSS^-) is oxidized by dioxygenase persulfide (SDO) producing sulfite (SO_3^{-2}) and glutathione (GS^-). This sulfite (SO_3^{-2}) may be used again by the SQOR or produce sulfate (SO_4^{-2}) with the simultaneous oxidation of cytochrome c in a reaction catalyzed by sulfite oxidase (SO). Alternatively, it has also been described that SQOR can directly catalyze the formation of glutathione persulfide (GSS^-) using hydrogen sulfide (H_2S) and glutathione (GS^-) as substrate and CoQ as electron acceptor (Kabil *et al.*, 2014) (Introduction figure 11).

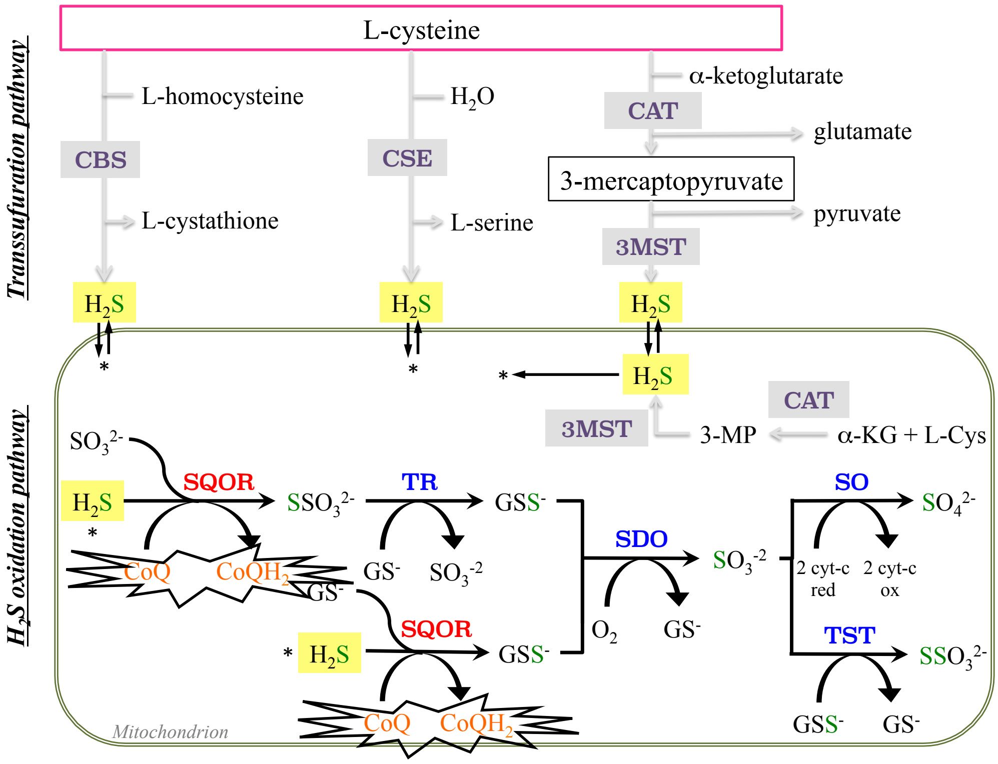
Transsufuration pathway
L-cysteine
L-homocysteine
CBS
L-cystathione
H2O
CSE
L-serine
α-ketoglutarate
CAT
glutamate
3-mercaptopyruvate
pyruvate
3MST
H2S
H2S
H2S
*
*
*
H2S
CAT
3MST
3-MP
α-KG + L-Cys
H2S oxidation pathway
SO3 2-
SQOR
H2S
*
SSO3 2-
TR
GSS-
CoQ
CoQH2
GS-
SO3 -2
GS-
SQOR
* H2S
GSS-
CoQ
CoQH2
SDO
SO3 -2
O2
GS-
SO
SO4 2-
2 cyt-c red
2 cyt-c ox
TST
SSO3 2-
GSS-
GS-
Mitochondrion

Introduction Figure 11. Influence of the Coenzyme Q in the sulfide metabolism pathway. Figure modified from (Quinzii *et al.*, 2017).

Oxidation and transulfuration pathways are interconnected to provide a regulation of levels of H_2S. Motteawa and colleagues showed this close connection between both pathways in patients with Crohn diseases who had increased numbers of microbial producers of H_2S and a reduction of the H_2S catabolic pathways in the gut. In fact, the same group demonstrated the importance of the H_2S oxidation in Crohn disease. They reduced the colitis coursed in the mice affected by Crohn disease by the administration of H_2S scavengers (Mottawea *et al*, 2016).

Sulfide metabolism is close related to CoQ, since it acts as cofactor of its first oxidation enzyme, SQOR. It has been proposed that, through SQOR, H_2S could act as electron donor to CoQ in the mitochondrial respiratory chain, in a similar way that NADH or $FADH_2$ use mitochondrial CI and CII, respectively (Modis *et al*, 2013). This system would work at lower H_2S concentration (1-10uM). However, in high concentrations (>10uM), H_2S could act as respiratory chain inhibitor through the inhibition of the heme a of the cytochrome C or the short-chain acyl CoA dehydrogenase (Di Meo *et al*, 2011; Lagoutte *et al*, 2010; Pedersen *et al*, 2003).

1.2 RARE DISEASES

Rare diseases are numerous, heterogeneous in nature and geographically disparate, defined, in the European Union (EU), as those diseases affecting fewer than 1 per 2,000 persons. Most of them are associated to a lack of available and effective treatment and a lack of research to discover such treatments. There are thousands of these diseases and, if we count them together, affect to a 6%-8% of the population, being the total number of affected persons between 27 and 36 millions in EU, which makes them a real problem for the health system. Some of the rare diseases include autosomal dominant, autosomal recesive, chromosomal anomaly, x-linked recesive, x-linked dominant, multigenic/multifactorial, both autosomal dominant and recesive, both autosomal and x-linked, other multiple inheritance, unknown factors and the called MD (Introduction figure 12). The lack of proper treatments to cure these diseases leads to a really considerable high cost in palliative cares (Angelis *et al*, 2015; Nguengang Wakap *et al*, 2020).

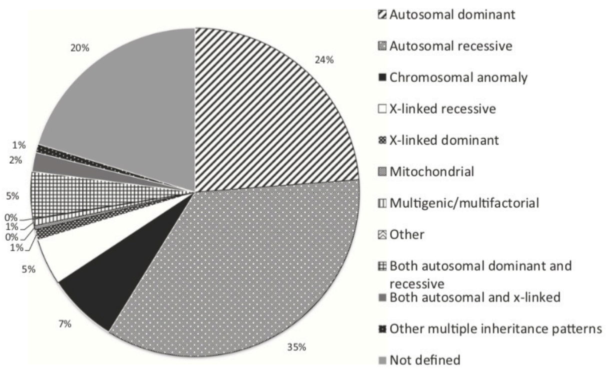

Introduction Figure 12. **Influence of the Coenzyme Q in the sulfide metabolism pathway** (Nguengang Wakap *et al.*, 2020).

1.2.1 MITOCHONDRIAL DISEASES

MD are a group of rare neurometabolic disorders that are extremely complex and refer to a heterogeneous group of genetic disorders resulting from abnormal oxidative phosphorylation, including the mtETC and leading to defective cellular energy production in the form of ATP (Gorman, 2019). Totally, it has been estimated the presence of about 1500 genes coding mitochondrial proteins. Actually, it has been experimentally identified 1158 proteins located into mitochondria (MitoCarta2.0, (Calvo *et al*, 2016)). MD can be caused by mutations in nuclear or mtDNA. In some special cases, it has been described *de novo* mutations both in nuclear or mtDNA, although they are not very frequent (King *et al*, 2018) (Introduction figure 13). In the case of mtDNA, the situation is even more complex since every cell has many copies of DNA and one copy can be mutated but other not, and, therefore, different levels of mutated copies can be found in a single cell. This concept is called ‘’heteroplasmy’’ and its value is important for the development of the clinical symptoms. MD can appear at any stage of life, and, normally, has multisystemic effect, so there are many clinical syndromes included as MD, divided in: *a)* childhood-onset MD, like Leigh Syndrome, Ataxia neuropathy spectrum (ANS), Alpers-Huttenlocher syndrome (AHS), Sengers syndrome, Congenital lactic acidosis (CLA) among others; and *b)* adult-onset MD, like Leber hereditary optic neuropathy (LHON), Kears-Sayre syndrome (KSS), Myoclonic epilepsy with ragged red fibres (MERF) and Mitochondrial neurogastrointestinal encephalopathy (MNGIE), among others (Gorman *et al.*, 2016) . Other affection considered as MD is primary CoQ deficiency, which can be associated to different phenotypes (Emmanuele *et al*, 2012). MD affect 12.5 per 100,000 (1/8,000) persons, and the management of these patients remains difficult since, in most cases, there are no interventions that provide a realistic prospect of cure, and the therapeutic options for these disorders are mostly limited to palliative care and remain woefully inadequate (Gorman, 2019; Wang *et al*, 2016). In many cases, even the treatments with the best results still fail in improving the mitochondrial bioenergetics and/or phenotypic features on mouse models, as weight or strength gaining, and consequently, the quality of life or survival are not improved (DiMauro *et al*, 2013; Wang *et al.*, 2016). So, it is of vital importance to find therapeutic options that approach to a real cure for these patients.

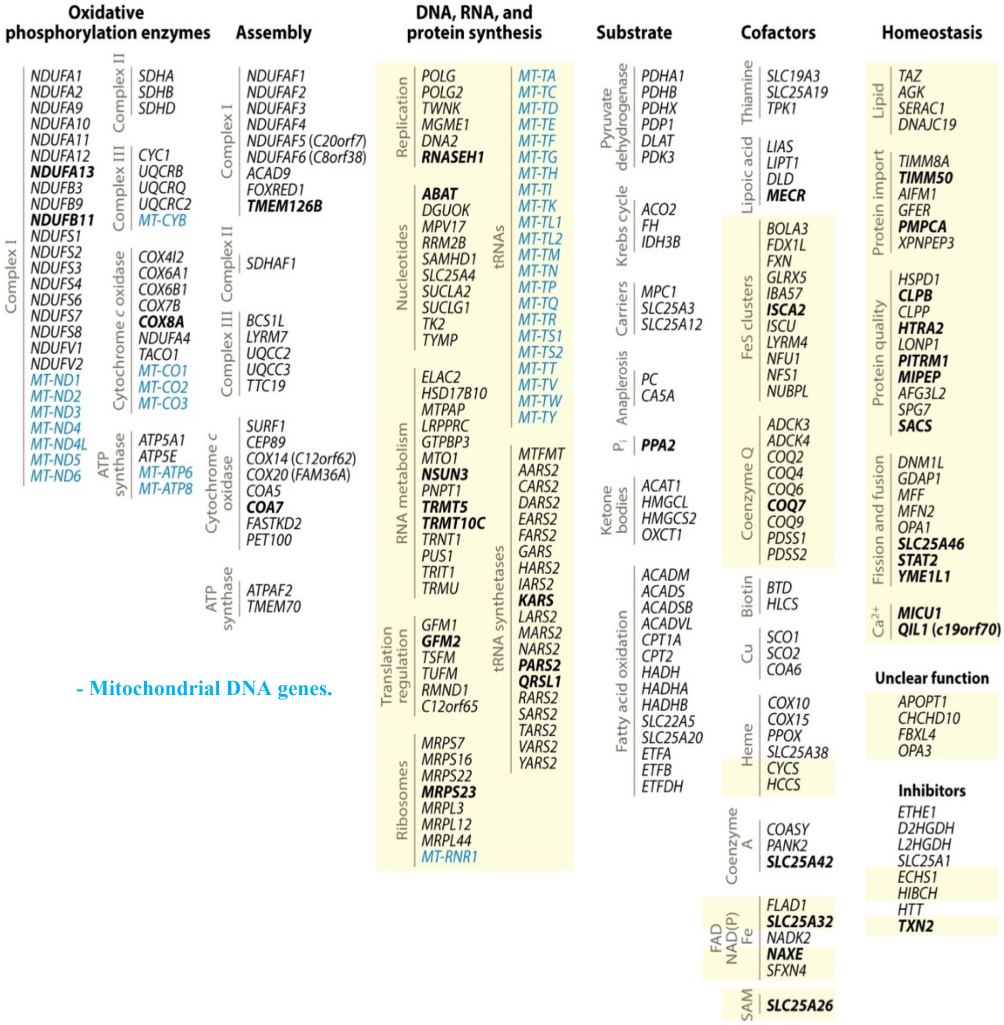
Oxidative phosphorylation enzymes
Complex I
NDUFA1
NDUFA2
NDUFA9
NDUFA10
NDUFA11
NDUFA12
NDUFA13
NDUFB3
NDUFB9
NDUFB11
NDUFS1
NDUFS2
NDUFS3
NDUFS4
NDUFS6
NDUFS7
NDUFS8
NDUFV1
NDUFV2
MT-ND1
MT-ND2
MT-ND3
MT-ND4
MT-ND4L
MT-ND5
MT-ND6
Complex II
SDHA
SDHB
SDHD
Complex III
CYC1
UQCRB
UQCRQ
UQCRC2
MT-CYB
Cytochrome c oxidase
COX4I2
COX6A1
COX6B1
COX7B
COX8A
NDUFA4
TACO1
MT-CO1
MT-CO2
MT-CO3
ATP synthase
ATP5A1
ATP5E
MT-ATP6
MT-ATP8
Assembly
Complex I
NDUFAF1
NDUFAF2
NDUFAF3
NDUFAF4
NDUFAF5 (C20orf7)
NDUFAF6 (C8orf38)
ACAD9
FOXRED1
TMEM126B
Complex II
SDHAF1
Complex III
BCS1L
LYRM7
UQCC2
UQCC3
TTC19
Cytochrome c oxidase
SURF1
CEP89
COX14 (C12orf62)
COX20 (FAM36A)
COA5
COA7
FASTKD2
PET100
ATP synthase
ATPAF2
TMEM70
- Mitochondrial DNA genes.
DNA, RNA, and protein synthesis
Replication
POLG
POLG2
TWNK
MGME1
DNA2
RNASEH1
Nucleotides
ABAT
DGUOK
MPV17
RRM2B
SAMHD1
SLC25A4
SUCLA2
SUCLG1
TK2
TYMP
RNA metabolism
ELAC2
HSD17B10
MTPAP
LRPPRC
GTPBP3
MTO1
NSUN3
PNPT1
TRMT5
TRMT10C
TRNT1
PUS1
TRIT1
TRMU
Translation regulation
GFM1
GFM2
TSFM
TUFM
RMND1
C12orf65
Ribosomes
MRPS7
MRPS16
MRPS22
MRPS23
MRPL3
MRPL12
MRPL44
MT-RNR1
tRNAs
MT-TA
MT-TC
MT-TD
MT-TE
MT-TF
MT-TG
MT-TH
MT-TI
MT-TK
MT-TL1
MT-TL2
MT-TM
MT-TN
MT-TP
MT-TQ
MT-TR
MT-TS1
MT-TS2
MT-TT
MT-TV
MT-TW
MT-TY
tRNA synthetases
MTFMT
AARS2
CARS2
DARS2
EARS2
FARS2
GARS
HARS2
IARS2
KARS
LARS2
MARS2
NARS2
PARS2
QRSL1
RARS2
SARS2
TARS2
VARS2
YARS2
Substrate
Pyruvate dehydrogenase
PDHA1
PDHB
PDHX
PDP1
DLAT
PDK3
Krebs cycle
ACO2
FH
IDH3B
Carriers
MPC1
SLC25A3
SLC25A12
Anaplerosis
PC
CA5A
Pᵢ
PPA2
Ketone bodies
ACAT1
HMGCL
HMGCS2
OXCT1
Fatty acid oxidation
ACADM
ACADS
ACADSB
ACADVL
CPT1A
CPT2
HADH
HADHA
HADHB
SLC22A5
SLC25A20
ETFA
ETFB
ETFDH
Cofactors
Thiamine
SLC19A3
SLC25A19
TPK1
Lipoic acid
LIAS
LIPT1
DLD
MECR
FeS clusters
BOLA3
FDX1L
FXN
GLRX5
IBA57
ISCA2
ISCU
LYRM4
NFU1
NFS1
NUBPL
Coenzyme Q
ADCK3
ADCK4
COQ2
COQ4
COQ6
COQ7
COQ9
PDSS1
PDSS2
Biotin
BTD
HLCS
Cu
SCO1
SCO2
COA6
Heme
COX10
COX15
PPOX
SLC25A38
CYCS
HCCS
Coenzyme A
COASY
PANK2
SLC25A42
FAD
NAD(P)
Fe
FLAD1
SLC25A32
NADK2
NAXE
SFXN4
SAM
SLC25A26
Homeostasis
Lipid
TAZ
AGK
SERAC1
DNAJC19
Protein import
TIMM8A
TIMM50
AIFM1
GFER
PMPCA
XPNPEP3
Protein quality
HSPD1
CLPB
CLPP
HTRA2
LONP1
PITRM1
MIPEP
AFG3L2
SPG7
SACS
Fission and fusion
DNM1L
GDAP1
MFF
MFN2
OPA1
SLC25A46
STAT2
YME1L1
Ca²⁺
MICU1
QIL1 (c19orf70)
Unclear function
APOPT1
CHCHD10
FBXL4
OPA3
Inhibitors
ETHE1
D2HGDH
L2HGDH
SLC25A1
ECHS1
HIBCH
HTT
TXN2

Introduction Figure 13. **Mitochondrial diseases and the genes involved.** Modified from (Craven *et al*, 2017).

1.2.1.1 CoQ deficiency

Considering the multiple and critical functions of CoQ, it is reasonable to think that a deficit in this molecule should cause a MD. Ogasahara and colleagues. described the first cases of CoQ deficiency in two siblings who, after a normal early development, showed exercise intolerance and muscle weakness in the legs. At five years of age, both had myoglobinuria and brain involvement, and, individually, one suffered convulsion and, the other, cerebellar syndrome. After the muscle biopsy study, these patients were found to have a severe CoQ deficiency with a marked OXPHOS defect. In addition, the presence of ragged red fibers and accumulation of lipid drops in type I fibers, both characteristic of mitochondrial myopathies, were detected (Ogasahara *et al*, 1989). Since then, more than 200 CoQ-deficient patients, in more than 130 families, with a wide range of clinical phenotypes, have been identified and published. Somehow, it has been estimated a much higher incidence of these defects using modern techniques of large-scale sequencing data, predicting about 124,000 patients over the world (Hughes *et al*, 2017). Genetically, CoQ deficiency is associated with an autosomal recessive disorder that is clinically manifested by a heterogeneous picture that, classically, has been grouped into five large phenotypes:

1. Encephalopathy characterized by brain involvement and recurrent myoglobinuria.
2. Childhood multisystem disorder with encephalopathy usually associated with nephropathy and involvement of other organs.
3. Cerebellar ataxia with atrophy of the cerebellum.
4. Isolated myopathy.
5. Steroid-resistant nephrotic syndrome.

Nowadays, however, the classification is not completely adequate since some clinical phenotypes are wider and, for example, it has not yet described any isolated myopathy (Alcazar-Fabra *et al.*, 2018).

The manifestation of these phenotypes is predominantly early (82% < 13 years, including 23% in childhood < 12 months). But cases have also been identified in adolescence (7% between 13 and 18 years), as well as in adulthood (11% > 18 years) (Emmanuele et al., 2012). CoQ deficiency may be caused by mutations in genes directly involved in its biosynthesis, in which case it is called primary CoQ deficiency (Alcazar-Fabra *et al.*, 2018).

Within this type, it has been described patients with molecular defects in *PDSS1* (Mollet *et al*, 2007), *PDSS2* (Lopez *et al*, 2006; Sadowski *et al*, 2015), *COQ2* (Justine Perrin *et al*, 2020; Mollet *et al.*, 2007; Procopio *et al*, 2019; Quinzii *et al*, 2006; Sadowski *et al.*, 2015; Wu *et al*, 2019), *COQ4* (Brea-Calvo *et al*, 2015; Caglayan *et al*, 2019; Chung *et al*, 2015; Sondheimer *et al*, 2017), *COQ5* (Malicdan *et al*, 2018), *COQ6* (Heeringa *et al*, 2011; Justine Perrin *et al.*, 2020; Sadowski *et al.*, 2015), *COQ7* (Wang *et al*, 2017), *COQ8A* (Gerards *et al*, 2010; Horvath *et al*, 2012; Lagier-Tourenne *et al*, 2008; Mollet *et al*, 2008), *COQ8B* (Adan Lanceta *et al*, 2020; Ashraf *et al*, 2013; Maeoka *et al*, 2020; Sondheimer *et al.*, 2017; Song *et al*, 2020) *COQ9* (Danhauser *et al*, 2015; Duncan *et al*, 2009; Smith *et al*, 2018) and *FDX2* (Gurgel-Giannetti *et al*, 2018). These mutations affect to different systems but, because of the low number of patients and the different clinical manifestation, it is difficult to explain why mutations in the same genes causes different phenotypes. Besides, there are patients with CoQ deficiency and mutations in genes that are not related to ubiquinone biosynthesis. These cases have been described as secondary CoQ deficiency, and it can involve any of the CoQ functions or its connection to other metabolic pathways, being more common than those involving a primary CoQ deficiency. Low levels of CoQ have been described in, nuclear or mtDNA, OXPHOS diseases and in a high number of diseases involving different mutations that are not related with the mtETC. For instance, secondary CoQ deficiency has been described in ataxia and oculomotor apraxia due to mutation in *APTX* (Quinzii *et al*, 2005), in isolated myopathy due to mutations in *ETFDH* (Gempel *et al*, 2007), in cardiofaciocutaneous syndrome due to mutations in *BRAF* (Aeby *et al*, 2007), in MD due to mutations in other genes of OXPHOS system (Kuhl *et al*, 2017), or in Leigh syndrome associated to a defect in *PARL* (Spinazzi *et al*, 2019). The pathology in these diseases are caused mainly by its original pathology involving muscular or central nervous system. So, the mechanism by which the CoQ levels are reduced remains unknown. It has been hypothesized that multiple factors may participate in decreasing the levels of CoQ, such as an error on the formation of the complex Q linked to mtETC, an increase of oxidative stress, interferences with CoQ biosynthesis pathways or a degeneration of the mitochondria (He *et al*, 2014; Miranda *et al*, 1999). Besides, CoQ deficiency can be present in other common diseases as cirrhosis, fibromyalgia, cardiomyopathies or in muscle and adipose tissue of patients with insulin resistance (Diaz-Casado *et al.*, 2019; Fazakerley *et al*, 2018; Rahman *et al*, 2012; Yubero *et al*, 2016). Also, Yubero and collaborators, described CoQ deficiency in patients with mtDNA depletion syndrome (Yubero *et al.*, 2016). In addition, it has been recently published CoQ deficiency in plasma from phenylketonuric patients and patients with mucopolysaccharidoses (Montero *et al*, 2019). However, not all patients with these diseases develop CoQ deficiency and it is not known why some patients are more susceptible than others to develop it, although some studies point out to genetic factors, such as certain polymorphisms. Besides, the symptoms associated to secondary CoQ deficiencies vary according to the original pathology of the patient, although muscular and neurological manifestations (muscle weakness, hypotonia, exercise intolerance, myoglobinuria or ataxia) are frequent. Therefore, from the point of view of molecular diagnosis, genetic analysis is necessary to differentiate between primary and secondary CoQ deficiency (Desbats *et al*, 2015) (Introduction figure 14).

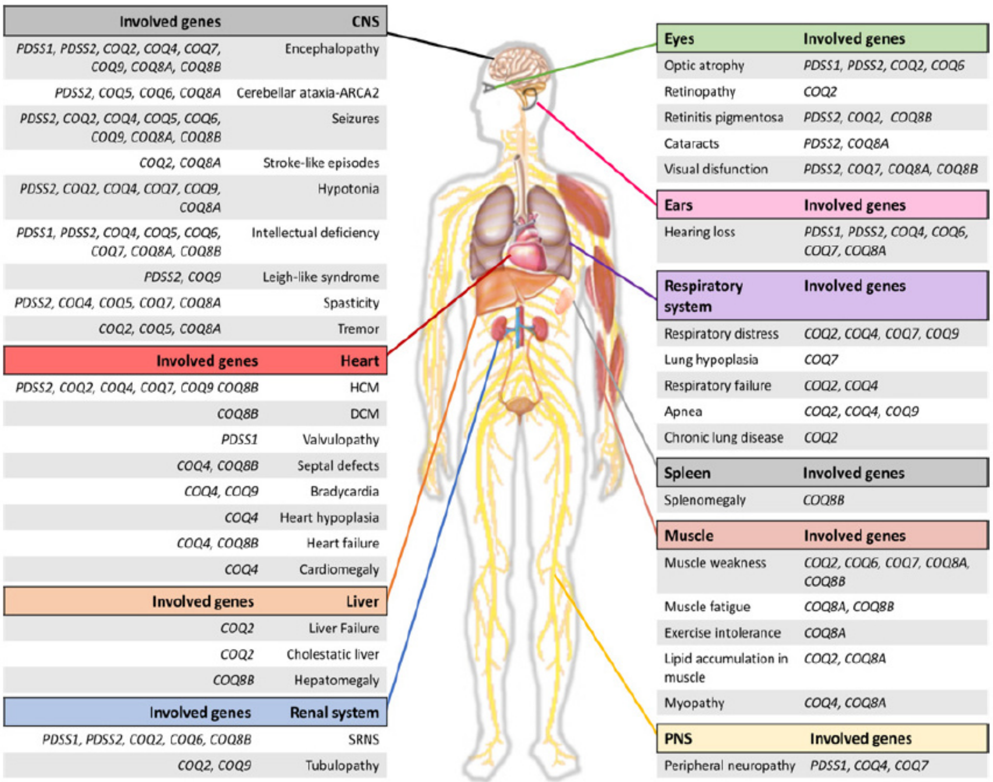

Involved genes	CNS
PDSS1, PDSS2, COQ2, COQ4, COQ7, COQ9, COQ8A, COQ8B	Encephalopathy
PDSS2, COQ5, COQ6, COQ8A	Cerebellar ataxia-ARCA2
PDSS2, COQ2, COQ4, COQ5, COQ6, COQ9, COQ8A, COQ8B	Seizures
COQ2, COQ8A	Stroke-like episodes
PDSS2, COQ2, COQ4, COQ7, COQ9, COQ8A	Hypotonia
PDSS1, PDSS2, COQ4, COQ5, COQ6, COQ7, COQ8A, COQ8B	Intellectual deficiency
PDSS2, COQ9	Leigh-like syndrome
PDSS2, COQ4, COQ5, COQ7, COQ8A	Spasticity
COQ2, COQ5, COQ8A	Tremor

Involved genes	Heart
PDSS2, COQ2, COQ4, COQ7, COQ9 COQ8B	HCM
COQ8B	DCM
PDSS1	Valvulopathy
COQ4, COQ8B	Septal defects
COQ4, COQ9	Bradycardia
COQ4	Heart hypoplasia
COQ4, COQ8B	Heart failure
COQ4	Cardiomegaly

Involved genes	Liver
COQ2	Liver Failure
COQ2	Cholestatic liver
COQ8B	Hepatomegaly

Involved genes	Renal system
PDSS1, PDSS2, COQ2, COQ6, COQ8B	SRNS
COQ2, COQ9	Tubulopathy

Eyes	Involved genes
Optic atrophy	*PDSS1, PDSS2, COQ2, COQ6*
Retinopathy	*COQ2*
Retinitis pigmentosa	*PDSS2, COQ2, COQ8B*
Cataracts	*PDSS2, COQ8A*
Visual disfunction	*PDSS2, COQ7, COQ8A, COQ8B*

Ears	Involved genes
Hearing loss	*PDSS1, PDSS2, COQ4, COQ6, COQ7, COQ8A*

Respiratory system	Involved genes
Respiratory distress	*COQ2, COQ4, COQ7, COQ9*
Lung hypoplasia	*COQ7*
Respiratory failure	*COQ2, COQ4*
Apnea	*COQ2, COQ4, COQ9*
Chronic lung disease	*COQ2*

Spleen	Involved genes
Splenomegaly	*COQ8B*

Muscle	Involved genes
Muscle weakness	*COQ2, COQ6, COQ7, COQ8A, COQ8B*
Muscle fatigue	*COQ8A, COQ8B*
Exercise intolerance	*COQ8A*
Lipid accumulation in muscle	*COQ2, COQ8A*
Myopathy	*COQ4, COQ8A*

PNS	Involved genes
Peripheral neuropathy	*PDSS1, COQ4, COQ7*

Introduction Figure 14. Organs and systems affected in CoQ defficiency patients (Alcazar-Fabra *et al.*, 2018).

1.2.1.1.1 Pathological mechanisms associated to CoQ deficiency: experimental studies

In order to understand the pathophysiological consequences of CoQ_{10} deficiency, some studies have been conducted in skin fibroblasts from patients with CoQ_{10} deficiency in the last decade. Firstly, Geromel and collaborators. showed that fibroblasts of two brothers with deficiency in CoQ_{10} of unknown genetic etiology, showed slight defects in mitochondrial respiration and growth rate, but no evidence of increased production of superoxide anion, lipid peroxidation or apoptosis were found (Geromel *et al*, 2001). Later on, Lopez-Martin et al. showed that fibroblasts of two brothers with mutation in *COQ2* presented an enzymatic deficit of the CoQ-dependent mitochondrial complexes and a reduction in cell growth rate that was normalized after 24h of treatment with CoQ_{10} (10 µM) (Lopez-Martin *et al*, 2007). On the other hand, in Dr. Hirano's laboratory, a study was carried out using fibroblasts with mutations in *COQ2*, *PDSS2* and *COQ9* previously described (Duncan *et al.*, 2009; Lopez *et al.*, 2006; Quinzii *et al.*, 2006). In metabolic conditions dependent on oxidative phosphorylation, the results showed clear differences between mutants, i.e., mutants in *PDSS2* and *COQ9*, with 10-15% CoQ_{10}, showed a marked reduction in ATP synthesis, but no signs of oxidative stress or alterations of antioxidant systems (Duncan *et al.*, 2009; Lopez *et al.*, 2006). In contrast, mutants in *COQ2*, with 30-50% CoQ_{10}, showed a partial reduction in ATP synthesis, a significant increase in the production of ROS, accompanied by lipid and protein oxidation, and cell death (Quinzii *et al*, 2010; Quinzii *et al*, 2008). The relationship between CoQ levels, bionergetics defect and oxidative stress has also been confirmed through the pharmacological inhibition of CoQ biosynthesis with 4-HB analogues (Duberley *et al*, 2013; Quinzii *et al*, 2013). Likewise, Rodríguez-Hernández and colleagues confirmed that fibroblasts in patients with CoQ_{10} deficiency (30%) caused by *COQ2* mutation have an increase in ROS (Rodriguez-Hernandez *et al*, 2009).

In addition, they showed an activation of the mitochondrial transition pore that triggers in apoptosis and that the induction of the autophagy would act as protection against apoptosis (Rodriguez-Hernandez *et al.*, 2009). In order to overcome the limitations of *in vitro* systems, as can be the limited information that they provide about tissue specificities, the first ubiquinone-deficient mouse model was published in 2001 by two independent groups due to the absence of *Coq7*, which encodes the COQ7 protein, an enzyme that, as we have mentioned, catalyzes the hydroxylation of DMQ producing 5-hydroxy-UQ (Levavasseur *et al*, 2001; Nakai *et al*, 2001; Stenmark *et al.*, 2001). Unfortunately, the knock-out mouse (KO) for *Coq7* was embryologically lethal (less than 10.5 days) because of a neurogenesis failure (Nakai *et al.*, 2001). Electron microscopy studies showed elongated mitochondria, with elongated lysosomes, containing traces of mitochondrial membranes. Biochemical studies showed that the absence of *Coq7* caused the accumulation of DMQ. Interestingly, mitochondrial respiration decreased by only 40%, despite of the total absence of ubiquinone and embryonic lethality, suggesting that DMQ may have some functionality in electron transport. However, in yeasts, DMQ does not show the ability to function as an electron carrier, either in the mitochondrial respiratory chain or as an antioxidant agent (Levavasseur *et al.*, 2001; Nakai *et al.*, 2001; Padilla *et al*, 2004). Besides, Dr. Morgan's group described a possible toxic effect of accumulation of DMQ by exchanging the quinones pools between wild type and *Coq7* mutant worms, that accumulates DMQ. The results revealed an inhibition of CI + III after the replenish of wild type quinones with the quinones from *Coq7* mutants (Yang *et al.*, 2011). Therefore, it is conceivable that other functions of ubiquinone could significantly contribute to the pathogenesis of ubiquinone deficiency. In any case, the mitochondrial pathogenesis of these mice was confirmed by Dr. Shirasawa's group, revealing that embryonic cells of these mice showed a significant increase in apoptosis, a reduction in membrane potential and ATP levels. Those abnormalities were partially restored with the supplementation of 25 μM of water-soluble CoQ_{10} for 5 hours (Takahashi *et al*, 2008). The absence of *in vivo* models, which recapitulated human clinical phenotypes, was the reason for our group to generate and characterize a single mouse model deficient in CoQ due to a mutation in the *Coq9* gene, the same one presented by the patient described by Dr. Rahman's group (Duncan *et al.*, 2009; Garcia-Corzo *et al.*, 2013). The *Coq9* (*Coq9*^{R239X}) knock-in mouse has a R239X change, truncating the 75 terminal amino acids of the COQ9 protein and producing certain levels of a truncated protein due to an inefficient Nonsense-mediated mRNA decay (NMD) that is not able to fully degrade the mutated mRNA (Luna-Sanchez *et al.*, 2015). The presence of the truncated protein destabilizes the multiprotein complex of CoQ synthesis, so the brain, cerebellum, heart, muscle, kidneys and liver from *Coq9*^{R239X} mice showed a reduction of 70-85% of CoQ_9 and CoQ_{10} levels with an accumulation of DMQ (the substrate for COQ7), a metabolite intermediate in CoQ biosynthesis. The CoQ deficit causes a specific decrease in the levels of the free III complex in the brain, which triggers a reduction in mitochondrial respiration and ATP synthesis, accompanied by increased oxidative stress and neuronal death mediated by apoptosis independent of the caspase pathway. This neuronal death was accompanied by severe reactive astrogliosis and spongiform degeneration, especially evident in the brain-stem, which caused reduction in the animal body weight, paralysis of the limbs between the 3-6 months of age and premature death due to cardiorespiratory arrest (Garcia-Corzo *et al.*, 2013) (Introduction figure 15). To understand the clinical heterogeneity of CoQ deficiency, our group has characterized another model with a different mutation in the *Coq9* gene, which produces a premature stop codon in amino acid 95 (*Coq9*^{Q95X} model), inducing a complete absence of the COQ9 protein due to a total efficiency of the messenger RNA degradation mechanism mediated by NMD to eliminate aberrant mRNA. This total absence of COQ9 does not induce destabilization of the CoQ synthesis multiprotein complex observed in *Coq9*^{R239X} and, consequently, *Coq9*^{Q95X} mice have a less severe CoQ deficiency, leading to a mild myopathy with exercise intolerance in females (Luna-Sanchez *et al.*, 2015) (Introduction figure 15). Therefore, the two models generated recapitulate two of the clinical phenotypes that are present in patients with CoQ_{10} deficiency and that are common in other MD, myopathies and encephalomyopathies.

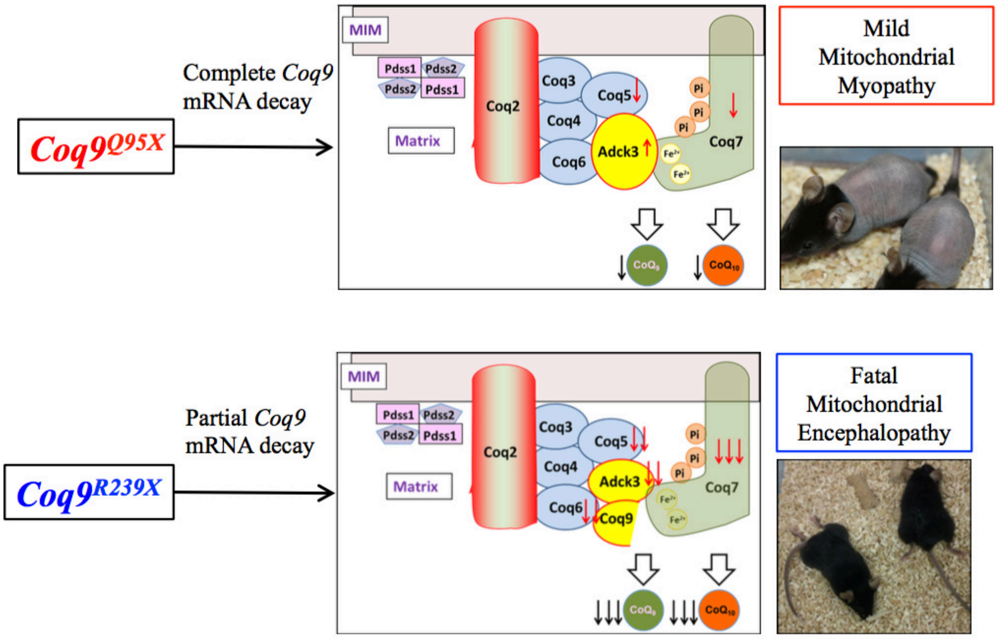
Complete *Coq9* mRNA decay
Coq9^{Q95X}
MIM
Pdss1
Pdss2
Matrix
Coq2
Coq3
Coq5
Coq4
Adck3
Coq6
Coq7
Pi
Fe
CoQ_9
CoQ_{10}
Mild Mitochondrial Myopathy
Partial *Coq9* mRNA decay
Coq9^{R239X}
Coq9
Fatal Mitochondrial Encephalopathy

Introduction Figure 15. **Example of different pathology involving different mutations of the same gene** (Luna-Sanchez *et al.*, 2015).

Importantly, two independent studies showed that CoQ deficiency, either *in vitro* in human cells or *in vivo* in mouse model, severely decreases the levels of SQOR, the first enzyme in the mitochondrial H_2S oxidation pathway. Thus, the decrease in SQOR leads to an impairment of H_2S oxidation, leading to accumulation of H_2S and depletion on the glutathione system (Luna-Sanchez *et al*, 2017; Ziosi *et al*, 2017). Altogether, these alterations could be influencing in the pathomechanisms associated to CoQ deficiency. On fact, other molecular defects in the mitochondrial H_2S oxidation pathway have been identified (Quinzii *et al.*, 2017). Specifically, mutations in *ETHE1*, *SUOX* and *SQOR* cause encephalopathies (Friederich *et al*, 2020; Mudd *et al*, 1967; Tiranti *et al*, 2009). Curiously, mutations in *ETHE1* are associated to CIV deficiency because of the accumulation of sulfide metabolites. Besides, the encephalopathic phenotype of *ETHE1* mutant mice is partially rescue (Viscomi *et al*, 2010), with the supplementation of N-acetylcisteine (NAC), a sulfur amino acid and precursor of glutathione.

1.2.1.1.2 Experimental treatments for CoQ deficiency.

The most rational therapeutic approach for CoQ deficiency is the supplementation with exogenous CoQ_{10}. Studies in human skin fibroblasts from patients with primary CoQ deficiency would support this rational approach. Rodríguez-Hernández and collaborators used CoQ_{10} deficient fibroblast due to *COQ2* defect and found a slight increase in II+III complex activity after the treatment with 100 μM CoQ_{10} for 72 hours (Rodriguez-Hernandez *et al.*, 2009). In the same way, Lopez and collaborators found that the levels of ATP and the ATP/ADP ratio were normalized in CoQ_{10} deficient fibroblast with mutations in *PDSS2*, *COQ2* and *COQ9* after the administration of 5 μM ubiquinone-10 for 1 week but not for 24 h (Duncan *et al.*, 2009; Lopez *et al*, 2010; Lopez *et al.*, 2006; Quinzii *et al.*, 2006). In contrast, treatment with short-chain ubiquinone analogues such as CoQ_2 or Idebenone, had no effects on mitochondrial bioenergetics (Lopez *et al.*, 2010). Consequently, the outcome of these i*n vitro* studies suggested that: a) exogenous CoQ_{10} has a prolonged pharmacokinetics to restore respiratory chain activity in CoQ_{10}-deficient cells (Bentinger *et al*, 2003), a factor that may contribute to the late clinical response to the oral supplementation of CoQ_{10} (Montini *et al*, 2008) and suggest that high doses of CoQ_{10} must be administered; and b) short-tail ubiquinone analogs cannot substitute CoQ_{10} in the mitochondrial respiratory chain revealing the importance of the decaprenyl tail.

In vivo, a mouse model with spontaneous mutation in *Pdss2*, CoQ deficiency and fatal nephropathy (Peng *et al*, 2004) was treated with hydrosoluble CoQ_{10} at a dose of 200-400mg/kg body weight/day in the water. The treated mice did not show a substantial increase their tissue levels of CoQ_{10} but an improvement in the development of nephritis was observed. Thus, the authors suggested that the therapeutic mechanism was due to a reduction in oxidative stress (Saiki *et al*, 2008). Later on, our group evaluated the administration of water-soluble $CoQ_{10}H_2$ (ubiquinol-10) in the *Coq9*^{R239X} mouse model. Although survival improved, still 50% of the *Coq9*^{R239X} mice treated with ubiquinol-10 died before 6 months of age (Garcia-Corzo *et al.*, 2013). Thus, due to its poor bioavailability, the therapeutic effects of exogenous CoQ_{10} are limited in some cases, especially in those involving the nervous system because of the presence of the BBB (Emmanuele *et al.*, 2012).

Therefore, novel therapeutics approaches are required to get better outcomes in the treatment of patients with CoQ deficiency.

1.2.1.1.3 Treatment of patients with CoQ deficiency.

Primary CoQ deficiency is considered one of the few treatable MD, although not all cases are successfully treated (Introduction table 1). As mentioned, the conventional treatment is the oral supplementation with high doses of CoQ_{10}, but the response to the treatment is very variable among patients, being in certain cases ineffective, especially in those patients with neurological symptoms (Introduction table 1). A high concentrations of CoQ_{10} was able to stop the progression of encephalopathy in a patient with the multisystem variant of the disease (Rotig *et al*, 2000); another case with mutation in the *COQ2* responded positively to the CoQ_{10} supplementation (Montini *et al.*, 2008); six patients with myopathy improved after CoQ_{10} supplementation, while another 28 patients with mutations in the *ETFDH*, coursing with CoQ_{10} deficiency, improved only with the addition of a riboflavin treatment (Gempel *et al.*, 2007); other patient with myopathy due to *COQ7* mutation reduced its symptoms by the treatment with CoQ_{10} (Freyer *et al*, 2015); and two more patients with mutations in *COQ4* seemed to be positively responsive to treatment with CoQ_{10} (Caglayan *et al.*, 2019) (Introduction table 1).

In contrast, CoQ_{10} supplementation was less effective in some forms of ataxia, such as those caused by the mutations in the *COQ8A* (*=ADCK3*) (Mollet *et al.*, 2008) (Lagier-Tourenne *et al.*, 2008); also, a homozygous patient for the *COQ9* mutation experienced a decrease in blood lactate during CoQ_{10} therapy but did not slow the progress of neurological and cardiac symptoms, leading to death at two years of life (Duncan *et al.*, 2009); in other patients with neurological symptoms harboring mutations in *COQ2*, *COQ4* or *COQ9* experimented only mild improvements in the neurological symptoms, and died at early age (Brea-Calvo *et al.*, 2015; Danhauser *et al.*, 2015; Jakobs *et al*, 2013) (Introduction table 1).

The reason why treatment fails in some cases is unclear. A key aspect, would be the early diagnosis of the disease that would enable an early start of treatment (Yubero *et al*, 2017; Yubero *et al*, 2018) (Introduction table 1). The optimal CoQ_{10} dose and formulation used would be another factor to consider. According to clinical experiences in recent years, the recommended dose of CoQ_{10} for patients with CoQ_{10} deficiency is 2,400 mg daily in adults and up to 30 mg/kg/day in children. Another important aspect to consider in the inefficiency of the therapy is the low absorption and bioavailability of CoQ_{10} when administered orally exogenously, which limits the intramitochondrial increase of CoQ_{10}, especially in the brain and cerebellum because of the extra difficulty of crossing the BBB (Emmanuele *et al.*, 2012). In any case, the results of these studies lead the search for alternative therapies that can increase the efficacy of the treatment.

Gen	Fams/ Pats.	Age		Manifestation	CoQ Treatment Effects
		Start	Last Examination		
PDSS1	2/3	First years	1.5yo* (1) 14-22yo (2)	Encephalopathy (2), peripheral neuropathy (2), optical atrophy (2), deafness (2), nephrotic syndrome and ESRD (1), valvulopathy (2)	NK
PDSS2	5/7	< 1yo (6) 2yo (1)	8mo* (2) 8yo*(1) 8-12yo (2) NC (2)	Leigh syndrome (1), encephalopathy (1), cerebellar ataxia (3), deafness (4), retinopathy (2), optical atrophy (1), nephrotic syndrome (7), ESRD (2), cardiomyopathic hypertrophy (2)	Yes (2). Not benefits
COQ2	18/22	< 2yo (15) 16-18yo (2) 70 (1) NK (4)	< 2yo* (9) 2-4yo (5) 12yo (1) 23-37yo (2) 71yo (1) NK (4)	Encephalopathy (7), cerebellar atrophy (1), MELAS (1), retinopathy (2), optical atrophy (1), nephrotic syndrome (17), ESRD (8), tubulopathy (1), muscle weakness (1), cardiomyopathic hypertrophy (3)	Yes (9). No benefits (2). No deterioration (2). Improved renal function (4). Improved neuromuscular function (1)
COQ4	11/14	Birth (13) 10mo (1)	< 4d* (6) 1m-2yo* (5) 3yo (1) 18yo (1) NK (1)	Encefalopatía (7), atrofia cerebelar (1), neuropatía periférica (1), sordera (1), miopatía (1), fallo cardiaco (2), hipertrofia cardiomiopática (7)	Yes (3). No benefits (1). Muscle enhancement (1). Improved lactic acidosis and heart function (1)
COQ5	1/3	Childhood (3)	14-22yo (3)	Cerebellar ataxia (3), cerebellar atrophy (1)	Yes (3). Improving ataxia (3)
COQ6	19/26	< 1.5yo (9) 2-6yo (13) NK (4)	5-6yo* (2) 17yo* (1) NK* (2) 6mo-11yo (14) NK (7)	Cerebellar ataxia (1), deafness (16), optical atrophy (1), nephrotic syndrome (23), ESRD (15), muscle weakness (2),	Yes (4). Proteinuria enhancement (3). Renal function enhancement (1). Growth retardation enhancement (1)
COQ7	2/2	< 1yo (2)	6-9yo (2)	Peripheral neuropathy (2), deafness (2), renal failure (1), muscle weakness (2), cardiomyopathic hypertrophy (1)	Yes (2). No deterioration (2)
COQ9	3/6	Birth (6)	Nac.* (2) 12h* (1) 3d* (1) 18d* (1) 2yo* (1)	Encephalopathy (2), Leigh syndrome (2), cerebellar atrophy (1), tubulopathy (1), cardiomyopathic hypertrophy (1)	Yes (3). No benefits (2). Lactate plasma reduction (1)
COQ8A/ ADCK3	29/45	1-4yo (24) 5-11yo (13) 14-27yo (8)	22yo* (1) 26yo* (1) 3-7yo (2) 15-50yo (40) 81yo (1)	Cerebellar atrophy (44), cerebellar ataxia (43), MELAS (6), encephalopathy (1), deafness (2), visual impairment, myopathy (1), muscle weakness (7), exercise intolerance (8), cardiomyopathy (1)	Yes (18). No benefits (8). Improves ataxia (4). Stabilises ataxia (1). Improves motor capacity (2). Improves fatigue (1)
COQ8B/ ADCK4	38/74	< 1-10yo (29) 11-21yo (38) 23-32yo (7)	15yo* (1) 25yo* (1) 29yo* (1) 1-9yo (6) 10-20yo (51) 21-39yo (14)	Encephalopathy (1), seizures (4), nephrotic syndrome (63), ESRD(45), chronic kidney disease (17), muscle weakness (1), cardiomyopathic hypertrophy (2), heart failure (1), cardiomyopathy (1)	Yes (28). No benefits (7). Proteinuria enhancement (17). Fatigue enhancement (1). Renal function stabilization (1). NC (2)

Introduction table 1. Primary CoQ Deficiiency. Its clincal manifestations and its response to exogenous CoQ treatment.

Extracted and modified from (Alcazar-Fabra et al., 2018) collected up to 2018. Fams: Families; Pats: Payients; NK:Not Known; y: years; m: months; d: days; h: hours; (*): Death. ESRD: End-stage regal disease. Until now has been described other two patients with mutations in COQ4 (Caglayan et al., 2019), two patients with mutations in COQ6 (Justine Perrin et al., 2020), five patients with mutations in COQ8B (Song et al., 2020) that positively responds to CoQ treatment. In the counterpart, it was described other patient with mutation in COQ2 that did not respond to CoQ treatment (Wu et al., 2019).

1.2.1.1.4 Alternative treatments for CoQ deficiency using analogs of 4HB

As we mention above, the biosynthesis of CoQ occurs in a complex biosynthetic pathway, in which the 4-HB is the initial substrate. This precursor of the benzoquinone ring of CoQ is first prenylated and then, a total of seven reactions (one decarboxylation, three hydroxylations, and three methylations) produce the fully substituted benzoquinone ring of CoQ. The molecular understanding of the CoQ biosynthetic pathway is now allowing the design of alternative therapies with the aim of increasing the endogenous CoQ biosynthesis. One of the hydroxylation steps is catalyzed by COQ7, a hydroxylase that needs another protein, COQ9, for its stability and normal function (Garcia-Corzo *et al.*, 2013; Lohman *et al.*, 2014; Luna-Sanchez *et al.*, 2015). The hydroxyl group incorporated by COQ7 into the benzoquinone ring is already present in the β-Resorcylic acid (β-RA) or 2,4-dihydroxybenzoic acid (2,4-diHB) molecule. Therefore, β-RA is a 4-HB analog that can be theoretically used in the CoQ biosynthesis pathway in order to bypass a defect of the hydroxylation step catalyzed by COQ7. This strategy was partially successful *in vitro* in COQ7 null yeasts, as well as in mice and human fibroblasts with mutations in *COQ7* or *COQ9* (Freyer *et al.*, 2015; Luna-Sanchez *et al.*, 2015; Wang *et al*, 2015; Wang *et al.*, 2017; Xie *et al*, 2012).

The same principle has been demonstrated *in vitro* with the use of 3,4-hydroxybenzoic acid (3,4-diHB) or vanillic acid (VA) in *COQ6* null yeasts (Doimo *et al*, 2014b). Furthermore, a recent study has shown that supplementation of 4-HB increases the levels of CoQ biosynthetic proteins and fully restores endogenous CoQ_{10}-biosynthesis in *COQ2*-deficient cells lines (Herebian *et al*, 2017).

HYPOTHESIS & OBJECTIVES

2. HYPOTHESIS & OBJECTIVES

Primary and secondary CoQ deficiencies constitute a mitochondrial syndrome with heterogeneous clinical presentations, involving different pathomechanims. The conventional treatment is based in the exogenous administration of high doses of CoQ_{10}. This treatment, however, has limited effects in a high percentage of patients due to different factors: 1) the low absorption and bioavailability of the exogenous CoQ_{10}, together with its low capacity to cross the BBB; 2) the lack of effect over the accumulation of intermediate metabolites in the synthesis of CoQ (importantly, some of these metabolites, e.g. DMQ, may contribute to the disease phenotype by inhibiting the transfer of electrons in the mtETC); and 3) the lack of effect over the Complex Q and the endogenous biosynthesis of CoQ. For that reason, CoQ_{10} therapy does not induce any change in the levels of CoQ_9.

Based on previous studies *in vitro*, we hypothesize that β-RA may have superior therapeutics outcomes because of three different reasons: 1) it is a water-soluble compound of low molecular weight, having, therefore, better absorption and bioavailability than CoQ_{10}; 2) it may bypass a defect in COQ7 or COQ9; and 3) it has the ability to modulate the Complex Q in order to minimize the accumulation of toxic intermediates, e.g. DMQ, and maximize CoQ biosynthesis, increasing the levels of both CoQ_9 and CoQ_{10}. In addition, we believe that the reduction in SQOR activity and accumulation of H_2S, as a consequence of the low levels of CoQ, are another pathomechanisms associated to CoQ deficiency. Thus, the modulation of the availability of sulfur amino acids in the diet, as sources of H_2S, could provide therapeutic benefits.

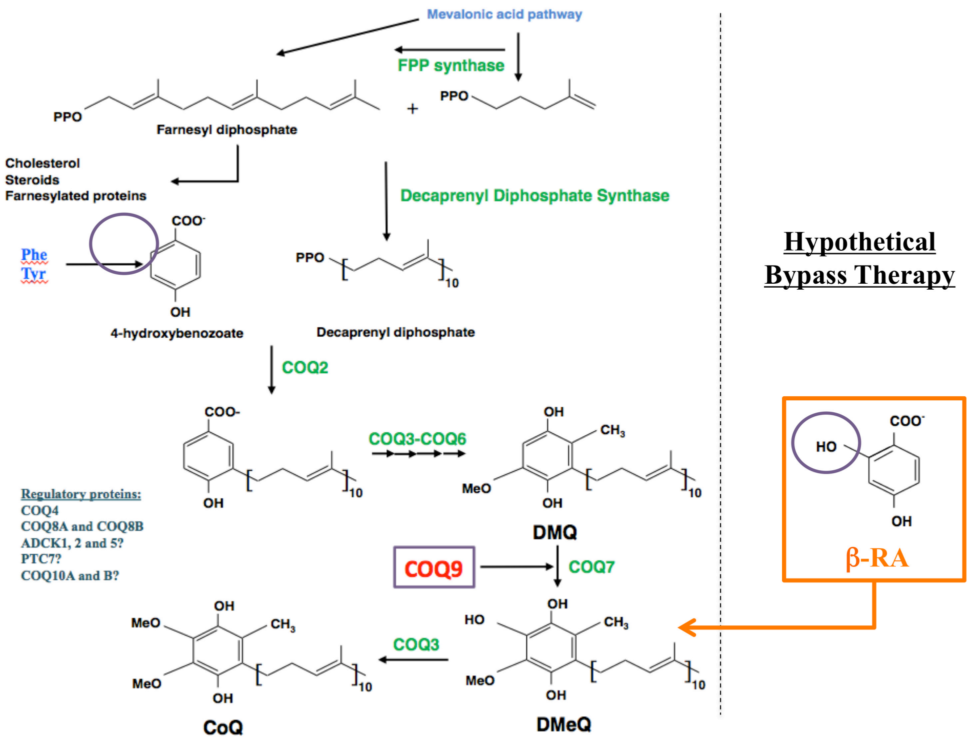
Mevalonic acid pathway
FPP synthase
PPO
+
PPO
Farnesyl diphosphate
Cholesterol
Steroids
Farnesylated proteins
Decaprenyl Diphosphate Synthase
Phe
Tyr
COO-
OH
4-hydroxybenozoate
PPO
10
Decaprenyl diphosphate
COQ2
COO-
OH
10
COQ3-COQ6
OH
CH3
MeO
OH
10
DMQ
Regulatory proteins:
COQ4
COQ8A and COQ8B
ADCK1, 2 and 5?
PTC7?
COQ10A and B?
COQ9
COQ7
OH
MeO
CH3
MeO
OH
10
CoQ
COQ3
HO
OH
CH3
MeO
OH
10
DMeQ
Hypothetical
Bypass Therapy
HO
COO-
OH
β-RA

Hypothesis Figure 1. **Possible bypass therapy using β-RA in the *Coq9*^{R239X} mice**.

To test those hypothesizes we propose to develop the following specific aims (SAs):

SA1: To test, *in vivo,* the efficacy of β-RA in the treatment of primary CoQ deficiency due to mutations in *Coq9*.

SA2: To perform a dose-response study with β-RA in the *Coq9*^{R239X} mouse model and their wild-type littermates.

SA3. To evaluate the therapeutic potential of NAC supplementation and a diet with sulfur amino acids restriction in the *Coq9*^{R239X} mouse.

MATERIALS & METHODS

3. MATERIALS & METHODS

3.1 EXPERIMENTAL DESIGN

Coq9$^{+/+}$ and *Coq9*^{R239X} mice were used in the study, all of them having a mix of C57BL/6N and C57BL/6J genetic background. The *Coq9*^{R239X} mouse model (MGI: 5473628) was previously generated and characterized (Garcia-Corzo *et al.*, 2013). All animal manipulations were performed according to a protocol approved by the Institutional Animal Care and Use Committee of the University of Granada (procedures numbers 18/02/2019/016 and 16/09/2019/153) and were in accordance with the European Convention for the Protection of Vertebrate Animals used for Experimental and Other Scientific Purposes (CETS # 123) and the Spanish law (R.D. 53/2013). Mice were housed in the Animal Facility of the University of Granada under an SPF zone with lights on at 7:00 AM and off at 7:00 PM. Mice had unlimited access to water and rodent chow. Unless stated otherwise, the analytical experiments were done in animals at 3 months of age, with the exception of the animals at "terminal stage" that range from two to five months of age.

β-Resorcylic acid (β-RA) was given to the mice in the chow at two different concentrations: 1% (high dose), and 0.33% (low dose). For a particular experiment, we doubled the high dose by adding β−RA into the drinking water at a concentration of 5 mg/ml, neutralizing the water with sodium bicarbonate.

A mix of β-RA and 4-HB (at a concentration of 0.5% each one) was also provided in the chow for particular experiments. Mice began receiving the assigned treatments at 1 month of age (except in the some exception, in which the treatments started at 2 or 6 months of age) and the analyses were done at the age indicated for each case. Also, a pilot survival study was done with β–RA in Ndufs4 knockout mice, which show microgliosis and neuroinflammation (Quintana *et al*, 2010). Animals were randomly assigned in experimental groups. In addition, to check whether the availability of sulfur amino acids affects sulfide metabolism in CoQ_{10} deficiency, *Coq9*^{R239X} mice (MGI: 5473628) were treated with L-NAC, added to drinking water at a concentration of 1%. Separately, mice were treated with sulfur amino acids restriction (SAAR) diet containing 0.15% Methionine and 0% Cystine, compared to control diet containing 0.6% Methionine and 0.42% Cystine. Data were randomly collected and processed as well.

The body weights were collected once a month. The motor coordination was evaluated by rotarod test at different months of age. Systolic blood pressure (SBP) and heart rate (HR) were measured in conscious, prewarmed, and restrained mice by tail-cuff plethysmography (Digital Pressure Meter LE 5001, Letica S.A., Barcelona, Spain) as described previously (Gomez-Guzman *et al*, 2014). Briefly, mice were held in a plastic tube, and their tail was put through a rubber cuff, and the cuff was inflated with air. The pressure level at which the first pulse appeared, after blood flow had been interrupted with the inflated cuff, was designated SBP. At least fifteen determinations were made in every session, and the mean of the lowest ten values within 5 mmHg was taken as the SBP level. HR values were obtained as average of several determinations simultaneously to SBP level.

The therapeutic potential of β-RA was also assessed in zebrafish embryos treated with the neurotoxin 1-methyl-4-phenyl- 1,2,3,6-tetrahydropyridine (MPTP), which is used to induce key features of Parkinson Disease, including CI inhibition and neuroinflammation (Diaz-Casado *et al*, 2018). The embryos were exposed to MPTP from 24 hpf to 72 hpf, and β-RA was added to the wells from 72 hpf to 120 hpf. After completing the experiment protocol, at 120 hpf, the mortality rate was calculated as the percentage of dead embryos with respect to total embryos. Oedema, the most common malformations, as well as tail and yolk abnormalities were macroscopically quantified (Diaz-Casado *et al.*, 2018).

3.2 HEMOGRAM, PLASMA AND URINE ANALYSIS

Blood samples were collected in K3-EDTA tubes using a golden rod lancet and the submandibular vein of mice as puncture site. The hemograms were obtained using a Mythic 22 CT in an automated hematology analyzer. The plasma was extracted from blood samples by centrifugation at 4,500g for 10 minutes at 4ºC. Biochemical analysis from urine and plasma were developed in a biochemical analyzer Bs-200 (Shenzhen Mindray Bio-Medical Electronics Co., Ttd) and reagents from Spinreact.

3.3 HISTOLOGY AND IMMUNOHISTOCHEMISTRY

Tissues were fixed in formalin and paraffin embedded. Multiple sections (4 µm thickness) were deparaffinized with xylene and stained with hematoxylin and eosin (H&E) or Masson's trichrome. Immunohistochemistry was carried out in the same sections, using the following primary antibodies: anti-GFAP (Millipore, MAB360) and anti-Iba-1 (Wako, 019-19741). Dako Animal Research Kit for mouse primary antibodies (Dako Diagnóstico S.A., Spain) was used for the qualitative identification of antigens by light microscopy. The detection of carbonyl groups as a marker of protein oxidation was performed using a commercial kit (OxyIHC™ Oxidative Stress Detection Kit (S7450, Millipore) (Garcia-Corzo *et al.*, 2013).

Type I and type II skeletal muscle fibers were examined through histochemical detection of cytochrome oxidase (COX) and succinate dehydrogenase (SDH) enzymes activity (Tanji & Bonilla, 2008).

Sections were examined at 40–400 magnifications with a Nikon Eclipse Ni-U microscope, and the images were scanned under equal light conditions with the NIS-Elements Br computer software.

3.4 IN VIVO MRI AND PROTON MRS

MRI and MRS studies were conducted with a 7 T horizontal bore magnet Bruker Biospec TM 70/20 USR designed for small animal experimentation. Mice were anesthetized by spontaneous breathing of 0.4–2.0 % (0.4-0.6 % in *Coq9*^{R239X} and 1.5-2.0% in *Coq9*$^{+/+}$) isofluorane and oxygen mixture through a nose cone using a MSS (Medical Suplies and Services) veterinary anesthesia unit. The mice were placed in an MRI-compatible cradle and their body temperature was maintained at 37ºC by a water bath circulation system. A pneumatic pillow and an accompanying pressure transducer monitored their respiratory rates. Both temperature and breathing were recorded by a small animal monitoring system. Anesthesia was adjusted to obtain a respiratory rate of about 40-60 breaths per minute. Following localizer scans, high- resolution axial and coronal T2-weighted datasets were acquired in order to visualize any cerebral or structural atrophy and to investigate for potential focal pathologies. A fast-spin echo sequence was used to acquire inter-leaved multislice T2-weighted, high-resolution mouse brain images with TR/TE = 2500 / 33 ms, field-of-view = 20 x 20 mm, slice thickness = 0.7 mm, inter-slice gap ⅓ 0.3 mm, and 48 excitations per phase-encoding step. The data were zero-filled to yield a final image with 78 x 78 μm in-plane resolution. Water-suppressed point-resolved spectroscopy was acquired in order to glean the metabolic status from the mouse brain. The MRI dataset was collected with the following settings: a voxel size of 2 × 2 × 2 mm, a bandwidth of 3 kHz, 2048 acquisition points, a TR period of 2500 ms, a TE period of 144 ms and 256 averages. The voxel was centered in the brainstem region. (Diaz *et al*, 2012).

3.5 TRANSCRIPTOME ANALYSIS BY RNA-seq

The RNeasy Lipid Tissue Mini Kit (Qiagen) was used to extract total RNAs from the braintem of five animals in each experimental group. The RNAs were precipitated and their quality and quantity assessed using an Agilent Bioanalyzer 2100 and an RNA 6000 chip (Agilent Technologies). The cDNA libraries were then constructed using the TruSeq RNA Sample Prep Kit v2 (Illumina, Inc.) and their quality checked using an Agilent Bioanalyzer 2100 and a DNA 1000 chip (Agilent Technologies). The libraries were Paired End sequenced in a HiSeq 4000 system (Illumina, Inc.). We aimed for 4 to 5 Giga Bases outcome per sample. The quality of the resulting sequencing reads was assessed using FastQC. The GRCm38.p5 fasta and gtf files of the reference mouse genome were downloaded from the Ensembl database and indexed using the bwtsw option of BWA (Linden *et al*, 2012). BWA, combined with xa2multi.pl and SAMtools (Li *et al*, 2009), was also used for aligning the sequencing reads against the reference genome, and HTSeq was used for counting the number of reads aligned to each genomic locus (Mishanina *et al*, 2015). The alignments and counting were carried out in our local server following the protocols as described (Brzywczy *et al*, 2002; Di Meo *et al.*, 2011).

After elimination of the genomic loci that aligned to less than 5 reads in less than 5 samples and normalization of the read counts by library size, the differential gene expression was detected using the Generalized Linear Model (glmLRT option) statistic in EdgeR (Hine *et al*, 2015). We used a 0.05 p-level threshold after False Discovery Rate correction for type I error. The heatmap figure was made using the heatmap function in R (https://www.r-project.org/). Annotation of the differentially expressed genes was obtained from the Mouse Genome Informatics (http://www.informatics.jax.org/).

The transcripts that filled the inclusion criteria were then subjected to gene classification, using a databank based on hand-curated literature mining for specific protein–protein interactions and regulatory networks (Ingenuity Pathway Analysis (IPA); Ingenuity Systems, Redwood City, CA, USA). The general canonical pathways, biological functions and diseases implicated for the significantly changed transcripts by Ingenuity Pathway Analysis were evaluated and P-values <0.01 were considered significant. Further, specific functional networks based on published knowledge on protein–protein interactions and regulatory networks were constructed by Ingenuity Pathway Analysis (Raimundo *et al*, 2009).

3.6 MITOCHONDRIAL PROTEOMICS ANALYSIS

Both *Coq9*$^{+/+}$ mice and *Coq9*$^{+/+}$ mice under 1% of β-RA supplementation were sacrificed and the brain and kidneys were removed and washed in saline buffer. The tissues were chopped with a scissors in 3 ml HEENK (10 mM HEPES, 1 mM EDTA, 1 mM EGTA, 10 mM NaCl, 150 mM KCl, pH 7.1, 300 mOsm/l) containing 1 mM phenylmethanesulfonyl fluoride (from 0.1 M stock in isopropanol) and 1x protease inhibitor cocktail (Pierce). The tissues were homogenized using a 3 ml dounce homogenizer (5 passes of a tight-fitting teflon piston). Each homogenate obtained was rapidly subdued to standard differential centrifugation methods until the mitochondrial pellet was obtained as described in elsewhere (Liu *et al*, 2018). Briefly, the homogenate was centrifuged at 600 g for 5 min at 4 °C (twice), and the resultant supernatant was centrifuged at 9,000 g for 5 min at 4 °C. The final pellet, corresponding to a crude mitochondrial fraction, was resuspended in 500 ul of HEENK medium without PMSF or protease inhibitor (Liu *et al.*, 2018). Protein concentration determined (using Bradford dye (BIO-RAD) and a Shimadzu spectrophotometer), resulting in approximately 3 mg protein for renal mitochondria and 1.5 mg for cerebral mitochondria. To verify the content of the mitochondrial fraction, Complex IV activity was determined by optical absorption of the difference spectrum at 550 nm, as previously described (Luna-Sanchez *et al.*, 2017).

The purified mitochondria were spin down to remove previous buffer and lysis buffer (1% sodium deoxycholate SDC in 100 mM tris at pH 8.5) was added to the pellets. Samples were boiled for 5 minutes at 99ºC to denature all the proteins and then sonicated by micro tip probe sonication (Hielscher UP100H Lab Homogenizer) for 2 min with pulses of 1s on and 1s off at 80% amplitude. Protein concentration was estimated by BCA assay and 200 µg were taken of each sample. 10 mM tris (2-carboxyethyl) phosphine and 40 mM chloroacetamide (final concentration) at 56 ºC were added to each of these 200 µg for 10 minutes in order to reduce and alkylate the disulfide bridges. After this step, samples were digested with LysC (Wako) in an enzyme/protein ratio of 1:100 (w/w) for 1 h, followed by trypsin (Promega) 1:50 (w/w) overnight. Protease activity was quenched by acidification with trifluoroacetic acid (TFA) to a final pH of ~2. Samples were then centrifuged at 5,000g for 10 minutes, in order to eliminate the insoluble SDC, and loaded on an OASIS HLB (Waters) 96-well plate. Sample were washed with 0.1% TFA, eluted with a 50/50 ACN and 0.1% TFA, dried by SpeedVac (Eppendorf, Germany), and resuspended in 2% formic acid prior to MS analysis. 5 µg were taken from each sample and pooled in order to be used for quality control for MS (1 QC was analyzed every 12 samples) and to be fractionated at high-pH for the Match between runs.

All samples with the QC and 7 high-pH fractions were acquired using an UHPLC 1290 system (Agilent Technologies; Santa Clara, USA) coupled online to an Q Exactive HF mass spectrometer (Thermo Scientific; Bremen, Germany). Peptides were first trapped (Dr. Maisch Reprosil C18, 3 μm, 2 cm × 100 μm) prior to separation on an analytical column (Agilent Poroshell EC-C18, 2.7 μm, 50 cm × 75 μm). Trapping was performed for 5 min in solvent A (0.1% v/v formic acid in water), and the gradient was as follows: 10% – 40% solvent B (0.1% v/v formic acid in 80% v/v ACN) in 95 min, 40– 100% B in 2 min, then the column was cleaned for 4 minutes and equilibrated for 10 min (flow was passively split to approximately 300 nL/min). The mass spectrometer was operated in a data-dependent mode. Full-scan MS spectra from m/z 300-1600 Th were acquired in the Orbitrap at a resolution of 120,000 after accumulation to a target value of 3E6 with a maximum injection time of 120 ms. The 15 most abundant ions were fragmented with a dynamic exclusion of 24 sec. HCD fragmentation spectra (MS/MS) were acquired in the Orbitrap at a resolution of 30,000 after accumulation to a target value of 1E5 with an isolation window of 1.4 Th and maximum injection time 54 ms.

All raw files were analyzed by MaxQuant v1.6.10 software (Cox & Mann, 2008) using the integrated Andromeda Search engine and searched against the mouse UniProt Reference Proteome (November 2019 release with 55412 protein sequences) with common contaminants. Trypsin was specified as the enzyme allowing up to two missed cleavages. Carbamidomethylation of cysteine was specified as fixed modification and protein N-terminal acetylation, oxidation of methionine, and deamidation of asparagine were considered variable modifications. We used all the automatic setting and activated the "Match between runs" (time window of 0.7 min and alignment time window of 20 min) and LFQ with standard parameters. The files generated by MaxQuant were open from Perseus for the preliminary data analysis: the LFQ data were first transformed in log2, then identifications present in at least N (3/5) biological replicates were kept for further analysis; missing values were then imputed using the standard settings of Perseus. For the volcano plot we set as threshold p-value of 0.01 and 1 for the difference in log2 of the LFQ values. IPA analysis was performed as described above (Raimundo *et al.*, 2009).

3.7 MITOCHONDRIAL RESPIRATION

To isolate fresh mitochondria, mice were sacrificed and the organs were extracted rapidly on ice. Brain was homogenated (1:10, w/v) in a respiration buffer C (0.32 M Sucrose, 1 mM EDTA-K+, 10 mM Tris-HCl, pH7.4) at 500 rpm at 4 °C in a glass-teflon homogenizer. The homogenate was centrifuged at 13,000 x g for 3 min at 4 ºC. The Supernatant (s1) was kept on ice and the pellet was re-suspended in 5 ml of buffer A and centrifuged at 13,000 x g for 3 min at 4 ºC. The subsequent supernatant (s2) was combined with s1 and centrifuged at 21,200 x g for 10 min at 4 ºC. Mitochondrial pellet of this step was re-suspended in 0.85 mL extraction buffer A containing 15% Percoll, poured into ultracentrifuge tubes containing a Percoll gradient formed by 1 ml 40% Percoll and 1 ml 23% Percoll in buffer A, and centrifuged at 63,000 x g for 30 min at 4ºC. Pure mitochondria, corresponding to the fraction between 23% and 40% Percoll, were collected, washed twice with 1 ml of buffer A at 10,300 x g for 10 min at 4ºC. Mitochondrial pellets were suspended in MAS 1X medium. Kidney was homogenated (1:10, w/v) in a respiration buffer A (250 mM Sucrose, 0.5 mM Na2EDTA, 10 mM Tris and 1 % free fatty acid albumin) at 800 rpm in a glass-teflon homogenizer. Then, homogenate was centrifuged at 500 x g for 7 min at 4 ºC and the supernatant was centrifuged at 7,800 x g for 10 min at 4 ºC. The pellet was then resuspended in respiration buffer B (250 mM Sucrose, 0.5 mM Na2EDTA and 10 mM Tris) and an aliquot was used for protein determination. The remaining sample was then centrifuged at 6,000 x g x 10 min at 4ºC. The pellet was resuspended in buffer A and centrifuged again at 6,000 x g x 10 min at 4ºC. The final crude mitochondrial pellet was re-suspended in MAS 1X medium.

Mitochondrial respiration was measured by using an XFe24 Extracellular Flux Analyzer (Seahorse Bioscience) (Rogers *et al*, 2011). Mitochondria were first diluted to the needed concentration required for plating in cold MAS 1X (3,5 ug/ in brain; 2 ug/well in kidney). Next, 50 ul of mitochondrial suspension was delivered to each well (except for background correction wells) while the plate was on ice. The plate was then centrifuged at 2,000 g for 10 min at 4°C. After centrifugation, 450 ul of MAS 1X + substrate (10 mM succinate, 2 mM malate, 2 mM glutamate and 10 mM pyruvate) was added to each well. Respiration by the mitochondria was sequentially measured in a coupled state with substrate present (basal respiration or State 2), followed by State 3o (phosphorylating respiration, in the presence of ADP and substrates); State 4 (non-phosphorylating or resting respiration) was measured after the addition of oligomycin when all ADP was consumed, and then maximal uncoupler-stimulated respiration (State 3u). Injections were as follows: port A, 50 ul of 40 mM ADP (4 mM final); port B, 55 ul of 30 ug/ml oligomycin (3 ug/ml final); port C, 60 ul of 40 uM FCCP (4 uM final); and port D, 65 ul of 40 uM antimycin A (4 uM final). All data were expressed in pmol/min/lg protein.

3.8 CoQ-DEPENDENT RESPIRATORY CHAIN ACTIVITIES

Coenzyme Q-dependent respiratory chain activities were measured in tissue samples of brain, kidney, skeletal muscle and heart. Tissue samples were homogenized in CPT medium (0.05 M Tris-HCl, 0.15 M KCl, pH 7.5) at 1,100 rpm in a glass–Teflon homogenizer. Homogenates were sonicated and centrifuged at 600 g for 20 min at 4 °C, and the supernatants obtained were used to measure CoQ-dependent respiratory chain activities (CI + III and CII + III) as previously described (Barriocanal-Casado *et al*, 2019). To test whether b-RA works as a CoQ substitute in the mitochondrial respiratory chain, we also measure the CI-III activity after adding 50 uM b-RA. The results were expressed in nmol reduced cyt c/min/mg prot.

3.9 EVALUATION OF SUPERCOMPLEXES FORMATION BY BNGE

BNGE was performed on crude mitochondrial fractions from mice kidneys and brain. Mitochondrial isolation was performed as previously described (Garcia-Corzo *et al.*, 2013). One aliquot of the crude mitochondrial fraction was used for protein determination. The remaining samples were then centrifuged at 13,000 × g for 3 min at 4 °C. The mitochondrial pellets were suspended in an appropriate volume of medium C (1 M aminocaproic acid, 50 mM Bis-Tris-HCl [pH 7.0]) to create a protein concentration of 10 mg/ml, and the membrane proteins were solubilized with digitonin (4 g/g) and incubated for 10 min in ice. After 30 min of centrifugation at 13,000 ×g (4 °C), the supernatants were collected, and 3 μL of 5% Brilliant Blue G dye prepared in 1 M aminocaproic acid was added. Mitochondrial proteins (100 μg) were then loaded and run on a 3–13% gradient native gel as previously described (Garcia-Corzo *et al.*, 2013). After electrophoresis, the complexes were electroblotted onto PVDF membranes and sequentially tested with specific antibodies against CI, anti-NDUFA9 (Abcam, ab14713), CIII, anti-ubiquinol-cytochrome c reductase core protein I (Abcam, ab110252) and VDAC1 (Abcam, ab14734).

3.10 SAMPLE PREPARATION AND WESTERN BLOT ANALYSIS IN TISSUES

For Western blot analyses in mouse tissues, samples were homogenized in T-PER® buffer (Thermo Scientific) with protease inhibitor cocktail (Pierce) at 1,100 rpm in a glass–Teflon homogenizer. Homogenates were sonicated and centrifuged at 1,000 × g for 5 mins at 4°C, and the resultant supernatants were used for Western blot analysis. For Western blot analyses in brain mitochondria, the pellets containing the mitochondrial fraction were re-suspended in RIPA buffer with protease inhibitor cocktail. 60 ug of protein from the sample extracts was electrophoresed in 12% Mini-PROTEAN TGX™ precast gels (Bio-Rad) using the electrophoresis system mini-PROTEAN Tetra Cell (Bio-Rad). Proteins were transferred onto PVDF 0.45-μm membranes using a mini Trans-blot Cell (Bio-Rad) or Trans-blot Cell (Bio-Rad) and probed with target antibodies. Protein–antibody interactions were detected with peroxidase-conjugated horse antimouse, anti-rabbit, or anti-goat IgG antibodies using Amersham ECL™ Prime Western Blotting Detection Reagent (GE Healthcare, Buckinghamshire, UK). Band quantification was carried out using an Image Station 2000R (Kodak, Spain) and a Kodak 1D 3.6 software. Protein band intensity was normalized to VDAC1 (mitochondrial proteins), and the data expressed in terms of percent relative to wild-type mice or control cells (Luna-Sanchez *et al.*, 2015). The following primary antibodies were used: anti-SQRDL (Proteintech, 17256-1-AP), anti-TST (Proteintech, 16311-1-AP), anti-CBS (Proteintech, 14787-1-AP), anti-PDSS2 (Proteintech, 13544-1-AP), anti-COQ2 (Origene, TA341982), anti-COQ4 (Proteintech, 16654-1-AP), anti-COQ5 (Proteintech, 17453-1-AP), anti-COQ6 (Proteintech, 12481-1-AP), anti-COQ7 (Proteintech, 15083-1-AP), anti-COQ8A (Proteintech, 15528-1-AP), anti-FGF21 (Abcam, ab171941) anti-VDAC1 (Abcam, ab14734), anti-GPx (Abcam, ab125066) and anti-GRd (Santa Cruz Biotechnology, sc-32886).

3.11 QUANTIFICATION OF CoQ_9 AND CoQ_{10} LEVELS IN MICE TISSUES

CoQ_9 and CoQ_{10} from mice tissues were extracted by mixing tissue extracts with 1- propanol. After 2 min vortex, the solution was centrifuged at 13,000 rpm for 5 min. The resultant supernatant was injected in a HPLC system (Gilson, WI, USA) and the lipid components were separated by a reverse phase Symmetry C18 3.5 μm, 4.6 x 150 mm column (Waters, Spain), using a mobile phase consisting of methanol, ethanol, 2- propanol, acetic acid (500:500:15:15) and 50 mM sodium acetate at a flow rate of 0.9 ml/min. The electrochemical detector consisted of an ESA Coulochem III with the following setting: guard cell (upstream of the injector) at +900 mV, conditioning cell at –600 mV (downstream of the column), followed by the analytical cell at +350 mV (32).

CoQ_9 and CoQ_{10} concentrations were estimated by comparison of the peak areas with those of standard solutions of known concentrations. The results were expressed in pmol CoQ/mg prot.

3.12 QUANTIFICATION OF β-RA AND 4-HB LEVELS IN MICE TISSUES

Tissues from mice were homogenized in water. The homogenate samples were then treated with a solution of methanol/water (80:20, v/v), shaked for 1 minute, sonicated for 15 minutes and then centrifuged at 5,000g for 25 minutes at 4ºC (Borges *et al*, 2017).

The supernatants were analyzed using a Thermo Scientific™ UltiMate™ 3000 UHPLC system (Waltham, Massachusetts, United States), consisting of an UltiMate™ 3000 UHPLC RS binary pump and an UltiMate™ 3000 UHPLC sample manager coupled to a Thermo Scientific™ Q Exactive™ Focus Hybrid Quadrupole-Orbitrap™ detector of mass spectrometer (MS/MS) with an electrospray ionization in negative mode (Waltham, Massachusetts, United States). The analytical separation column was a Hypersil GOLD™ C18, 3 µm, 4.6 × 150 mm column (Thermo Scientific™) and the flow rate was 0.6 ml/min. The mobile phase consisted of two solutions: eluent A (H2O + 0.1% Formic acid, MS grade, Thermo Scientific™) and eluent B (acetonitrile + 0.1% Formic acid, MS grade, Thermo Scientific™). Samples were eluted over 30 min with a gradient as follow: 0 min, 95% eluent A 0-25 min, 70% eluent A; 25-25.1 min, 95 % eluent A; 25.1-30 min, 95% eluent A. Capillary and auxiliary gas temperatures were set at 275 and 450 °C, respectively. Sheath gas flow rate used was at 55 arbitrary units, auxiliary gas flow rate used was at 15 arbitrary units, sweep gas flow was used at 3 arbitrary units. Mass spectrometry analyses were carried out in full scan mode between 110 and 190 uma. To quantify the levels of 4-HB and β–RA, we use a standard curve with both compounds at a concentration of 100 ng/ml, 10 ng/ml and 1 ng/ml.

3.13 QUANTIFICATION OF PRO-INFLAMMATORY MEDIATORS IN MURINE RAW 264.7 MACROPHAGES AND BRAINSTEM EXTRACTS

Concentrations of interleukin (IL)-1β, IL-2, interferon-γ (IFN-γ), tumor necrosis factor-α (TNF-α) and growth regulated oncogene-α (GRO-α) were quantified in duplicates in the supernatant of the cell culture of murine RAW 264.7 macrophages and brainstem tissue using ProcartaPlexTM Multiplex immunoassays (eBioscience), as previously described and according to the manufacturer instructions (Hinz *et al*, 2000; Reichmann *et al*, 2015).

3.14 STATISTICAL ANALYSIS

Number of animals in each group were calculated in order to detect gross ~60% changes in the biomarker's measurements (based upon alpha=0.05 and power of beta=0.8). We used the application available in: http://www.biomath.info/power/index.htm. Animals were genotyped and randomly assigned in experimental groups in separate cages by the technician of the animal facility. Most statistical analyses were performed using the Prism 6 scientific software. Data are expressed as the mean ± SD of six-ten experiments per group. A one-way ANOVA with a Tukey's post hoc test was used to compare the differences between three experimental groups. Studies with two experimental groups were evaluated using unpaired Student's t-test. A P-value of < 0.05 was considered to be statistically significant. Survival curve was analyzed by log-rank (Mantel-Cox) and the Gehan-Breslow-Wilcoxon tests. The statistical tests used for the transcriptomics and proteomics analyses are described in their respective section.

3.15 DATA AVAILABILITY

RNA-Seq data were generated as described above. The files have been uploaded to the National Center for Biotechnology Information (NCBI) database. Submission ID: SUB7245113; BioProject ID: PRJNA623208; http://www.ncbi.nlm.nih.gov/bioproject/623208.

The mass spectrometry proteomics data have been deposited to the ProteomeXchange (http://proteomecentral.proteomexchange.org) Consortium via the PRIDE partner repository with the dataset identifier PXD018311.

RESULTS

Part of the results showed in this thesis form part of the following international papers:

1. “*β-RA reduces DMQ/CoQ ratio and rescues the encephalopathic phenotype in Coq9*^{R239X} *mice*”. EMBO Molecular Medicine, 2019. DOI: 10.15252/emmm.201809466. **Article awarded with best paper of the month (February)** by the Biochemistry and Molecular Biology Spanish Society (SEBBM).

   Agustín Hidalgo-Gutiérrez, Eliana Barriocanal-Casado, Mohammed Bakkali, M Elena Díaz-Casado, Laura Sánchez-Maldonado, Miguel Romero, Ramy K Sayed, Cornelia Prehn, Germaine Escames, Juan Duarte, Darío Acuña-Castroviejo, Luis C López.

2. “*Coenzyme Q10 modulates sulfide metabolism and links the mitochondrial respiratory chain to pathways associated to one carbon metabolism*”. Human Molecular Genetics, 2020. DOI: 10.1093/hmg/ddaa214.

   Pilar González-García, **Agustín Hidalgo-Gutiérrez** (**Co-First Author**), Cristina Mascaraque, Eliana Barriocanal-Casado, Mohammed Bakkali, Marcello Ziosi, Ussipbek Botagoz Abdihankyzy, Sabina Sánchez-Hernández, Germaine Escames, Holger Prokisch, Francisco Martín, Catarina M. Quinzii and Luis C. López.

3. “*Toxic vs Therapeutic: The Dose-Dependent Effects of β-Resorcylic Acid Depend on Mitochondrial Metabolism*”. Authorea Repository, 2020. **Pending of submission** DOI: 10.22541/au.158938611.16011582. **Agustín Hidalgo-Gutiérrez**, Elena Díaz-Casado, Eliana Barriocanal-Casado, Pilar González-García, Mohammed Bakkali, Riccardo Chiozzi, Marcos Martínez-Ruíz, Dario Ancuna-Castroviejo, Luis C López

4. RESULTS

4.1 CoQ DEFICIENCY ALTERNATIVE THERAPY: 4-HB ANALOGUE. β-RESORCYLIC ACID

4.1.1 THE TREATMENT WITH β-RA RESCUES THE PHENOTYPE OF *Coq9*^{R239X} MICE

We previously demonstrated that *Coq9*^{R239X} mice have reduced size and body weight, and die between 3 to 7 months of age (Garcia-Corzo *et al.*, 2013). Moreover, we proved that ubiquinol-10 treatment induces biochemical and histopathological improvements in the brain of *Coq9*^{R239X} mice (Garcia-Corzo *et al*, 2014). These improvements leaded to a significant increase in the survival of *Coq9*^{R239X} mice treated with ubiquinol-10, compared to the *Coq9*^{R239X} mice. While the *Coq9*^{R239X} mice reached a maximum age of 7 months, with a median survival of 5 months of age, the *Coq9*^{R239X} mice treated with ubiquinol-10 reached a maximum age of 17 months, with a median survival of 13 months of age (Fig 1A). Interestingly, the therapeutic effect of oral β–RA supplementation resulted in an even greater increase in the survival of *Coq9*^{R239X} mice, reaching a maximum lifespan of 25 months of age, with a median survival of 22 months of age (Fig 1A). Therefore, the extension in the lifespan achieved by β–RA in *Coq9*^{R239X} mice reached values close to the lifespan in wild-type mice (Fig 1A). Analysis using the log-rank (Mantel-Cox) and the Gehan-Breslow-Wilcoxon tests show significant differences ($p < 0.0001$, and $p = 0.0017$, respectively) between *Coq9*^{R239X} mice and *Coq9*^{R239X} mice treated with β–RA (Fig 1A). Moreover, if the β–RA treatment started at 3 months of age (symptomatic period) instead of 1 month of age (asymptomatic period), 100% of the treated mice remained alive at 14 months of age (Fig 3B).

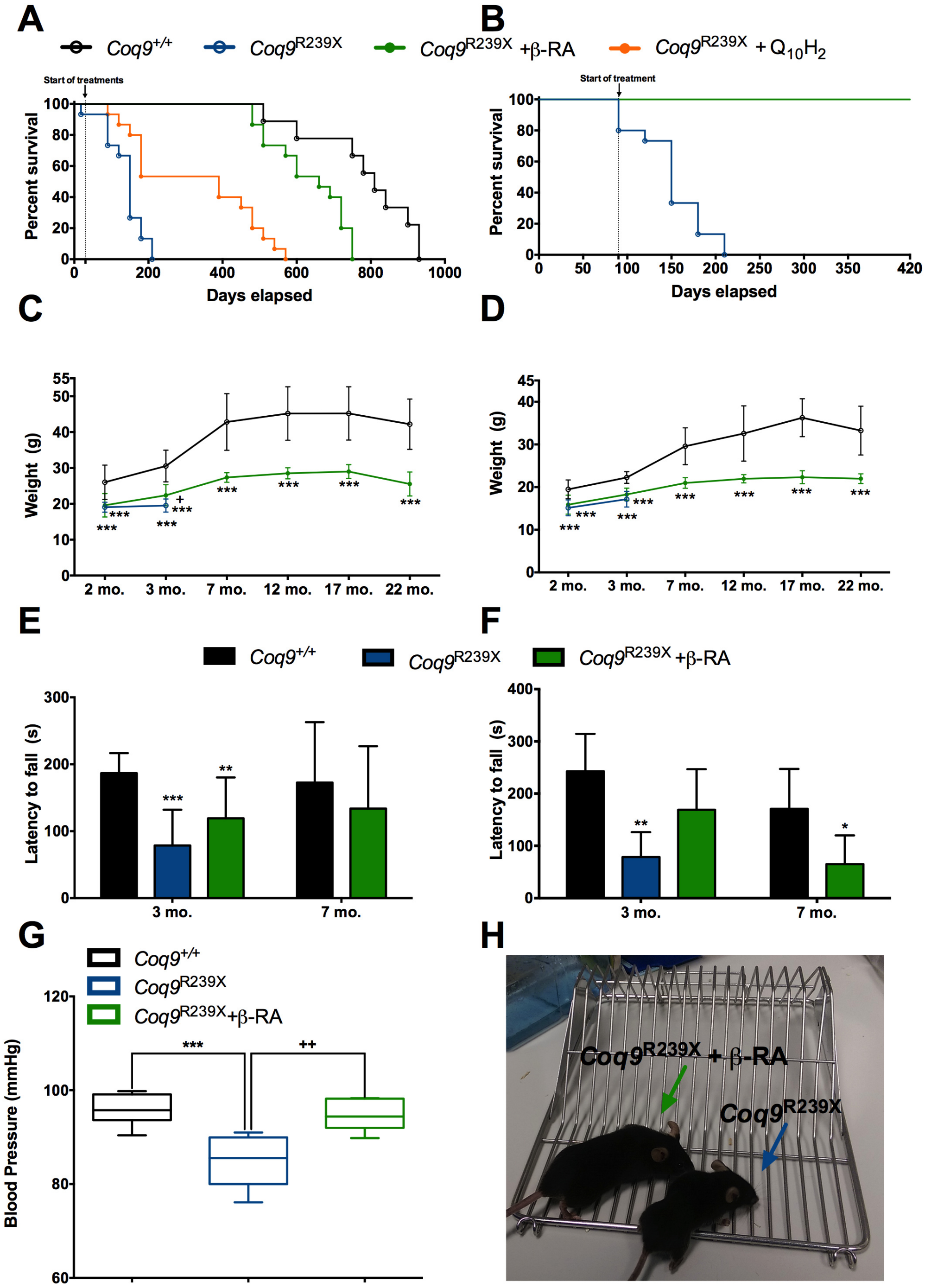

Figure 1. **Survival and phenotypic characterization of** ***Coq9***^{R239X} **mice after β–RA treatment.**

A Survival curve of the *Coq9*$^{+/+}$ mice, *Coq9*^{R239X} mice and *Coq9*^{R239X} mice after β–RA treatment and *Coq9*^{R239X} after ubiquinol-10 treatment. The treatments started at 1 month of age.
B Survival curve of the *Coq9*^{R239X} mice and *Coq9*^{R239X} mice after β–RA treatment started at 3 months of age.
C, D Body weight of males (C) and females (D) *Coq9*$^{+/+}$ mice, *Coq9*^{R239X} mice and *Coq9*^{R239X} mice after β–RA treatment.
E, F Rotarod test of male and female *Coq9*$^{+/+}$ mice, *Coq9*^{R239X} mice and *Coq9*^{R239X} mice after β–RA treatment.
G Blood pressure of *Coq9*$^{+/+}$ mice, *Coq9*^{R239X} mice and *Coq9*^{R239X} mice after β–RA treatment. Data from male and female mice are represented together.
H Comparative image of a *Coq9*^{R239X} mouse and a *Coq9*^{R239X} mouse after β–RA treatment at 4 months of age.
Data are expressed as mean ± SD. $^*P < 0.05$; $^{**}P < 0.01$; $^{***}P < 0.001$; *Coq9*^{R239X} or *Coq9*^{R239X} after β–RA treatment versus *Coq9*$^{+/+}$. $+P < 0.05$; *Coq9*^{R239X} versus *Coq9*^{R239X} after β–RA treatment (one-way ANOVA with a Tukey's post hoc test; n = 13–24 for each group).

The striking increase in survival was in parallel of/accompanied by a phenotypic improvement. *Coq9*$^{\mathrm{R239X}}$ mice treated with β–RA showed a slight increase in the body weight, although the values did not reach the wild-type levels (Fig 1C and D). The motor coordination tested by rotarod assay showed a decrease in the latency to fall in *Coq9*$^{\mathrm{R239X}}$ mice compared to *Coq9*$^{+/+}$ mice. The treatment with β–RA significantly attenuated the motor phenotype in *Coq9*$^{\mathrm{R239X}}$ mice, both in males and females (Fig 1E and F). The treatment also normalized the blood pressure (Fig 1G), while the blood cells and hemoglobin levels did not change in the experimental groups (Fig 2). The general health improvement of *Coq9*$^{\mathrm{R239X}}$ mice treated with β–RA was remarkable and their healthier aspect, compared to the untreated *Coq9*$^{\mathrm{R239X}}$ mice, was visible and could be easily appreciated (Fig 1H).

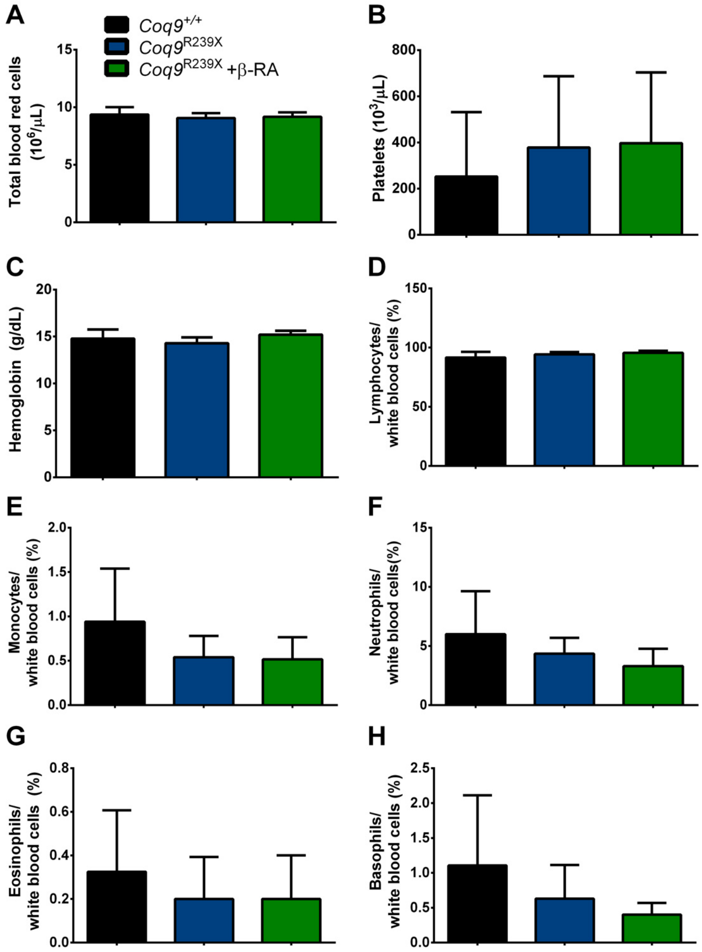

Figure 2. Hemogram after β-RA treatment.

A-H (A) Total blood cells, (B) number of platelets, (C) Hemoglobin levels, (D) percentage of lymphocytes, (E) percentage of monocytes, (F) percentage of neutrophils, (G) percentage of eosinophils and (H) percentage of basophils in $Coq9^{+/+}$ mice, $Coq9^{R239X}$ mice and $Coq9^{R239X}$ mice after β–RA treatment. Data are expressed as mean ± SD. (one-way ANOVA with Tukey's post hoc test; n = 6–10 for each group). No changes were observed after the treatment.

4.1.2 THE TREATMENT WITH Β-RA INDUCES A REDUCTION IN THE HISTOPATHOLOGICAL SIGNS OF THE ENCEPHALOPATHY

Because of the striking effect of the treatment on the survival and health status of the *Coq9*^{R239X} mice, we performed a histopathological evaluation of the brain, the main symptomatic tissue. The spongiform degeneration and reactive astrogliosis characteristic in the diencephalon and the pons of the *Coq9*^{R239X} mice (Fig 3B1, E1, H1 and K1; Fig 4) (Garcia-Corzo *et al.*, 2013), compared to *Coq9*$^{+/+}$ mice (Fig 3A1, D1, G1 and J1; Fig 4), almost disappeared after the β–RA treatment (Fig 3C1, F1, I1 and L1; Fig 4). The microglia distribution did not show any difference between the three experimental groups (Fig 3M1 to R1; Fig 4). Moreover, the increased protein oxidation observed in the diencephalon of *Coq9*^{R239X} mice (Fig 3T1), compared to *Coq9*$^{+/+}$ mice (Fig 3), was attenuated in *Coq9*^{R239X} mice treated with β–RA (Fig 3U1).

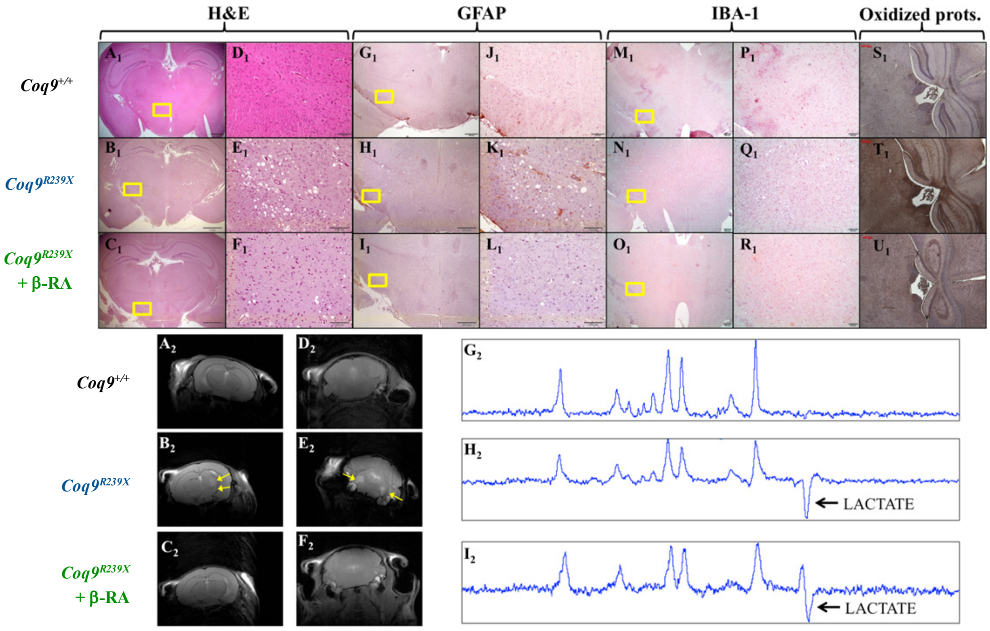
H&E
GFAP
IBA-1
Oxidized prots.
Coq9+/+
Coq9R239X
Coq9R239X + β-RA
A1
D1
G1
J1
M1
P1
S1
B1
E1
H1
K1
N1
Q1
T1
C1
F1
I1
L1
O1
R1
U1
Coq9+/+
Coq9R239X
Coq9R239X + β-RA
A2
D2
G2
B2
E2
H2
C2
F2
I2
LACTATE
LACTATE

Figure 3. **Pathological features in the brain of *Coq9*^{R239X} mice after β–RA treatment.**
A_1-F_1 H&E stain in the diencephalon of *Coq9*$^{+/+}$ mice (A_1 and D_1), *Coq9*^{R239X} mice (B_1 and E_1) and *Coq9*^{R239X} mice after β–RA treatment (C_1 and F_1).
G_1-L_1 Anti-GFAP stain in the diencephalon of *Coq9*$^{+/+}$ mice (G_1 and J_1), *Coq9*^{R239X} mice (H_1 and K_1) and *Coq9*^{R239X} mice after β–RA treatment (I_1 and L_1).
M_1-R1 Anti-Iba1 stain in the diencephalon of *Coq9*$^{+/+}$ mice (M_1 and P_1), *Coq9*^{R239X} mice (N_1 and Q_1) and *Coq9*^{R239X} mice after β–RA treatment (O_1 and R_1).
S_1-U_1 Protein oxidation in the diencephalon of *Coq9*$^{+/+}$ mice (S_1), *Coq9*^{R239X} mice (T_1) and *Coq9*^{R239X} mice after β–RA treatment (U_1).
A_2-C_2 Magnetic Resonance Images of the diencephalon of *Coq9*$^{+/+}$ mice (A_2), *Coq9*^{R239X} mice (B_2) and *Coq9*^{R239X} mice after β–RA treatment (C_2).
D_2-F_2 Magnetic Resonance Images of the pons of *Coq9*$^{+/+}$ mice (D_2), *Coq9*^{R239X} mice (E_2) and *Coq9*^{R239X} mice after β–RA treatment (F_2).
G_2-I_2 Lactate peak in the brain of *Coq9*$^{+/+}$ mice (G_2), *Coq9*^{R239X} mice (H_2) and *Coq9*^{R239X} mice after β–RA treatment (I_2).

The improvements in the histopathological features were further corroborated by magnetic resonance imaging (MRI). Brain injuries were observed in the diencephalon and the pons of *Coq9*^{R239X} mice (Fig 3B2 to E2; Fig 4). In *Coq9*$^{+/+}$ mice and *Coq9*^{R239X} mice treated with β–RA, however, we did not detect any sign of brain injury (Fig 3A2 and D2, and C2 and F2; Fig 4), suggesting that the treatment normalized the cerebral structure.

Nevertheless, the cerebral lactate levels, that are increased in *Coq9*^{R239X} mice (Fig 3H2) compared to *Coq9*$^{+/+}$ mice (Fig 3G2), remained increased in *Coq9*^{R239X} mice after the treatment (Fig 3I2).

In the skeletal muscle, the cytochrome c oxidase (COX) and succinate dehydrogenase (SDH) stainings showed an increase in type II fibers in

Coq9$^{\mathrm{R239X}}$ mice. After the treatment with β–RA, the proportion of type I and type II fibers was normalized (Fig 5).

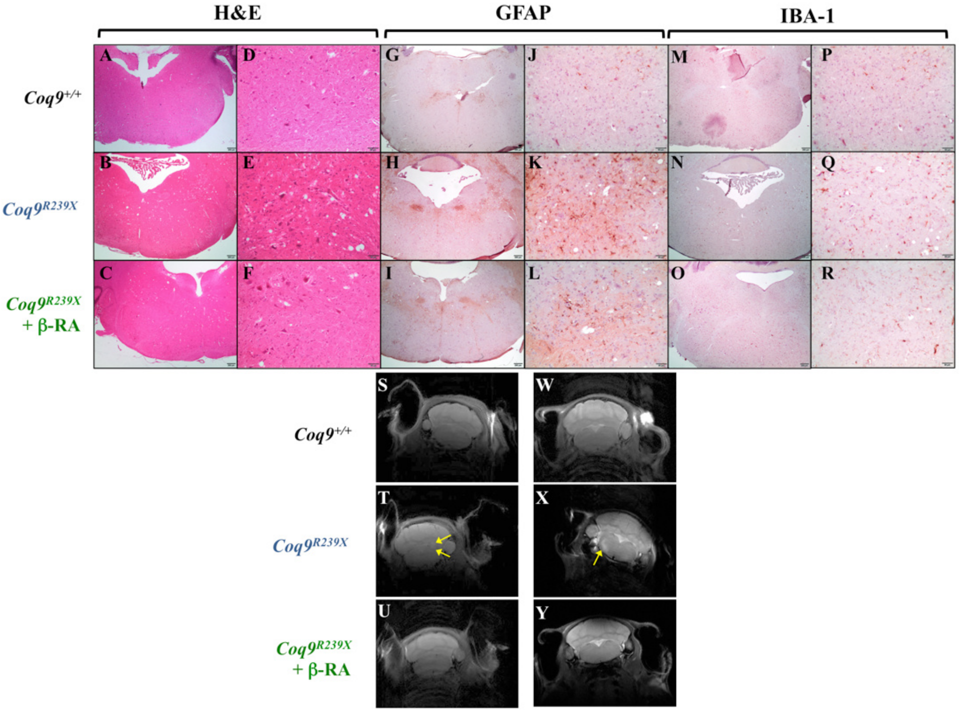
H&E
GFAP
IBA-1
Coq9$^{+/+}$
Coq9^{R239X}
Coq9^{R239X} + β-RA
A
D
G
J
M
P
B
E
H
K
N
Q
C
F
I
L
O
R
Coq9$^{+/+}$
Coq9^{R239X}
Coq9^{R239X} + β-RA
S
W
T
X
U
Y

Figure 4. **Structural changes and distribution of astrocytes and microglia in the pons of *Coq9*^{R239X} mice after β–RA treatment.**

A-F H&E stain in the pons of *Coq9*$^{+/+}$ mice (A and D), *Coq9*^{R239X} mice (B and E) and *Coq9*^{R239X} mice after β–RA treatment (C and F).

G-L Anti-GFAP stain in the pons of *Coq9*$^{+/+}$ mice (G and J), *Coq9*^{R239X} mice (H and K) and *Coq9*^{R239X} mice after β–RA treatment (I and L).

M-R Anti-Iba1 stain in the pons of *Coq9*$^{+/+}$ mice (M and P), *Coq9*^{R239X} mice (N and Q) and *Coq9*^{R239X} mice after β–RA treatment (O and R).

S-Y Magnetic Resonance Images of the diencephalon of *Coq9*$^{+/+}$ mice (S and W), *Coq9*^{R239X} mice (T and X) and *Coq9*^{R239X} mice after β–RA treatment (U and Y).

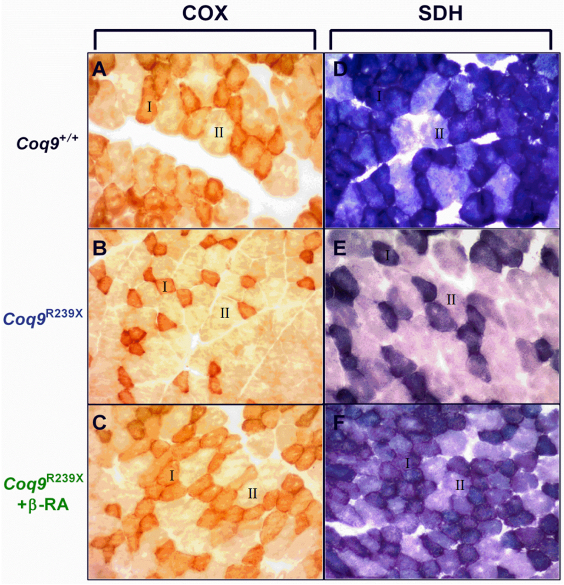

Figure 5. COX and SDH staining of grastrocnemius pons of *Coq9*^{R239X} mice after β–RA treatment.

A–C COX stains in *gastrocnemius* of *Coq9*$^{+/+}$ mice (A), *Coq9*^{R239X} mice (B), and *Coq9*^{R239X} mice after β-RA treatment (C).

D–F SDH stain in *gastrocnemius* of *Coq9*$^{+/+}$ mice (D), *Coq9*^{R239X} mice (E), and *Coq9*^{R239X} mice after β-RA treatment (F).Data information: “I” indicated fiber types I and “II” indicates fiber types II.

4.1.3 TRANSCRIPTOMICS PROFILE REVEALS A REDUCTION IN THE NEUROINFLAMMATORY GENES

Next, we carried out an RNA-Seq experiment on brainstems from the three experimental mice groups, e.g. *Coq9*$^{+/+}$, *Coq9*^{R239X} and *Coq9*^{R239X} treated with β–RA. The over 9x109 bases of the 101-bases sequencing reads aligned to 27291 loci of the reference mouse genome. As Fig 6A shows, 298 genes were over-expressed in the *Coq9*^{R239X} mice compared to the *Coq9*$^{+/+}$ mice, while

161 were under-expressed. On the other hand, 187 genes were over-expressed in the *Coq9*$^{\mathrm{R239X}}$ mice compared to the *Coq9*$^{\mathrm{R239X}}$ mice treated with β−RA, while 160 were under-expressed (Fig 6A). When comparing the pathways to which these differentially expressed genes belong, we observed a noticeably higher presence of genes belonging to inflammation signaling pathways in the *Coq9*$^{\mathrm{R239X}}$ mice compared to the β−RA treated *Coq9*$^{\mathrm{R239X}}$ or *Coq9*$^{+/+}$ mice (Fig 6B).

Of the 459 genes whose expression is significantly altered in *Coq9*$^{\mathrm{R239X}}$ mice compared to *Coq9*$^{+/+}$, 27 were significantly altered in *Coq9*$^{\mathrm{R239X}}$ mice treated with β−RA compared to *Coq9*$^{\mathrm{R239X}}$ mice. Interestingly, among these 27 genes, the ones that were over-expressed in *Coq9*$^{\mathrm{R239X}}$ mice, compared to the *Coq9*$^{+/+}$ mice, became under-expressed in *Coq9*$^{\mathrm{R239X}}$ mice treated with β−RA, compared to *Coq9*$^{\mathrm{R239X}}$ mice, and viceversa (Fig 6C). Thus, the levels of these 27 genes were normalized. Most of these genes showed higher expression in *Coq9*$^{\mathrm{R239X}}$ mice compared to *Coq9*$^{+/+}$ mice, and they mainly have inflammation and immune-related functions. For example, the inflammatory genes Bgn (biglycan), Ccl6 (chemokine C-C motif ligand 6), Cst7 (cystatin F), Ifi27l2a (interferon, alpha-inducible protein 27 like 2A), Ifitm3 (interferon induced transmembrane protein 3), Itgax (integrin alpha X) and Vav1 are up-regulated in *Coq9*$^{\mathrm{R239X}}$ mice and normalized after the treatment.

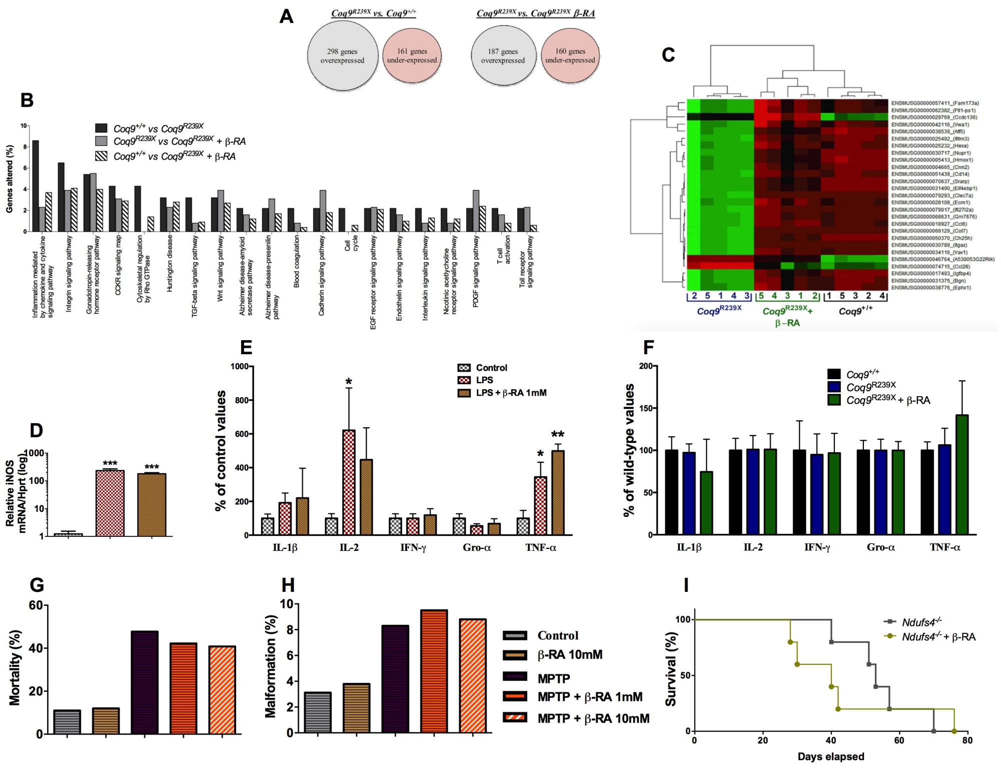

Figure 6. Effect of the β–RA treatment on genes expression profiles and neuroinflammatory-ralated features.

A Global differences in the levels of gene expression between experimental groups.

B Only pathways with more than one gene significantly altered in *Coq9*^{R239X} compared to *Coq9*$^{+/+}$ mice are considered for this figure (more details in Data file S1). The Y-axis represents the percentage of genes corresponding to a pathway in the sample of genes whose expression level is significantly altered in a comparison between mice samples.

C Heatmap showing the comparative landscape of the expression level per sample of the 27 genes whose expression was altered by the mutation and normalized by the β–RA treatment**.** The column numbers correspond to the different samples and the row names are genes codes composed of the ENSEMBL gene ID and the gene symbol (between parentheses). The green means comparatively higher, red means comparatively lower and black means no difference in expression level.

D iNOS expression levels in RAW cells after stimulation with LPS.

E Cytokines levels in the culture supernatant of RAW cells after stimulation with LPS;

F Cytokines levels in the brainstem of *Coq9*$^{+/+}$ mice, *Coq9*^{R239X} mice and *Coq9*^{R239X} mice treated with β–RA.

G, H Mortality rate (G) and (H) percentage of malformations in zebrafish embryos treated with MPT and the effect of β–RA treatment.

I Survival curve of *Ndufs4* knockout mice and *Ndufs4* knockout mice treated with β–RA. Data are expressed as mean ± SD. $^*P < 0.05$; $^{**}P < 0.01$; $^{**}P < 0.001$; LPS or LPS + β–RA *versus* control; also *Coq9*^{R239X} or *Coq9*^{R239X} after β–RA treatment versus *Coq9*$^{+/+}$. $^+P < 0.05$; LPS or LPS + β–RA versus control; also *Coq9*^{R239X} after treatment with β–RA *versus* *Coq9*^{R239X} (one-way ANOVA with a Tukey's post hoc test; n = 5–7 for each group).

4.1.4 β-RA DOES NOT DIRECTLY ACT AS ANTI-INFLAMMATORY AGENT

Because the transcriptomics profile uncovers a possible involvement of neuroinflammation in the therapeutic effect of β–RA, and since this molecule is an analogue of the anti-inflammatory salicylic acid, we tested whether β–RA may have a direct anti-inflammatory action. First, we incubated RAW cells with 1 μg/ml LPS, which induces a NF-kB-mediated inflammatory response, as it is shown by the induction of iNOS (Fig 6D) and the release of IL-1β, IL-2 and TNF-α (Fig 6E). The pre-incubation with β–RA, however, did not modify the cellular iNOS expression (Fig 6D) or the cytokines levels in the cells supernatants (Fig 6E). Second, we quantified the cytokines levels in the brainstem of the three animals' experimental groups. The levels of IL-1β, IL-2, IFN-γ, Gro-α and TNF-a did not experience major changes (Fig 6F). Third, we tested whether β–RA may increase the survival in two models of neuroinflammation and early death due to mitochondrial Complex I deficiency, i.e. the zebrafish embryos treated with MPTP, which mimics Parkinson Disease (Diaz-Casado *et al.*, 2018); and the Ndufs4 knockout mouse model, which mimics Leigh Syndrome (Quintana *et al.*, 2010). In both cases, the treatment with β–RA did not induce any change in the animal survival (Fig 1, G and I) or the presence of malformations (Fig 6H). Because the inhibition of mTORC1 may mediate the anti-inflammatory actions of salicylates (Cameron *et al*, 2016), we also quantified the S6RP/S6R ratio as a marker of mTORC1 activity. Consistently with the other data, the β–RA did not modify the S6RP/S6R ratio in the brain (Fig 7A) and the kidneys (Fig 7B) of *Coq9*^{R239X} mice treated with β–RA, suggesting that this molecule does not inhibit mTORC1 in vivo. Overall, these results do not support a direct role of β–RA in the repression of the typical neuroinflammatory pathways.

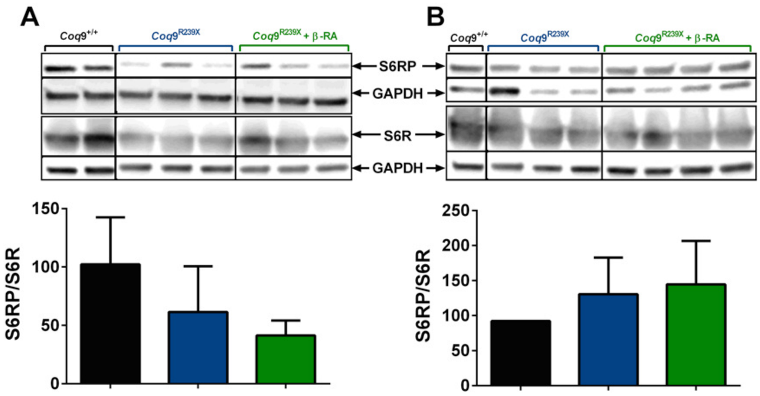

Figure 7. Assessment of the potential capacity of β–RA to inhibit mTORC1.
A–B S6PR/S6R ratio in the brain (A) and the kidneys (B) of *Coq9*$^{+/+}$ mice, *Coq9*^{R239X} mice and *Coq9*^{R239X} mice treated with β–RA.

4.1.5 β-RA IMPROVES MITOCHONDRIAL BIOENERGETICS IN PERIPHERAL TISSUES OF *Coq9*^{R239X} MICE

The persistent lactate peak observed in the brain spectroscopy after the β–RA treatment suggests that the treatment does not have any effect on mitochondrial bioenergetics in the brain. To confirm this premise, we evaluated the mitochondrial function in the brain, but also in the kidneys, muscle and heart (tissues clinically important in CoQ deficiency syndrome) of *Coq9*$^{+/+}$ mice, *Coq9*^{R239X} mice and *Coq9*^{R239X} mice treated with β–RA.

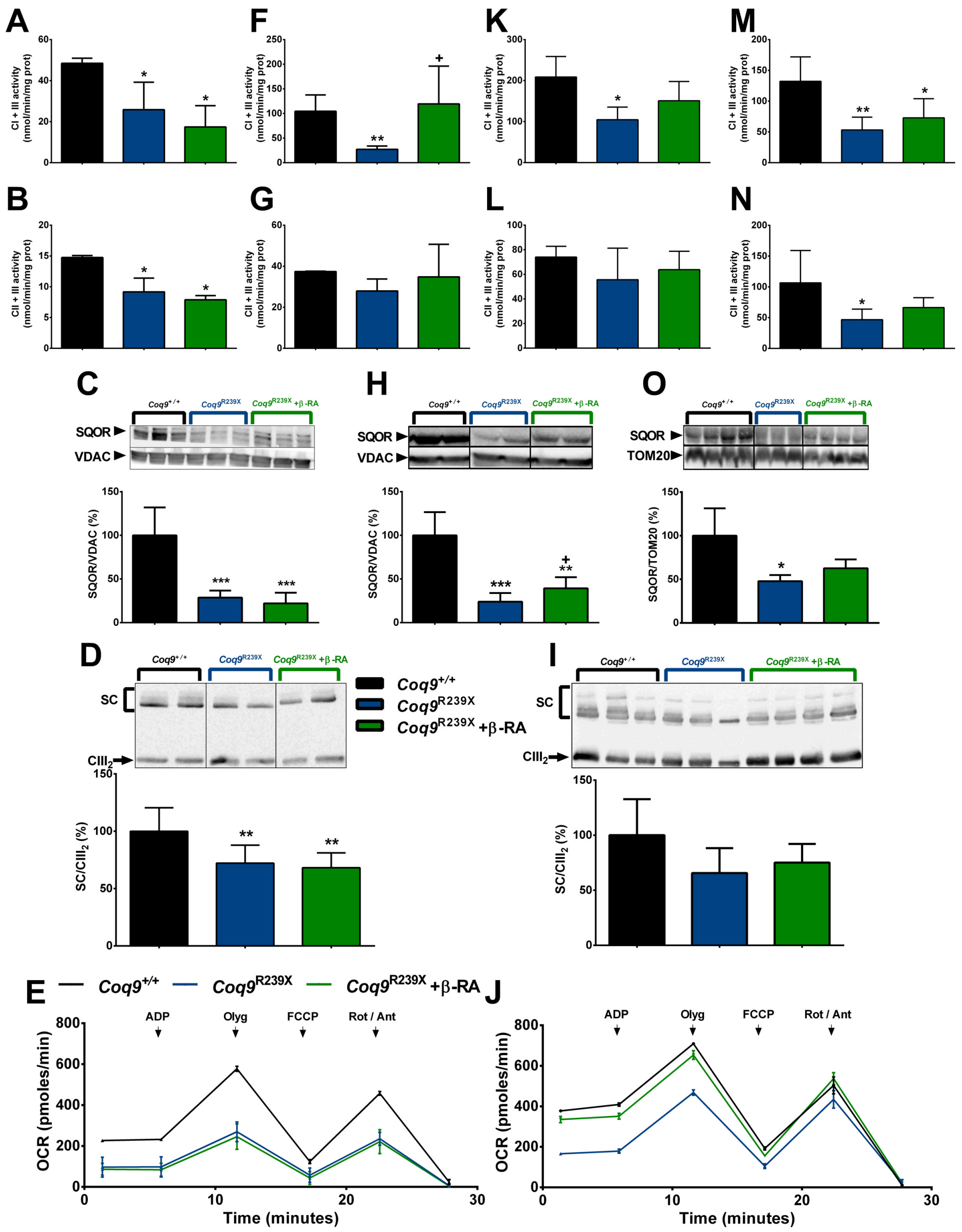

Figure 8. Tissue-specific differences in mitochondrial function after β–RA treatment in *Coq9^{R239X}* mice.

A, F, K, M CoQ-dependent Complex I + III activities in brain (A) and kidneys (F), skeletal muscle (K) and heart (M)

B, G, L, N CoQ-dependent Complex II + III activities in brain (B) and kidneys (G), skeletal muscle (L) and heart (N).

C, H, O Representative Western blot and quantitation of Western blot bands of SQOR in mitochondrial fractions of brain (C) and homogenates extracts from kidneys (H) and heart (O).
D, I BNGE followed by C-III immunoblotting analysis of mitochondrial supercomplexes in brain (D) and kidneys (I).
E, J Mitochondrial Oxygen Consumption rate (represented as State 3o, in the presence of ADP and substrates) in brain (E) and kidneys (J). *Coq9*$^{+/+}$ mice, *Coq9*^{R239X} mice and *Coq9*^{R239X} mice after β–RA treatment were included in all graphs. Data are expressed as mean ± SD. *P < 0.05; **P < 0.01; *Coq9*^{R239X} or *Coq9*^{R239X} after β–RA treatment versus *Coq9*$^{+/+}$. +P < 0.05; *Coq9*^{R239X} versus and *Coq9*^{R239X} after β–RA treatment (one-way ANOVA with a Tukey's post hoc test; n = 6–9 for each group).

In the brain of the mutant mice, the activities of the CoQ-dependent mitochondrial Complexes I+III (CI+III) and CII+III, the levels of SQOR, the assembly of CIII into the supercomplexes (SC) and the mitochondrial oxygen consumption rate (OCR) were significantly decreased (Fig 8A to E) compared to the values of wild-type animals. The β–RA treatment did not induce any change in those parameters in the brain of *Coq9*^{R239X} mice (Fig 8A to E). In the kidneys of the mutant mice, the activity of the CI+III, the levels of SQOR and the OCR were significantly decreased (Fig 8F to J), compared to the values of wild-type animals. These changes were not due to a potential capability of β–RA to act as an electron carrier in the mitochondrial respiratory chain because the CI+III activity did not change after adding 50 μM β–RA (Fig 9). The β–RA treatment normalized the CI+III activity and induced a significant increase of SQOR levels and the OCR (Fig 8F to J). On the contrary, assembly of CI into the supercomplexes did not change in any experimental group (Fig 10A and B). In the skeletal muscle of the mutant mice, the activity of the CI+III was significantly decreased while the CII+III activity did not change (Fig 8K and L), compared to the values of wild-type animals. The β–RA treatment normalized the CI+III activity (Fig 8K). In the heart of *Coq9*^{R239X} mice, the activities of the CI+III and CII+III, as well as the levels of SQOR were significantly decreased (Fig 8M to O), compared to the values of wild-type animals. Again, the β–RA treatment partially normalized the CI+III, CII+III activities and the levels of SQOR, although partially in this case (Fig 8M to O). Therefore, these results illustrate tissue-specific responses to β–RA treatment in the mitochondrial bioenergetics.

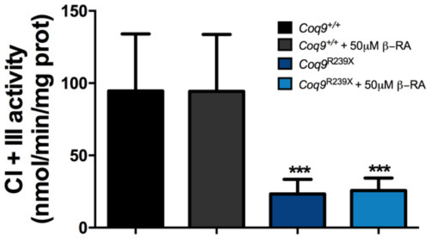

Figure 9. Effect of the addition of 50 μM β–RA into the reaction mix for measuring CI+III activity in isolated mitochondria from kidneys.

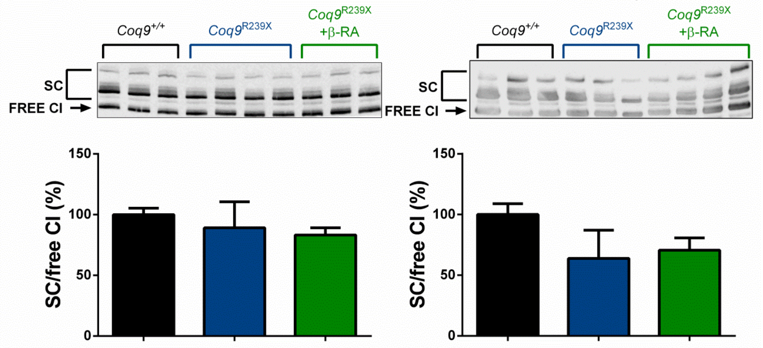

Figure 10. Mitochondrial complex I superassembly in the brain (A) and kidneys (B) of *Coq9*$^{+/+}$ mice, *Coq9*^{R239X} mice and *Coq9*^{R239X} mice after β–RA treatment.

4.1.6 β-RA REDUCES DMQ$_9$ IN PERIPHERAL TISSUES OF *Coq9*^{R239X} MICE

Coq9^{R239X} mice present widespread deficiency of CoQ$_9$ (major CoQ form in rodents) and CoQ$_{10}$ (minor CoQ form in rodents). Because COQ9 protein is needed for the COQ7 hydroxylation reaction, *Coq9*^{R239X} mice also show accumulation of DMQ$_9$, the substrate of COQ7 (Garcia-Corzo *et al.*, 2013). To test whether the general health improvement after β–RA treatment was due to the effects of this compound on CoQ biosynthesis, and to check whether the tissue-specific differences in mitochondrial bioenergetics were due to variances in the CoQ metabolism, we measured the levels of CoQ$_9$, CoQ$_{10}$ and DMQ$_9$ in the most relevant tissues. As previously reported, the levels of CoQ$_9$ (Fig 11A, E, I, M and Q) and CoQ$_{10}$ (Fig 11B, F, J, N and R) were severely decreased in the brain (Fig 11A and B), kidneys (Fig 11E and F), liver (Fig 11I and J), skeletal muscle (Fig 11M and N) and heart (Fig 11Q and R) of *Coq9*^{R239X} mice. In parallel, the levels of DMQ$_9$ were significantly increased in the same tissues (Fig 11C, G, K, O and S) and, therefore, the DMQ$_9$/CoQ$_9$ ratios were significantly increased (Fig 11D, H, L, P and T) in *Coq9*^{R239X} mice. After the treatment with β–RA, the levels of CoQ$_9$ significantly increased only in the kidneys (Fig 11E), but not in the other tissues (Fig 11A, I, M and Q) of the mutant mice. CoQ_{10} also showed a trend toward increased levels in the kidneys of *Coq9*^{R239X} mice after β–RA treatment (Fig 11F), although in the other tissues the levels of CoQ_{10} did not change after β–RA treatment (Fig 11B, J, N and R). Importantly, the levels of DMQ_9 and, consequently, the DMQ_9/CoQ_9 ratios were significantly decreased in the kidneys (Fig 11G and H), liver (Fig 11K and L), skeletal muscle (Fig 11O and P) and heart (Fig 11S and T) of *Coq9*^{R239X} mice treated with β–RA, suggesting that β–RA exerts an influence in the CoQ biosynthetic pathway. In the brain, however, the β–RA treatment did not induce changes in the levels of DMQ_9 or DMQ_9/CoQ_9 ratio (Fig 11C and D). Taken together, these results suggest that the improvement of mitochondrial bioenergetics occurs only in the tissues with decreased DMQ_9/CoQ_9 ratio after the treatment.

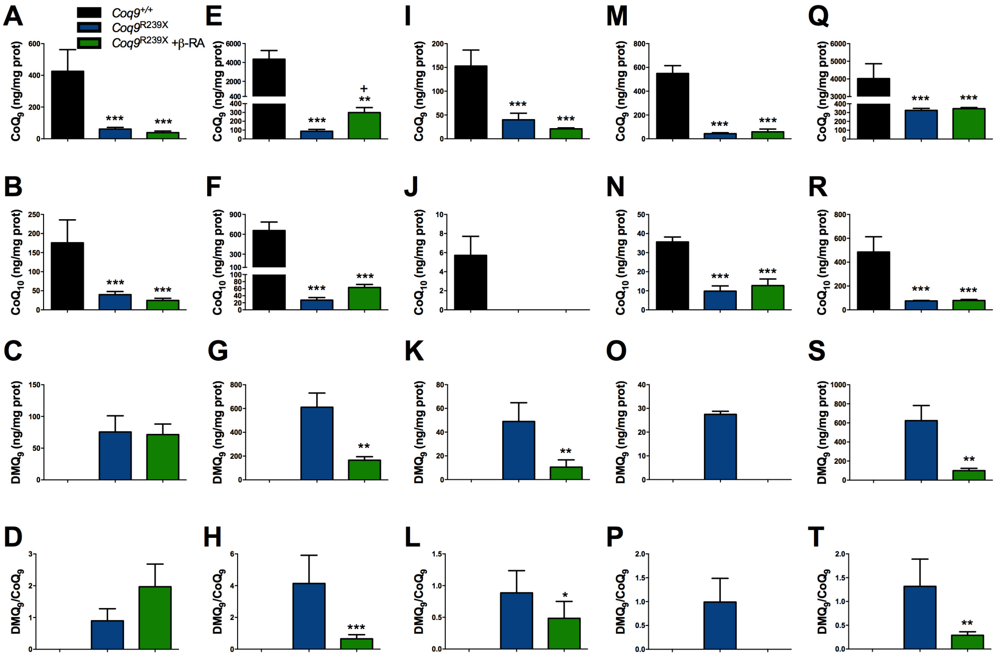

Figure 11. Tissue-specific differences in the levels of CoQ$_9$, CoQ$_{10}$ and DMQ$_9$, and in the DMQ$_9$/CoQ$_9$ ratio after β–RA treatment in *Coq9*^{R239X} mice.
A-T Levels of CoQ$_9$ (A, E, I, M, Q), CoQ$_{10}$ (B, F, J, N, R) and DMQ$_9$ (C, G, K, O, S), as well as and DMQ$_9$/CoQ$_9$ ratio (D, H, L, P, T) in brain (A-D), kidney (E-H), liver (I-L), skeletal muscle (M-P) and heart (Q-T) of *Coq9*$^{+/+}$ mice*, Coq9*^{R239X} mice and *Coq9*^{R239X} mice after β–RA treatment. Data are expressed as mean ± SD. $*P < 0.05$; $**P < 0.01$; $***P < 0.001$; *Coq9*^{R239X} or *Coq9*^{R239X} after β–RA treatment versus *Coq9*$^{+/+}$. $+P < 0.05$; $++P < 0.01$; $+P < 0.001$; *Coq9*^{R239X} versus *Coq9*^{R239X} after β–RA treatment (one-way ANOVA with a Tukey's post hoc test; n = 5–6 for each group).

To check whether the levels of CoQ$_9$ and DMQ$_9$ can be further modified during the time of the treatment or with a higher dose of β–RA, we also quantified the levels of both quinones in tissues of mice after 9 month of treatment or with the double dose of β–RA. The results showed that the levels of DMQ$_9$ levels and the DMQ$_9$ ratio were decreased in these two other experimental variants (Table 1 and Fig 12 and 13). However, no major differences were found in the results obtained under three experimental situations.

Table 1. Relative levels CoQ$_9$ and DMQ$_9$/CoQ$_9$ ratio in tissues of mice treated with β–RA.

		1 g of β-RA/kg b.w./day - 2 months after treatment			
		***Coq9*$^{+/+}$**	***Coq9*^{R239X}**	***Coq9*^{R239X}+β-RA**	**Fold change**
CoQ$_9$ (% relative to *Coq9*$^{+/+}$)	Brain	**100**	14.34 ± 2.51	9.07 ± 2.36	0.63
	Kidney	**100**	2.00 ± 0.47	6.87 ± 1.29	3.43
	Skeletal muscle	**100**	7.85 ± 1.47	10.58 ± 4.26	1.34
DMQ$_9$/CoQ$_9$	Brain	**0**	1.21 ± 0.23	1.97 ± 0.71	1.63
	Kidney	**0**	6.14 ± 0.6	0.65 ± 0.26	0.11
	Skeletal muscle	**0**	0.65 ±0.09	0	0
		1 g of β-RA/kg b.w./day - 9 months after treatment			
		***Coq9*$^{+/+}$**	***Coq9*^{R239X}**	***Coq9*^{R239X}+β-RA**	**Fold change**
CoQ$_9$ (% relative to *Coq9*$^{+/+}$)	Brain	**100**	-	9.91 ± 4.16	-
	Kidney	**100**	-	7.29 ± 2.8	-
	Skeletal muscle	**100**	-	8.28 ± 2.36	-
DMQ$_9$/CoQ$_9$	Brain	**0**	-	1.06 ± 0.5	-
	Kidney	**0**	-	0.32 ± 0.07	-
	Skeletal muscle	**0**	-	0	-
		2 g of β-RA*kg b.w./day - 1 month after treatment			
		***Coq9*$^{+/+}$**	***Coq9*^{R239X}**	***Coq9*^{R239X}+β-RA**	**Fold change**
CoQ$_9$ (% relative to *Coq9*$^{+/+}$)	Brain	**100**	11.47 ± 6.47	8.53 ± 2.56	0.74
	Kidney	**100**	3.79 ± 2.27	9.67 ± 5	2.55
	Skeletal muscle	**100**	8.96 ± 3.58	15.95 ± 7.11	1.78
DMQ$_9$/CoQ$_9$	Brain	**0**	0.92 ± 0.48	0.87 ± 0.17	0.95
	Kidney	**0**	6.59 ± 0.96	0.26 ± 0.13	0.04
	Skeletal muscle	**0**	0.87 ± 0.61	0	0

The measurements were done in tissues of mice under three experimental conditions: 1) two months after the treatment with β–RA at a dose of 1 g of β–RA/kg b.w./day (upper segment of the table); 2) nine months after the treatment with β–RA at a dose of 1 g of β–RA/kg b.w./day (intermediate segment of the table); and 3) one month after the treatment with β–RA at a dose of 2 g of β–RA/kg b.w./day (lower segment of the table). The fold change values have been calculated by dividing the results in *Coq9*^{R239X} mice and *Coq9*^{R239X} mice treated with β–RA.

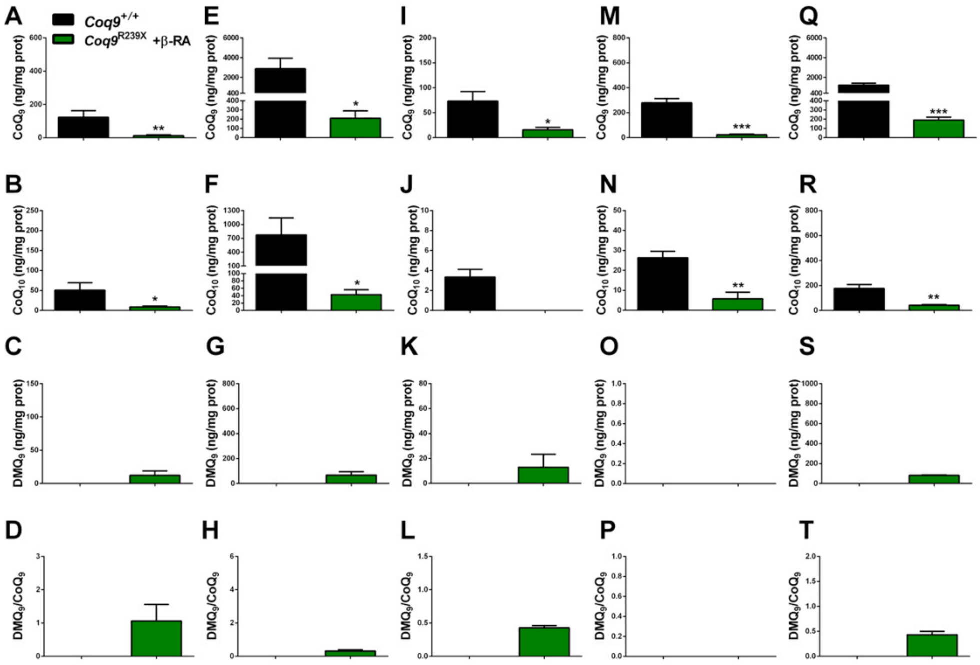

Figure 12. Tissue-specific differences in the levels of CoQ$_9$, CoQ$_{10}$ and DMQ$_9$, and in the DMQ$_9$/CoQ$_9$ ratio after 9 months of β -RA treatment in *Coq9*^{R239X} mice.

A-T Levels of CoQ$_9$ (A, E, I, M, Q), CoQ$_{10}$ (B, F, J, N, R) and DMQ$_9$ (C, G, K, O, S), as well as and DMQ$_9$/CoQ$_9$ ratio (D, H, L, P, T) in brain (A-D), kidney (E-H), liver (I-L), skeletal muscle (M-P) and heart (Q-T) of *Coq9*$^{+/+}$ mice and *Coq9*^{R239X} mice after β -RA treatment. Note that data from Coq9^{R239X} mice are not shown since 100 % the animals are dead at 7 months of age. Data are expressed as mean ± SD. *P < 0.05; **P < 0.01; ***P < 0.001; *Coq9*^{R239X} or *Coq9*^{R239X} after β -RA treatment versus *Coq9*$^{+/+}$. +P < 0.05; ++P < 0.01; +P < 0.001; *Coq9*^{R239X} versus *Coq9*^{R239X} after β -RA treatment (one-way ANOVA with a Tukey's post hoc test; n = 3-4 for each group).

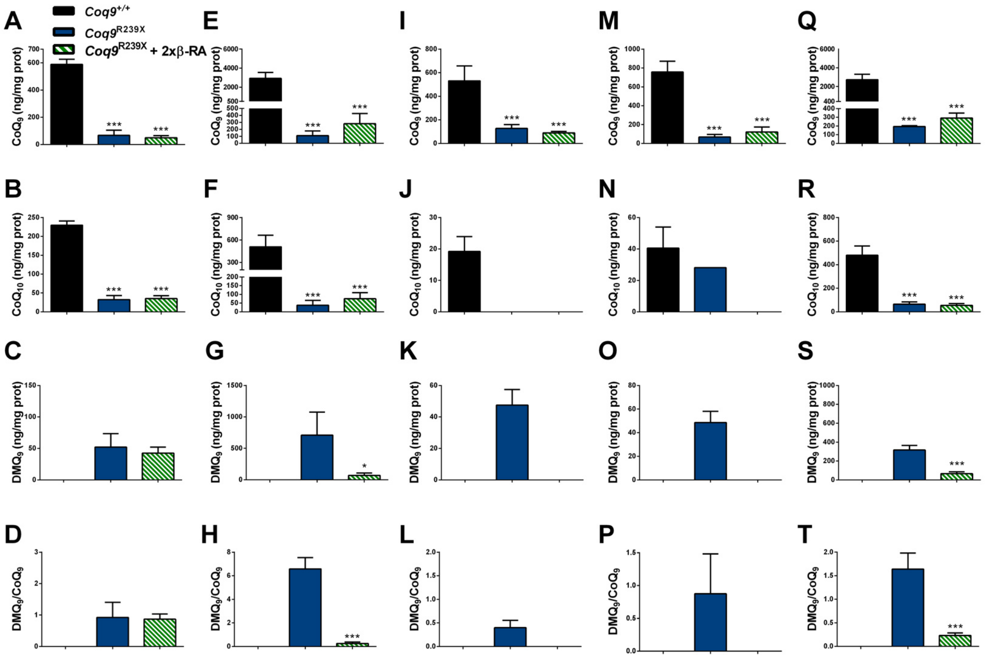

Figure 13. Tissue-specific differences in the levels of CoQ$_9$, CoQ$_{10}$ and DMQ$_9$, and in the DMQ$_9$/CoQ$_9$ ratio after 1 month of β-RA treatment at a dose of 3 g/kg b.w./day.

A-T Levels of CoQ$_9$ (A, E, I, M, Q), CoQ$_{10}$ (B, F, J, N, R) and DMQ$_9$ (C, G, K, O, S), as well as and DMQ$_9$/CoQ$_9$ ratio (D, H, L, P, T) in brain (A-D), kidney (E-H), liver (I-L), skeletal muscle (M-P) and heart (Q-T) of *Coq9*$^{+/+}$ mice and *Coq9*^{R239X} mice after β-RA treatment. 2x = double dose. Data are expressed as mean ± SD. *P < 0.05; **P < 0.01; ***P < 0.001; *Coq9*^{R239X} or *Coq9*^{R239X} after β-RA treatment versus *Coq9*$^{+/+}$. +P < 0.05; ++P < 0.01; +P < 0.001; *Coq9*^{R239X} versus *Coq9*^{R239X} after β-RA treatment (one-way ANOVA with a Tukey's post hoc test; n = 3–4 for each group).

Because the tissue-specific differences observed in DMQ$_9$/CoQ$_9$ ratio after β–RA treatment could be due to the bioavailability of this compound in the tissues after oral supplementation, we quantified the levels of β–RA in *Coq9*^{R239X} mice after oral supplementation and compared the data to those obtained after acute intraperitoneal (i.p.) administration. The compound was detected in all the examined tissues, including the brain, by both oral and i.p. administration (Table 2 and Fig 14). The highest values of β–RA were found in plasma and kidneys, while the results in brain and liver were similar (Table 2 and Fig 14). In the non-treated animals, β−RA was not detected, except in the kidney of one animal (Table 2 and Fig 14). The other hydroxybenzoic acid detected in the samples was the 4-HB, but no statistic differences were found between the experimental groups (Table 3). Therefore, the bioavailability of β−RA does not completely explain the tissue-specific differences in CoQ metabolism since brain and liver showed similar levels of β−RA.

Table 2. Levels of 4-HB in plasma and tissues of the mutant mice after oral or i.p. administration of β-RA.

Genotype	**Administration Route**	**Time of sample collection**	**Number of samples with detected levels of 4-HB**	**Type of Samples**	**Levels of 4-HB (pg/mg prot)**
Coq9$^{+/+}$	not treated	7:30-9:00	2/3	Brain	90.63 ± 22.89
Coq9^{R239X}	not treated	7:30-9:00	3/3	Brain	78.69 ± 2.35
Coq9^{R239X}	oral	7:30-9:00	6/6	Brain	82.35 ± 48.91
Coq9$^{+/+}$	not treated	7:30-9:00	3/3	Liver	61.08 ± 14.53
Coq9^{R239X}	not treated	7:30-9:00	2/3	Liver	39.16 ± 6.24
Coq9^{R239X}	oral	7:30-9:00	6/6	Liver	82.30 ± 35.73
Coq9$^{+/+}$	not treated	7:30-9:00	3/3	Kidney	144.72 ± 76.52
Coq9^{R239X}	not treated	7:30-9:00	3/3	Kidney	105.78 ± 40.93
Coq9^{R239X}	oral	7:30-9:00	6/6	Kidney	139.86 ± 37.5

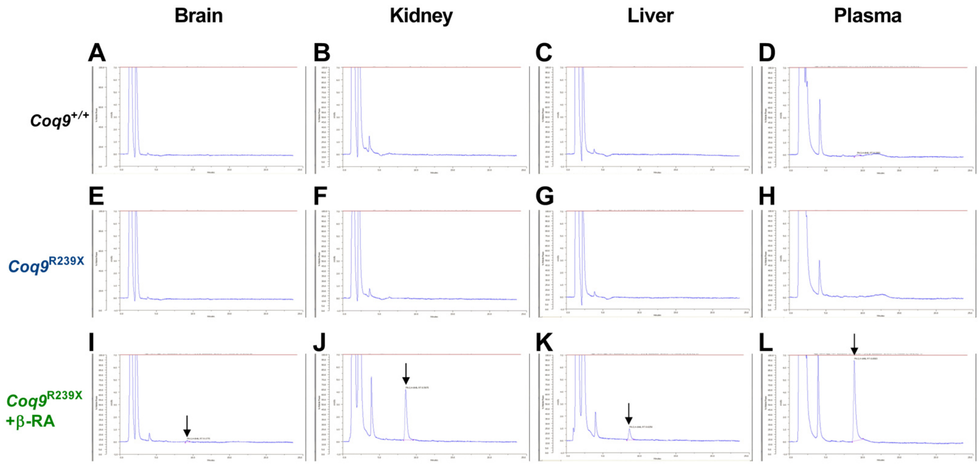

Figure 14. Representative chromatographs showing the peak of β–RA in mice tissues and plasma after the treatment.

A-D Chromatographs for β-RA in tissues and plasma from *Coq9*$^{+/+}$ mice; (E to H) Chromatographs for β-RA in tissues and samples from *Coq9*^{R239X}, (I to L) Chromatographs for β -RA in tissues and samples from *Coq9*^{R239X} after β-RA treatment.

Table 3. Levels of β-RA in plasma and tissues of the mutant mice after oral or i.p. administration of β-RA

Genotype	Administration Route	Time of sample collection	Number of samples with detected levels of β-RA	Type of Samples	Levels of β-RA (μg/mg prot)
Coq9^{R239X}	not treated	7:30-9:00	0/3	Brain	UND
Coq9^{R239X}	oral	7:30-9:00	3/8	Brain	21.3 ± 1.32
Coq9^{R239X}	i.p.	30 min after injection	3/3	Brain	14.49 ± 2.17
Coq9^{R239X}	not treated	7:30-9:00	0/3	Liver	UND
Coq9^{R239X}	oral	7:30-9:00	6/8	Liver	37.34 ± 14.28
Coq9^{R239X}	i.p.	30 min after injection	3/3	Liver	20.91 ± 6.21
Coq9^{R239X}	not treated	7:30-9:00	1/3	Kidney	21.9
Coq9^{R239X}	oral	7:30-9:00	8/8	Kidney	163.08 ± 133.84
Coq9^{R239X}	i.p.	30 min after injection	3/3	Kidney	89.74 ±34.81
Coq9^{R239X}	not treated	7:30-9:00	0/2	Plasma	UND
Coq9^{R239X}	oral	7:30-9:00	5/5	Plasma	360.71 ± 265.29
Coq9^{R239X}	i.p.	30 min after injection	3/3	Plasma	116.3 ±13.62

i.p. = intraperitoneal; UND = undetected

4.1.7 THE EFFECT OF β-RA OVER CoQ BIOSYNTHETIC PATHWAY IS PARTIALLY MEDIATED BY A STABILIZATION OF THE COMPLEX Q

To try to understand the mechanism involved in the reduction in the levels of DMQ_9 observed after β–RA treatment, we quantified the levels of main CoQ biosynthetic proteins. The levels of PDSS2 and COQ2, which do not form part of the Complex Q, did not experience major changes in the brain (Fig 15A and B), kidneys (Fig 15C and D) and heart (Fig 15E and F) of the three experimental groups, and only a decrease in the COQ2 levels was appreciated in the kidneys of *Coq9*^{R239X} mice (Fig 15D). The levels of COQ4, COQ5, COQ6, COQ7 and COQ8A, which are components of the Complex Q, were consistently decreased in the brain (Fig 16A to F), kidneys (Fig 16G to K) and heart (Fig 16L to P) of *Coq9*^{R239X} mice compared to the same tissues in *Coq9*$^{+/+}$ mice. Interestingly, the treatment with β−RA induced a trend toward increase on the levels of COQ4, COQ5, COQ6 and COQ8A in the kidneys (Fig 16G, H, I, K) and heart (Fig 16L, M, N, P), but not in the brain (Fig 16A, B, D, F). On the contrary, the levels of COQ7, which physically interacts with COQ9, were not modified by the β−RA treatment in any of the three tissues (Fig 16D, J, T). Overall, these results suggest that β−RA may induce the stabilization of the Complex Q, resulting in a decrease in the DMQ_9/CoQ_9 ratio.

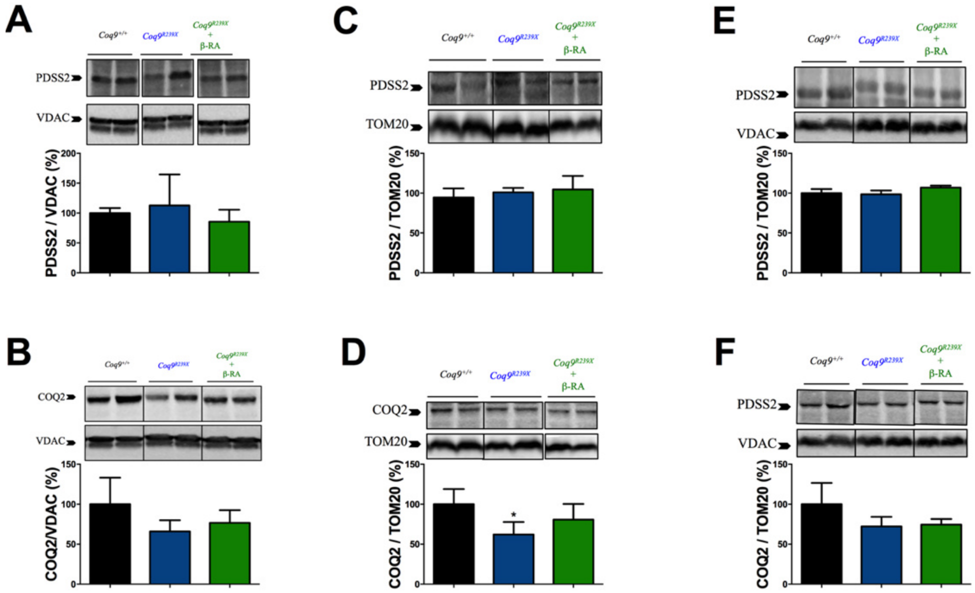

Figure 15. Effect of β–RA treatment in the tissue levels of CoQ biosynthetic proteins not involved in Complex Q.

A-F Representative images of western blots of the CoQ biosynthetic proteins PDSS2 and COQ2 and the quantitation of the protein bands in the brain (A and B), kidneys (C and D) and heart (E to F) of *Coq9*$^{+/+}$, *Coq9*^{R239X} *and Coq9*^{R239X} mice treated with β–RA. *Coq9*$^{+/+}$ mice*,* *Coq9*^{R239X} mice and *Coq9*^{R239X} mice after β–RA treatment were included in all graphs. Data are expressed as mean ± SD. *P < 0.05; **P < 0.01; ***P < 0.001; *Coq9*^{R239X} or *Coq9*^{R239X} after β–RA treatment versus *Coq9*$^{+/+}$. +P < 0.05; *Coq9*^{R239X} versus and *Coq9*^{R239X} after β–RA treatment (one-way ANOVA with a Tukey's post hoc test; n = 4–6 for each group).

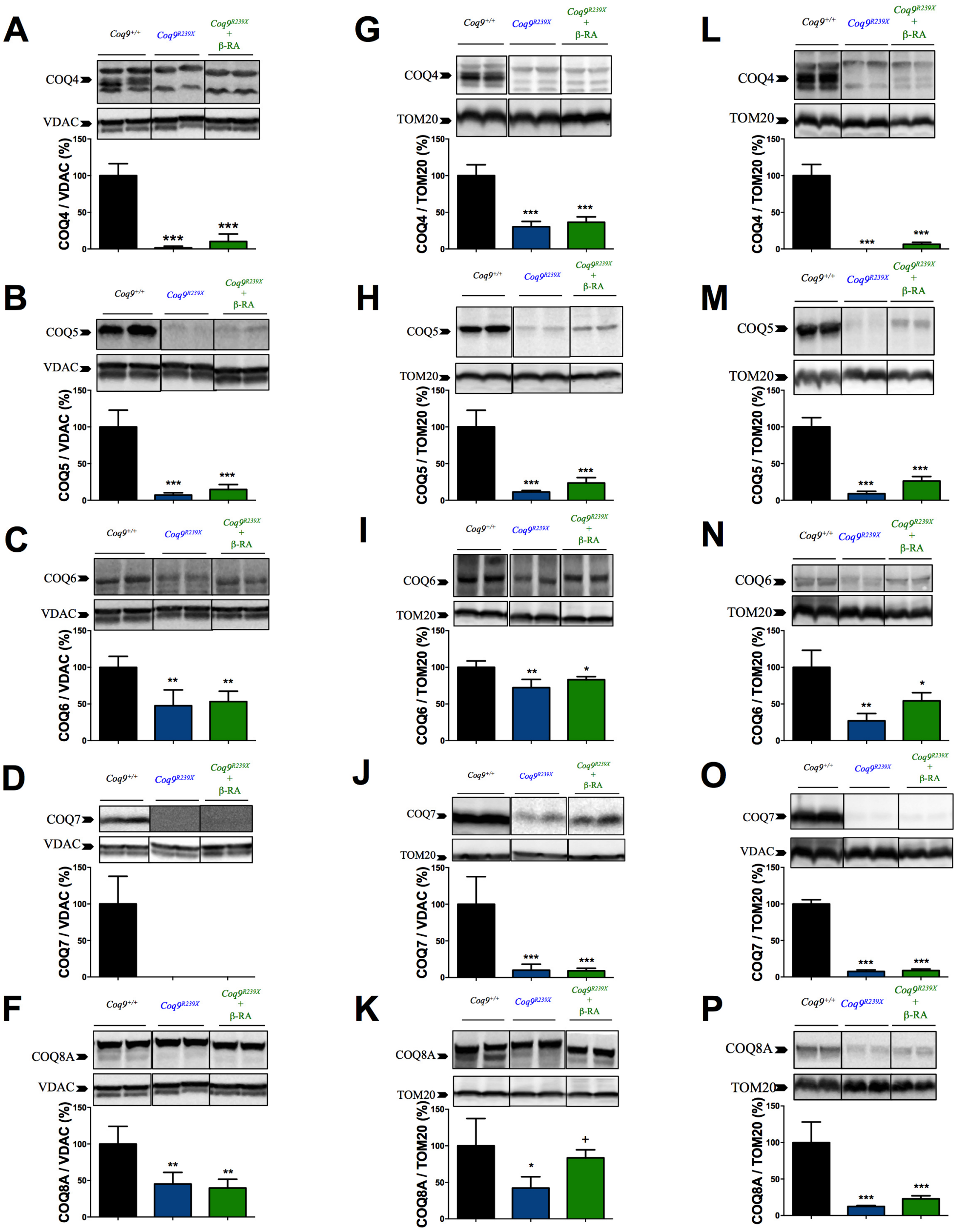

Figure 16. Effect of β–RA treatment in the tissue levels of CoQ biosynthetic proteins involved in Complex Q.

A-P Representative images of western blots of the CoQ biosynthetic proteins COQ4, COQ5, COQ6, COQ7 and COQ8A and the quantitation of the protein bands in the brain (A-F), kidneys (G-K) and heart (L-P) of $Coq9^{+/+}$, $Coq9^{R239X}$ *and* $Coq9^{R239X}$ mice treated with β–RA. $Coq9^{+/+}$ mice, $Coq9^{R239X}$ mice and $Coq9^{R239X}$ mice after β–RA treatment were included in all graphs. Data are expressed as mean ± SD. $^{*}P < 0.05$; $^{**}P < 0.01$; $^{***}P < 0.001$; $Coq9^{R239X}$ or $Coq9^{R239X}$ after β–RA treatment versus $Coq9^{+/+}$. $^{+}P < 0.05$; $Coq9^{R239X}$ versus and $Coq9^{R239X}$

after β–RA treatment (one-way ANOVA with a Tukey's post hoc test; n = 4–6 for each group).

4.1.8 THE LEVELS OF DMQ$_9$ CONTRIBUTE TO THE DISEASE PHENOTYPE.

The results of the previous sections suggest that the DMQ$_9$/CoQ$_9$ ratio is a key factor in the disease phenotype. To validate those results, we calculated the DMQ$_9$/CoQ$_9$ ratio in the tissues of two additional experimental models: 1) the *Coq9*^{Q95X} mouse model, which have widespread CoQ deficiency without compromising the lifespan (Luna-Sanchez *et al.*, 2015); and 2) the *Coq9*^{R239X} mice treated with ubiquinol-10, which show an increase in the levels of CoQ$_{10}$ (Garcia-Corzo *et al.*, 2014), resulting in an increase in the lifespan (Fig 1A); yet, this increased lifespan is not comparable to the one observed under β–RA treatment (Fig 1A). Our results show that, at one month of age, the DMQ$_9$/CoQ$_9$ ratios in the tissues of *Coq9*^{Q95X} mice were significantly lower than in the tissues of *Coq9*^{R239X} mice (Fig 17A and B; Fig 18). At three month of age, the DMQ$_9$ almost disappeared in the tissues of *Coq9*^{Q95X}, but not in *Coq9*^{R239X} mice (Fig 17C and E; Fig 18). In *Coq9*^{R239X} mice, the treatment with ubiquinol-10 did not affect the levels of DMQ$_9$ and, therefore, the DMQ$_9$/CoQ$_9$ ratios were still high in all tissues, while the CoQ$_{10}$ was increased

(Fig 18E and F; Fig 19). Therefore, those results corroborate the correlation between DMQ$_9$/CoQ$_9$ ratio and the severity of the disease phenotype.

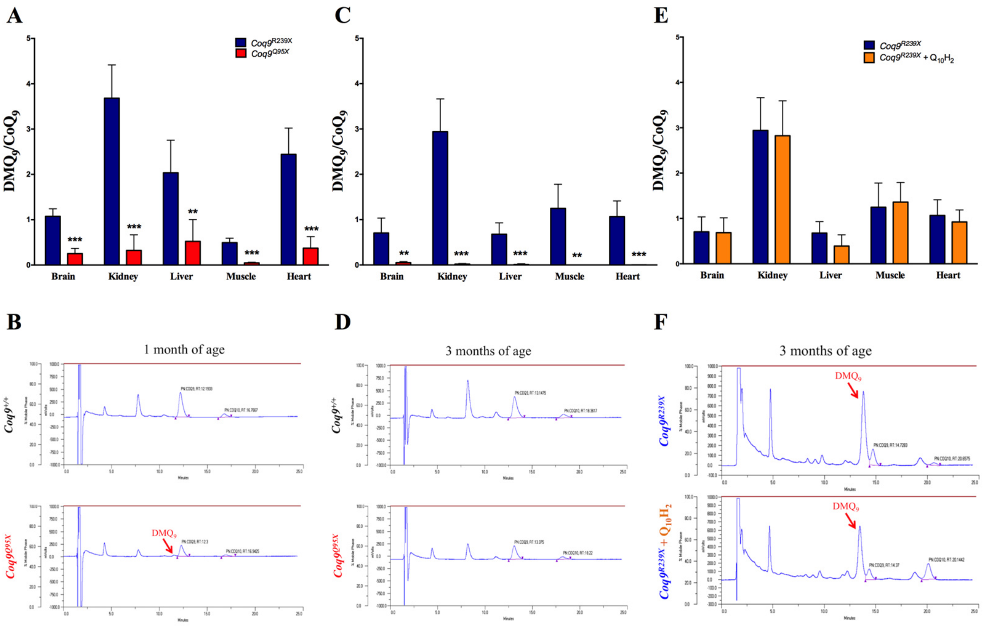

Figure 17. DMQ$_9$/CoQ$_9$ ratio in other experimental conditions.

A DMQ$_9$/CoQ$_9$ ratio in tissues from *Coq9*^{R239X} and *Coq9*^{Q95X} mice at 1 month of age.

C DMQ$_9$/CoQ$_9$ ratio in tissues from *Coq9*^{R239X} and *Coq9*^{Q95X} mice at 3 months of age.

E DMQ$_9$/CoQ$_9$ ratio in tissues from *Coq9*^{R239X} mice and *Coq9*^{R239X} mice treated with ubiquinol-10 during two months.

B, D, F Representative cromatographs showing the different quinones in the kidneys. Data are expressed as mean ± SD. ***$P < 0.001$; *Coq9*^{Q95X} versus *Coq9*^{R239X}. (one-way ANOVA with a Tukey's post hoc test; n = 5–7 for each group).

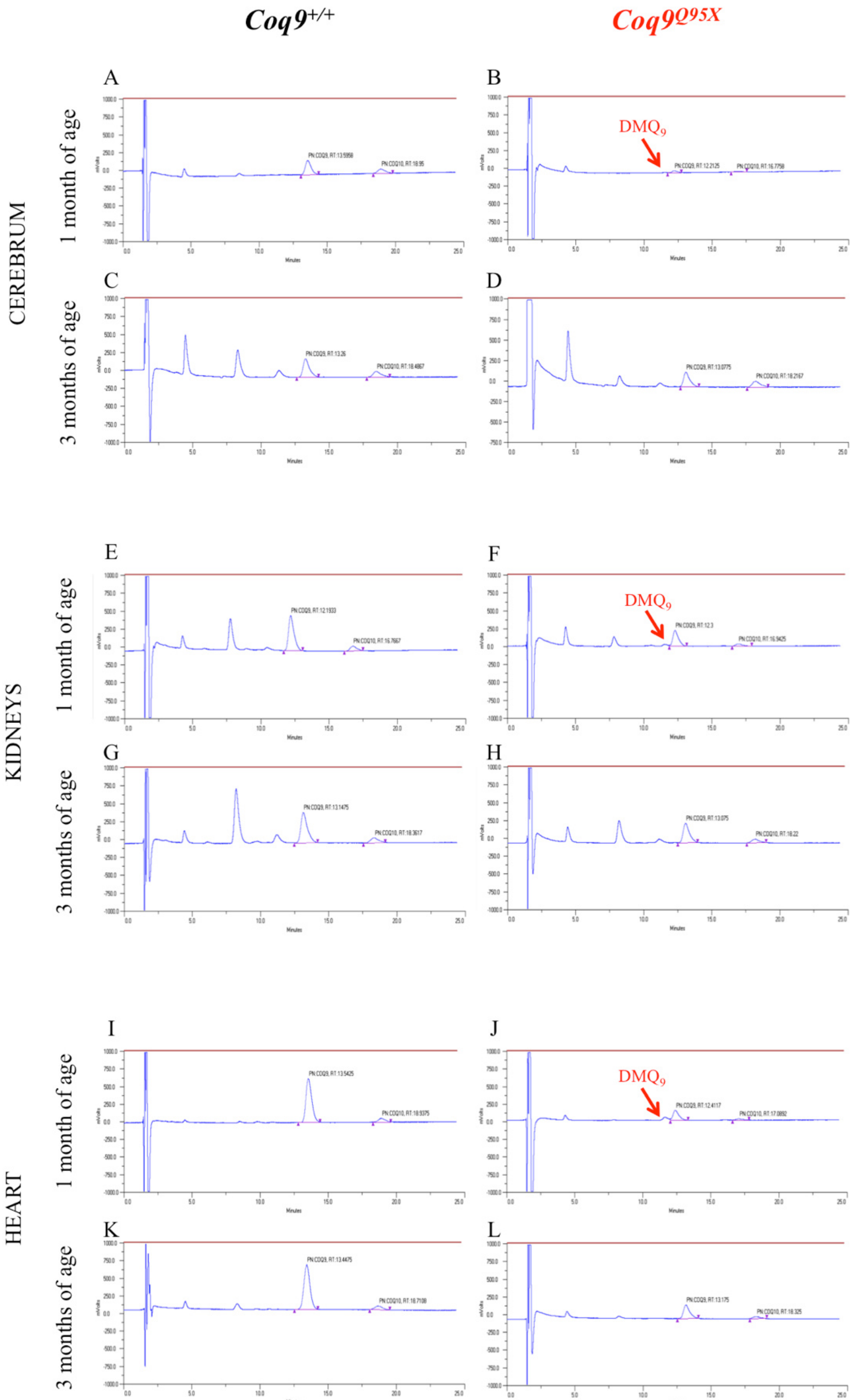
$Coq9^{+/+}$
$Coq9^{Q95X}$
CEREBRUM
KIDNEYS
HEART
1 month of age
3 months of age
A
B
C
D
E
F
G
H
I
J
K
L
DMQ$_9$
PN:COQ9, RT:13.5958
PN:COQ10, RT:18.95
PN:COQ9, RT:12.2125
PN:COQ10, RT:16.7758
PN:COQ9, RT:13.26
PN:COQ10, RT:18.4867
PN:COQ9, RT:13.0775
PN:COQ10, RT:18.2167
PN:COQ9, RT:12.1933
PN:COQ10, RT:16.7667
PN:COQ9, RT:12.3
PN:COQ10, RT:16.9425
PN:COQ9, RT:13.1475
PN:COQ10, RT:19.3617
PN:COQ9, RT:13.075
PN:COQ10, RT:18.22
PN:COQ9, RT:13.5425
PN:COQ10, RT:18.9375
PN:COQ9, RT:12.4117
PN:COQ10, RT:17.0892
PN:COQ9, RT:13.4475
PN:COQ10, RT:18.7108
PN:COQ9, RT:13.175
PN:COQ10, RT:18.325
mVolts
Minutes
1000.0
750.0
500.0
250.0
0.0
-250.0
-500.0
-750.0
-1000.0
0.0
5.0
10.0
15.0
20.0
25.0

Figure 18. Representative chromatographs showing the peak of DMQ9 in tissues from *Coq9*$^{+/+}$ and *Coq9*^{Q95X} mice at 1 and 3 months of age.
A-L (A to D) Chromatographs in the cerebrum; (E to H) Chromatographs in the kidneys; (I to L) Chromatographs in the heart. The DMQ9 peak is only detected in cerebrum, kidneys and heart of *Coq9*^{Q95X} mice at 1 month of age (B, F and J).

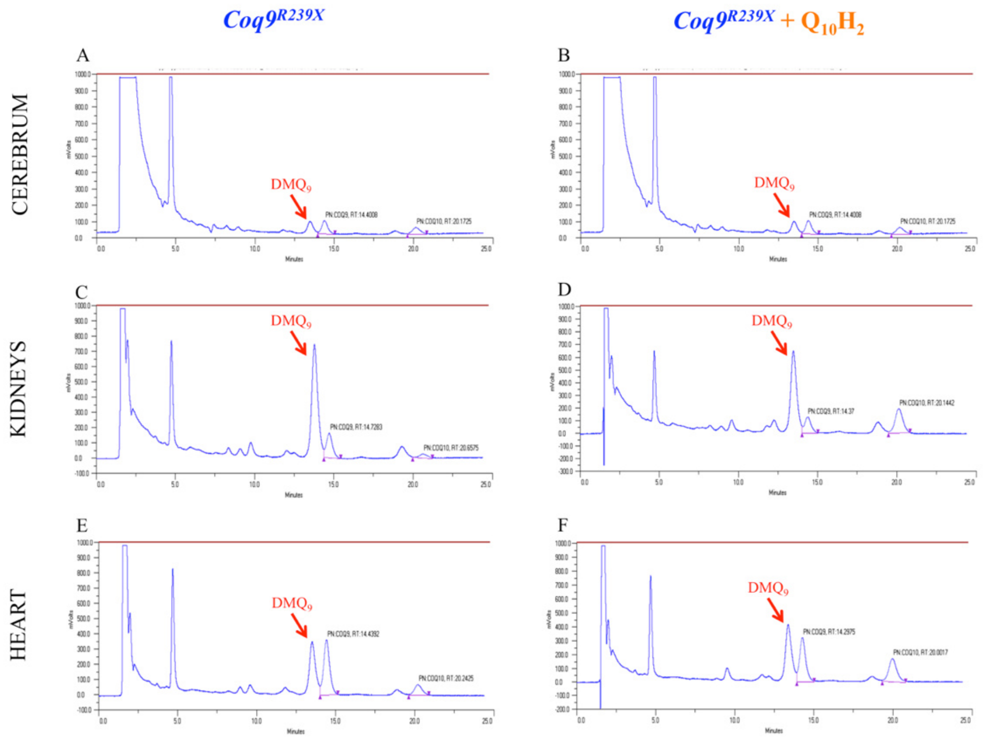

Figure 19. Representative chromatographs showing the peak of DMQ9 in tissues from *Coq9*^{R239X} mice and *Coq9*^{R239X} mice treated with ubiquinol-10 ($Q_{10}H_2$) during two months.
A-F (A and B) Chromatographs in the cerebrum; (C and D) Chromatographs in the kidneys; (E and F) Chromatographs in the heart. The treatment with ubiquinol-10 did not modify the levels of DMQ9.

4.1.9 STEROIDS HORMONES OR FGF21 DO NOT MEDIATE THE TISSUES COMMUNICATION UNDER COQ DEFICIENCY.

Because our data suggest that the modification of CoQ metabolism in peripheral tissues induces a reduction in the brain pathology in *Coq9*$^{\mathrm{R239X}}$ mice treated with β–RA, we tried to identify a circulating signal molecule that may provide this tissue communication (e.g. kidney-brain, muscle-brain, heart-brain or liver-brain). With that purpose, we quantified the steroids hormones, since some steps of their biosynthesis are localized in mitochondria; and FGF21, a recently identified biomarker for mitochondrial myopathies (Lehtonen *et al*, 2020). The results did not show any differences in the levels of corticosterone between the three experimental groups, both in males and females (Fig 20A and B). In male *Coq9*$^{\mathrm{R239X}}$ mice, the levels of androstenodione and testosterone were significantly lower than those in male *Coq9*$^{+/+}$ mice (Fig 20C and D). After β–RA treatment, the levels of both hormones were still lower than those in control animals (Fig 20C and D).

The levels of FGF21 in the target organ, the brain, were similar in *Coq9*$^{+/+}$ and *Coq9*$^{\mathrm{R239X}}$ mice, while a slight increase was detected in the precursor form in *Coq9*$^{\mathrm{R239X}}$ mice treated with β–RA, compared to *Coq9*$^{\mathrm{R239X}}$ mice (Fig 20E). In the liver, the main secretory organ of FGF21, the levels of FGF21 (both the precursor and the mature form) were similar in the three experimental groups (Fig 20F).

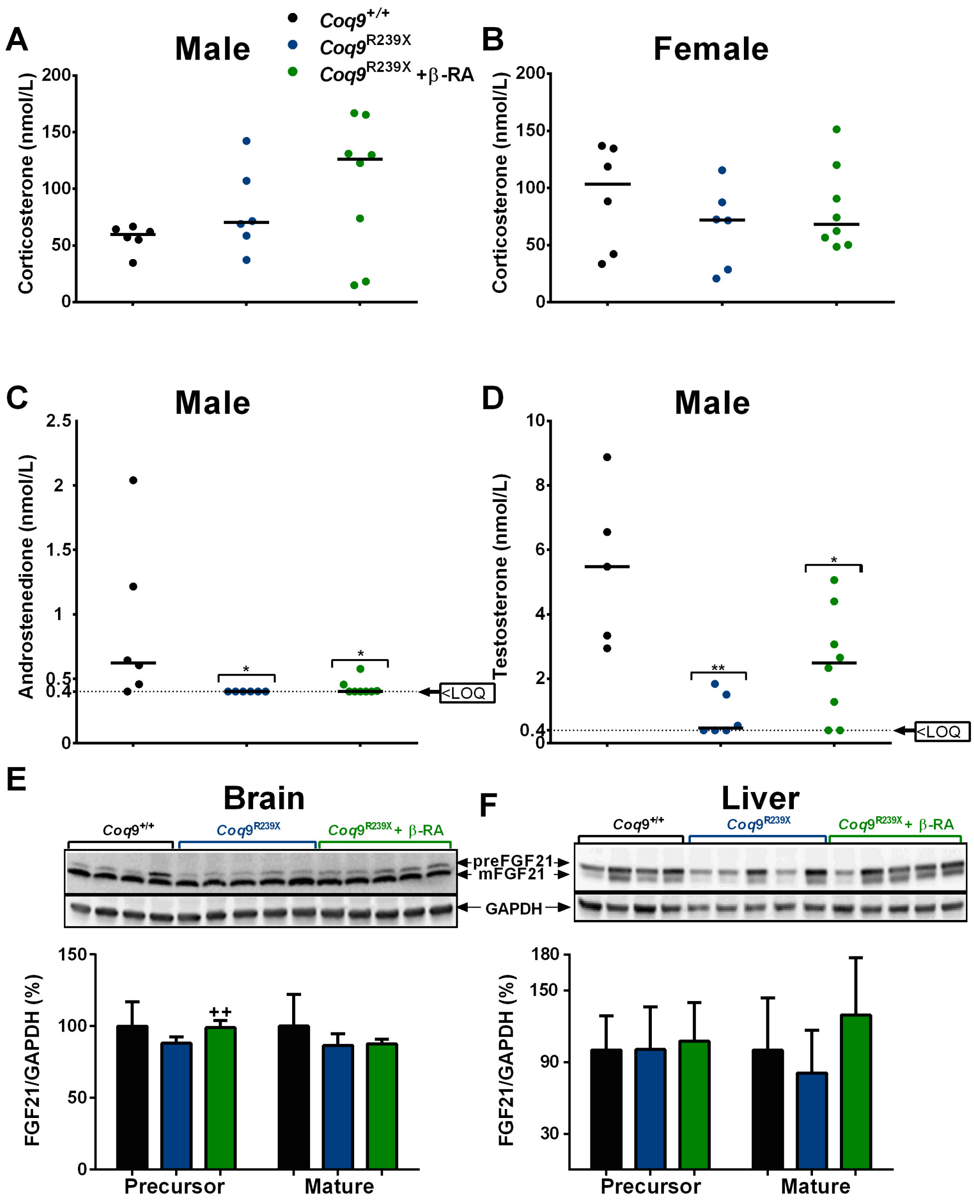

Figure 20. Figure S12. Levels of steroid hormones and FGF21.

A-F (A and B) Corticosterone levels in blood of male and female mice, respectively; (C) Androstenedione levels in blood of males mice; and (D) Testosterone levels in blood of males mice. (E and F) FGF21 levels in mice brains (E) and livers (F). *Coq9*$^{+/+}$ mice, *Coq9*^{R239X} mice and *Coq9*^{R239X} mice after β–RA treatment were included in all graphs. Data are expressed as median. *P < 0.05; **P < 0.01; *Coq9*^{R239X} and *Coq9*^{R239X} after β–RA treatment mice versus *Coq9*$^{+/+}$ mice. ++P < 0.01; *Coq9*^{R239X} versus *Coq9*^{R239X} after β–RA treatment (Mann-Whitney test; n = 6-8 for each group).

4.2 TOXIC OR THERAPEUTIC? - THE DOSE-DEPENDENT EFFECTS OF β-RESORCYLIC ACID DEPEND ON MITOCHONDRIAL METABOLISM

4.2.1 THE HIGH DOSE OF β-RA INDUCES DETRIMENTAL EFFECTS IN THE PHENOTYPE OF WILD-TYPE ANIMALS, WITH SEVERE MORPHOLOGICAL AND FUNCTIONAL ALTERATIONS IN THE LIVER, KIDNEYS AND BRAIN.

We have demonstrated that β–RA rescues the encephalopathic phenotype in a mouse model of primary CoQ deficiency. In the previous study, β–RA was administered in the chow at 1%, which gives a dose of 1-3 g/kg bw/day, referred from now as "high dose". Unexpectedly, this dose of β–RA significantly reduces the survival in wild-type mice when the supplementation starts at 1 month of age (Fig 21A). This mortality increase is independent of the moment when the supplementation starts (Fig 22A and D), but it seems to be affected by sex as males (Fig 22B and E) start to die later than the females (Fig 22C and F). The effect of the high dose of β–RA is also observed in the animals' body weight, with a significant decrease after the first month of supplementation, both in males (Fig 21B) and females (Fig 21C). Nevertheless, the motor coordination, measured by the rotarod test, is not compromised, neither in males (Fig 21D) nor in females (Fig 21E). Nonetheless, the equilibrium is partially lost in approximately 5% of the treated mice , suggesting an involvement of the CNS. Two-five days before death, the animals show a “terminal stage” manifested by a decrease of more than 50% of the body weight and a decreased ambulation (Fig 21F and G).

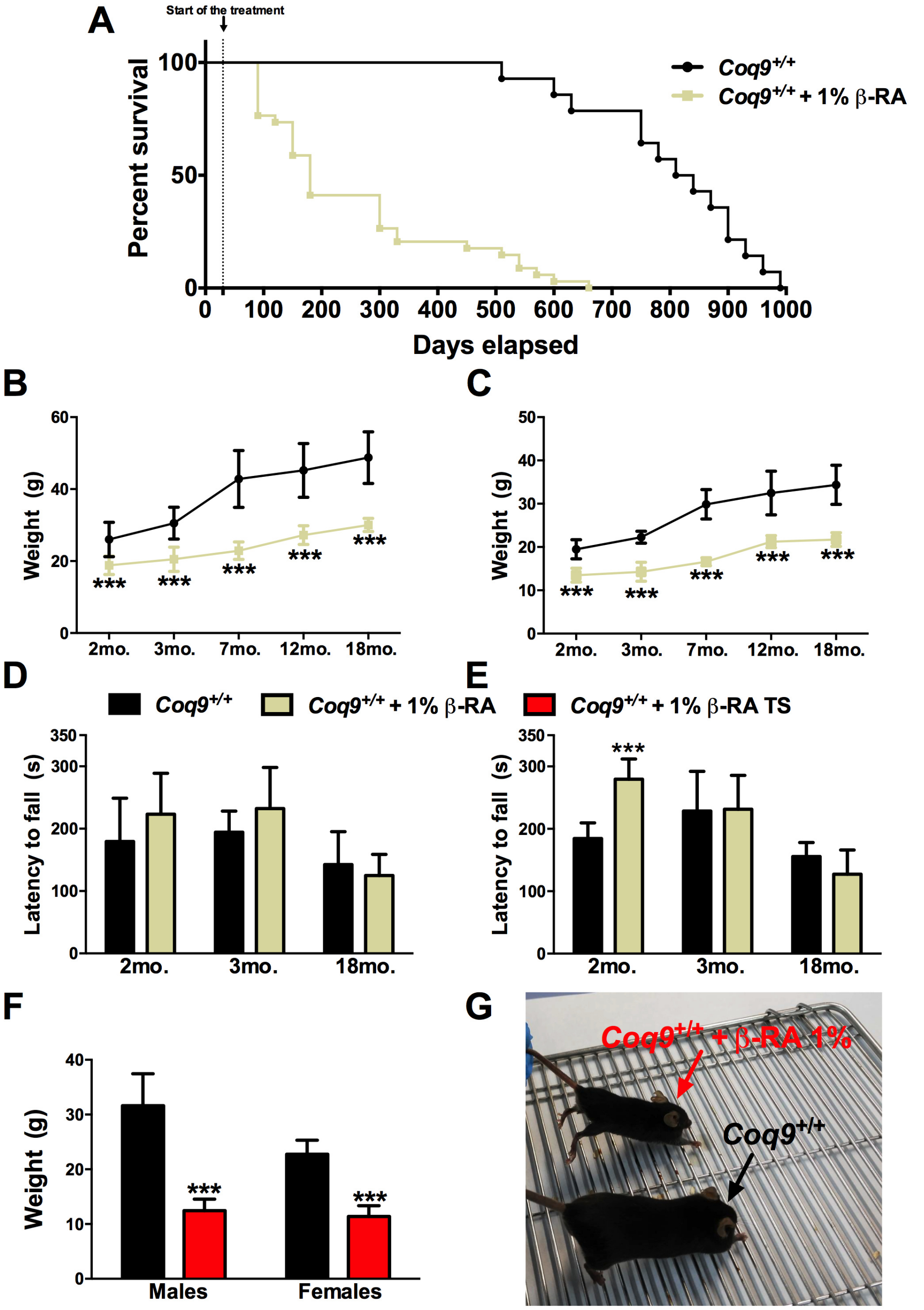

Figure 21. **Survival and phenotypic characterization of *Coq9*^{R239X} mice after β–RA treatment.**

A Survival curve of the *Coq9*$^{+/+}$ mice and *Coq9*$^{+/+}$ mice under 1% of β–RA supplementation. The treatments started at 1 month of age.

B,C Body weight of males and females *Coq9*$^{+/+}$ mice and *Coq9*$^{+/+}$ mice under 1% of β–RA supplementation.

D,E Rotarod test of male and female *Coq9*$^{+/+}$ mice and *Coq9*$^{+/+}$ mice under 1% of β–RA supplementation.

F Body weight of males and females *Coq9*$^{+/+}$ mice and *Coq9*$^{+/+}$ mice under 1% of β–RA supplementation at “terminal stage” (TS), at 2-5 months of age.

G Comparative image of a *Coq9*$^{+/+}$ mouse and a *Coq9*$^{+/+}$ mouse supplemented with 1% of β–RA at 3 months of age. Data are expressed as mean SD. *P < 0.05; **P < 0.01; ***P < 0.001; *Coq9*$^{+/+}$ mice under 1% of β–RA supplementation versus *Coq9*$^{+/+}$. (t-test; n = 5–34 for each group).

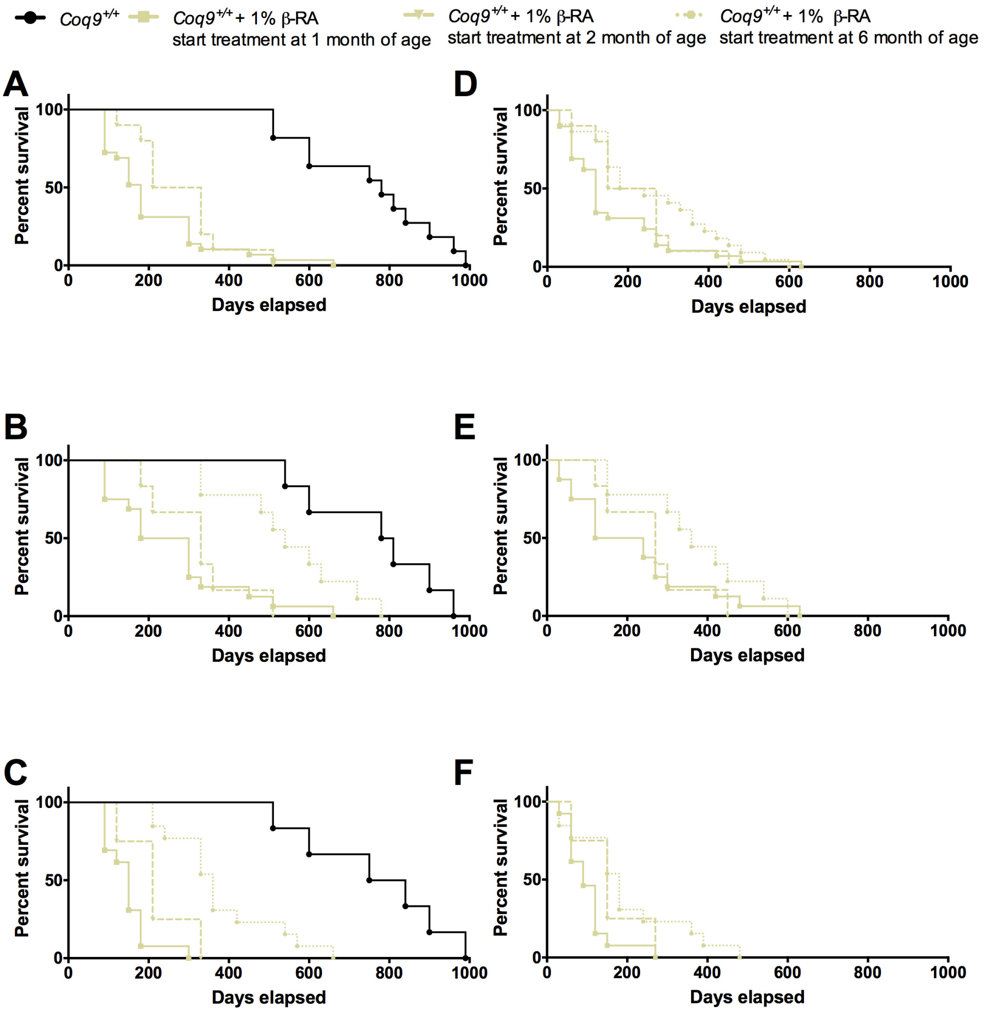

Figure 22. **Survival curve of *Coq9*$^{+/+}$ mice and *Coq9*$^{+/+}$ mice under 1% of β–RA supplementation, comparing the outcomes attending at the moment that the supplementation begins.**
A-F The treatments started at 1 month, 2 months or 6 months of age. Results of both sex (A,D), males (B,E) or females (C,F); in a general view (A-C) or normalizing the data attending to the moment that the treatment started (D-F).

The phenotypic changes observed in the wild-type animals supplemented with the high dose of β–RA are mainly due to structural and functional alterations in the liver, kidneys and brain. The livers of the treated mice have a fibrotic appearance and smaller size (Fig 23B to C), compared to the untreated animals (Fig 23A). Morphologically, they show bigger and binuclear hepatocytes with altered organization (Fig 23D to I), that become more evident in the animals at the terminal stage (Fig 23H to I). Accordingly, the activities of GOT, GPT and AP are increased in the plasma of wild-type animals supplemented with the high dose of β–RA at the terminal stage (Fig 23J to L), indicating that the damage to the liver is very severe at that moment. Also, the levels of bilirubin in plasma and uric acid in urine are increased in wild-type animals supplemented with the high dose of β–RA at the terminal stage (Fig 23M to O), although the levels of urea in urine are more variable (Fig 23N). The kidneys of the treated animals, especially those at the terminal stage, show a yellowish appearance (Fig 23P to R) and, morphologically, they show severe tubular degeneration, with necrotic areas, vacuolization and signs of fibrosis (Fig 23S to X). Accordingly, the levels of creatinine (Fig 23Y) are increased in plasma of wild-type animals supplemented with high dose of β–RA at the terminal stage, while the levels of albumin are decreased (Fig 23Z), all being signs of kidney disease. In the urine, the levels of total proteins and albumin are increased (Fig 23AA to AB), which may indicate a problem in the glomerular filtration. The levels of creatinine and phosphorous do not change under β–RA supplementation (Fig 23AC to AD). However, the levels of calcium are increased in wild-type animals supplemented with high dose of β–RA, while the opposite effect is observed in the levels of magnesium (Fig 23AE to AF); and the urine pH decreases in the wild-type animals supplemented with 1% β–RA at the terminal stage (Fig 23AG). These data may also indicate that the supplementation with the high dose of β–RA induces a disruption of the tubular homeostasis in wild-type animals. Despite all these pathophysiological features, the levels of hemoglobin and the counts of the different blood cells remain unaltered under the supplementation with high dose of β–RA (Fig 24).

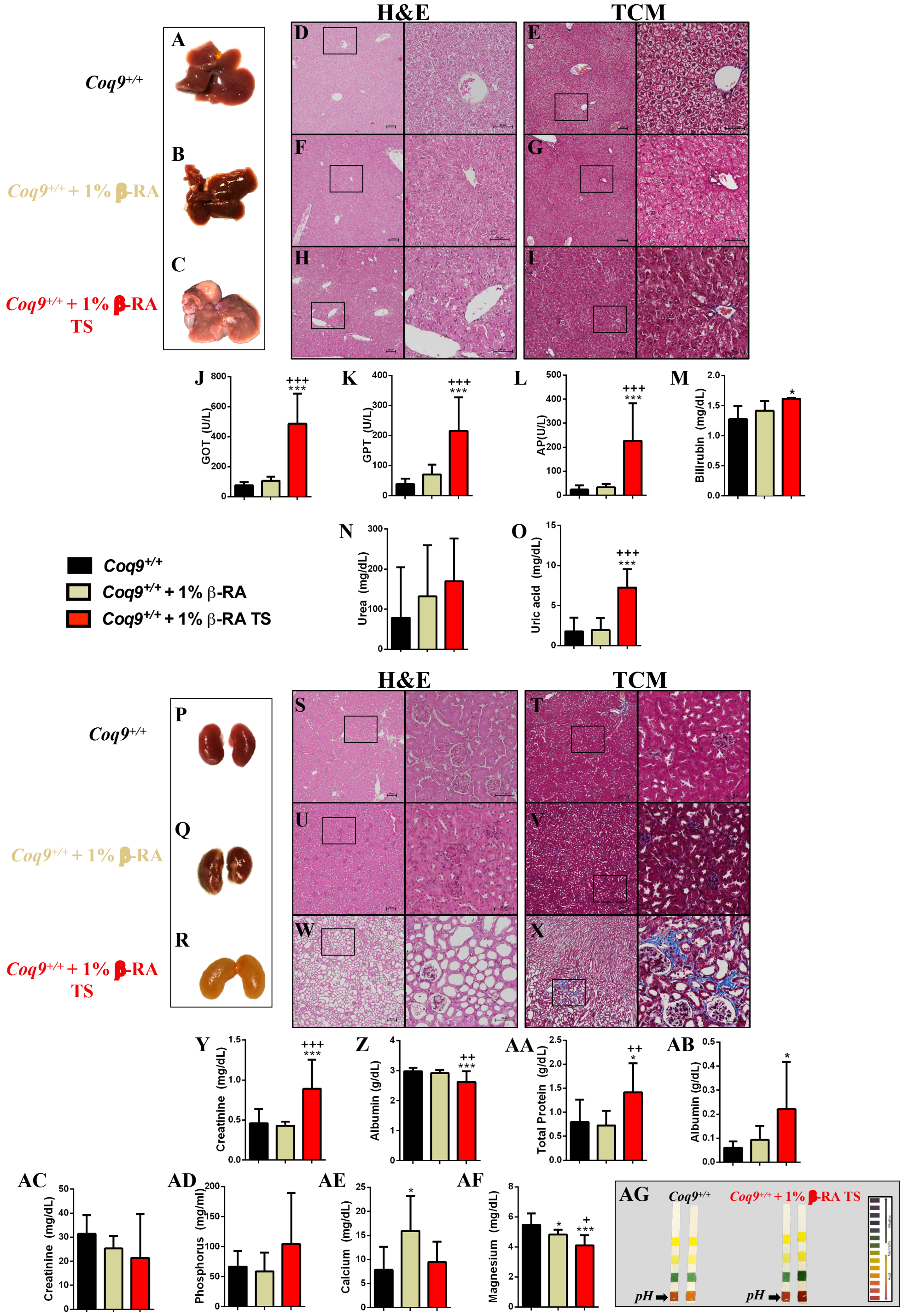
H&E
TCM
A
B
C
D
E
F
G
H
I
Coq9+/+
Coq9+/+ + 1% β-RA
Coq9+/+ + 1% β-RA TS
J
GOT (U/L)
K
GPT (U/L)
L
AP(U/L)
M
Bilirubin (mg/dL)
+++
***
*
N
Urea (mg/dL)
O
Uric acid (mg/dL)
■ Coq9+/+
□ Coq9+/+ + 1% β-RA
■ Coq9+/+ + 1% β-RA TS
P
Q
R
S
T
U
V
W
X
Y
Creatinine (mg/dL)
Z
Albumin (g/dL)
AA
Total Protein (g/dL)
AB
Albumin (g/dL)
++
AC
Creatinine (mg/dL)
AD
Phosphorus (mg/ml)
AE
Calcium (mg/dL)
AF
Magnesium (mg/dL)
+
AG
pH

Figure 23. **Morphological and physiological evaluation of the kidneys and the liver of *Coq9*$^{+/+}$ mice under 1% β–RA supplementation.**

A-C Visual appearance of the liver from *Coq9*$^{+/+}$ mice, *Coq9*$^{+/+}$ mice under 1% of β–RA supplementation and *Coq9*$^{+/+}$ mice under 1% of β–RA supplementation at terminal stage (TS).

D-I H&E and Masson's Trichrome stains in the liver from *Coq9*$^{+/+}$ mice, *Coq9*$^{+/+}$ mice under 1% of β–RA supplementation and *Coq9*$^{+/+}$ mice under 1% of β–RA supplementation at terminal stage (TS).

J-M Markers of hepatic function in the plasma from *Coq9*$^{+/+}$ mice and *Coq9*$^{+/+}$ mice, *Coq9*$^{+/+}$ mice under 1% of β–RA supplementation and *Coq9*$^{+/+}$ mice under 1% of β–RA supplementation at terminal stage (TS). GOT = glutamate-oxaloacetate transaminase; GPT = glutamate-pyruvate transaminase; AP = alkaline phosphatase.

N-O Markers of hepatic function in the urine from *Coq9*$^{+/+}$ mice, *Coq9*$^{+/+}$ mice under 1% of β–RA supplementation and *Coq9*$^{+/+}$ mice under 1% of β–RA supplementation at terminal stage (TS).

P-R Visual appearance of the kidney from *Coq9*$^{+/+}$ mice, *Coq9*$^{+/+}$ mice under 1% of β–RA supplementation and *Coq9*$^{+/+}$ mice under 1% of β–RA supplementation at terminal stage (TS).

S-X H&E and Masson's Trichrome stains in the kidney from *Coq9*$^{+/+}$ mice, *Coq9*$^{+/+}$ mice under 1% of β–RA supplementation and *Coq9*$^{+/+}$ mice under 1% of β–RA supplementation at terminal stage (TS).

Y,Z Markers of renal function in the plasma from *Coq9*$^{+/+}$ mice and *Coq9*$^{+/+}$ mice, *Coq9*$^{+/+}$ mice under 1% of β–RA supplementation and *Coq9*$^{+/+}$ mice under 1% of β–RA supplementation at terminal stage (TS).

AA-AF Markers of renal function in the urine from *Coq9*$^{+/+}$ mice, *Coq9*$^{+/+}$ mice under 1% of β–RA supplementation and *Coq9*$^{+/+}$ mice under 1% of β–RA supplementation at terminal stage (TS). Data are expressed as mean ± SD. *P < 0.05; **P < 0.01; ***P < 0.001; *Coq9*$^{+/+}$ under 1% of β–RA supplementation or *Coq9*$^{+/+}$ under 1% of β–RA supplementation at TS versus *Coq9*$^{+/+}$. +P < 0.05; ++P < 0.01; +++P < 0.001 *Coq9*$^{+/+}$ under 1% of β–RA supplementation at TS versus *Coq9*$^{+/+}$ under 1% of β–RA supplementation (t-test; n = 5–17 for each group).

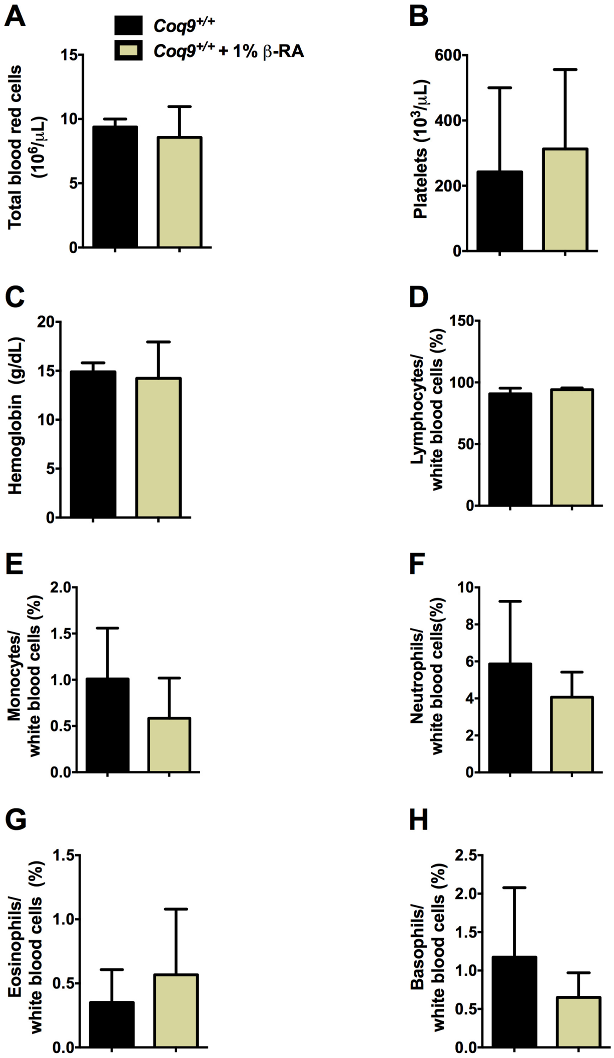

Figure 24. **Hemogram of *Coq9*$^{+/+}$ *and Coq9*$^{+/+}$ mice under 1% of β–RA supplementation.** A-H (A) Total blood cells, (B) number of platelets, (C) Hemoglobin levels, (D) percentage of lymphocytes, (E) percentage of monocytes, (F) percentage of neutrophils, (G) percentage of eosinophils and (H) percentage of basophils of *Coq9*$^{+/+}$ mice and *Coq9*$^{+/+}$ mice under 1% of β–RA supplementation.

The size of the brains of the wild-type animals treated with the high dose of β–RA is smaller than that of the untreated animals (Fig 25A to C), especially at the terminal stage (Fig 25C). In the diencephalon, the high dose of β–RA induces a mild increase of small vacuoles at the terminal stage (Fig 25F), compared to treated (Fig 25E) and untreated (Fig 25D) *Coq9*$^{+/+}$ mice. Also, mild proliferation of astrocytes is observed (Fig 25G to I), especially at the terminal stage (Fig 25I). Other tissues, such as spleen and heart, are smaller but, together with the gut, they do not show major morphological alterations (Fig 26). Since some spongiosis and astrogliosis are observed in diencephalon and the brainstem, we also performed RNA-Seq of the brains from untreated and treated animals, followed by a multi-dimensional transcriptome analyses in the datasets, aiming at the identification of diseases, functions, canonical pathways and networks that are altered by the supplementation with the high dose of β–RA. Our analyses reveal that the high dose of β–RA induces changes in the expression of genes associated to neurological diseases and brain damage. The canonical pathway analysis of the differentially regulated genes showed enrichment of pathways related to endoplasmic reticulum, such as unfolded protein response (Hsp90b1, Hspa5, Hsph1, Srebf1, Xbp1), endoplasmic reticulum stress (Hsp90b1, Hspa5, Xbp1), FXR/RXR activation (Agt, Apod, Foxa1, Foxa2, IL33, Srebf1) and LXR/RXR activation (Agt, Apod, Cyp51a1, IL33, Srebf1) (Fig 27). The analysis also reveals enrichment of pathways related to the metabolism of monoamine neurotransmitters (Fig 27), mainly those associated to serotonin receptor signaling (Gch1, Slc18a2, Slc6a4, Tph2) and dopamine receptor signaling (Drd2, Drd4, Gch1, Slc18a2, Slc6a3) (Fig 27). Interestingly, monoamine neurotransmitters derivate from phenylalanine, tyrosine and tryptophan, share a common pathway with the biosynthesis of 4-HB, the natural precursor of CoQ (Fig 25).

Therefore, the morphological, functional and transcriptomic analyses point out that the liver, kidneys and brain of wild-type animals are negatively affected by the supplementation of the high dose of β–RA.

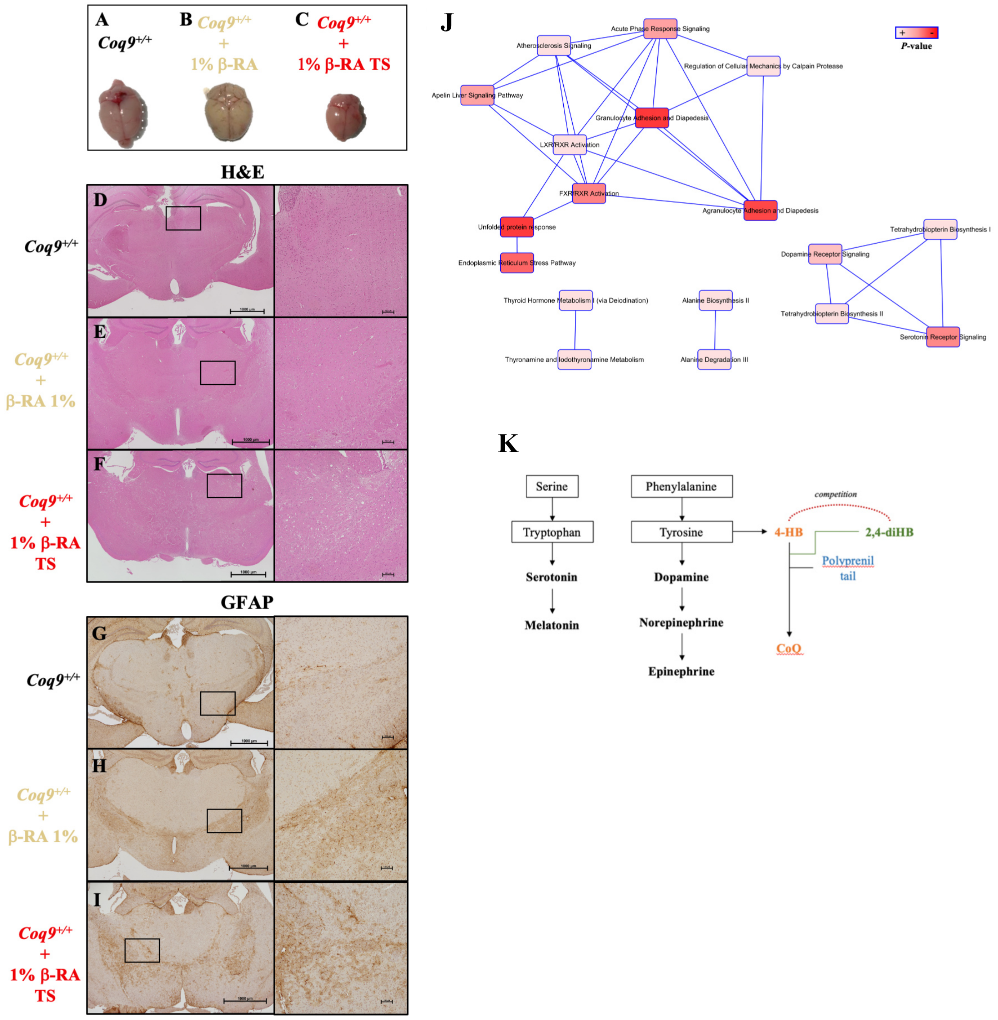
A
Coq9+/+
B Coq9+/+
+
1% β-RA
C Coq9+/+
+
1% β-RA TS
H&E
D
E
F
Coq9+/+
Coq9+/+
+
β-RA 1%
Coq9+/+
+
1% β-RA
TS
GFAP
G
H
I
J
P-value
Acute Phase Response Signaling
Atherosclerosis Signaling
Regulation of Cellular Mechanics by Calpain Protease
Apelin Liver Signaling Pathway
Granulocyte Adhesion and Diapedesis
LXR/RXR Activation
FXR/RXR Activation
Agranulocyte Adhesion and Diapedesis
Unfolded protein response
Endoplasmic Reticulum Stress Pathway
Tetrahydrobiopterin Biosynthesis I
Dopamine Receptor Signaling
Thyroid Hormone Metabolism I (via Deiodination)
Alanine Biosynthesis II
Tetrahydrobiopterin Biosynthesis II
Serotonin Receptor Signaling
Thyronamine and Iodothyronamine Metabolism
Alanine Degradation III
K
Serine
Tryptophan
Serotonin
Melatonin
Phenylalanine
Tyrosine
Dopamine
Norepinephrine
Epinephrine
competition
4-HB
2,4-diHB
Polyprenil tail
CoQ

Figure 25. Morphological evaluation of the brain and changes in the cerebral transcriptome in *Coq9*$^{+/+}$ mice under 1% of β–RA supplementation.

A-C Visual appearance of the brain from *Coq9*$^{+/+}$ mice, *Coq9*$^{+/+}$ mice under 1% of β–RA supplementation and *Coq9*$^{+/+}$ mice under 1% of β–RA supplementation at terminal stage (TS).

D-I H&E stain and anti-GFAP stains in the diencephalon from *Coq9*$^{+/+}$ mice, *Coq9*$^{+/+}$ mice under 1% of β–RA supplementation and *Coq9*$^{+/+}$ mice under 1% of β–RA supplementation at terminal stage (TS).

J Network based on the enriched canonical pathways in brain of Coq9+/+ mice after 1% b-RA treatment.

K Schematic summary of the pathways for the biosynthesis monoamine neurotransmitters and 4-HB, the natural precursor of CoQ, indicating the common use of tyrosine.

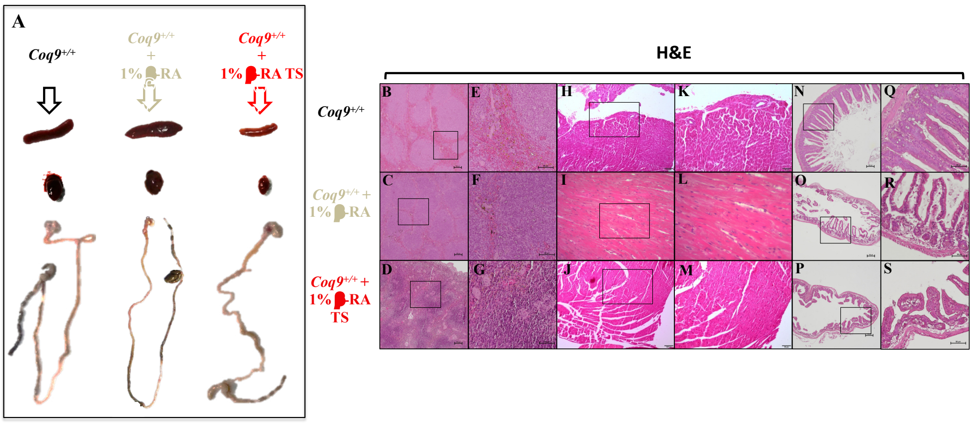

Figure 26. Morphological and histological features from spleen, heart and gut of *Coq9*$^{+/+}$ *and Coq9*$^{+/+}$ mice under 1% of β–RA supplementation.

A Visual appearance of spleen, heart and gut of *Coq9*$^{+/+}$ mice and *Coq9*$^{+/+}$ mice under 1% of β–RA supplementation.

B-G H&E stain in the spleen from *Coq9*$^{+/+}$ mice and *Coq9*$^{+/+}$ mice under 1% of β–RA supplementation.

H-M H&E stain in the heart from *Coq9*$^{+/+}$ mice and *Coq9*$^{+/+}$ mice under 1% of β–RA supplementation.

N-S H&E stain in the gut from *Coq9*$^{+/+}$ mice and *Coq9*$^{+/+}$ mice under 1% of β–RA supplementation. TS = terminal stage.

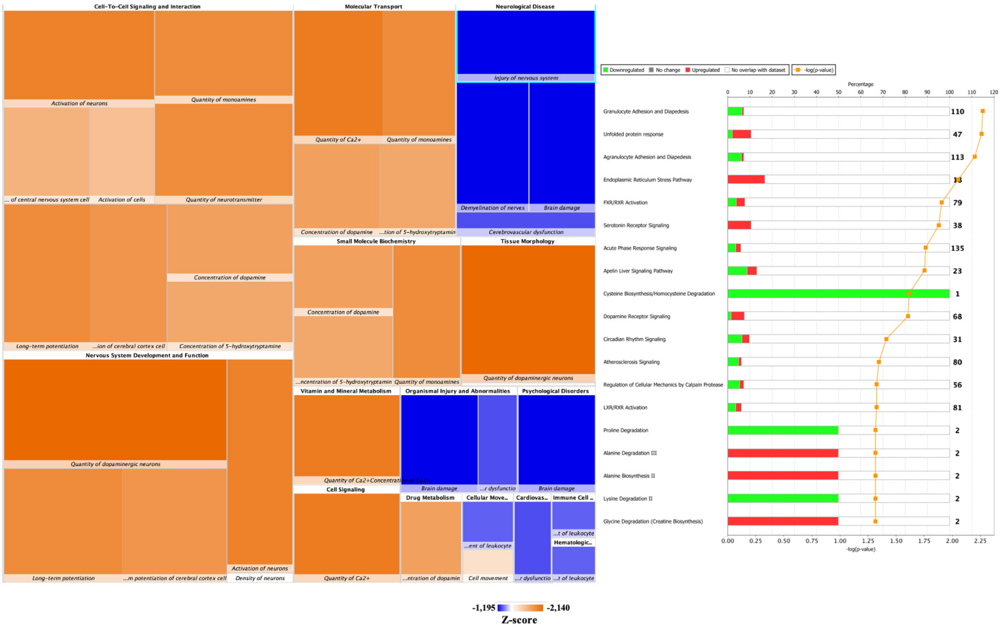

Figure 27. Heatmap and enriched canonical pathways from brain of *Coq9*$^{+/+}$ *and Coq9*$^{+/+}$ mice under 1% of β–RA supplementation.
Heatmap showing the diseases and biological functions that are stimulated or repressed by the supplementation of 1% of β–RA in the brain of *Coq9*$^{+/+}$ mice. Orange means that a significant number of genes that are related with that particular function of disease are upregulated in the brain *Coq9*$^{+/+}$ mice supplemented with 1% of β–RA; blue means that a significant number of genes that are related with that particular function of disease are downregulated in the brain *Coq9*$^{+/+}$ mice supplemented with 1% of β–RA
Top twenty enriched canonical pathways in the brain of *Coq9*$^{+/+}$ mice after 1% b-RA treatment.

4.2.2 THE HIGH DOSE OF β-RA AFFECTS THE HOMEOSTASIS OF THE MITOCHONDRIAL PROTEOME AND CoQ METABOLISM IN WILD-TYPE ANIMALS.

To further profile the molecular consequences of β–RA toxicity, we performed quantitative proteomics on mitochondrial fractions of brain and kidneys from wild-type mice treated with the high dose of β–RA and untreated wild-type mice. In the brain, 143 mitochondrial proteins are differentially expressed (Fig 28A), 35 over-expressed and 108 under-expressed (Fig 28B), in wild-type mice treated with the high dose of β–RA, compared to untreated wild-type mice. Among those proteins, PARL, a protein that causes CoQ deficiency when it is dysfunctional (Spinazzi *et al.*, 2019), is under-expressed in the treated wild-type animals, while COQ4 (Belogrudov *et al.*, 2001), a CoQ biosynthetic protein is over-expressed (Fig 28B). Canonical pathway (Fig 28C; Fig 29A) analysis show enrichment of pathways of mitochondrial dysfunction, oxidative phosphorylation and sirtuin signaling, all these related with the altered functions of Complex I assembly, transmembrane potential, protein synthesis, generation of free radicals and apoptosis.

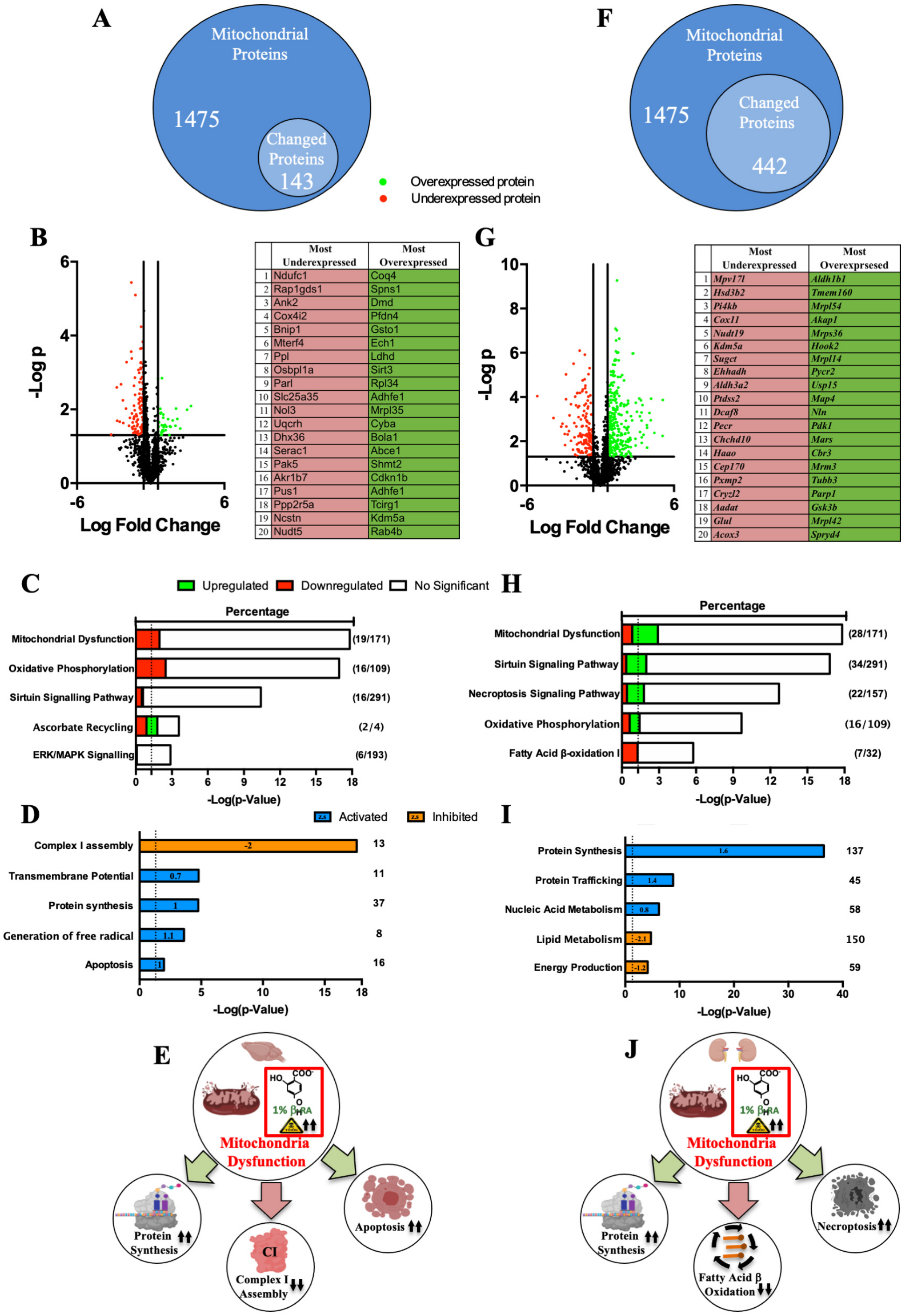

	Most Underexpressed	Most Overexpressed
1	Ndufc1	Coq4
2	Rap1gds1	Spns1
3	Ank2	Dmd
4	Cox4i2	Pfdn4
5	Bnip1	Gsto1
6	Mterf4	Ech1
7	Ppl	Ldhd
8	Osbpl1a	Sirt3
9	Parl	Rpl34
10	Slc25a35	Adhfe1
11	Nol3	Mrpl35
12	Uqcrh	Cyba
13	Dhx36	Bola1
14	Serac1	Abce1
15	Pak5	Shmt2
16	Akr1b7	Cdkn1b
17	Pus1	Adhfe1
18	Ppp2r5a	Tcirg1
19	Ncstn	Kdm5a
20	Nudt5	Rab4b

	Most Underexpressed	Most Overexprsesed
1	*Mpv17l*	*Aldh1b1*
2	*Hsd3b2*	*Tmem160*
3	*Pi4kb*	*Mrpl54*
4	*Cox11*	*Akap1*
5	*Nudt19*	*Mrps36*
6	*Kdm5a*	*Hook2*
7	*Sugct*	*Mrpl14*
8	*Ehhadh*	*Pycr2*
9	*Aldh3a2*	*Usp15*
10	*Ptdss2*	*Map4*
11	*Dcaf8*	*Nln*
12	*Pecr*	*Pdk1*
13	*Chchd10*	*Mars*
14	*Haao*	*Cbr3*
15	*Cep170*	*Mrm3*
16	*Pxmp2*	*Tubb3*
17	*Cryzl2*	*Parp1*
18	*Aadat*	*Gsk3b*
19	*Glul*	*Mrpl42*
20	*Acox3*	*Spryd4*

Figure 28. Mitochondrial proteome alterations in the brain and the kidneys of *Coq9*$^{+/+}$ mice after 1% β–RA treatment.

A,F Venn diagram of significantly changed mitochondrial proteins in the brain (A) and the kidneys (F) from *Coq9*$^{+/+}$ mice after 1% of β–RA treatment.
B,G Volcano plot of mitochondrial proteins altered in the brain and the kidneys from *Coq9*$^{+/+}$ mice under 1% of β–RA supplementation, compared to non-supplemented *Coq9*$^{+/+}$ mice. Green represents the most overexpressed proteins and red the most underexpressed protein.
C,H Top five enriched canonical pathways in the cerebral (C) and renal (H) mitochondrial proteomes from *Coq9*$^{+/+}$ mice after 1% of β–RA treatment. Dotted line: Adjusted $p = 0.05$. Parentheses indicate the number of proteins changed in that category per total number of proteins classified in that category. Green means the percentage of proteins upregulated in the specific category. Red means the percentage of proteins downregulated in the specific category.
D,I Top five enriched biological functions in the cerebral (D) and renal (I) mitochondrial proteomes from *Coq9*$^{+/+}$ mice after 1% of β–RA treatment. Dotted line: Adjusted $p = 0.05$. Blue means that the category is expected to be activated according to the z-score; orange means that the category is expected to be inhibited according to the z-score.
E,J Schematic figure of the most important changes in the mitochondrial proteomes from the brain (E) and the kidneys (J) from *Coq9*$^{+/+}$ mice after 1% of β–RA treatment.

In the kidneys, 442 mitochondrial proteins are differentially expressed (Fig 28F), 300 over-expressed and 142 under-expressed (Fig 28G), in wild-type mice treated with the high dose of β–RA, compared to untreated wild-type mice. Canonical pathway analysis show enrichment of pathways of mitochondrial dysfunction, sirtuin signaling, necroptosis and fatty acid oxidation, among others (Fig 28H, Fig 29). This is consistent with an inhibition of lipid metabolism and energy production (Fig 28I). It is also remarkable that more than 80 of the altered proteins are directly related to mitochondrial protein synthesis, and most of them are upregulated (Fig 28I to J). Furthermore, we need to point out that the CoQ biosynthetic proteins COQ3, COQ6 and COQ8A are upregulated in wild-type animals supplemented with the high dose of β–RA, probably as a compensatory response.

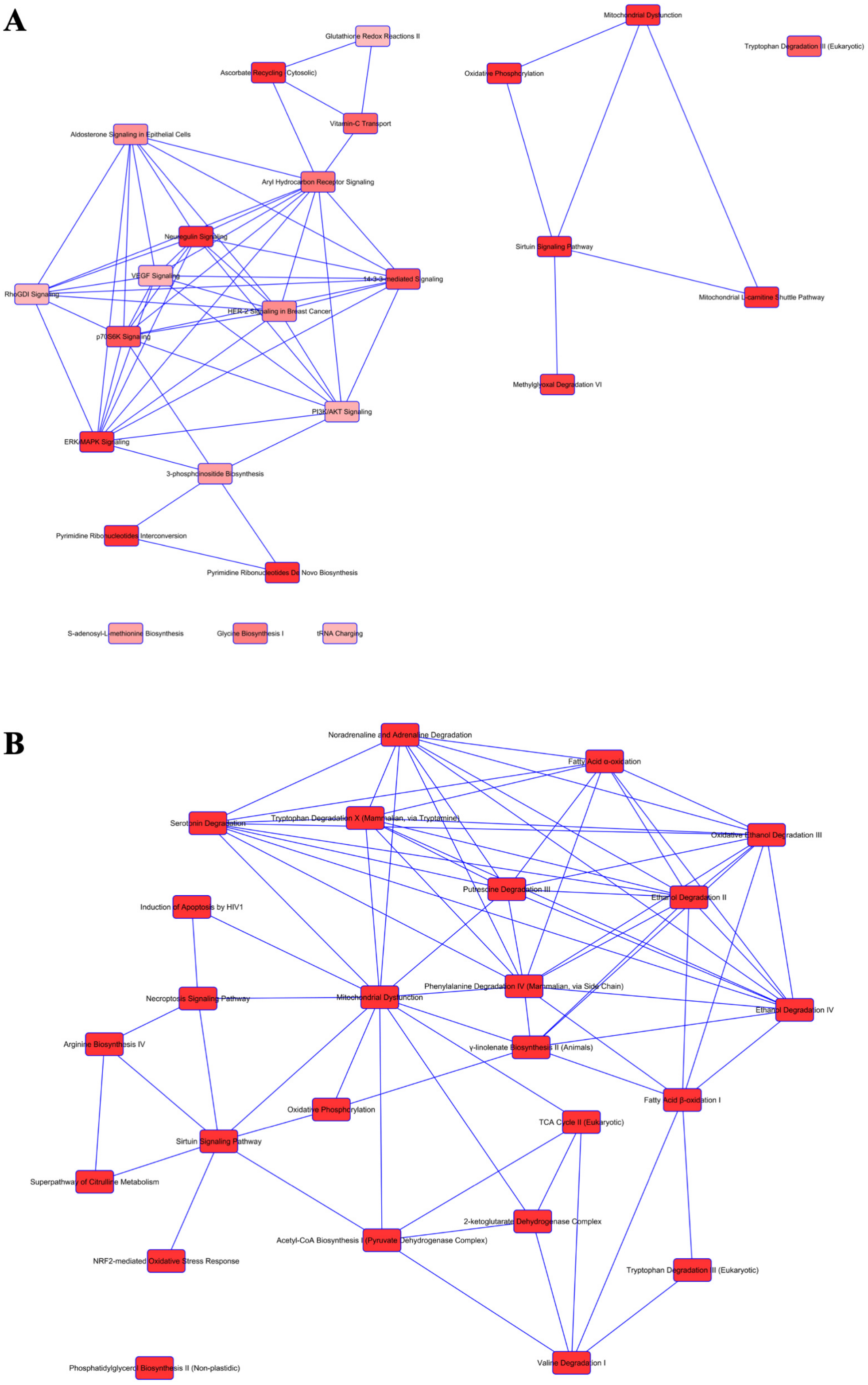
A
Glutathione Redox Reactions II
Ascorbate Recycling (Cytosolic)
Vitamin-C Transport
Aldosterone Signaling in Epithelial Cells
Aryl Hydrocarbon Receptor Signaling
Neuregulin Signaling
VEGF Signaling
14-3-3-mediated Signaling
RhoGDI Signaling
HER-2 Signaling in Breast Cancer
p70S6K Signaling
PI3K/AKT Signaling
ERK/MAPK Signaling
3-phosphoinositide Biosynthesis
Pyrimidine Ribonucleotides Interconversion
Pyrimidine Ribonucleotides De Novo Biosynthesis
S-adenosyl-L-methionine Biosynthesis
Glycine Biosynthesis I
tRNA Charging
Mitochondrial Dysfunction
Tryptophan Degradation III (Eukaryotic)
Oxidative Phosphorylation
Sirtuin Signaling Pathway
Mitochondrial L-carnitine Shuttle Pathway
Methylglyoxal Degradation VI
B
Noradrenaline and Adrenaline Degradation
Fatty Acid α-oxidation
Serotonin Degradation
Tryptophan Degradation X (Mammalian, via Tryptamine)
Oxidative Ethanol Degradation III
Putrescine Degradation III
Ethanol Degradation II
Induction of Apoptosis by HIV1
Phenylalanine Degradation IV (Mammalian, via Side Chain)
Necroptosis Signaling Pathway
Mitochondrial Dysfunction
Ethanol Degradation IV
Arginine Biosynthesis IV
γ-linolenate Biosynthesis II (Animals)
Fatty Acid β-oxidation I
Oxidative Phosphorylation
TCA Cycle II (Eukaryotic)
Sirtuin Signaling Pathway
Superpathway of Citrulline Metabolism
2-ketoglutarate Dehydrogenase Complex
Acetyl-CoA Biosynthesis I (Pyruvate Dehydrogenase Complex)
NRF2-mediated Oxidative Stress Response
Tryptophan Degradation III (Eukaryotic)
Phosphatidylglycerol Biosynthesis II (Non-plastidic)
Valine Degradation I

Figure 29. **Network of canonical pathways, associated to the mitochondrial proteome, altered in the brain and the kidneys of *Coq9*$^{+/+}$ mice under 1% of β−RA supplementation.**
A Network based on the canonical pathways altered in the mitochondrial proteome of the brain from *Coq9*$^{+/+}$ mice under 1% of β−RA supplementation.
B Network based on the canonical pathways altered in the mitochondrial proteome of the kidneys from *Coq9*$^{+/+}$ mice under 1% of β−RA supplementation.

To try to understand why β−RA produces toxic effects in wild-type mice but therapeutic outcomes in *Coq9*^{R239X} mice, we quantified the tissue levels of β−RA, as well as the levels of the natural CoQ precursor, 4-HB. As expected, a significant amount of β−RA is detected in the brain (Fig 30A) and the kidneys (Fig 31B), as well as in other tissues (Fig 31), of the treated animals, being the levels higher in the animals at the terminal stage. Importantly, the levels of β−RA are higher in the treated wild-type mice than in the treated *Coq9*^{R239X} mice, especially at the terminal stage (Fig 30A to B and Fig 31). Additionally, the tissue levels of 4-HB are also higher in the treated wild-type mice than in the treated *Coq9*^{R239X} mice (Fig 30C to D and Fig 31), except in the brain (Fig 30C). Thus, the higher levels of 4-HB in the wild-type animals may limit the use of β−RA by the CoQ biosynthetic pathway and, therefore, induce the accumulation of β−RA. However, certain amount of β−RA must be used by the CoQ biosynthetic pathway since a mild reduction of CoQ_9 and/or CoQ_{10} is observed in the brain (Fig 30E to F), the skeletal muscle (Fig 31H to I) and the heart (Fig 31O) of the animals treated with the high dose of β−RA, although the decrease is not statistically significant in the kidneys (Fig 30H to

I), liver (Fig 31C to D) and heart (Fig 31P). Additionally, small amounts of DMQ_9, an intermediate in the CoQ biosynthetic pathways that may inhibit the transfer of electrons in the Q junction (Yang *et al.*, 2011) are detected in the kidneys (Fig 30J), liver (Fig 31E) and skeletal muscle (Fig 31J) of the animals treated with the high dose of β–RA, but not in the brain (Fig 30G) or the heart (Fig 31Q). Those mild changes in the levels of CoQ and DMQ do not compromise the activities of the CoQ-dependent mitochondrial complexes I + III and II + III in any tissue (Fig 30K to N; Fig 31K to L and R to S).

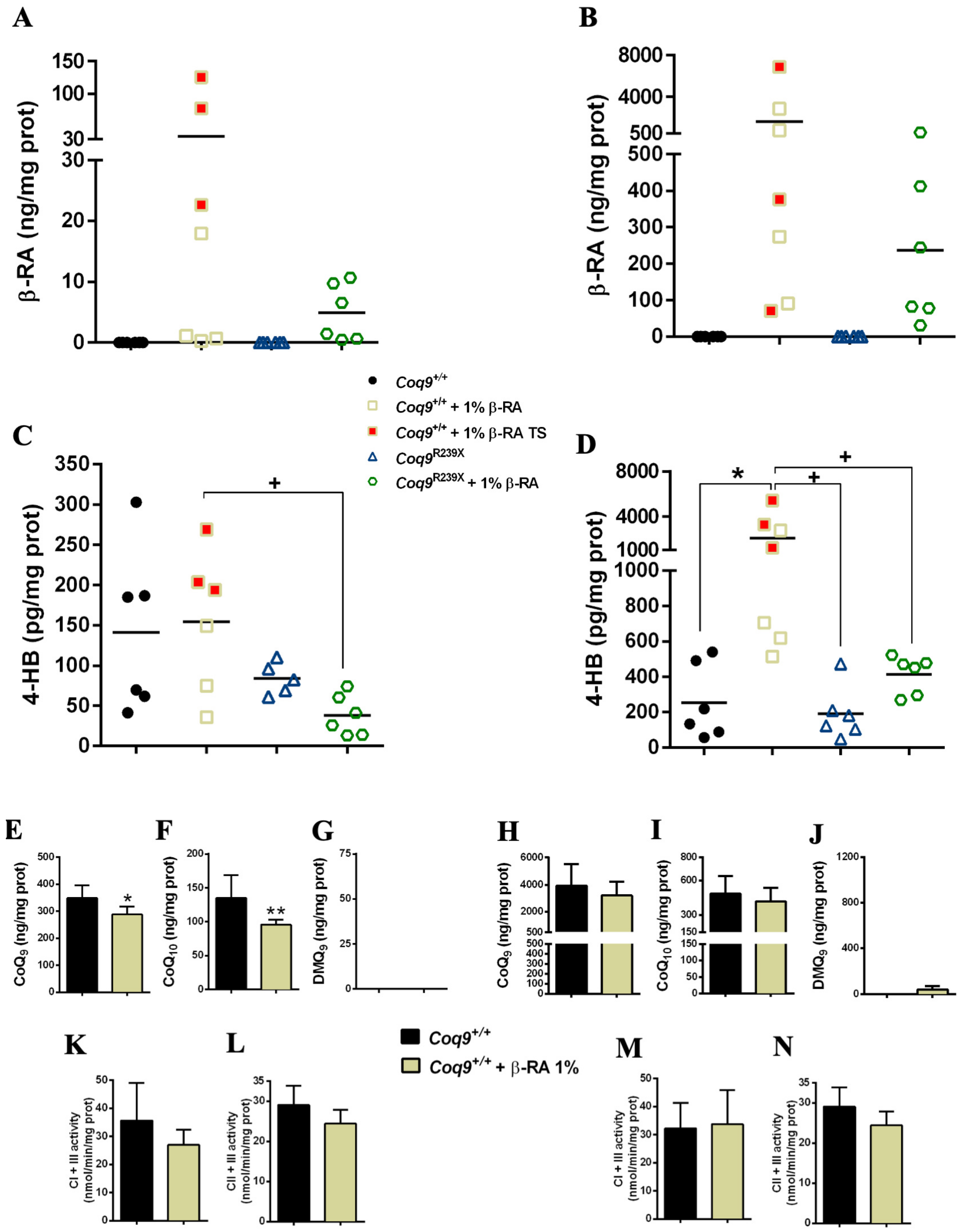

Figure 30. **CoQ metabolism and mitochondrial function in response to 1% β–RA supplementation in the brain and the kidneys from *Coq9*$^{+/+}$ mice.**

A,B Levels of β–RA in the brain (A) and the kidneys (B) from *Coq9*$^{+/+}$ mice, *Coq9*$^{+/+}$ mice under 1% of β–RA supplementation, *Coq9*^{R239X} mice and *Coq9*^{R239X} mice under 1% of β–RA supplementation.

C,D Levels of 4-HB in the brain (C) and the kidneys (D) from *Coq9*$^{+/+}$ mice, *Coq9*$^{+/+}$ mice under 1% of β–RA supplementation, *Coq9*^{R239X} mice and *Coq9*^{R239X} mice under 1% of β–RA supplementation.

E-J Levels of CoQ_9, CoQ_{10} and DMQ_9 in brain (E-G) and kidneys (H-J) from *Coq9*$^{+/+}$ mice and *Coq9*$^{+/+}$ mice under 1% of β–RA supplementation.
K-N Complex I + III (CI + III) and Complex II + III (CII + III) activities in the brain (K-L) and the kidneys (M-N) from *Coq9*$^{+/+}$ mice and *Coq9*$^{+/+}$ mice under 1% of β–RA supplementation. Data are expressed as mean ± SD. $^*P < 0.05$; $^{**}P < 0.01$; $^{***}P < 0.001$; *Coq9*$^{+/+}$ under 1% of β–RA supplementation or *Coq9*$^{+/+}$ under 1% of β–RA supplementation TS versus *Coq9*$^{+/+}$. $^+P < 0.05$; $^{++}P < 0.01$; $^{+++}P < 0.001$ *Coq9*$^{+/+}$ under 1% of β–RA supplementation TS versus *Coq9*$^{+/+}$ under 1% of β–RA supplementation (one-way ANOVA with a Tukey's post hoc test or t-test; n = 5–7 for each group).

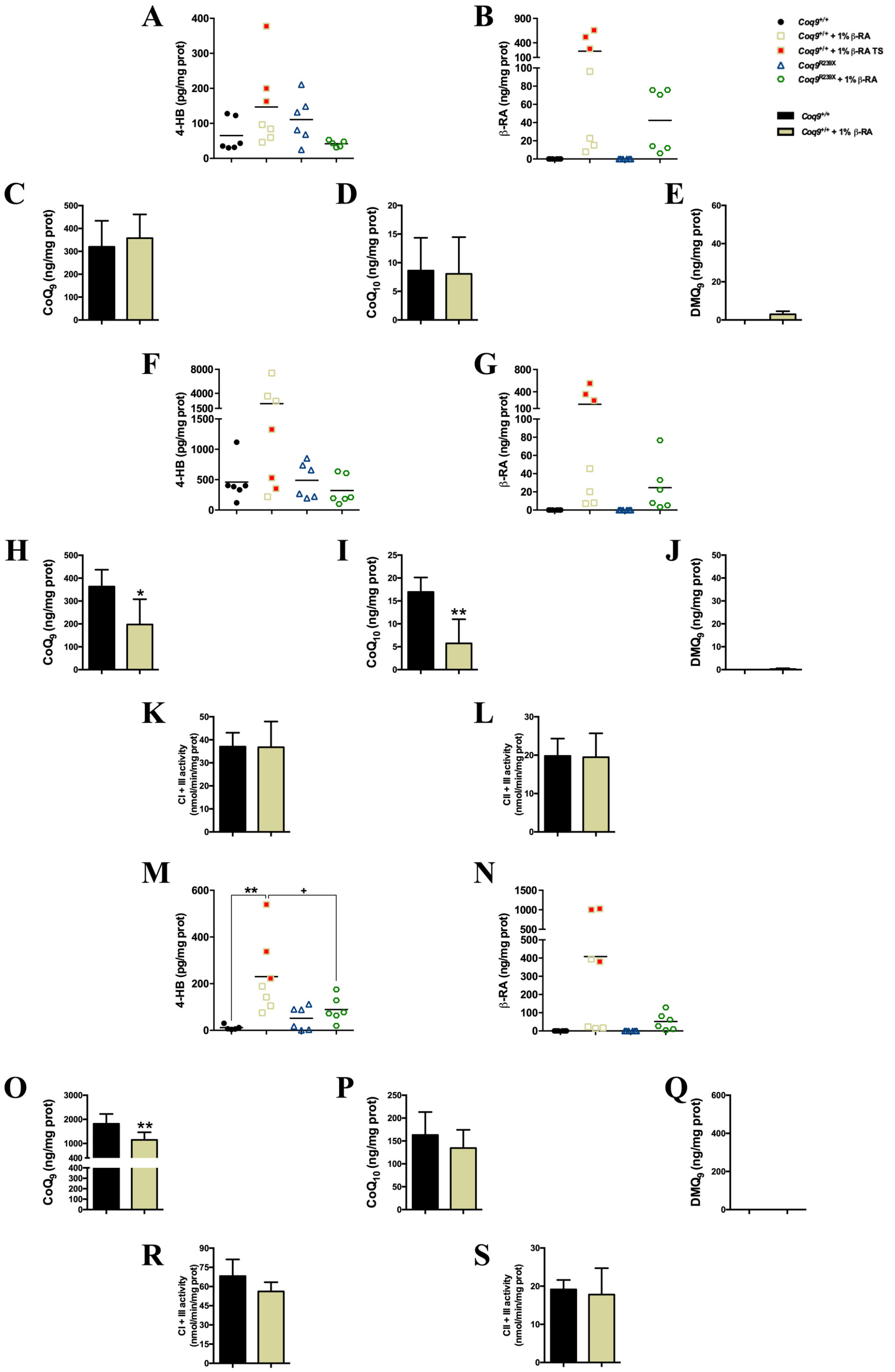
A
4-HB (pg/mg prot)
B
β-RA (ng/mg prot)
$Coq9^{+/+}$
$Coq9^{+/+}$ + 1% β-RA
$Coq9^{+/+}$ + 1% β-RA TS
$Coq9^{R239X}$
$Coq9^{R239X}$ + 1% β-RA
$Coq9^{+/+}$
$Coq9^{+/+}$ + 1% β-RA
C
CoQ_9 (ng/mg prot)
D
CoQ_{10} (ng/mg prot)
E
DMQ_9 (ng/mg prot)
F
4-HB (pg/mg prot)
G
β-RA (ng/mg prot)
H
CoQ_9 (ng/mg prot)
*
I
CoQ_{10} (ng/mg prot)
**
J
DMQ_9 (ng/mg prot)
K
CI + III activity (nmol/min/mg prot)
L
CII + III activity (nmol/min/mg prot)
M
4-HB (pg/mg prot)
**
+
N
β-RA (ng/mg prot)
O
CoQ_9 (ng/mg prot)
**
P
CoQ_{10} (ng/mg prot)
Q
DMQ_9 (ng/mg prot)
R
CI + III activity (nmol/min/mg prot)
S
CII + III activity (nmol/min/mg prot)

Figure 31. **CoQ metabolism and mitochondrial function in the liver, skeletal muscle and heart from $Coq9^{+/+}$ mice under 1% β–RA supplementation.**
A,B Levels of 4-HB and β–RA in the liver from $Coq9^{+/+}$ mice, $Coq9^{+/+}$ mice under 1% of β–RA supplementation, $Coq9^{R239X}$ mice and $Coq9^{R239X}$ mice under 1% of β–RA treatement.
C-E Levels of CoQ_9, CoQ_{10} and DMQ_9 in the liver from $Coq9^{+/+}$ mice and $Coq9^{+/+}$ mice under 1% of β–RA supplementation.
F,G Levels of 4-HB and β–RA in skeletal muscle of $Coq9^{+/+}$ mice, $Coq9^{+/+}$ mice under 1% of β–RA supplementation, $Coq9^{R239X}$ mice and $Coq9^{R239X}$ mice after 1% of β–RA treatment.
H-J Levels of CoQ_9, CoQ_{10} and DMQ_9 in the skeletal muscle from $Coq9^{+/+}$ mice, $Coq9^{+/+}$ mice under 1% of β–RA supplementation.
K,L Complex I + III (CI + III) and Complex II + III (CII + III) activities in skeletal muscle from $Coq9^{+/+}$ mice, $Coq9^{+/+}$ mice under 1% of β–RA supplementation.
M,N Levels of 4-HB and β–RA in the heart from $Coq9^{+/+}$ mice, $Coq9^{+/+}$ mice under 1% of β–RA supplementation, $Coq9^{R239X}$ mice and $Coq9^{R239X}$ mice under 1% of β–RA treatment.
O-Q Levels of CoQ_9, CoQ_{10} and DMQ_9 in the heart from $Coq9^{+/+}$ mice, $Coq9^{+/+}$ mice under 1% of β–RA supplementation.
R,S Complex I + III (CI + III) and Complex II + III (CII + III) activities in the heart from $Coq9^{+/+}$ mice, $Coq9^{+/+}$ mice under 1% of β–RA supplementation. Data are expressed as mean ± SD. *P < 0.05; **P < 0.01; ***P < 0.001; differences versus $Coq9^{+/+}$. +P < 0.05; ++P < 0.01; +++P < 0.001 differences versus $Coq9^{+/+}$ after 0.33% of β-RA treatment. (one-way ANOVA with a Tukey's post hoc test or t-test; n = 5–7 for each group).
TS = terminal stage

4.2.3 A LOWER DOSE OF β-RA AVOIDS ITS TOXIC EFFECTS IN WILD-TYPE ANIMALS, MAINTAINING ITS POTENTIAL TO REDUCE THE PHENOTYPIC AND HISTOPATHOLOGICAL SIGNS IN $Coq9^{R239X}$ MICE.

Because of the severe toxicity of the high dose of β–RA in wild-type animals, we decided to test the effect of a lower dose of β–RA in both wild-type and $Coq9^{R239X}$ mice. This low dose is a third of the dose previously used, i.e. 0.33 % of β–RA in the chow, which gives a dose of 0.3-1 g/kg bw/day. The low dose of β–RA does not affect the survival of $Coq9^{+/+}$ mice (Fig 32A), although the animals body weight is reduced in both males and females (Fig 32B to C). In *Coq9*^{R239X} mice, the treatment with the low dose of β–RA increases the survival (Fig 32A), although that increase is less intense than the one reported with the high dose of β–RA. Also, the locomotor activity and coordination increase in *Coq9*^{R239X} mice treated with the low dose of β–RA, compared to the untreated *Coq9*^{R239X} mice, while the treatment does not affect the results of the rotarod test in wild-type animals (Fig 32D to E). Consequently, both *Coq9*$^{+/+}$ and *Coq9*^{R239X} mice treated with the low dose of β–RA have a healthy appearance.

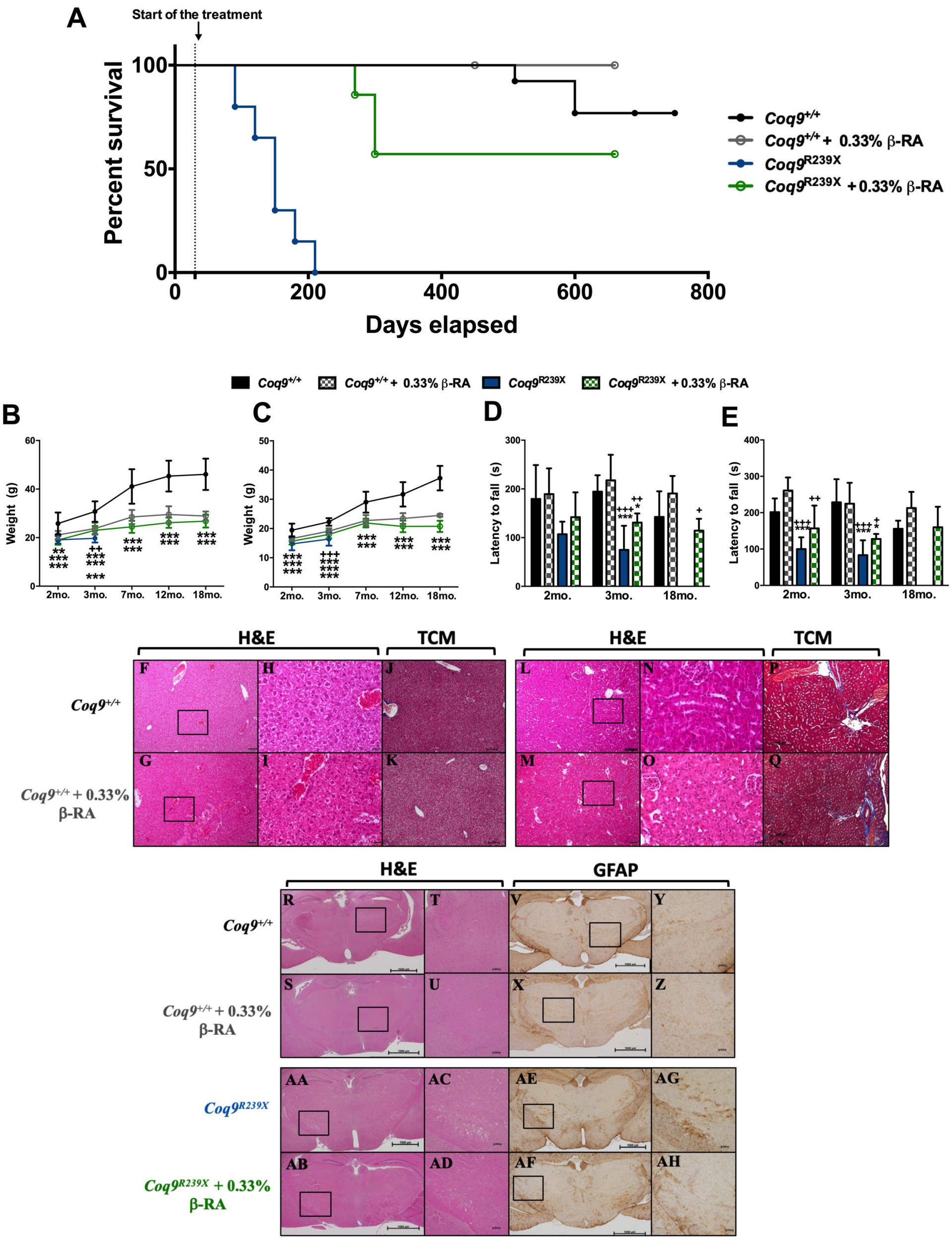

Figure 32. Survival and phenotypic-morphological characterization of *Coq9*$^{+/+}$ *and Coq9*^{R239X} mice after 0.33% of β–RA treatment.

A Survival curve of *Coq9*$^{+/+}$ mice, *Coq9*$^{+/+}$ mice under 0.33% of β–RA treatment, *Coq9*^{R239X} mice and *Coq9*^{R239X} mice under 0.33% of β–RA treatment. The treatments started at 1 month of age.

B,C Body weight of males (B) and females (C) of *Coq9*$^{+/+}$ mice*,* *Coq9*$^{+/+}$ mice under 0.33% of β–RA treatment, *Coq9*^{R239X} mice and *Coq9*^{R239X} mice under 0.33% of β–RA treatment.

D,E Rotarod test of males (D) and females (E) of *Coq9*$^{+/+}$ mice*,* *Coq9*$^{+/+}$ mice under 0.33% of β–RA treatment, *Coq9*^{R239X} mice and *Coq9*^{R239X} mice under 0.33% of β-RA treatment.
F-K H&E and Masson's Trichrome stains in the liver of *Coq9*$^{+/+}$ mice (F,H,J) and *Coq9*$^{+/+}$ mice under 0.33% β–RA supplementation (G,J,K).
L-Q H&E and Masson's Trichrome stains in the kidneys of *Coq9*$^{+/+}$ mice (L,N,P) and *Coq9*$^{+/+}$ mice under 0.33% β–RA treatment (M,O,Q).
R-Z H&E stain (R-U) and anti-GFAP stain (V-Z) in the diencephalon of *Coq9*$^{+/+}$ mice (R,T,V,I) and *Coq9*$^{+/+}$ mice under 0.33% β–RA supplementation (S,U,X,Z).
AA-AH H&E stain (AA-AD) and Anti-GFAP stain (AE-AH) in the diencephalon of *Coq9*^{R239X} mice (AA,AC,AE,AG) and *Coq9*^{R239X} mice under 0.33% of β–RA treatment (AB,AD,AF,AH). Data are expressed as mean ± SD. *P < 0.05; **P < 0.01; ***P < 0.001; differences versus *Coq9*$^{+/+}$. +P < 0.05; ++P < 0.01; +++P < 0.001 differences versus *Coq9*$^{+/+}$ under 0.33% of β–RA treatment (one-way ANOVA with a Tukey's post hoc test or t-test; n = 4–36 for each group).

Morphologically, the low dose of β–RA does not produce significant alterations in the liver (Fig 32F to K), kidneys (Fig 32L to Q) and brain (Fig 32R to Z) of wild-type animals, and the blood and urine markers of renal and hepatic functions are similar between the treated and untreated groups (Table 4). In *Coq9*^{R239X} mice, the most important histopathological features, i.e. the spongiosis (Fig 32AA to AC) and astrogliosis (Fig 32AE to AG), are decreased under the treatment with the low dose of β–RA (Fig 32AB to AD and AF to AH). Therefore, the therapeutic effect of the low dose in mutant animals is similar to the therapeutic effect previously described for the high dose.

Table 4. **Markers of hepatic and renal function in the plasma and urine from *Coq9*$^{+/+}$ mice and *Coq9*$^{+/+}$ mice under 0.33% of β–RA supplementation.**

PLASMA		
	***Coq9*$^{+/+}$**	***Coq9*$^{+/+}$ + 0.33 % β-RA**
	Mean ± SD	
GOT (U/L)	76.20 ± 21.75	66.95 ± 8.48
GPT (U/L)	41.70 ± 19.63	25.20 ± 9.81 *
AP (U/L)	24.58 ± 17.86	18.77 ± 15.49
Urea (mg/dl)	143.60 ± 147.93	5.97 ± 13.28 *
Creatinin (mg/dl)	0.50 ± 0.17	0.41 ± 0.086
Abumin (g/dl)	2.98 ± 0.11	2.90 ± 0.089
Bilirrubin (mg/dl)	1.28 ± 0.22	1.15 ± 0.26
URINE		
	***Coq9*$^{+/+}$**	***Coq9*$^{+/+}$ + 0.33 % β-RA**
	Mean ± SD	
Albumin (g/dl)	0.06 ± 0.026	0.03 ± 0.021
Total Protein (g/dl)	0.80 ± 0.46	0.72 ± 0.21
Creatinin (mg/dl)	31.39 ± 7.71	30.40 ± 4.24
Urea (mg/dl)	78.96 ± 125.65	3.72 ± 1.54
Uric Acid (mg/dl)	1.80 ± 1.70	1.72 ± 0.82
Phosphorus (mg/ml)	66.63 ± 26	77.02 ± 18.14
Calcium (mg/dl)	7.83 ± 4.83	6.79 ± 3.07
Magnesium (mg/dl)	5.47 ± 0.77	5.65 ± 1.77

GOT = glutamate-oxaloacetate transaminase; GPT = glutamate-pyruvate transaminase; AP = alkaline phosphatase.

4.2.4 THE THERAPEUTIC EFFECT OF THE LOW DOSE OF β-RA IS DUE TO THE REDUCTION OF THE DMQ/CoQ RATIO IN PERIPHERAL TISSUES OF *Coq9*^{R239X} MICE, LEADING TO A BIOENERGETICS IMPROVEMENT.

The decrease in the levels of DMQ was previously described as the main therapeutic mechanism of the high dose of β–RA in the treatment of *Coq9*^{R239X}

mice. We have then checked whether the low dose of β−RA induces a similar effect on the CoQ biosynthetic pathway. In general, β−RA interferes with CoQ metabolism in peripheral tissues but not in the brain. In *Coq9*^{R239X} mice, the low dose of β−RA induces a mild increase in the levels of CoQ_9 in the kidneys (Fig 33E) and in the levels of CoQ_{10} in the kidneys (Fig 33F) and the skeletal muscle (Fig 34D), compared to the untreated *Coq9*^{R239X} mice. However, the levels of CoQ_9 and CoQ_{10} did not change in the brain, skeletal muscle and heart of *Coq9*^{R239X} mice after the β−RA treatment (Fig 33A and B; Fig 34A to F). Remarkably, the levels of DMQ_9 and, consequently, the DMQ_9/CoQ_9 ratio, are significantly decreased in the kidneys (Fig 33G and H), liver (Fig 34G and H), skeletal muscle (Fig 34I and J) and heart (Fig 34K and L) of the *Coq9*^{R239X} treated with the low dose of β−RA, compared to untreated *Coq9*^{R239X} mice. However, the low dose of β−RA does not reduce the levels of DMQ_9 or DMQ_9/CoQ_9 ratio in the brain of the *Coq9*^{R239X} mice (Fig 33C and D), as happened for the treatment with the higher dose of β−RA. Therefore, the effect of the low dose of β−RA on CoQ metabolism in both *Coq9*$^{+/+}$ and *Coq9*^{R239X} mice is similar to the effect showed above and described for the treatment with the high dose of β−RA. In the *Coq9*$^{+/+}$ mice, the low dose of β−RA induces very mild changes in the tissue levels of CoQ_9, CoQ_{10} and DMQ_9 (Fig 33A to H and Fig 34A to L).

The tissue-specific reduction in the levels of DMQ on *Coq9*$^{\mathrm{R239X}}$ mice seems to correlate with the increase of β−RA levels, since the levels of β−RA are higher in the kidneys (Fig 33K), liver (Fig 34M) and heart (Fig 34Q), but not in the brain (Fig 33I) and skeletal muscle (Fig 34O), of the treated *Coq9*$^{\mathrm{R239X}}$ mice compared to the treated *Coq9*$^{+/+}$ mice. However, the levels of 4-HB do not increase in response to the treatment with the low dose of β−RA in either *Coq9*$^{+/+}$ or *Coq9*$^{\mathrm{R239X}}$ (Fig 33J and L; Fig 34N,P,R).

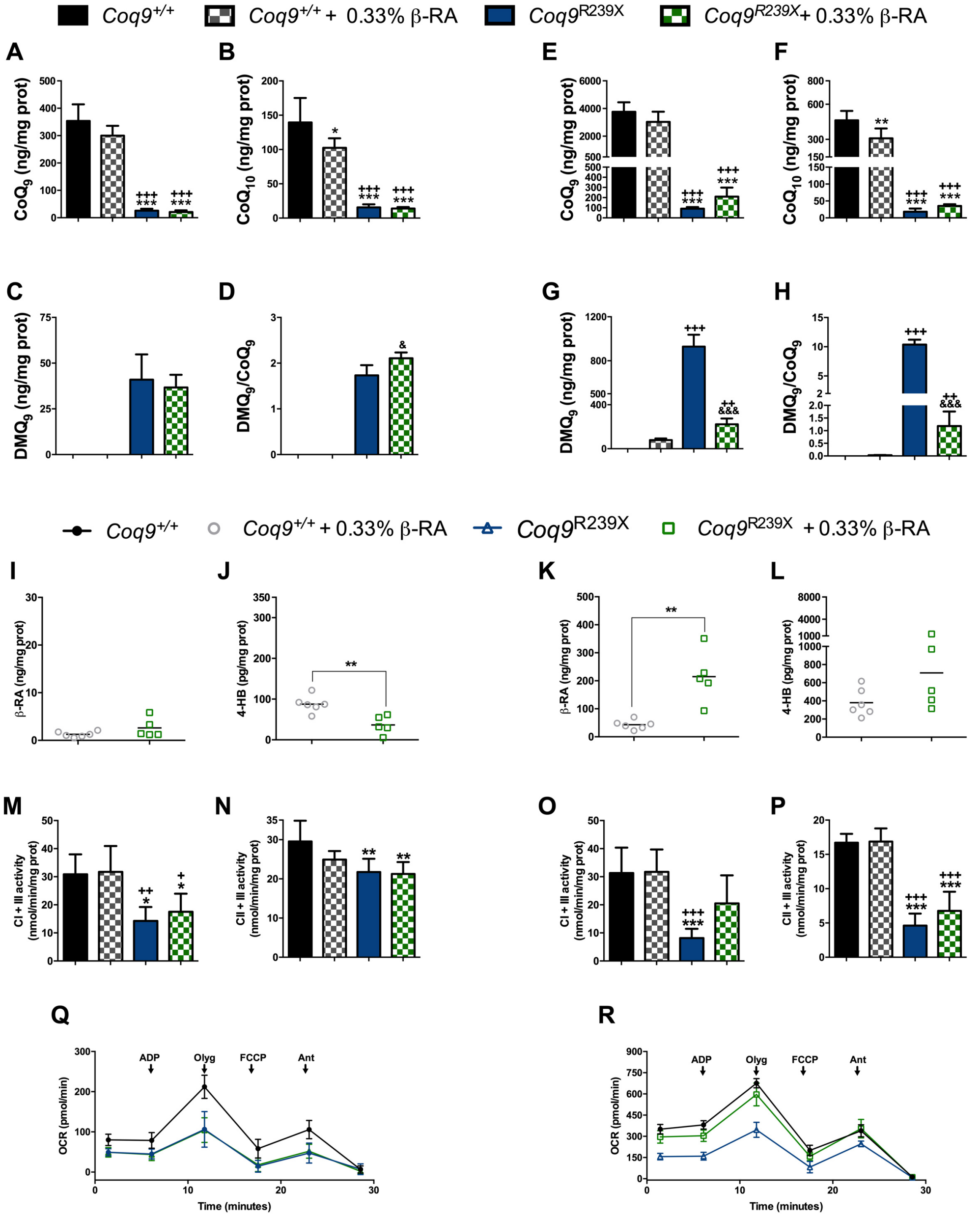

Figure 33. CoQ metabolism and mitochondrial function in the brain and the kidneys from $Coq9^{+/+}$ mice, $Coq9^{+/+}$ mice after 0.33% of β–RA treatment, $Coq9^{R239X}$ mice and $Coq9^{R239X}$ mice under 0.33% of β–RA treatment.

A-H Levels of CoQ$_9$, CoQ$_{10}$, DMQ$_9$ and the ratio DMQ$_9$/ CoQ$_9$ in the brain and the kidneys from $Coq9^{+/+}$ mice, $Coq9^{+/+}$ mice under 0.33% of β–RA treatment, $Coq9^{R239X}$ mice and $Coq9^{R239X}$ mice under 0.33% of β–RA treatment.

I-L Levels of β–RA and 4-HB in the brain and the kidneys from *Coq9*$^{+/+}$ mice, *Coq9*$^{+/+}$ mice under 0.33% of β–RA treatment, *Coq9*^{R239X} mice and *Coq9*^{R239X} mice under 0.33% of β–RA treatment.
M-P Complex I + III (CI + III) and Complex II + III (CII + III) activities in the brain and the kidneys from *Coq9*$^{+/+}$ mice, *Coq9*$^{+/+}$ mice under 0.33% of β–RA treatment, *Coq9*^{R239X} mice and *Coq9*^{R239X} mice under 0.33% of β–RA treatment.
Q,R Mitochondrial Oxygen Consumption rate (represented as State 3o, in the presence of ADP and substrates) in the brain and the kidneys from *Coq9*$^{+/+}$ mice, *Coq9*^{R239X} mice and *Coq9*^{R239X} mice under 0.33% of β–RA treatment. Data are expressed as mean ± SD. *P < 0.05; **P < 0.01; ***P < 0.001; differences versus *Coq9*$^{+/+}$. +P < 0.05; ++P < 0.01; +++P < 0.001 differences versus *Coq9*$^{+/+}$ after 0.33% of β-RA treatment. &P < 0.05; &&P < 0.01; &&&P < 0.001 differences versus *Coq9*^{R239X} (one-way ANOVA with a Tukey's post hoc test or t-test; n = 3–7 for each group).

Bioenergetically, the treatment with the low dose of β–RA does not produce any changes in the brain in either *Coq9*$^{+/+}$ or *Coq9*$^{\mathrm{R239X}}$ mice (Fig 33M,N,Q), but it induces an increase of the activities of complexes I + III and II + III (Fig 33O and P), as well as of the mitochondrial respiration in the kidneys of the treated *Coq9*$^{\mathrm{R239X}}$ mice (Fig 33R), compared to the untreated *Coq9*$^{\mathrm{R239X}}$ mice. These data are comparable to the data showed before for the treatment with the high dose of β–RA. Other tissues do not experience major changes in mitochondrial bioenergetics (Fig 34S to V).

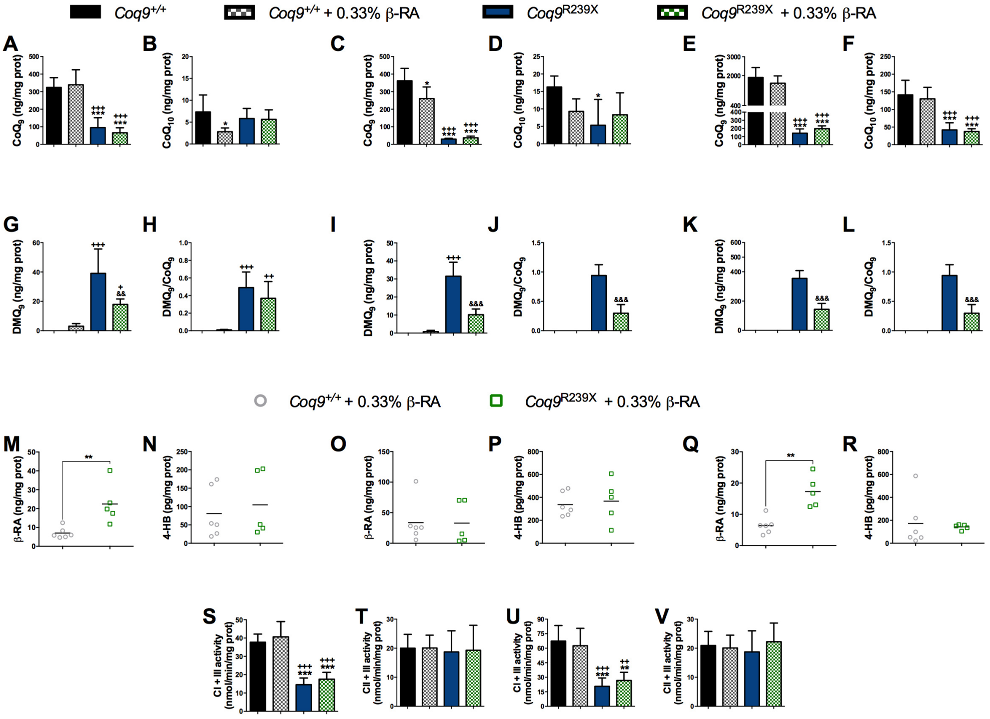

Figure 34. **CoQ metabolism and mitochondrial function in the liver, skeletal muscle and heart from *Coq9*$^{+/+}$ mice, *Coq9*$^{+/+}$ mice under 0.33% of β–RA treatment, *Coq9*^{R239X} mice and *Coq9*^{R239X} mice ander 0.33% of β–RA treatment.**

A-F Levels of CoQ$_9$ and CoQ$_{10}$ in the liver (A,B), skeletal muscle (C,D) and heart (E,F) from *Coq9*$^{+/+}$ mice*, Coq9*$^{+/+}$ mice under 0.33% of β–RA treatment, *Coq9*^{R239X} mice and *Coq9*^{R239X} mice under 0.33% of β–RA treatment.
G-L Levels of DMQ$_9$ and DMQ$_9$/CoQ$_9$ ratio in the liver (G,H), skeletal muscle (I,J) and heart (K,L) from *Coq9*$^{+/+}$ mice*, Coq9*$^{+/+}$ mice under 0.33% of β–RA treatment, *Coq9*^{R239X} mice and *Coq9*^{R239X} mice under 0.33% of β–RA treatment.
M-R Levels of β–RA and □□□□ in the liver (M,N), skeletal muscle (O,P) and heart (Q,R) from *Coq9*$^{+/+}$ mice*, Coq9*$^{+/+}$ mice under 0.33% of β–RA treatment, *Coq9*^{R239X} mice and *Coq9*^{R239X} mice under 0.33% of β–RA treatment.
S-V Complex I + III (CI + III) and Complex II + III (CII + III) activities in the skeletal muscle

(V,W) and heart (X,Y) from *Coq9*$^{+/+}$ mice*, Coq9*$^{+/+}$ mice under 0.33% of β–RA treatment,

Coq9^{R239X} + mice and *Coq9*^{R239X} mice under 0.33% of β–RA treatment. Data are expressed as

mean ± SD. *P < 0.05; **P < 0.01; ***P < 0.001; differences versus *Coq9*$^{+/+}$. +P < 0.05; ++P

< 0.01; +++P < 0.001 differences versus *Coq9*$^{+/+}$ after 0.33% of β-RA treatment. &P < 0.05;

&&P < 0.01; &&&P < 0.001 differences versus *Coq9*^{R239X} (one-way ANOVA with a Tukey's post hoc test or t-test; n = 5–6 for each group).

4.2.5 CO-ADMINISTRATION OF 4-HB MODIFIES THE EFFECTS OF β-RA

Our data suggest that either the toxic effect of β−RA in *Coq9*$^{+/+}$ mice or the therapeutic results in *Coq9*^{R239X} mice can be modulated by 4-HB, since both 4-HB and β−RA compete to enter in the CoQ biosynthetic pathway through the activity of COQ2. To check this premise, we supplemented *Coq9*$^{+/+}$ and *Coq9*^{R239X} mice with an equal amount of 4-HB and β−RA incorporated into the chow. Interestingly, the co-administration of 4-HB and β−RA suppresses the inhibitory effect of β−RA over CoQ_9 (Fig 35A to E) and CoQ_{10} biosynthesis (Fig 35F to J) in all tissues of the *Coq9*$^{+/+}$ mice (compared to Fig 33 and 34, 36). Even more, the levels of CoQ_9 increases in the brain (Fig 35A) and the kidneys (Fig 35B) of the *Coq9*$^{+/+}$ mice treated with the combination of 4-HB and β−RA, compared to the untreated *Coq9*$^{+/+}$ mice. In *Coq9*^{R239X} mice, the untreated and treated groups show similar levels of both CoQ_9 (Fig 35A to E) and CoQ_{10} (Fig 35F to J). Importantly, the reduction of the levels of DMQ_9 and of the DMQ_9/CoQ_9 ratio induced by β−RA (Fig 33 and 34) in *Coq9*^{R239X} mice is suppressed by the co-administration of 4-HB and β−RA (Fig 35K to T and 36). Consequently, the co-administration of 4-HB and β−RA does not induce an increase of survival of *Coq9*^{R239X} mice (Fig 35U). Together, these data confirm that the adequate levels of 4-HB are essential for the toxic or therapeutic effect of β−RA in *Coq9*$^{+/+}$ or *Coq9*^{R239X} mice, respectively.

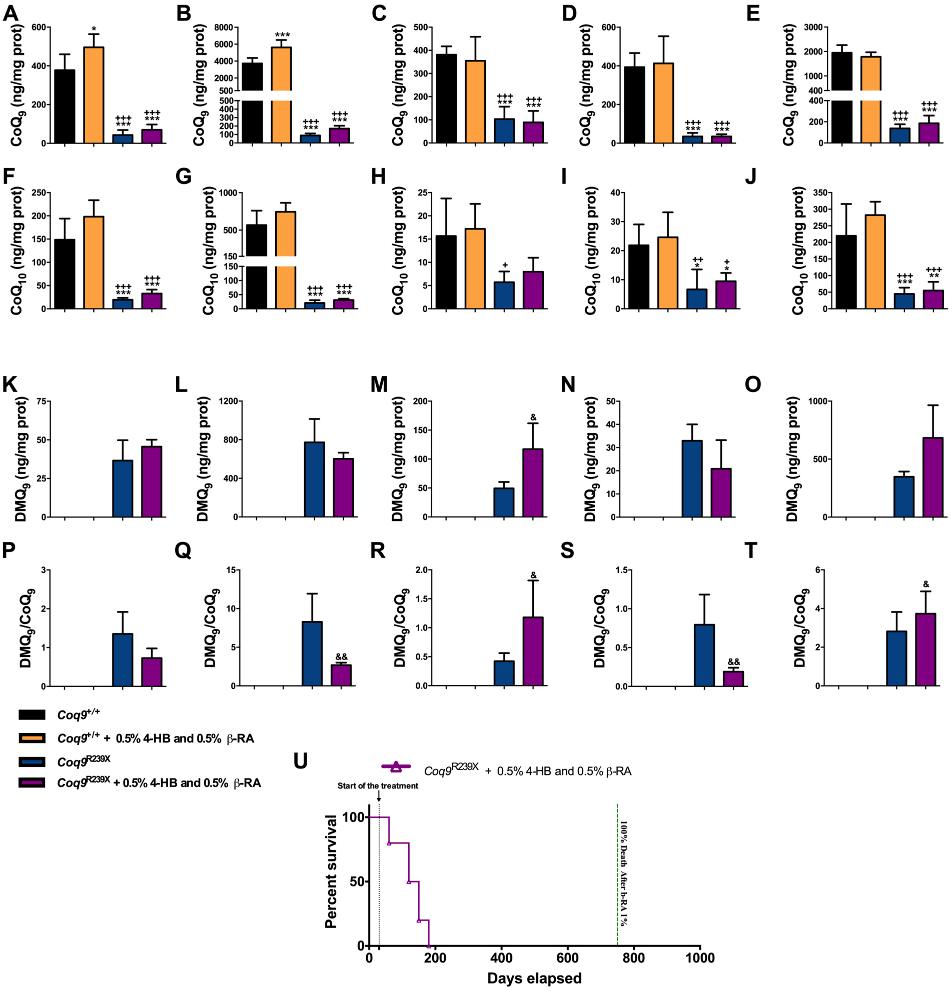

Figure 35. **Co-administration of 4-HB suppresses the effects of β−RA treatment in *Coq9*$^{+/+}$ and *Coq9*^{R239X} mice.**

A-E Levels of CoQ_9 in the brain, kidneys, liver, skeletal muscle and heart from *Coq9*$^{+/+}$ mice, *Coq9*$^{+/+}$ mice under 0.5% of 4-HB + 0.5% of β-RA treatment, *Coq9*^{R239X} mice and *Coq9*^{R239X} mice under 0.5% of 4-HB + 0.5% of β-RA treatment.

F-J Levels of CoQ_{10} in the brain, kidneys, liver, skeletal muscle and heart from *Coq9*$^{+/+}$ mice, *Coq9*$^{+/+}$ mice under 0.5% of 4-HB + 0.5% of β-RA treatment, *Coq9*^{R239X} mice and *Coq9*^{R239X} mice under 0.5% of 4-HB + 0.5% of β-RA treatment.
K-O Levels of DMQ_9 in the brain, kidneys, liver, skeletal muscle and heart from *Coq9*$^{+/+}$ mice, *Coq9*$^{+/+}$ mice under 0.5% of 4-HB + 0.5% of β-RA treatment, *Coq9*^{R239X} mice and *Coq9*^{R239X} mice under 0.5% of 4-HB + 0.5% of β-RA treatment.
P-T Ratio DMQ_9/ CoQ_9 in the brain, kidneys, liver, skeletal muscle and heart from *Coq9*$^{+/+}$ mice, *Coq9*$^{+/+}$ mice under 0.5% of 4-HB + 0.5% of β-RA treatment, *Coq9*^{R239X} mice and *Coq9*^{R239X} mice under 0.5% of 4-HB + 0.5% of β-RA treatment.
U Survival curve of *Coq9*^{R239X} mice under 0.5% of 4-HB + 0.5% of β-RA treatment. Data are expressed as mean ± SD. $^*P < 0.05$; $^{**}P < 0.01$; $^{***}P < 0.001$; differences versus *Coq9*$^{+/+}$. $^+P < 0.05$; $^{++}P < 0.01$; $^{+++}P < 0.001$ differences versus *Coq9*$^{+/+}$ after 0.5% of 4-HB and 0.5% of β-RA treatment. &P < 0.05; &&P < 0.01; &&&P < 0.001 differences versus *Coq9*^{R239X} (one-way ANOVA with a Tukey's post hoc test or t-test; n = 5–10 for each group).

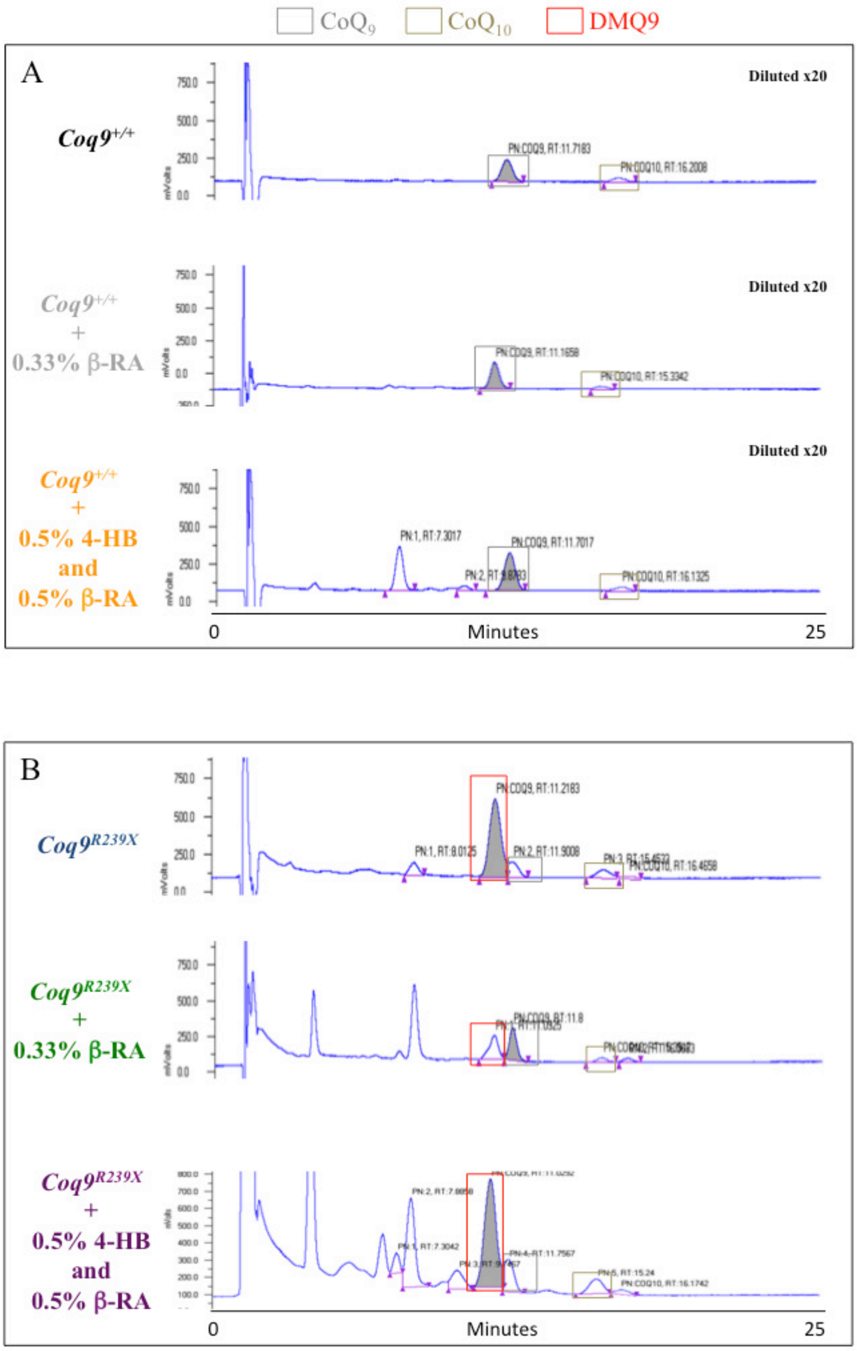

Figure 36. **Representative chromatographs showing the peaks of CoQ_9 and DMQ_9 in the kidneys.**

A Chromatographs for CoQ_9 in the kidney of a *Coq9*$^{+/+}$ mouse, *Coq9*$^{+/+}$ mouse under 0.33% of β–RA treatment and *Coq9*$^{+/+}$ mouse under 0.5% of 4-HB + 0.5% of β–RA treatment.

B Chromatographs for CoQ_9 and DMQ_9 in the kidney of a *Coq9*^{R239X} mouse, *Coq9*^{R239X} mouse under 0.33% of β–RA treatment and *Coq9*^{R239X} mouse under 0.5% of 4-HB + 0.5% of β–RA treatment.

4.3 SULFIDE METABOLISM AND CoQ DEFICIENCY

4.3.1 MODULATION OF SULFIDE METABOLISM TO PREVENT THE PATHOLOGIC FEATURES IN *Coq9*^{R239X} MICE

To assess the effects of different sulfur amino acids availability on SQOR levels *in vivo*, we measured SQOR levels in the kidney of *Coq9*^{R239X} mice under supplementation with NAC, a sulfur-containing amino acid, or a diet with SAAR, since the kidney has a very active sulfide metabolism and it has reduced levels of SQOR in *Coq9*^{R239X} mice. To evaluate whether the transsulfuration pathway may adapt to the changes on SQOR levels, we also quantified the levels of CBS. The levels of SQOR are significantly lower in the kidneys of *Coq9*^{R239X} mice than in the kidneys of *Coq9*$^{+/+}$, and they are not rescued by NAC or SAAR supplementation (Fig 37A). Besides, in the kidneys of *Coq9*^{R239X} mice, the levels of CBS were slightly increased compared to *Coq9*$^{+/+}$ mice and this change was maintained under supplementation with NAC or SAAR (Fig 37B). Therefore, there is an inverse correlation between SQOR and CBS. In addition, we checked the glutathione metabolism. The kidneys of *Coq9*^{R239X} mice, showed decreased levels of total glutathione, and that decrease is preserved after the supplementation with NAC or SAAR (Fig 37C). Moreover, the GSSG/GSH ratio is reduced in untreated *Coq9*^{R239X} mice, as well as in *Coq9*^{R239X} mice treated with NAC or SAAR, compared to *Coq9*$^{+/+}$ mice (Fig 37D). The levels of the glutathione enzymes, GPx and GRd, are mildly decreased in the three experimental groups of *Coq9*^{R239X} mice, compared to *Coq9*$^{+/+}$ mice, although the decrease is statistically significant only in the case of GPx in untreated *Coq9*^{R239X} mice (Fig 37E). These results indicate that CoQ_{10} regulates the levels of SQOR *in vivo*, independently of the sulfur amino acids availability. Since NAC or SAAR did not induce any change on sulfide metabolism, the survival of *Coq9*^{R239X} mice were not improved after those treatments (Fig 37F).

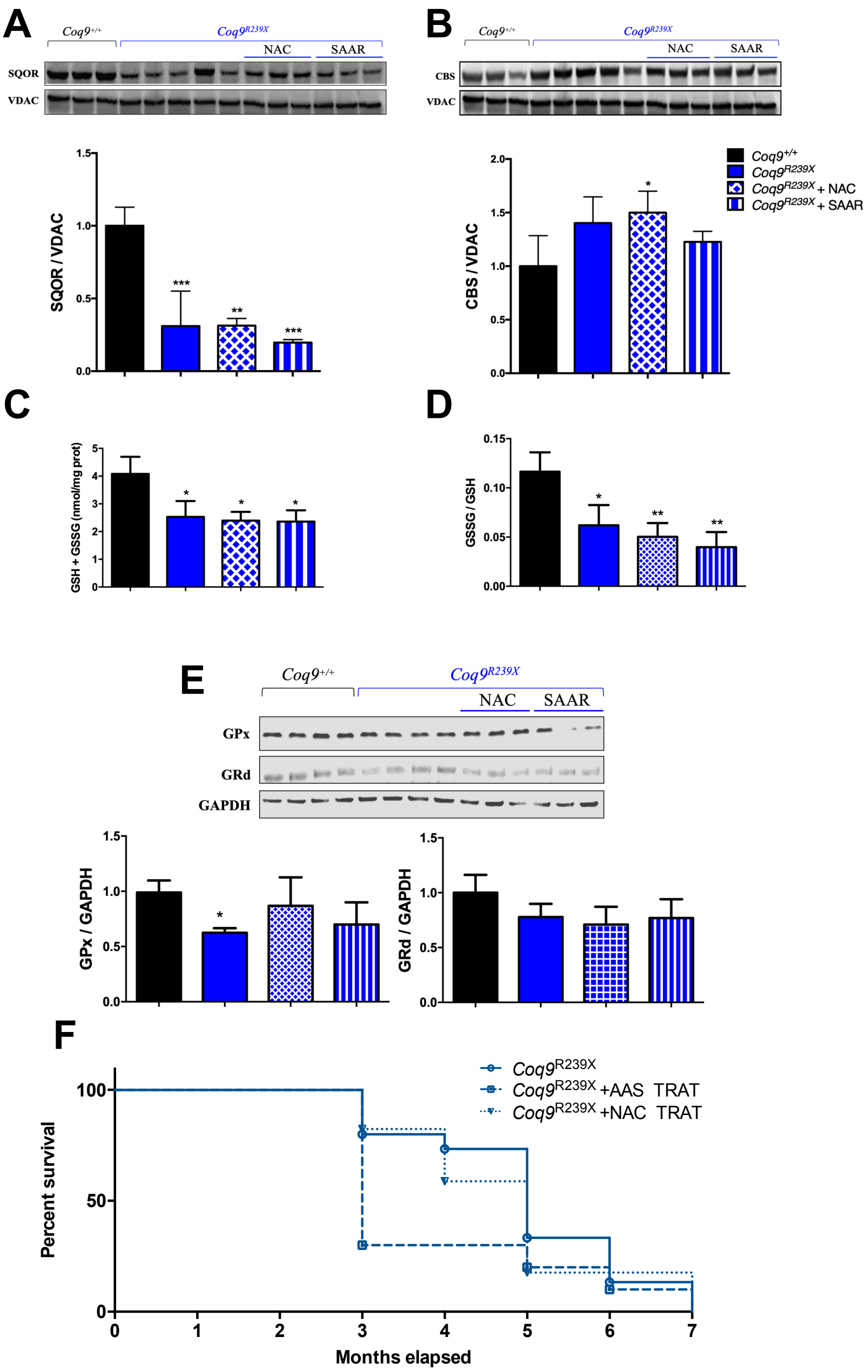

Figure 37. **Sulfide metabolism oxidation (SQOR) and transulfuration (CBS) proteins levels, and subsequent survival, are independent of the sulfur amino acids availability in mice tissues.**

A,B SQR and CBS protein levels (*A and B*) in kidneys of *Coq9*$^{+/+}$, *Coq9*^{R239X} and *Coq9*^{R239X} under NAC or SAAR treatment mice.

C Survival of *Coq9*^{R239X} and *Coq9*^{R239X} under NAC or SAAR treatment mice (C). Data are expressed as mean ± SD. **P* < 0.05; ***P* < 0.01; ****P* < 0.001; *Coq9*^{R239X} and *Coq9*^{R239X} under NAC or SAAR treatment versus *Coq9*$^{+/+}$ mice. (one-way ANOVA with a Tukey's *post hoc* test; n = 5-16 for each group).

DISCUSSION

5. DISCUSSION

5.1 β-RA SUPLEMENTATION AS ALTERNATIVE THERAPY FOR PRIMARY CoQ DEFICIENCY.

The treatment of primary or secondary mitochondrial diseases is, in most cases, still limited to a palliative care. Primary and secondary CoQ deficiencies constitute a mitochondrial syndrome with heterogeneous clinical presentations, involving different pathomechanims. The conventional treatment is based in the exogenous administration of high doses of CoQ_{10}. This treatment, however, has limited effects in a high percentage of patients due to different factors: 1) the low absorption and bioavailability of the exogenous CoQ_{10}, together with its low capacity to cross the BBB; 2) the lack of effect over the accumulation of intermediate metabolites in the synthesis of CoQ (importantly, some of these metabolites, e.g. DMQ, may contribute to the disease phenotype by inhibiting the transfer of electrons in the mtETC); and 3) the lack of effect over the Complex Q and the endogenous biosynthesis of CoQ. For that reason, CoQ_{10} therapy does not induce any change in the levels of CoQ_9.

In this study, we identify a novel treatment for primary CoQ deficiency. The treatment is based on the administration of β–RA, which reduces the molecular, histopathologic, and clinical signs of mitochondrial encephalopathy in a mouse model of encephalopathy associated with CoQ deficiency. The remarkable increase of survival after β−RA treatment was superior to that observed after ubiquinol-10 treatment, and the therapeutic effect was succeeded even if the treatment started in a symptomatic period. The striking increase in animal survival and the general health improvement after the β−RA treatment was achieved even though the levels of CoQ and mitochondrial function were not increased in the brain, which is the most relevant tissue for the development of the disease. In peripheral tissues, however, β−RA induced a decrease in the DMQ_9/CoQ_9 ratio, resulting in a bioenergetics improvement that may exert a key influence on the brain pathology. Accordingly, we provide additional data about the DMQ_9/CoQ_9 ratio in the *Coq9*^{Q95X} mouse model and in *Coq9*^{R239X} mice treated with ubiquinol-10, and both cases support the importance of the DMQ_9/CoQ_9 ratio in the progression of the clinical symptoms associated with CoQ deficiency syndrome.

The initial hypothesis for this study was that β−RA could be used in the CoQ biosynthetic pathway and bypasses the defect in COQ9-COQ7, increasing the endogenous levels of CoQ (Luna-Sanchez *et al.*, 2015; Pierrel, 2017). However, our results show that the bypass effect would be limited because only the kidneys, the tissue with higher levels of β−RA, showed a moderate increase in the levels of CoQ in the mutant mice after the treatment.

Nevertheless, the levels of DMQ_9 were significantly decreased not only in the kidneys but also in the skeletal muscle, liver, and heart. Those results hint that the CoQ biosynthetic pathway might use β–RA as a substrate whose Km is probably higher than the natural substrate, 4-HB, and for that reason the reduction of the DMQ_9 levels is not accompanied by an increase of CoQ_9 in tissues where the β–RA does not reach a threshold (Pierrel, 2017). Also, the stabilization of the Complex Q may contribute to this effect, since the levels of COQ4, COQ5, COQ6, and COQ8A were slightly increased in the kidneys and heart after β–RA treatment. Consistent with those results, 4-HB or vanillic acid induced an increase of the CoQ biosynthetic protein *in vitro* (Herebian *et al.*, 2017). Also, β–RA was able to rescue the decreased levels of COQ5, but not COQ3 or COQ7, in a glomerular podocytes-specific *ADCK4* mutant mice (Widmeier *et al*, 2020). Moreover, we must also consider that the β–RA administration was able to increase the levels of CoQ_9 in renal and cardiac mitochondria, as well as in muscle tissue in a conditional *Coq7* KO model, which lacks COQ7 protein (Wang *et al.*, 2015; Wang *et al.*, 2017). Nevertheless, the cerebral CoQ_9 levels after β–RA supplementation were not determined in the conditional *Coq7* KO mice (Wang *et al.*, 2015; Wang *et al.*, 2017). Also, the levels of CoQ were not shown in two recent reports about the theraputic effects of β–RA in two glomerular podocytes-specific *Coq6* and *Adck4* knockout mice (Widmeier *et al*, 2019; Widmeier *et al.*, 2020). Because

Coq9^{R239X} mice has reduced levels not only of COQ7 but also of COQ4, COQ5, COQ6, and COQ8A (Luna-Sanchez *et al.*, 2015), it is also possible that the limitation of the β–RA to generally increase the CoQ_9 levels in *Coq9*^{R239X} mice could be due to the disruption of the Complex Q observed in this mouse model. The combination of both arguments could explain the lack of effect over the CoQ biosynthesis pathway in the brain. In either case, our data on the *Coq9*^{R239X} mouse model together with those obtained in the *Coq6*, *Coq7* and *Adck4* conditional KO models indicate that it is possible to influence the CoQ biosynthesis *in vivo* with the use of the appropriated 4-HB analog(s). These results partially corroborate previous data *in vitro* using mutant yeasts and human skin fibroblasts derived from patients with primary CoQ deficiency (Doimo *et al*, 2014a; Freyer *et al.*, 2015; Herebian *et al.*, 2017; Luna-Sanchez *et al.*, 2015; Ozeir *et al*, 2011; Pierrel, 2017; Wang *et al.*, 2017; Xie *et al.*, 2012).

While the levels of CoQ_9 and CoQ_{10} were doubled in the kidneys of *Coq9*^{R239X} mice after the treatment, the levels reached after the treatment were barely 5% of the wild-type levels. The reduction in the DMQ_9 levels after the therapy, and as a consequence, the DMQ_9/CoQ_9 ratio, was more important in terms of absolute values, as well as more consistent because the response was similar in all peripheral tissues. Importantly, the decrease in DMQ_9/CoQ_9 ratio in peripheral tissues (like kidneys, heart, and muscle) was enough to increase the CoQ-dependent complexes activities up to normalizing the mitochondrial respiration. Therefore, the effect of the β–RA treatment in the function of the renal, muscular, and cardiac mitochondria must be due to the reduction of the DMQ_9/CoQ_9 ratio. In line with it, the altered renal function of the *Coq6* and *Adck4* glomerular podocytes-specific KO models were rescued by the treatment with β–RA but no quinone levels, DMQ or CoQ, were shown (Widmeier *et al.*, 2019; Widmeier *et al.*, 2020). While DMQ is not commercial available to develop more direct experiments, Yang and collaborators were able to exchange the quinone pools between the mitochondria from wild-type and *Clk-1* (= *Coq7*) mutated worms, demonstrating that DMQ_9 was the responsible of the inhibition of the electron transfer from complex I to ubiquinone in the mitochondrial respiratory chain (Yang *et al.*, 2011), probably due to the competition of CoQ and DMQ for the same binding site, together with the inability of DMQ to transfer electrons (Arroyo *et al*, 2006). Our results in mice suggest that DMQ could also inhibit the electron transfer from complex II to ubiquinone, a fact that was not observed in worms (Yang *et al.*, 2011). Those differences may reflect the diverse structure and functionality of the mitochondria in different organisms, tissues, and cell types (Vafai & Mootha, 2012). Thus, our study points out the importance of the DMQ_9/CoQ_9 ratio in the disease phenotype, a fact that is further supported by several evidences: (i) The *Coq9*^{Q95X} mouse model has low levels of DMQ_9 and higher levels of CoQ biosynthetic proteins (compared to the *Coq9*^{R239X} mouse model), and the lifespan is not compromised; (ii) the treatment with ubiquinol-10 in *Coq9*^{R239X} mice does not change the DMQ$_9$ levels and its therapeutic effects are significantly lower than those after β–RA treatment; (iii) the reduction in the DMQ$_9$ levels in the *Coq7* conditional KO mice after β–RA therapy may also contribute to the increased survival observed in this mouse model, although the phenotype of this mouse model were not profound described (Wang *et al.*, 2015); and (iv) patients with high levels of DMQ$_{10}$ in the samples used for the diagnostic (muscle and/or skin fibroblasts) are associated to severe clinical presentations (Danhauser *et al.*, 2015; Duncan *et al.*, 2009; Freyer *et al.*, 2015; Smith *et al.*, 2018; Wang *et al.*, 2017).

Because the levels of CoQ$_9$ and DMQ$_9$ did not change in the brain of the *Coq9*^{R239X} mice after the treatment, this tissue did not experience any improvement in the mitochondrial function after β–RA therapy. However, even if the treatment does not have any detectable effect at the cerebral mitochondria, the *Coq9*^{R239X} mice showed a clear and profound reduction in the spongiform degeneration, reactive astrogliosis, and oxidative damage, leading to an absence of brain injuries after the β–RA therapy. Those effects are, therefore, independent of the CoQ$_9$ and DMQ$_9$ levels in the brain. Thus, two complementary hypotheses could explain the therapeutic effects of β–RA in the brain of *Coq9*^{R239X} mice. First, β–RA may have CoQ-independent functions with therapeutic potential for mitochondrial encephalopathies. The transcriptomics data showing a decrease in the expression levels of some inflammatory genes, and the fact that β–RA is a structural analogue of salicylic acid (Gomez-Guzman *et al.*, 2014), would support this hypothesis. However, our experimental data do not support this hypothesis because: (i) The microglia distribution and the cytokines levels did not experience major changes between *Coq9*^{R239X} mice and *Coq9*^{R239X} mice treated with β–RA; (ii) β–RA did not reduce iNOS expression or cytokines release in RAW cells stimulated with LPS; (iii) β–RA did not have therapeutic effects in pharmacological or genetic models of neuroinflammation, e.g., the MPTP-induced zebrafish model of Parkinson disease and the *Ndufs4* mouse model of Leigh syndrome; and (iv) β–RA did not inhibit mTORC1 *in vivo*. Thus, the changes in the expression levels of some inflammatory genes may reflect the reduction in the astrogliosis. In fact, some genes associated with chemokine (e.g., C-C Motif Chemokine Ligands family) and cytokine signaling (e.g., Cd14, Ifitm3, Hmox1), immune response (Nurp1), cell cycle (e.g., Eif4bpp1), cell adhesion (e.g., Ecm1, Igfb4), and lipid metabolism (e.g., Ch25) have been also associated to reactive astrogliosis (Colombo & Farina, 2016; Zamanian *et al*, 2012) and, therefore, the reduction observed in these genes could be due to the reduction in the astrogliosis. Our data also suggest that, similarly to other mitochondrial encephalopathies (Lax *et al*, 2012; Tegelberg *et al*, 2017), the neuroinflammation associated with microglia activation is not an important factor in the mitochondrial encephalopathy associated with CoQ deficiency.

The second hypothesis is that the reduction in DMQ_9/CoQ_9 ratio in peripheral tissues and the subsequent improvement of mitochondrial bioenergetics may provide some tissue–brain cross-talk in order to reduce the astrogliosis, spongiosis, and its associated brain injury. While we were not able to reveal how the peripheral tissues communicate with the brain in this situation, a recent study about gene therapy in a mouse model of Leigh syndrome also suggests that the correction of the gene defect in peripheral tissues is important to reduce brain pathology (Di Meo *et al*, 2017). The studies about the kidney–brain, heart–brain, or liver–brain cross-talk, as well as the presence of a gut–brain axis, would support the concept of an influence of peripheral tissues in the brain pathology, and reactive astrogliosis in particular (Butterworth, 2016; Mayo *et al*, 2014; Miranda *et al*, 2017; Rothhammer *et al*, 2017; Rothhammer *et al*, 2016; Thackeray *et al*, 2018).

In conclusion, our study shows that β–RA is a powerful therapeutic agent for the mitochondrial encephalopathy due to CoQ deficiency, a disease that is increasingly diagnosed with exome sequencing, with an estimation of more the 124,000 cases worldwide (Hughes *et al.*, 2017). The therapeutic results are greater than those obtained by the classical oral CoQ supplementation because of the decrease of the DMQ/CoQ ratio. Therefore, β–RA should be preferentially considered for the treatment of human CoQ_{10} deficiency with accumulation of DMQ_{10}, as it has been reported in patients with mutations in *COQ9, COQ7,* or *COQ4* (Danhauser *et al.*, 2015; Duncan *et al.*, 2009; Freyer *et al.*, 2015; Smith *et al.*, 2018; Wang *et al.*, 2017) but also in cells under siRNA knockdown of *COQ3*, *COQ5* and *COQ6* (Herebian *et al.*, 2017). Moreover, the positive therapeutic effects of β–RA in *Coq6* and *Adck4* glomerular podocytes-specific KO mice also suggest that this molecule could be used as a therapy in cases of *COQ6* and *COQ4* mutations, although the therapeutics mechanisms need to be elucidated (Widmeier *et al.*, 2019; Widmeier *et al.*, 2020). Similar principles could be applied for 3,4-hydroxybenzoic acid, vanillic acid, 2-methyl-4-hydroxybenzoic acid, or 2,3-dimethoxy-4- hydroxybenzoic acid in the cases of mutations in *COQ6*, *COQ5*, or *COQ3* (Gigante *et al*, 2017; Heeringa *et al.*, 2011; Herebian *et al.*, 2017; Pierrel, 2017; Ribas *et al*, 2014; Yoo *et al*, 2012), respectively. Furthermore, 4-HB analogs may provide therapeutic effects in other conditions, e.g., mitochondrial disorders, since secondary CoQ deficiency due to decreased levels of CoQ biosynthetic proteins have been recently reported in various mouse models of mitochondrial diseases (Kuhl *et al.*, 2017); or metabolic diseases due to insulin resistance since secondary CoQ deficiency due to decreased levels of CoQ biosynthetic proteins have been recently described in in vitro insulin resistance models and adipose tissue from insulin-resistant humans (Fazakerley *et al.*, 2018). To apply the β–RA treatment into the clinic, the safety and dose–response studies included in a clinical trial should be first developed. Nevertheless, β–RA is a natural compound that is used as a flavor by the food industry (Adams *et al*, 2005), and its administration in wild-type mice at high doses does not have detrimental effects on the survival (Wang *et al.*, 2015). Therefore, the safety study has a good prognosis and would allow the use of this compound at least as a compassionate option in cases of severe CoQ deficiencies due to mutations in *COQ4*, *COQ6*, *COQ7*, *COQ9* or *ADCK4* (Hidalgo-Gutierrez *et al.*, 2019; Wang *et al.*, 2015; Widmeier *et al.*, 2019; Widmeier *et al.*, 2020).

5.2 DUAL EFFECTS OF β–RA: THE INFLUENCE OF CoQ METABOLISM.

Some HBAs, e.g. salicylic acid, are used in the clinic and long track records in their use are available. Toxicity has been reported with the use of high doses of salicylates in pediatric population, inducing Reye's syndrome, a condition with non-precisely defined pathomechanisms. β–RA is another HBA with therapeutic potential, since, as previously mentioned, recent preclinical studies have shown it to have powerful therapeutic effects in CoQ deficiency models caused by mutations in *Coq6, Coq7, Adck4* or *Coq9* (Hidalgo-Gutierrez *et al.*, 2019; Wang *et al.*, 2015; Widmeier *et al.*, 2019; Widmeier *et al.*, 2020). Those studies have used high doses of oral β−RA but a detailed study about the effects of these high doses of β−RA in wild-type animals has not been developed. The only data about β−RA toxicity is, one article published in 1958 that described that the administration of β−RA to patients with rheumatic fever at the oral dose of 5,330–6,000 mg per day for up to 16 days did not have severe side effects (Clarke *et al*, 1958). However, the treatment used in the rheumatic fever patients were up to 16 days and, in the case of the CoQ deficient mutants mice, the treatment used is cronic (Hidalgo-Gutierrez *et al.*, 2019; Wang *et al.*, 2015; Widmeier *et al.*, 2019; Widmeier *et al.*, 2020). Besides, another article, published in 1976, stablished that the median lethal dose (LD_{50}) of β−RA is 800 mg/kg body weight in rats (Grady *et al*, 1976). The LD_{50} data would been in agreement with our results, since the high dose of β−RA, corresponding to more than 1g/kg body weight/day in mice, induces severe morphological, molecular and biochemical alterations in the kidneys, liver and brain of wild-type mice, leading to premature death.

β−RA (or 2,4-diHB) is an analog of salicylic acid (or 2-HB), and toxicity associated to high doses of salicylates induces Reye's syndrome in the pediatric population. Reye's syndrome is clinically manifested by an impairment of the liver function, with abnormal mitochondria and dysfunctional fatty-acid oxidation, and encephalopathy with various degrees of neurological impairment (Belay *et al*, 1999; Casteels-Van Daele *et al*, 2000; Hurwitz *et al*, 1987). Some cases also show acute renal failure with enlarged vacuoles (Hin *et al*, 1990; Mor *et al*, 1979). Since the kidney is the organ that accumulates more β–RA, this acute renal failure with enlarged vacuoles is a common feature in the animals treated with β–RA at terminal stage. Thus, the toxicity of β–RA reported here share some of the pathological features of Reye's syndrome, as it was also reported by benzoic acid (McCune *et al*, 1982). Importantly, our data demonstrate that the toxicity of β–RA depends on the levels of 4-HB, the natural precursor of CoQ biosynthesis. The levels of 4-HB are increased in response to the high levels of β–RA, probably as a compensatory mechanism to preserve CoQ biosynthesis, a fact that cannot be tested because the biosynthetic steps of 4-HB biosynthesis from tyrosine in mammals have not been characterized yet (Pierrel, 2017). β–RA and 4-HB compete to enter into the CoQ biosynthetic pathway through the activity of COQ2, but the km for 4-HB must be lower than the km for β–RA (Pierrel, 2017). Thus, the higher levels of 4-HB observed in the treated wild-type animals, compared to the untreated wild-type and *Coq9*^{R239X} mice, may limit the use of β–RA in the CoQ biosynthetic pathway, and, consequently, it could induce a greater accumulation in cells and tissues of wild-type mice than in those of *Coq9*^{R239X} mice. Since our results show that the toxicity of β−RA is dose-dependent, this accumulation of higher levels of β−RA must contribute to its pathological consequences and may explain the absence of toxicity in *Coq9*^{R239X} mice and *Coq*9$^{+/+}$ treated with the low dose of β−RA. Consequently, the toxicity of other HBAs that have been tested *in vitro* for the treatment of CoQ deficiency, e.g. vanillic acid (Doimo *et al.*, 2014b; Herebian *et al.*, 2017), must be evaluated. Furthermore, these data are also important because Reye's syndrome may share this CoQ biosynthesis-dependent mechanism, since an early study from Dallner's group showed that the supplementation of acetylsalicylic acid to rats interferes with CoQ biosynthesis in the liver, kidneys and muscle (Aberg *et al*, 1996).

Even more important, our study identifies novel potential molecular mechanisms through the first transcriptomics and mitochondrial proteomics analyses developed on the brain and the kidneys in response to an HBA. Specifically, we show that β−RA induces a marked reduction in the levels of Complex I subunits in the brain, a fact that may be related to the interaction of the β−RA with the Fe-S cluster of mitochondrial Complex I, inducing an increased generation of free radicals and apoptosis (Battaglia *et al*, 2005). All these alterations in the mitochondrial proteome may induce ER stress and the activation of unfolded protein response (Kim *et al*, 2008; Restelli *et al*, 2018), as reflected in the transcriptomic analysis. Moreover, we have detected an over-expression of genes related with the metabolism of the monoamine neurotransmitters, which derivate from phenylalanine or tyrosine, like the 4-HB, the natural precursor of CoQ. Since the levels of 4-HB are increased in the wild-type animals treated with the high dose of β−RA, we can speculate that the stimulation of the synthesis of 4-HB could influence the synthesis of monoamine neurotransmitters and, consequently, induces an overexpression of the transporters/receptors of these neurotransmitters.

Additionally, the analysis of the renal mitochondrial proteome reveals key molecular alterations that contribute to understand the toxicity induced by β−RA: 1) the increase in the levels of nuclear-encoded subunits of mitochondrial Complex I, probably as a compensatory mechanism to the interaction of the β−RA with the Fe-S cluster of mitochondrial Complex I (Battaglia *et al.*, 2005), leading to its partial inhibition (Sandoval-Acuna *et al*, 2012); 2) the decrease in the levels of enzymes involved in fatty acids oxidation, which is common in the salicylic acid or benzoic acid toxicity (Begriche *et al*, 2011; McCune *et al.*, 1982); 3) the induction of apoptosis through the upregulation of proapoptotic proteins and downregulation of anti-apoptotic proteins (Barnett & Cummings, 2019); and 4) the increase of several components of the mitoribosome, without changes in the mitochondrial-encoded subunits, a mechanism that, to our knowledge, has not been reported for other drugs that induce mitochondrial toxicity (Barnett & Cummings, 2019; Begriche *et al.*, 2011; Krahenbuhl, 2001). This stimulation of the mitoribosome could also reflect a compensatory mechanism to the mitochondrial toxicity or, alternatively, could be related to the induction of apoptosis since some mitoribosomal proteins have also a role in promoting apoptosis in human diseases (Cavdar Koc *et al*, 2001; Gopisetty & Thangarajan, 2016).

Considering the toxic effects of β–RA reported here, we tried to identify a dose of β–RA that has therapeutic effects in *Coq9*$^{\mathrm{R239X}}$ mice but has no toxic effects in wild-type animals. A third of the dose initially used preserved a powerful therapeutic effect, avoiding the pathophysiological consequences in wild-type animals. The data from wild-type animals that were treated with this lower dose of β–RA are similar to those reported by other groups (Hidalgo-Gutierrez *et al.*, 2019; Wang *et al.*, 2015; Widmeier *et al.*, 2019; Widmeier *et al.*, 2020), and manifest the dose-dependent effects of β–RA from both the toxicological and therapeutic points of views. Furthermore, our results demonstrate that the effects of β–RA depend on its competition with 4-HB in the CoQ biosynthetic pathways, and confirm that the reduction on the DMQ/CoQ ratio in peripheral tissues is a key factor in the treatment of CoQ deficiency due to mutations in *COQ9*.

Overall, this study shows a dose-dependent toxicity of the β−RA in the kidneys, liver and brain of wild-type animals, and presents novel molecular mechanisms of mitochondrial toxicity of this natural compound. Remarkably, these dose-dependent effects depend on CoQ metabolism and the underlying mechanisms could be common to other HBAs used in the clinic and experimentally. Accordingly, an accurate and early genetic diagnosis is required to initiate the treatment with β−RA in patients with CoQ deficiency, and the monitorization of renal and hepatic blood markers is highly recommended in the patients that initiate the treatment. Also, the potential use of β−RA in secondary CoQ deficiencies, as reported in other genetic diseases or insulin resistance (Aeby *et al.*, 2007; Fazakerley *et al.*, 2018; Kuhl *et al.*, 2017; Quinzii *et al.*, 2005; Yubero *et al.*, 2016), must require, at least, further research and a gradual adjustment of the dose. Therefore, the data of the present work are relevant for the future translation of the treatment with β−RA and other HBAs into the clinic.

5.3 MODULATION OF SULFIDE METABOLISM AS THERAPEUTIC APPROACH FOR PRIMARY COQ DEFICIENCY.

Our group, together with the group of Dr. Catarina Quinzii, have recently demonstrated, in two independent studies, that CoQ deficiency severely decreases the levels of SQOR, the first enzyme in the mitochondrial H_2S

oxidation pathway, leading to accumulation of H_2S and depletion on the glutathione system (Luna-Sanchez *et al.*, 2017; Ziosi *et al.*, 2017). Accordingly, the reduction in SQOR activity, accumulation of H_2S and reduction in the levels of GSH are additional pathomechanisms associated to CoQ deficiency. Therefore, therapeutic interventions aiming to modulate those metabolic pathways, as the availability of sulfur amino acids in the diet, as sources of H_2S, may provide therapeutic outcomes. Thus, we treated *Coq9*^{R239X} mice with NAC, which can also stimulate glutathione biosynthesis, or a diet with SAAR.

Our results showed that the decreased levels of SQOR and increased levels of CBS in the kidneys of *Coq9*^{R239X} mice, were preserved after the supplementation with NAC or SAAR diet. Those results contradict to those in yeasts, where the addition of cysteine reduces the H_2S production with CoQ deficiency, suggesting that H_2S and cysteine biosynthetic pathways are coordinately regulated by feedback mechanisms (Zhang *et al*, 2008). Also, our data are not in agreement with a recent study in mouse, where SAAR increased the expression of the enzyme CSE in the liver, resulting in increased H_2S production and decreased levels of GSH (Hine *et al.*, 2015). Therefore, the low levels of CoQ may limit the effects of NAC or SAAR diet, in sulfide metabolism, in mice.

While the sources of cysteine are apparently different in mammals, the therapeutic effects of NAC, a prodrug of L-cysteine utilized to increase GSH, in *ETHE1* knockout mice suggest that mitochondrial sulfide oxidation pathway may exert some influence on GSH metabolism (Viscomi *et al.*, 2010). However, neither NAC supplementation of SAAR diet were able to counteract the decrease in glutathione levels in the kidneys of *Coq9*$^{\mathrm{R239X}}$ mice. Also, the levels of the glutathione enzymes, GPx and GRd, were mildly decreased in the three experimental groups of *Coq9*$^{\mathrm{R239X}}$ mice, compared to *Coq9*$^{+/+}$ mice, although the decreased was statistically significant only in the case of GPx in untreated *Coq9*$^{\mathrm{R239X}}$ mice. Therefore, our results suggest that sulfide metabolism influences the levels of glutathione, independently of the sulfur amino acids availability; and that GSH metabolism could not be modulated by sulfur amino acids availability under CoQ deficiency.

Finally, we checked whether NAC supplementation or the SAAR diet could influence the survival of *Coq9*$^{\mathrm{R239X}}$ mice. However, no therapeutic effects were observed after the treatments. Therefore, we were not able to reproduce the therapeutic effects reported by NAC in the ethylmalonic encephalopathy due to mutations in *ETHE1*, both in patients and in the mouse model, where the levels of H_2S were reduced and the GSH levels increased (Sahebekhtiari *et al*, 2019; Tiranti *et al.*, 2009).

CONCLUSSIONS

6. CONCLUSIONS

1. β-RA is a powerful therapeutic agent for the mitochondrial encephalopathy due to *Coq9* mutation, with better results than those obtained by the conventional oral CoQ supplementation.

2. The therapeutic effect of β-RA is mainly due to a decrease of the DMQ/CoQ ratio. Therefore, β-RA should be preferentially considered for the treatment of human CoQ_{10} deficiency with accumulation of DMQ_{10}, as it has been reported in patients with mutations in *COQ9*, *COQ7*, or *COQ4*, but also in cells under siRNA knockdown of COQ3, COQ5 and COQ6.

3. A high dose of β-RA is toxic for the kidneys, liver and brain of wild-type animals, leading to premature death. However, a third of that dose is safe for wild-type animals, while preserving the therapeutics effects in *Coq9*^{R239X} mice. These dose-dependent effects of β-RA depend on CoQ metabolism.

4. An accurate and early genetic diagnosis is required to initiate the treatment with β-RA in patients with CoQ deficiency and, the monitorization of renal and hepatic blood markers is highly recommended in the patients that initiate the treatment.

5. The sulfide metabolism influences the levels of glutathione, independently of the sulfur amino acids availability.
6. The modulation of sulfur amino acids availability does not produce therapeutic effects on *Coq9*$^{\mathrm{R239X}}$ mice.

BIBLIOGRAPHY

7. BIBLIOGRAPHY

Abby SS, Kazemzadeh K, Vragniau C, Pelosi L, Pierrel F (2020) Advances in bacterial pathways for the biosynthesis of ubiquinone. *Biochim Biophys Acta Bioenerg* 1861: 148259

Aberg F, Zhang Y, Teclebrhan H, Appelkvist EL, Dallner G (1996) Increases in tissue levels of ubiquinone in association with peroxisome proliferation. *Chem Biol Interact* 99: 205-218

Acin-Perez R, Fernandez-Silva P, Peleato ML, Perez-Martos A, Enriquez JA (2008) Respiratory active mitochondrial supercomplexes. *Mol Cell* 32: 529-539

Acosta MJ, Vazquez Fonseca L, Desbats MA, Cerqua C, Zordan R, Trevisson E, Salviati L (2016) Coenzyme Q biosynthesis in health and disease. *Biochim Biophys Acta* 1857: 1079-1085

Adams TB, Cohen SM, Doull J, Feron VJ, Goodman JI, Marnett LJ, Munro IC, Portoghese PS, Smith RL, Waddell WJ *et al* (2005) The FEMA GRAS assessment of hydroxy- and alkoxy-substituted benzyl derivatives used as flavor ingredients. *Food Chem Toxicol* 43: 1241-1271

Adan Lanceta V, Romero Salas Y, Justa Roldan ML, Garcia Jimenez MC, Ariceta Iraola G (2020) [Encephalopathy, kidney failure and retinopathy. CoQ10 deficiency due to COQ8B mutation]. *An Pediatr (Barc)*

Aeby A, Sznajer Y, Cave H, Rebuffat E, Van Coster R, Rigal O, Van Bogaert P (2007) Cardiofaciocutaneous (CFC) syndrome associated with muscular coenzyme Q10 deficiency. *J Inherit Metab Dis* 30: 827

Alcazar-Fabra M, Navas P, Brea-Calvo G (2016) Coenzyme Q biosynthesis and its role in the respiratory chain structure. *Biochim Biophys Acta* 1857: 1073-1078

Alcazar-Fabra M, Trevisson E, Brea-Calvo G (2018) Clinical syndromes associated with Coenzyme Q10 deficiency. *Essays Biochem* 62: 377-398

Allan CM, Awad AM, Johnson JS, Shirasaki DI, Wang C, Blaby-Haas CE, Merchant SS, Loo JA, Clarke CF (2015) Identification of Coq11, a new coenzyme Q biosynthetic protein in the CoQ-synthome in Saccharomyces cerevisiae. *J Biol Chem* 290: 7517-7534

Angelis A, Tordrup D, Kanavos P (2015) Socio-economic burden of rare diseases: A systematic review of cost of illness evidence. *Health Policy* 119: 964-979

Arroyo A, Santos-Ocana C, Ruiz-Ferrer M, Padilla S, Gavilan A, Rodriguez-Aguilera JC, Navas P (2006) Coenzyme Q is irreplaceable by demethoxy-coenzyme Q in plasma membrane of Caenorhabditis elegans. *FEBS Lett* 580: 1740-1746

Ashraf S, Gee HY, Woerner S, Xie LX, Vega-Warner V, Lovric S, Fang H, Song X, Cattran DC, Avila-Casado C *et al* (2013) ADCK4 mutations promote steroid-resistant nephrotic syndrome through CoQ10 biosynthesis disruption. *J Clin Invest* 123: 5179-5189

Awad AM, Bradley MC, Fernandez-Del-Rio L, Nag A, Tsui HS, Clarke CF (2018) Coenzyme Q10 deficiencies: pathways in yeast and humans. *Essays Biochem* 62: 361-376

Awad AM, Nag A, Pham NVB, Bradley MC, Jabassini N, Nathaniel J, Clarke CF (2020) Intragenic suppressor mutations of the COQ8 protein kinase homolog restore coenzyme Q biosynthesis and function in Saccharomyces cerevisiae. *PLoS One* 15: e0234192

Baba SW, Belogrudov GI, Lee JC, Lee PT, Strahan J, Shepherd JN, Clarke CF (2004) Yeast Coq5 C-methyltransferase is required for stability of other polypeptides involved in coenzyme Q biosynthesis. *J Biol Chem* 279: 10052-10059

Barnett LMA, Cummings BS (2019) Cellular and Molecular Mechanisms of Kidney Toxicity. *Semin Nephrol* 39: 141-151

Barriocanal-Casado E, Hidalgo-Gutierrez A, Raimundo N, Gonzalez-Garcia P, Acuna-Castroviejo D, Escames G, Lopez LC (2019) Rapamycin administration is not a valid therapeutic strategy for every case of mitochondrial disease. *EBioMedicine*

Barros MH, Johnson A, Gin P, Marbois BN, Clarke CF, Tzagoloff A (2005) The Saccharomyces cerevisiae COQ10 gene encodes a START domain protein required for function of coenzyme Q in respiration. *J Biol Chem* 280: 42627-42635

Battaglia V, Salvi M, Toninello A (2005) Oxidative stress is responsible for mitochondrial permeability transition induction by salicylate in liver mitochondria. *J Biol Chem* 280: 33864-33872

Baum DA (2015) A comparison of autogenous theories for the origin of eukaryotic cells. *Am J Bot* 102: 1954-1965

Begriche K, Massart J, Robin MA, Borgne-Sanchez A, Fromenty B (2011) Drug-induced toxicity on mitochondria and lipid metabolism: mechanistic diversity and deleterious consequences for the liver. *J Hepatol* 54: 773-794

Belay ED, Bresee JS, Holman RC, Khan AS, Shahriari A, Schonberger LB (1999) Reye's syndrome in the United States from 1981 through 1997. *N Engl J Med* 340: 1377-1382

Belogrudov GI, Lee PT, Jonassen T, Hsu AY, Gin P, Clarke CF (2001) Yeast COQ4 encodes a mitochondrial protein required for coenzyme Q synthesis. *Arch Biochem Biophys* 392: 48-58

Bentinger M, Brismar K, Dallner G (2007) The antioxidant role of coenzyme Q. *Mitochondrion* 7 Suppl: S41-50

Bentinger M, Dallner G, Chojnacki T, Swiezewska E (2003) Distribution and breakdown of labeled coenzyme Q10 in rat. *Free Radic Biol Med* 34: 563-575

Bentinger M, Tekle M, Dallner G (2010) Coenzyme Q--biosynthesis and functions. *Biochem Biophys Res Commun* 396: 74-79

Berthold DA, Stenmark P (2003) Membrane-bound diiron carboxylate proteins. *Annu Rev Plant Biol* 54: 497-517

Borges TH, Pereira JA, Cabrera-Vique C, Lara L, Oliveira AF, Seiquer I (2017) Characterization of Arbequina virgin olive oils produced in different regions of Brazil and Spain: Physicochemical properties, oxidative stability and fatty acid profile. *Food Chem* 215: 454-462

Brea-Calvo G, Haack TB, Karall D, Ohtake A, Invernizzi F, Carrozzo R, Kremer L, Dusi S, Fauth C, Scholl-Burgi S *et al* (2015) COQ4 mutations cause a broad spectrum of mitochondrial disorders associated with CoQ10 deficiency. *Am J Hum Genet* 96: 309-317

Brea-Calvo G, Siendones E, Sanchez-Alcazar JA, de Cabo R, Navas P (2009) Cell survival from chemotherapy depends on NF-kappaB transcriptional up-regulation of coenzyme Q biosynthesis. *PLoS One* 4: e5301

Brown JA, Sammy MJ, Ballinger SW (2020) An evolutionary, or "Mitocentric" perspective on cellular function and disease. *Redox Biol* 36: 101568

Brzywczy J, Sienko M, Kucharska A, Paszewski A (2002) Sulphur amino acid synthesis in Schizosaccharomyces pombe represents a specific variant of sulphur metabolism in fungi. *Yeast* 19: 29-35

Butterworth RF (2016) Pathogenesis of hepatic encephalopathy in cirrhosis: the concept of synergism revisited. *Metab Brain Dis* 31: 1211-1215

Caglayan AO, Gumus H, Sandford E, Kubisiak TL, Ma Q, Ozel AB, Per H, Li JZ, Shakkottai VG, Burmeister M (2019) COQ4 Mutation Leads to Childhood-Onset Ataxia Improved by CoQ10 Administration. *Cerebellum* 18: 665-669

Calvo SE, Clauser KR, Mootha VK (2016) MitoCarta2.0: an updated inventory of mammalian mitochondrial proteins. *Nucleic Acids Res* 44: D1251-1257

Cameron AR, Logie L, Patel K, Bacon S, Forteath C, Harthill J, Roberts A, Sutherland C, Stewart D, Viollet B *et al* (2016) Investigation of salicylate hepatic responses in comparison with chemical analogues of the drug. *Biochim Biophys Acta* 1862: 1412-1422

Casteels-Van Daele M, Van Geet C, Wouters C, Eggermont E (2000) Reye syndrome revisited: a descriptive term covering a group of heterogeneous disorders. *Eur J Pediatr* 159: 641-648

Cavdar Koc E, Ranasinghe A, Burkhart W, Blackburn K, Koc H, Moseley A, Spremulli LL (2001) A new face on apoptosis: death-associated protein 3 and PDCD9 are mitochondrial ribosomal proteins. *FEBS Lett* 492: 166-170

Chahbouni M, Escames G, Venegas C, Sevilla B, Garcia JA, Lopez LC, Munoz-Hoyos A, Molina-Carballo A, Acuna-Castroviejo D (2010) Melatonin treatment normalizes plasma pro-inflammatory cytokines and nitrosative/oxidative stress in patients suffering from Duchenne muscular dystrophy. *J Pineal Res* 48: 282-289

Chance B, Estabrook RW, Lee CP (1963) Electron Transport in the Oxysome. *Science* 140: 379-380

Chung WK, Martin K, Jalas C, Braddock SR, Juusola J, Monaghan KG, Warner B, Franks S, Yudkoff M, Lulis L *et al* (2015) Mutations in COQ4, an essential component of coenzyme Q biosynthesis, cause lethal neonatal mitochondrial encephalomyopathy. *J Med Genet* 52: 627-635

Clarke NE, Clarke CN, Mosher RE (1958) Phenolic compounds in chemotherapy of rheumatic fever. *Am J Med Sci* 235: 7-22

Cogliati S, Enriquez JA, Scorrano L (2016) Mitochondrial Cristae: Where Beauty Meets Functionality. *Trends Biochem Sci* 41: 261-273

Colombo E, Farina C (2016) Astrocytes: Key Regulators of Neuroinflammation. *Trends Immunol* 37: 608-620

Cox J, Mann M (2008) MaxQuant enables high peptide identification rates, individualized p.p.b.-range mass accuracies and proteome-wide protein quantification. *Nat Biotechnol* 26: 1367-1372

Crane FL, Dilley RA (1963) Determination of Coenzyme Q (Ubiquinone). *Methods Biochem Anal* 11: 279-306

Crane FL, Hatefi Y, Lester RL, Widmer C (1957) Isolation of a quinone from beef heart mitochondria. *Biochim Biophys Acta* 25: 220-221

Craven L, Alston CL, Taylor RW, Turnbull DM (2017) Recent Advances in Mitochondrial Disease. *Annu Rev Genomics Hum Genet* 18: 257-275

D'Autreaux B, Toledano MB (2007) ROS as signalling molecules: mechanisms that generate specificity in ROS homeostasis. *Nat Rev Mol Cell Biol* 8: 813-824

Danhauser K, Herebian D, Haack TB, Rodenburg RJ, Strom TM, Meitinger T, Klee D, Mayatepek E, Prokisch H, Distelmaier F (2015) Fatal neonatal encephalopathy and lactic acidosis caused by a homozygous loss-of-function variant in COQ9. *Eur J Hum Genet*

Desbats MA, Lunardi G, Doimo M, Trevisson E, Salviati L (2015) Genetic bases and clinical manifestations of coenzyme Q10 (CoQ 10) deficiency. *J Inherit Metab Dis* 38: 145-156

Di Meo I, Fagiolari G, Prelle A, Viscomi C, Zeviani M, Tiranti V (2011) Chronic exposure to sulfide causes accelerated degradation of cytochrome c oxidase in ethylmalonic encephalopathy. *Antioxid Redox Signal* 15: 353-362

Di Meo I, Marchet S, Lamperti C, Zeviani M, Viscomi C (2017) AAV9-based gene therapy partially ameliorates the clinical phenotype of a mouse model of Leigh syndrome. *Gene Ther* 24: 661-667

Diaz F, Garcia S, Padgett KR, Moraes CT (2012) A defect in the mitochondrial complex III, but not complex IV, triggers early ROS-dependent damage in defined brain regions. *Hum Mol Genet* 21: 5066-5077

Diaz-Casado ME, Quiles JL, Barriocanal-Casado E, Gonzalez-Garcia P, Battino M, Lopez LC, Varela-Lopez A (2019) The Paradox of Coenzyme Q10 in Aging. *Nutrients* 11

Diaz-Casado ME, Rusanova I, Aranda P, Fernandez-Ortiz M, Sayed RKA, Fernandez-Gil BI, Hidalgo-Gutierrez A, Escames G, Lopez LC, Acuna-Castroviejo D (2018) In Vivo Determination of Mitochondrial Respiration in 1-Methyl-4-Phenyl-1,2,3,6-

Tetrahydropyridine-Treated Zebrafish Reveals the Efficacy of Melatonin in Restoring Mitochondrial Normalcy. *Zebrafish* 15: 15-26

DiMauro S, Schon EA, Carelli V, Hirano M (2013) The clinical maze of mitochondrial neurology. *Nat Rev Neurol* 9: 429-444

Doimo M, Desbats MA, Cerqua C, Cassina M, Trevisson E, Salviati L (2014a) Genetics of coenzyme q10 deficiency. *Mol Syndromol* 5: 156-162

Doimo M, Trevisson E, Airik R, Bergdoll M, Santos-Ocana C, Hildebrandt F, Navas P, Pierrel F, Salviati L (2014b) Effect of vanillic acid on COQ6 mutants identified in patients with coenzyme Q10 deficiency. *Biochim Biophys Acta* 1842: 1-6

Duberley KE, Abramov AY, Chalasani A, Heales SJ, Rahman S, Hargreaves IP (2013) Human neuronal coenzyme Q10 deficiency results in global loss of mitochondrial respiratory chain activity, increased mitochondrial oxidative stress and reversal of ATP synthase activity: implications for pathogenesis and treatment. *J Inherit Metab Dis* 36: 63-73

Duncan AJ, Bitner-Glindzicz M, Meunier B, Costello H, Hargreaves IP, Lopez LC, Hirano M, Quinzii CM, Sadowski MI, Hardy J *et al* (2009) A nonsense mutation in COQ9 causes autosomal-recessive neonatal-onset primary coenzyme Q10 deficiency: a potentially treatable form of mitochondrial disease. *Am J Hum Genet* 84: 558-566

Echtay KS, Winkler E, Frischmuth K, Klingenberg M (2001) Uncoupling proteins 2 and 3 are highly active H(+) transporters and highly nucleotide sensitive when activated by coenzyme Q (ubiquinone). *Proc Natl Acad Sci U S A* 98: 1416-1421

Echtay KS, Winkler E, Klingenberg M (2000) Coenzyme Q is an obligatory cofactor for uncoupling protein function. *Nature* 408: 609-613

Emmanuele V, Lopez LC, Berardo A, Naini A, Tadesse S, Wen B, D'Agostino E, Solomon M, DiMauro S, Quinzii C *et al* (2012) Heterogeneity of coenzyme Q10 deficiency: patient study and literature review. *Arch Neurol* 69: 978-983

Enriquez JA (2016) Supramolecular Organization of Respiratory Complexes. *Annu Rev Physiol* 78: 533-561

Enriquez JA, Lenaz G (2014) Coenzyme q and the respiratory chain: coenzyme q pool and mitochondrial supercomplexes. *Mol Syndromol* 5: 119-140

Ernster L, Dallner G (1995) Biochemical, physiological and medical aspects of ubiquinone function. *Biochim Biophys Acta* 1271: 195-204

Ernster L, Lee IY, Norling B, Persson B (1969) Studies with ubiquinone-depleted submitochondrial particles. Essentiality of ubiquinone for the interaction of succinate dehydrogenase, NADH dehydrogenase, and cytochrome b. *Eur J Biochem* 9: 299-310

Esteves TC, Echtay KS, Jonassen T, Clarke CF, Brand MD (2004) Ubiquinone is not required for proton conductance by uncoupling protein 1 in yeast mitochondria. *Biochem J* 379: 309-315

Fazakerley DJ, Chaudhuri R, Yang P, Maghzal GJ, Thomas KC, Krycer JR, Humphrey SJ, Parker BL, Fisher-Wellman KH, Meoli CC *et al* (2018) Mitochondrial CoQ deficiency is a common driver of mitochondrial oxidants and insulin resistance. *Elife* 7

Fernandez-Ayala DJ, Brea-Calvo G, Lopez-Lluch G, Navas P (2005) Coenzyme Q distribution in HL-60 human cells depends on the endomembrane system. *Biochim Biophys Acta* 1713: 129-137

Festenstein GN, Heaton FW, Lowe JS, Morton RA (1955) A constituent of the unsaponifiable portion of animal tissue lipids (lambda max. 272 m mu). *Biochem J* 59: 558-566

Fontaine E, Ichas F, Bernardi P (1998) A ubiquinone-binding site regulates the mitochondrial permeability transition pore. *J Biol Chem* 273: 25734-25740

Forsmark-Andree P, Dallner G, Ernster L (1995) Endogenous ubiquinol prevents protein modification accompanying lipid peroxidation in beef heart submitochondrial particles. *Free Radic Biol Med* 19: 749-757

Freyer C, Stranneheim H, Naess K, Mourier A, Felser A, Maffezzini C, Lesko N, Bruhn H, Engvall M, Wibom R *et al* (2015) Rescue of primary ubiquinone deficiency due to a novel COQ7 defect using 2,4-dihydroxybensoic acid. *J Med Genet* 52: 779-783

Friederich MW, Elias AF, Kuster A, Laugwitz L, Larson AA, Landry AP, Ellwood-Digel L, Mirsky DM, Dimmock D, Haven J *et al* (2020) Pathogenic variants in SQOR encoding sulfide:quinone oxidoreductase are a potentially treatable cause of Leigh disease. *J Inherit Metab Dis* 43: 1024-1036

Garcia-Corzo L, Luna-Sanchez M, Doerrier C, Garcia JA, Guaras A, Acin-Perez R, Bullejos-Peregrin J, Lopez A, Escames G, Enriquez JA *et al* (2013) Dysfunctional Coq9 protein causes predominant encephalomyopathy associated with CoQ deficiency. *Hum Mol Genet* 22: 1233-1248

Garcia-Corzo L, Luna-Sanchez M, Doerrier C, Ortiz F, Escames G, Acuna-Castroviejo D, Lopez LC (2014) Ubiquinol-10 ameliorates mitochondrial encephalopathy associated with CoQ deficiency. *Biochim Biophys Acta* 1842: 893-901

Gempel K, Topaloglu H, Talim B, Schneiderat P, Schoser BG, Hans VH, Palmafy B, Kale G, Tokatli A, Quinzii C *et al* (2007) The myopathic form of coenzyme Q10 deficiency is caused by mutations in the electron-transferring-flavoprotein dehydrogenase (ETFDH) gene. *Brain* 130: 2037-2044

Gerards M, van den Bosch B, Calis C, Schoonderwoerd K, van Engelen K, Tijssen M, de Coo R, van der Kooi A, Smeets H (2010) Nonsense mutations in CABC1/ADCK3 cause progressive cerebellar ataxia and atrophy. *Mitochondrion* 10: 510-515

Geromel V, Kadhom N, Ceballos-Picot I, Chretien D, Munnich A, Rotig A, Rustin P (2001) Human cultured skin fibroblasts survive profound inherited ubiquinone depletion. *Free Radic Res* 35: 11-21

Gigante M, Diella S, Santangelo L, Trevisson E, Acosta MJ, Amatruda M, Finzi G, Caridi G, Murer L, Accetturo M *et al* (2017) Further phenotypic heterogeneity of CoQ10 deficiency associated with steroid resistant nephrotic syndrome and novel COQ2 and COQ6 variants. *Clin Genet* 92: 224-226

Gomez-Guzman M, Jimenez R, Romero M, Sanchez M, Zarzuelo MJ, Gomez-Morales M, O'Valle F, Lopez-Farre AJ, Algieri F, Galvez J *et al* (2014) Chronic hydroxychloroquine improves endothelial dysfunction and protects kidney in a mouse model of systemic lupus erythematosus. *Hypertension* 64: 330-337

Gopisetty G, Thangarajan R (2016) Mammalian mitochondrial ribosomal small subunit (MRPS) genes: A putative role in human disease. *Gene* 589: 27-35

Gorman ASALG, 2019. Epidemiology of Mitochondrial Disease, in: Klopstock M.M.T. (Ed.) Diagnosis and Management of Mitochondrial Disorders, 1 ed. Springer International Publishing, p. 382.

Gorman GS, Chinnery PF, DiMauro S, Hirano M, Koga Y, McFarland R, Suomalainen A, Thorburn DR, Zeviani M, Turnbull DM (2016) Mitochondrial diseases. *Nat Rev Dis Primers* 2: 16080

Grady RW, Graziano JH, Akers HA, Cerami A (1976) The development of new iron-chelating drugs. *J Pharmacol Exp Ther* 196: 478-485

Green DE, Tzagoloff A (1966) The mitochondrial electron transfer chain. *Arch Biochem Biophys* 116: 293-304

Green DR, Reed JC (1998) Mitochondria and apoptosis. *Science* 281: 1309-1312

Guaras A, Perales-Clemente E, Calvo E, Acin-Perez R, Loureiro-Lopez M, Pujol C, Martinez-Carrascoso I, Nunez E, Garcia-Marques F, Rodriguez-Hernandez MA *et al* (2016) The CoQH2/CoQ Ratio Serves as a Sensor of Respiratory Chain Efficiency. *Cell Rep* 15: 197-209

Gurgel-Giannetti J, Lynch DS, Paiva ARB, Lucato LT, Yamamoto G, Thomsen C, Basu S, Freua F, Giannetti AV, de Assis BDR *et al* (2018) A novel complex neurological phenotype due to a homozygous mutation in FDX2. *Brain* 141: 2289-2298

Hackenbrock CR, Chazotte B, Gupte SS (1986) The random collision model and a critical assessment of diffusion and collision in mitochondrial electron transport. *J Bioenerg Biomembr* 18: 331-368

He CH, Xie LX, Allan CM, Tran UC, Clarke CF (2014) Coenzyme Q supplementation or over-expression of the yeast Coq8 putative kinase stabilizes multi-subunit Coq polypeptide complexes in yeast coq null mutants. *Biochim Biophys Acta* 1841: 630-644

Heeringa SF, Chernin G, Chaki M, Zhou W, Sloan AJ, Ji Z, Xie LX, Salviati L, Hurd TW, Vega-Warner V *et al* (2011) COQ6 mutations in human patients produce nephrotic syndrome with sensorineural deafness. *J Clin Invest* 121: 2013-2024

Herebian D, Seibt A, Smits SHJ, Rodenburg RJ, Mayatepek E, Distelmaier F (2017) 4-Hydroxybenzoic acid restores CoQ10 biosynthesis in human COQ2 deficiency. *Ann Clin Transl Neurol* 4: 902-908

Hernandez-Camacho JD, Bernier M, Lopez-Lluch G, Navas P (2018) Coenzyme Q10 Supplementation in Aging and Disease. *Front Physiol* 9: 44

Hidalgo-Gutierrez A, Barriocanal-Casado E, Bakkali M, Diaz-Casado ME, Sanchez-Maldonado L, Romero M, Sayed RK, Prehn C, Escames G, Duarte J *et al* (2019) beta-RA reduces DMQ/CoQ ratio and rescues the encephalopathic phenotype in Coq9 (R239X) mice. *EMBO Mol Med* 11

Hin SA, Reginald LK, Lim TC (1990) Acute renal failure in Reye's syndrome. *J Singapore Paediatr Soc* 32: 36-39

Hine C, Harputlugil E, Zhang Y, Ruckenstuhl C, Lee BC, Brace L, Longchamp A, Trevino-Villarreal JH, Mejia P, Ozaki CK *et al* (2015) Endogenous hydrogen sulfide production is essential for dietary restriction benefits. *Cell* 160: 132-144

Hinz B, Kraus V, Pahl A, Brune K (2000) Salicylate metabolites inhibit cyclooxygenase-2-dependent prostaglandin E(2) synthesis in murine macrophages. *Biochem Biophys Res Commun* 274: 197-202

Holmgren A, Bjornstedt M (1995) Thioredoxin and thioredoxin reductase. *Methods Enzymol* 252: 199-208

Horvath R, Czermin B, Gulati S, Demuth S, Houge G, Pyle A, Dineiger C, Blakely EL, Hassani A, Foley C *et al* (2012) Adult-onset cerebellar ataxia due to mutations in CABC1/ADCK3. *J Neurol Neurosurg Psychiatry* 83: 174-178

Hsieh EJ, Gin P, Gulmezian M, Tran UC, Saiki R, Marbois BN, Clarke CF (2007) Saccharomyces cerevisiae Coq9 polypeptide is a subunit of the mitochondrial coenzyme Q biosynthetic complex. *Arch Biochem Biophys* 463: 19-26

Hughes BG, Harrison PM, Hekimi S (2017) Estimating the occurrence of primary ubiquinone deficiency by analysis of large-scale sequencing data. *Sci Rep* 7: 17744

Hurwitz ES, Barrett MJ, Bregman D, Gunn WJ, Pinsky P, Schonberger LB, Drage JS, Kaslow RA, Burlington DB, Quinnan GV *et al* (1987) Public Health Service study of Reye's syndrome and medications. Report of the main study. *JAMA* 257: 1905-1911

Ibrahim W, Lee US, Yeh CC, Szabo J, Bruckner G, Chow CK (1997) Oxidative stress and antioxidant status in mouse liver: effects of dietary lipid, vitamin E and iron. *J Nutr* 127: 1401-1406

Jaburek M, Garlid KD (2003) Reconstitution of recombinant uncoupling proteins: UCP1, -2, and -3 have similar affinities for ATP and are unaffected by coenzyme Q10. *J Biol Chem* 278: 25825-25831

Jakobs BS, van den Heuvel LP, Smeets RJ, de Vries MC, Hien S, Schaible T, Smeitink JA, Wevers RA, Wortmann SB, Rodenburg RJ (2013) A novel mutation in COQ2 leading to fatal infantile multisystem disease. *J Neurol Sci* 326: 24-28

Jiang N, Levavasseur F, McCright B, Shoubridge EA, Hekimi S (2001) Mouse CLK-1 is imported into mitochondria by an unusual process that requires a leader sequence but no membrane potential. *J Biol Chem* 276: 29218-29225

Justine Perrin R, Rousset-Rouviere C, Garaix F, Cano A, Conrath J, Boyer O, Tsimaratos M (2020) COQ6 mutation in patients with nephrotic syndrome, sensorineural deafness, and optic atrophy. *JIMD Rep* 54: 37-44

Kabil O, Vitvitsky V, Banerjee R (2014) Sulfur as a signaling nutrient through hydrogen sulfide. *Annu Rev Nutr* 34: 171-205

Kalen A, Norling B, Appelkvist EL, Dallner G (1987) Ubiquinone biosynthesis by the microsomal fraction from rat liver. *Biochim Biophys Acta* 926: 70-78

Kawamukai M (2009) Biosynthesis and bioproduction of coenzyme Q10 by yeasts and other organisms. *Biotechnol Appl Biochem* 53: 217-226

Kawamukai M (2016) Biosynthesis of coenzyme Q in eukaryotes. *Biosci Biotechnol Biochem* 80: 23-33

Keilin D, Hartree EF (1947) Activity of the cytochrome system in heart muscle preparations. *Biochem J* 41: 500-502

Kim I, Xu W, Reed JC (2008) Cell death and endoplasmic reticulum stress: disease relevance and therapeutic opportunities. *Nat Rev Drug Discov* 7: 1013-1030

King MS, Thompson K, Hopton S, He L, Kunji ERS, Taylor RW, Ortiz-Gonzalez XR (2018) Expanding the phenotype of de novo SLC25A4-linked mitochondrial disease to include mild myopathy. *Neurol Genet* 4: e256

Kovacs WJ, Olivier LM, Krisans SK (2002) Central role of peroxisomes in isoprenoid biosynthesis. *Prog Lipid Res* 41: 369-391

Krahenbuhl S (2001) Mitochondria: important target for drug toxicity? *J Hepatol* 34: 334-336

Kuhl I, Miranda M, Atanassov I, Kuznetsova I, Hinze Y, Mourier A, Filipovska A, Larsson NG (2017) Transcriptomic and proteomic landscape of mitochondrial dysfunction reveals secondary coenzyme Q deficiency in mammals. *Elife* 6

Kuhlbrandt W (2015) Structure and function of mitochondrial membrane protein complexes. *BMC Biol* 13: 89

Kuznetsov AV, Margreiter R (2009) Heterogeneity of mitochondria and mitochondrial function within cells as another level of mitochondrial complexity. *Int J Mol Sci* 10: 1911-1929

Lagier-Tourenne C, Tazir M, Lopez LC, Quinzii CM, Assoum M, Drouot N, Busso C, Makri S, Ali-Pacha L, Benhassine T *et al* (2008) ADCK3, an ancestral kinase, is mutated in a form of recessive ataxia associated with coenzyme Q10 deficiency. *Am J Hum Genet* 82: 661-672

Lagoutte E, Mimoun S, Andriamihaja M, Chaumontet C, Blachier F, Bouillaud F (2010) Oxidation of hydrogen sulfide remains a priority in mammalian cells and causes reverse electron transfer in colonocytes. *Biochim Biophys Acta* 1797: 1500-1511

Lapointe CP, Stefely JA, Jochem A, Hutchins PD, Wilson GM, Kwiecien NW, Coon JJ, Wickens M, Pagliarini DJ (2018) Multi-omics Reveal Specific Targets of the RNA-Binding Protein Puf3p and Its Orchestration of Mitochondrial Biogenesis. *Cell Syst* 6: 125-135 e126

Lapuente-Brun E, Moreno-Loshuertos R, Acin-Perez R, Latorre-Pellicer A, Colas C, Balsa E, Perales-Clemente E, Quiros PM, Calvo E, Rodriguez-Hernandez MA *et al* (2013) Supercomplex assembly determines electron flux in the mitochondrial electron transport chain. *Science* 340: 1567-1570

Lax NZ, Hepplewhite PD, Reeve AK, Nesbitt V, McFarland R, Jaros E, Taylor RW, Turnbull DM (2012) Cerebellar ataxia in patients with mitochondrial DNA disease: a molecular clinicopathological study. *J Neuropathol Exp Neurol* 71: 148-161

Lehtonen JM, Auranen M, Darin N, Sofou K, Bindoff L, Hikmat O, Uusimaa J, Vieira P, Tulinius M, Lonnqvist T *et al* (2020) Diagnostic value of serum biomarkers FGF21 and GDF15 compared to muscle sample in mitochondrial disease. *J Inherit Metab Dis*

Lenaz G, Fato R, Formiggini G, Genova ML (2007) The role of Coenzyme Q in mitochondrial electron transport. *Mitochondrion* 7 Suppl: S8-33

Levavasseur F, Miyadera H, Sirois J, Tremblay ML, Kita K, Shoubridge E, Hekimi S (2001) Ubiquinone is necessary for mouse embryonic development but is not essential for mitochondrial respiration. *J Biol Chem* 276: 46160-46164

Li H, Handsaker B, Wysoker A, Fennell T, Ruan J, Homer N, Marth G, Abecasis G, Durbin R, Genome Project Data Processing S (2009) The Sequence Alignment/Map format and SAMtools. *Bioinformatics* 25: 2078-2079

Liesa M, Shirihai OS (2013) Mitochondrial dynamics in the regulation of nutrient utilization and energy expenditure. *Cell Metab* 17: 491-506

Linden DR, Furne J, Stoltz GJ, Abdel-Rehim MS, Levitt MD, Szurszewski JH (2012) Sulphide quinone reductase contributes to hydrogen sulphide metabolism in murine peripheral tissues but not in the CNS. *Br J Pharmacol* 165: 2178-2190

Liu F, Lossl P, Rabbitts BM, Balaban RS, Heck AJR (2018) The interactome of intact mitochondria by cross-linking mass spectrometry provides evidence for coexisting respiratory supercomplexes. *Mol Cell Proteomics* 17: 216-232

Lohman DC, Forouhar F, Beebe ET, Stefely MS, Minogue CE, Ulbrich A, Stefely JA, Sukumar S, Luna-Sanchez M, Jochem A *et al* (2014) Mitochondrial COQ9 is a lipid-binding protein that associates with COQ7 to enable coenzyme Q biosynthesis. *Proc Natl Acad Sci U S A* 111: E4697-4705

Lopez LC, Quinzii CM, Area E, Naini A, Rahman S, Schuelke M, Salviati L, Dimauro S, Hirano M (2010) Treatment of CoQ(10) deficient fibroblasts with ubiquinone, CoQ analogs, and vitamin C: time- and compound-dependent effects. *PLoS One* 5: e11897

Lopez LC, Schuelke M, Quinzii CM, Kanki T, Rodenburg RJ, Naini A, Dimauro S, Hirano M (2006) Leigh syndrome with nephropathy and CoQ10 deficiency due to decaprenyl diphosphate synthase subunit 2 (PDSS2) mutations. *Am J Hum Genet* 79: 1125-1129

Lopez-Martin JM, Salviati L, Trevisson E, Montini G, DiMauro S, Quinzii C, Hirano M, Rodriguez-Hernandez A, Cordero MD, Sanchez-Alcazar JA *et al* (2007) Missense mutation of the COQ2 gene causes defects of bioenergetics and de novo pyrimidine synthesis. *Hum Mol Genet* 16: 1091-1097

Luna-Sanchez M, Diaz-Casado E, Barca E, Tejada MA, Montilla-Garcia A, Cobos EJ, Escames G, Acuna-Castroviejo D, Quinzii CM, Lopez LC (2015) The clinical heterogeneity of coenzyme Q10 deficiency results from genotypic differences in the Coq9 gene. *EMBO Mol Med* 7: 670-687

Luna-Sanchez M, Hidalgo-Gutierrez A, Hildebrandt TM, Chaves-Serrano J, Barriocanal-Casado E, Santos-Fandila A, Romero M, Sayed RK, Duarte J, Prokisch H *et al* (2017) CoQ deficiency causes disruption of mitochondrial sulfide oxidation, a new pathomechanism associated with this syndrome. *EMBO Mol Med* 9: 78-95

Maeoka Y, Doi T, Aizawa M, Miyasako K, Hirashio S, Masuda Y, Kishita Y, Okazaki Y, Murayama K, Imasawa T *et al* (2020) A case report of adult-onset COQ8B nephropathy presenting focal segmental glomerulosclerosis with granular swollen podocytes. *BMC Nephrol* 21: 376

Malicdan MCV, Vilboux T, Ben-Zeev B, Guo J, Eliyahu A, Pode-Shakked B, Dori A, Kakani S, Chandrasekharappa SC, Ferreira CR *et al* (2018) A novel inborn error of the coenzyme Q10 biosynthesis pathway: cerebellar ataxia and static encephalomyopathy due to COQ5 C-methyltransferase deficiency. *Hum Mutat* 39: 69-79

Margulis L (1970) *Origin of Eukaryotic Cells: Evidence and Research Implications for a Theory of the Origin and Evolution of Microbial, Plant, and Animal Cells on the Precambrian Earth*

Martin WF, Muller, Miklos (2007) *Origin of Mitochondria and Hydrogenosomes*. Springer

Martin-Montalvo A, Gonzalez-Mariscal I, Pomares-Viciana T, Padilla-Lopez S, Ballesteros M, Vazquez-Fonseca L, Gandolfo P, Brautigan DL, Navas P, Santos-Ocana C (2013) The phosphatase Ptc7 induces coenzyme Q biosynthesis by activating the hydroxylase Coq7 in yeast. *J Biol Chem* 288: 28126-28137

Martinez-Rodriguez A, Cuestas-Calero BJ, Hernandez-Garcia M, Martiez-Olcina M, Vicente-Martinez M, Rubio-Arias JA (2020) Effect of Supplements on Endurance Exercise in the Older Population: Systematic Review. *Int J Environ Res Public Health* 17

Mayo L, Trauger SA, Blain M, Nadeau M, Patel B, Alvarez JI, Mascanfroni ID, Yeste A, Kivisakk P, Kallas K *et al* (2014) Regulation of astrocyte activation by glycolipids drives chronic CNS inflammation. *Nat Med* 20: 1147-1156

McCune SA, Durant PJ, Flanders LE, Harris RA (1982) Inhibition of hepatic gluconeogenesis and lipogenesis by benzoic acid, p-tert.-butylbenzoic acid, and a structurally related hypolipidemic agent SC-33459. *Arch Biochem Biophys* 214: 124-133

Miranda AS, Cordeiro TM, Dos Santos Lacerda Soares TM, Ferreira RN, Simoes ESAC (2017) Kidney-brain axis inflammatory cross-talk: from bench to bedside. *Clin Sci (Lond)* 131: 1093-1105

Miranda S, Foncea R, Guerrero J, Leighton F (1999) Oxidative stress and upregulation of mitochondrial biogenesis genes in mitochondrial DNA-depleted HeLa cells. *Biochem Biophys Res Commun* 258: 44-49

Mishanina TV, Libiad M, Banerjee R (2015) Biogenesis of reactive sulfur species for signaling by hydrogen sulfide oxidation pathways. *Nat Chem Biol* 11: 457-464

Modis K, Coletta C, Erdelyi K, Papapetropoulos A, Szabo C (2013) Intramitochondrial hydrogen sulfide production by 3-mercaptopyruvate sulfurtransferase maintains mitochondrial electron flow and supports cellular bioenergetics. *FASEB J* 27: 601-611

Mollet J, Delahodde A, Serre V, Chretien D, Schlemmer D, Lombes A, Boddaert N, Desguerre I, de Lonlay P, de Baulny HO *et al* (2008) CABC1 gene mutations cause ubiquinone deficiency with cerebellar ataxia and seizures. *Am J Hum Genet* 82: 623-630

Mollet J, Giurgea I, Schlemmer D, Dallner G, Chretien D, Delahodde A, Bacq D, de Lonlay P, Munnich A, Rotig A (2007) Prenyldiphosphate synthase, subunit 1 (PDSS1) and OH-benzoate polyprenyltransferase (COQ2) mutations in ubiquinone deficiency and oxidative phosphorylation disorders. *J Clin Invest* 117: 765-772

Montero R, Yubero D, Salgado MC, Gonzalez MJ, Campistol J, O'Callaghan MDM, Pineda M, Delgadillo V, Maynou J, Fernandez G *et al* (2019) Plasma coenzyme Q10 status is impaired in selected genetic conditions. *Sci Rep* 9: 793

Montini G, Malaventura C, Salviati L (2008) Early coenzyme Q10 supplementation in primary coenzyme Q10 deficiency. *N Engl J Med* 358: 2849-2850

Mor J, Susin M, Kahn E, Davm F, Teichberg S, McVicar M (1979) Acute renal failure in Reye syndrome. *J Pediatr* 94: 69-72

Mottawea W, Chiang CK, Muhlbauer M, Starr AE, Butcher J, Abujamel T, Deeke SA, Brandel A, Zhou H, Shokralla S *et al* (2016) Altered intestinal microbiota-host mitochondria crosstalk in new onset Crohn's disease. *Nat Commun* 7: 13419

Mudd SH, Irreverre F, Laster L (1967) Sulfite oxidase deficiency in man: demonstration of the enzymatic defect. *Science* 156: 1599-1602

Nakai D, Yuasa S, Takahashi M, Shimizu T, Asaumi S, Isono K, Takao T, Suzuki Y, Kuroyanagi H, Hirokawa K *et al* (2001) Mouse homologue of coq7/clk-1, longevity gene in Caenorhabditis elegans, is essential for coenzyme Q synthesis, maintenance of mitochondrial integrity, and neurogenesis. *Biochem Biophys Res Commun* 289: 463-471

Nedergaard J, Golozoubova V, Matthias A, Asadi A, Jacobsson A, Cannon B (2001) UCP1: the only protein able to mediate adaptive non-shivering thermogenesis and metabolic inefficiency. *Biochim Biophys Acta* 1504: 82-106

Nguengang Wakap S, Lambert DM, Olry A, Rodwell C, Gueydan C, Lanneau V, Murphy D, Le Cam Y, Rath A (2020) Estimating cumulative point prevalence of rare diseases: analysis of the Orphanet database. *Eur J Hum Genet* 28: 165-173

Nunnari J, Suomalainen A (2012) Mitochondria: in sickness and in health. *Cell* 148: 1145-1159

Ogasahara S, Engel AG, Frens D, Mack D (1989) Muscle coenzyme Q deficiency in familial mitochondrial encephalomyopathy. *Proc Natl Acad Sci U S A* 86: 2379-2382

Okada K, Suzuki K, Kamiya Y, Zhu X, Fujisaki S, Nishimura Y, Nishino T, Nakagawa T, Kawamukai M, Matsuda H (1996) Polyprenyl diphosphate synthase essentially defines the length of the side chain of ubiquinone. *Biochim Biophys Acta* 1302: 217-223

Ozeir M, Muhlenhoff U, Webert H, Lill R, Fontecave M, Pierrel F (2011) Coenzyme Q biosynthesis: Coq6 is required for the C5-hydroxylation reaction and substrate analogs rescue Coq6 deficiency. *Chem Biol* 18: 1134-1142

Padilla S, Jonassen T, Jimenez-Hidalgo MA, Fernandez-Ayala DJ, Lopez-Lluch G, Marbois B, Navas P, Clarke CF, Santos-Ocana C (2004) Demethoxy-Q, an intermediate of coenzyme Q biosynthesis, fails to support respiration in Saccharomyces cerevisiae and lacks antioxidant activity. *J Biol Chem* 279: 25995-26004

Papucci L, Schiavone N, Witort E, Donnini M, Lapucci A, Tempestini A, Formigli L, Zecchi-Orlandini S, Orlandini G, Carella G *et al* (2003) Coenzyme q10 prevents apoptosis by inhibiting mitochondrial depolarization independently of its free radical scavenging property. *J Biol Chem* 278: 28220-28228

Payet LA, Leroux M, Willison JC, Kihara A, Pelosi L, Pierrel F (2016) Mechanistic Details of Early Steps in Coenzyme Q Biosynthesis Pathway in Yeast. *Cell Chem Biol* 23: 1241-1250

Pedersen CB, Bross P, Winter VS, Corydon TJ, Bolund L, Bartlett K, Vockley J, Gregersen N (2003) Misfolding, degradation, and aggregation of variant proteins. The molecular pathogenesis of short chain acyl-CoA dehydrogenase (SCAD) deficiency. *J Biol Chem* 278: 47449-47458

Peng M, Jarett L, Meade R, Madaio MP, Hancock WW, George AL, Jr., Neilson EG, Gasser DL (2004) Mutant prenyltransferase-like mitochondrial protein (PLMP) and mitochondrial abnormalities in kd/kd mice. *Kidney Int* 66: 20-28

Pfanner N, Warscheid B, Wiedemann N (2019) Mitochondrial proteins: from biogenesis to functional networks. *Nat Rev Mol Cell Biol* 20: 267-284

Pierrel F (2017) Impact of Chemical Analogs of 4-Hydroxybenzoic Acid on Coenzyme Q Biosynthesis: From Inhibition to Bypass of Coenzyme Q Deficiency. *Front Physiol* 8: 436

Poon WW, Barkovich RJ, Hsu AY, Frankel A, Lee PT, Shepherd JN, Myles DC, Clarke CF (1999) Yeast and rat Coq3 and Escherichia coli UbiG polypeptides catalyze both O-methyltransferase steps in coenzyme Q biosynthesis. *J Biol Chem* 274: 21665-21672

Procopio R, Gagliardi M, Brighina L, Nicoletti G, Morelli M, Ferrarese C, Annesi G, Quattrone A (2019) Genetic mutation analysis of the COQ2 gene in Italian patients with multiple system atrophy. *Gene* 716: 144037

Quintana A, Kruse SE, Kapur RP, Sanz E, Palmiter RD (2010) Complex I deficiency due to loss of Ndufs4 in the brain results in progressive encephalopathy resembling Leigh syndrome. *Proc Natl Acad Sci U S A* 107: 10996-11001

Quinzii C, Naini A, Salviati L, Trevisson E, Navas P, Dimauro S, Hirano M (2006) A mutation in para-hydroxybenzoate-polyprenyl transferase (COQ2) causes primary coenzyme Q10 deficiency. *Am J Hum Genet* 78: 345-349

Quinzii CM, Garone C, Emmanuele V, Tadesse S, Krishna S, Dorado B, Hirano M (2013) Tissue-specific oxidative stress and loss of mitochondria in CoQ-deficient Pdss2 mutant mice. *FASEB J* 27: 612-621

Quinzii CM, Kattah AG, Naini A, Akman HO, Mootha VK, DiMauro S, Hirano M (2005) Coenzyme Q deficiency and cerebellar ataxia associated with an aprataxin mutation. *Neurology* 64: 539-541

Quinzii CM, Lopez LC, Gilkerson RW, Dorado B, Coku J, Naini AB, Lagier-Tourenne C, Schuelke M, Salviati L, Carrozzo R *et al* (2010) Reactive oxygen species, oxidative stress, and cell death correlate with level of CoQ10 deficiency. *FASEB J* 24: 3733-3743

Quinzii CM, Lopez LC, Von-Moltke J, Naini A, Krishna S, Schuelke M, Salviati L, Navas P, DiMauro S, Hirano M (2008) Respiratory chain dysfunction and oxidative stress correlate with severity of primary CoQ10 deficiency. *FASEB J* 22: 1874-1885

Quinzii CM, Luna-Sanchez M, Ziosi M, Hidalgo-Gutierrez A, Kleiner G, Lopez LC (2017) The Role of Sulfide Oxidation Impairment in the Pathogenesis of Primary CoQ Deficiency. *Front Physiol* 8: 525

Rahman S, Clarke CF, Hirano M (2012) 176th ENMC International Workshop: diagnosis and treatment of coenzyme Q(1)(0) deficiency. *Neuromuscul Disord* 22: 76-86

Raimundo N, Vanharanta S, Aaltonen LA, Hovatta I, Suomalainen A (2009) Downregulation of SRF-FOS-JUNB pathway in fumarate hydratase deficiency and in uterine leiomyomas. *Oncogene* 28: 1261-1273

Reichmann F, Hassan AM, Farzi A, Jain P, Schuligoi R, Holzer P (2015) Dextran sulfate sodium-induced colitis alters stress-associated behaviour and neuropeptide gene expression in the amygdala-hippocampus network of mice. *Sci Rep* 5: 9970

Restelli LM, Oettinghaus B, Halliday M, Agca C, Licci M, Sironi L, Savoia C, Hench J, Tolnay M, Neutzner A *et al* (2018) Neuronal Mitochondrial Dysfunction Activates the Integrated Stress Response to Induce Fibroblast Growth Factor 21. *Cell Rep* 24: 1407-1414

Ribas V, Garcia-Ruiz C, Fernandez-Checa JC (2014) Glutathione and mitochondria. *Front Pharmacol* 5: 151

Rodriguez-Hernandez A, Cordero MD, Salviati L, Artuch R, Pineda M, Briones P, Gomez Izquierdo L, Cotan D, Navas P, Sanchez-Alcazar JA (2009) Coenzyme Q deficiency triggers mitochondria degradation by mitophagy. *Autophagy* 5: 19-32

Rogers GW, Brand MD, Petrosyan S, Ashok D, Elorza AA, Ferrick DA, Murphy AN (2011) High throughput microplate respiratory measurements using minimal quantities of isolated mitochondria. *PLoS One* 6: e21746

Rothhammer V, Kenison JE, Tjon E, Takenaka MC, de Lima KA, Borucki DM, Chao CC, Wilz A, Blain M, Healy L *et al* (2017) Sphingosine 1-phosphate receptor modulation suppresses pathogenic astrocyte activation and chronic progressive CNS inflammation. *Proc Natl Acad Sci U S A* 114: 2012-2017

Rothhammer V, Mascanfroni ID, Bunse L, Takenaka MC, Kenison JE, Mayo L, Chao CC, Patel B, Yan R, Blain M *et al* (2016) Type I interferons and microbial metabolites of tryptophan modulate astrocyte activity and central nervous system inflammation via the aryl hydrocarbon receptor. *Nat Med* 22: 586-597

Rotig A, Appelkvist EL, Geromel V, Chretien D, Kadhom N, Edery P, Lebideau M, Dallner G, Munnich A, Ernster L *et al* (2000) Quinone-responsive multiple respiratory-chain dysfunction due to widespread coenzyme Q10 deficiency. *Lancet* 356: 391-395

Sadowski CE, Lovric S, Ashraf S, Pabst WL, Gee HY, Kohl S, Engelmann S, Vega-Warner V, Fang H, Halbritter J *et al* (2015) A single-gene cause in 29.5% of cases of steroid-resistant nephrotic syndrome. *J Am Soc Nephrol* 26: 1279-1289

Sahebekhtiari N, Fernandez-Guerra P, Nochi Z, Carlsen J, Bross P, Palmfeldt J (2019) Deficiency of the mitochondrial sulfide regulator ETHE1 disturbs cell growth, glutathione level and causes proteome alterations outside mitochondria. *Biochim Biophys Acta Mol Basis Dis* 1865: 126-135

Saiki R, Lunceford AL, Shi Y, Marbois B, King R, Pachuski J, Kawamukai M, Gasser DL, Clarke CF (2008) Coenzyme Q10 supplementation rescues renal disease in Pdss2kd/kd mice with mutations in prenyl diphosphate synthase subunit 2. *Am J Physiol Renal Physiol* 295: F1535-1544

Sandoval-Acuna C, Lopez-Alarcon C, Aliaga ME, Speisky H (2012) Inhibition of mitochondrial complex I by various non-steroidal anti-inflammatory drugs and its protection by quercetin via a coenzyme Q-like action. *Chem Biol Interact* 199: 18-28

Santos-Ocana C, Villalba JM, Cordoba F, Padilla S, Crane FL, Clarke CF, Navas P (1998) Genetic evidence for coenzyme Q requirement in plasma membrane electron transport. *J Bioenerg Biomembr* 30: 465-475

Satoh M, Kuroiwa T (1991) Organization of multiple nucleoids and DNA molecules in mitochondria of a human cell. *Exp Cell Res* 196: 137-140

Schagger H, Pfeiffer K (2000) Supercomplexes in the respiratory chains of yeast and mammalian mitochondria. *EMBO J* 19: 1777-1783

Scheffler IE (2007) *Mitochondria*

Smith AC, Ito Y, Ahmed A, Schwartzentruber JA, Beaulieu CL, Aberg E, Majewski J, Bulman DE, Horsting-Wethly K, Koning DV *et al* (2018) A family segregating lethal neonatal coenzyme Q10 deficiency caused by mutations in COQ9. *J Inherit Metab Dis* 41: 719-729

Sondheimer N, Hewson S, Cameron JM, Somers GR, Broadbent JD, Ziosi M, Quinzii CM, Naini AB (2017) Novel recessive mutations in COQ4 cause severe infantile cardiomyopathy and encephalopathy associated with CoQ10 deficiency. *Mol Genet Metab Rep* 12: 23-27

Song X, Fang X, Tang X, Cao Q, Zhai Y, Chen J, Liu J, Zhang Z, Xiang T, Qian Y *et al* (2020) COQ8B nephropathy: Early detection and optimal treatment. *Mol Genet Genomic Med* 8: e1360

Spinazzi M, Radaelli E, Horre K, Arranz AM, Gounko NV, Agostinis P, Maia TM, Impens F, Morais VA, Lopez-Lluch G *et al* (2019) PARL deficiency in mouse causes Complex III defects, coenzyme Q depletion, and Leigh-like syndrome. *Proc Natl Acad Sci U S A* 116: 277-286

Spinelli JB, Haigis MC (2018) The multifaceted contributions of mitochondria to cellular metabolism. *Nat Cell Biol* 20: 745-754

Stefely JA, Pagliarini DJ (2017) Biochemistry of Mitochondrial Coenzyme Q Biosynthesis. *Trends Biochem Sci* 42: 824-843

Stenmark P, Grunler J, Mattsson J, Sindelar PJ, Nordlund P, Berthold DA (2001) A new member of the family of di-iron carboxylate proteins. Coq7 (clk-1), a membrane-bound hydroxylase involved in ubiquinone biosynthesis. *J Biol Chem* 276: 33297-33300

Sul D, Kaneshiro ES (2001) Pneumocystis carinii f. sp. carinii synthesizes de novo four homologs of ubiquinone. *J Eukaryot Microbiol* 48: 182-187

Takahashi M, Shimizu T, Moriizumi E, Shirasawa T (2008) Clk-1 deficiency induces apoptosis associated with mitochondrial dysfunction in mouse embryos. *Mech Ageing Dev* 129: 291-298

Takahashi T, Okamoto T, Mori K, Sayo H, Kishi T (1993) Distribution of ubiquinone and ubiquinol homologues in rat tissues and subcellular fractions. *Lipids* 28: 803-809

Takayanagi R, Takeshige K, Minakami S (1980) NADH- and NADPH-dependent lipid peroxidation in bovine heart submitochondrial particles. Dependence on the rate of electron flow in the respiratory chain and an antioxidant role of ubiquinol. *Biochem J* 192: 853-860

Tanji K, Bonilla E (2008) Light microscopic methods to visualize mitochondria on tissue sections. *Methods* 46: 274-280

Tegelberg S, Tomasic N, Kallijarvi J, Purhonen J, Elmer E, Lindberg E, Nord DG, Soller M, Lesko N, Wedell A *et al* (2017) Respiratory chain complex III deficiency due to mutated BCS1L: a novel phenotype with encephalomyopathy, partially phenocopied in a Bcs1l mutant mouse model. *Orphanet J Rare Dis* 12: 73

Tekle M, Bentinger M, Nordman T, Appelkvist EL, Chojnacki T, Olsson JM (2002) Ubiquinone biosynthesis in rat liver peroxisomes. *Biochem Biophys Res Commun* 291: 1128-1133

Thackeray JT, Hupe HC, Wang Y, Bankstahl JP, Berding G, Ross TL, Bauersachs J, Wollert KC, Bengel FM (2018) Myocardial Inflammation Predicts Remodeling and Neuroinflammation After Myocardial Infarction. *J Am Coll Cardiol* 71: 263-275

Tiranti V, Viscomi C, Hildebrandt T, Di Meo I, Mineri R, Tiveron C, Levitt MD, Prelle A, Fagiolari G, Rimoldi M *et al* (2009) Loss of ETHE1, a mitochondrial dioxygenase, causes fatal sulfide toxicity in ethylmalonic encephalopathy. *Nat Med* 15: 200-205

Tran UC, Clarke CF (2007) Endogenous synthesis of coenzyme Q in eukaryotes. *Mitochondrion* 7 Suppl: S62-71

Turunen M, Olsson J, Dallner G (2004) Metabolism and function of coenzyme Q. *Biochim Biophys Acta* 1660: 171-199

Vafai SB, Mootha VK (2012) Mitochondrial disorders as windows into an ancient organelle. *Nature* 491: 374-383

van der Laan M, Horvath SE, Pfanner N (2016) Mitochondrial contact site and cristae organizing system. *Curr Opin Cell Biol* 41: 33-42

Viscomi C, Burlina AB, Dweikat I, Savoiardo M, Lamperti C, Hildebrandt T, Tiranti V, Zeviani M (2010) Combined treatment with oral metronidazole and N-acetylcysteine is effective in ethylmalonic encephalopathy. *Nat Med* 16: 869-871

Wallace DC (2016) Genetics: Mitochondrial DNA in evolution and disease. *Nature* 535: 498-500

Wang W, Karamanlidis G, Tian R (2016) Novel targets for mitochondrial medicine. *Sci Transl Med* 8: 326rv323

Wang Y, Oxer D, Hekimi S (2015) Mitochondrial function and lifespan of mice with controlled ubiquinone biosynthesis. *Nat Commun* 6: 6393

Wang Y, Smith C, Parboosingh JS, Khan A, Innes M, Hekimi S (2017) Pathogenicity of two COQ7 mutations and responses to 2,4-dihydroxybenzoate bypass treatment. *J Cell Mol Med* 21: 2329-2343

Widmeier E, Airik M, Hugo H, Schapiro D, Wedel J, Ghosh CC, Nakayama M, Schneider R, Awad AM, Nag A *et al* (2019) Treatment with 2,4-Dihydroxybenzoic Acid Prevents FSGS Progression and Renal Fibrosis in Podocyte-Specific Coq6 Knockout Mice. *J Am Soc Nephrol*

Widmeier E, Yu S, Nag A, Chung YW, Nakayama M, Fernandez-Del-Rio L, Hugo H, Schapiro D, Buerger F, Choi WI *et al* (2020) ADCK4 Deficiency Destabilizes the Coenzyme Q Complex, Which Is Rescued by 2,4-Dihydroxybenzoic Acid Treatment. *J Am Soc Nephrol* 31: 1191-1211

Wolf DE, Hoffman CH, Trenner NR, Arison BH, Shunk CH, Linn BO, Mcpherson JF, Folkers K (1958) Coenzyme Q .1. Structure Studies on the Coenzyme Q-Group. *J Am Chem Soc* 80: 4752-4752

Wu X, Wang W, Liu Y, Chen W, Zhao L (2019) A steroid-resistant nephrotic syndrome in an infant resulting from a consanguineous marriage with COQ2 and ARSB gene mutations: a case report. *BMC Med Genet* 20: 165

Xie LX, Ozeir M, Tang JY, Chen JY, Jaquinod SK, Fontecave M, Clarke CF, Pierrel F (2012) Overexpression of the Coq8 kinase in Saccharomyces cerevisiae coq null mutants allows for accumulation of diagnostic intermediates of the coenzyme Q6 biosynthetic pathway. *J Biol Chem* 287: 23571-23581

Yang YY, Vasta V, Hahn S, Gangoiti JA, Opheim E, Sedensky MM, Morgan PG (2011) The role of DMQ(9) in the long-lived mutant clk-1. *Mech Ageing Dev* 132: 331-339

Yoo SE, Chen L, Na R, Liu Y, Rios C, Van Remmen H, Richardson A, Ran Q (2012) Gpx4 ablation in adult mice results in a lethal phenotype accompanied by neuronal loss in brain. *Free Radic Biol Med* 52: 1820-1827

Yubero D, Allen G, Artuch R, Montero R (2017) The Value of Coenzyme Q10 Determination in Mitochondrial Patients. *J Clin Med* 6

Yubero D, Montero R, Martin MA, Montoya J, Ribes A, Grazina M, Trevisson E, Rodriguez-Aguilera JC, Hargreaves IP, Salviati L *et al* (2016) Secondary coenzyme Q10 deficiencies in oxidative phosphorylation (OXPHOS) and non-OXPHOS disorders. *Mitochondrion* 30: 51-58

Yubero D, Montero R, Santos-Ocana C, Salviati L, Navas P, Artuch R (2018) Molecular diagnosis of coenzyme Q10 deficiency: an update. *Expert Rev Mol Diagn* 18: 491-498

Zachar I, Boza G (2020) Endosymbiosis before eukaryotes: mitochondrial establishment in protoeukaryotes. *Cell Mol Life Sci* 77: 3503-3523

Zamanian JL, Xu L, Foo LC, Nouri N, Zhou L, Giffard RG, Barres BA (2012) Genomic analysis of reactive astrogliosis. *J Neurosci* 32: 6391-6410

Zhang M, Wakitani S, Hayashi K, Miki R, Kawamukai M (2008) High production of sulfide in coenzyme Q deficient fission yeast. *Biofactors* 32: 91-98

Zhao J, Lendahl U, Nister M (2013) Regulation of mitochondrial dynamics: convergences and divergences between yeast and vertebrates. *Cell Mol Life Sci* 70: 951-976

Ziosi M, Di Meo I, Kleiner G, Gao XH, Barca E, Sanchez-Quintero MJ, Tadesse S, Jiang H, Qiao C, Rodenburg RJ *et al* (2017) Coenzyme Q deficiency causes impairment of the sulfide oxidation pathway. *EMBO Mol Med* 9: 96-111